THE UNIVERSITY
of EDINBURGH

This thesis has been submitted in fulfilment of the requirements for a postgraduate degree (e.g. PhD, MPhil, DClinPsychol) at the University of Edinburgh. Please note the following terms and conditions of use:

This work is protected by copyright and other intellectual property rights, which are retained by the thesis author, unless otherwise stated.
A copy can be downloaded for personal non-commercial research or study, without prior permission or charge.
This thesis cannot be reproduced or quoted extensively from without first obtaining permission in writing from the author.
The content must not be changed in any way or sold commercially in any format or medium without the formal permission of the author.
When referring to this work, full bibliographic details including the author, title, awarding institution and date of the thesis must be given.

Investigating the reversibility of senescence

Britanto Dani Wicaksono

THE UNIVERSITY
of EDINBURGH

PhD in Cell and Molecular Biology – Cell Biology

The University of Edinburgh

2019

Declaration

I declare that this thesis was composed by myself, that the work contained herein is my own except where explicitly stated otherwise in the text, and that this work has not been submitted for any other degree or professional qualification except as specified.

Edinburgh, 03 December 2019

Britanto Dani Wicaksono

Abstract

Senescence is defined as a permanent and irreversible cell cycle arrest. The initiating stimuli can be diverse, such as oncogene expression, reactive oxygen species and critically short telomeres. Irrespective of the nature of the trigger, p53-dependent DNA damage response (DDR) is initiated, leading to cell cycle arrest in G1. A prolonged DDR activation can further reinforce the arrest through the activation of the cyclin-dependent kinase inhibitor p16. The inability of the semi-conservative DNA replication machinery to completely copy the ends of linear eukaryotic chromosomes results in a gradual telomere shortening that is counteracted by telomerase, a ribonucleoprotein which can add telomeric repeats to the 3' end of a chromosome. However, during human embryonic development, telomerase is downregulated through decreased expression of the telomerase catalytic subunit hTERT. Consequently, human somatic cells undergo progressive telomere shortening that will ultimately lead to eroded telomeres being recognised by the DDR and induction of replicative senescence. Reconstitution of hTERT in several human somatic cells has been shown to prevent replicative senescence. During cancer development, cell immortalisation requires escaping senescence and telomerase reactivation is the prevalent route to this end. However, while it is clear that the presence of telomerase can counteract entry into the senescence, it is not known if, once senescence has been established, telomerase could drive cells out of the arrest. In this work, I address the reversibility of senescence triggered by critically short telomeres by: 1) reactivating telomerase expression in senescent cells; 2) reactivating expression and tethering telomerase to telomeres during senescence; and 3) reactivating telomerase expression together with transient DDR inhibition. By taking advantage of telomerase fused to a conditional degron, I have tested if telomerase stabilisation in senescent MRC5 human fibroblasts could bypass the arrest. My results show that the presence of telomerase was not sufficient to overcome senescence. Since it has been shown that yeast telomerase can only gain access to telomeres during DNA replication, one possibility is that telomerase reactivated in senescent cells was unable to localise to telomeres. To address this

possibility, I have expressed an hPOT1-hTERT fusion to tether telomerase to telomeres irrespective of the cell cycle stage. In a parallel approach, I have set up a system to allow senescent cells to enter the S-phase by transient inhibition of DDR, by IPTG-inducible knock-down of p53 and p16. This study contributes to improving our understanding of molecular mechanisms of senescence and its reversibility as a possible approach for the therapy of age-related diseases.

Lay Summary

Most human cells can divide for certain amount of times before indefinitely stopped dividing in a state called cellular senescence or the aging of cells. Senescence in human cells is known to be linked to the shortening of the telomeres, the physical ends of chromosomes. Throughout its lifetime, cells can accumulate damage which could result in the cells becoming cancer cells, if damage is not repaired. Senescence can prevent this by limiting the cell's ability to divide when accumulation of damage is intolerable. On the other hand, the build-up of senescent cells is also known to be harmful, as it plays a role in the aging of tissues and the body of an organism. Furthermore, studies have shown that cancer cells may arise from cells that have escaped senescence. In this study, I am exploring how cells can escape senescence using human fibroblasts as a model, by introducing an enzyme that can elongate telomeres called telomerase to the cells. Furthermore, I have also attempted in modulating the senescence signalling in the cells, to study whether this can help cells escape senescence. The results of this study may have implications in our understanding of how senescent cells become cancer cells and also how we can treat diseases related to early aging.

Acknowledgements

Firstly, I would like to thank the Indonesia endowment fund for education (Lembaga Pengelola Dana Pendidikan/LPDP) of the ministry of finance of the republic of Indonesia for funding my studies at the University of Edinburgh. The school of biological sciences of the University of Edinburgh have also helped immensely in funding my research, particularly in the last two years of my PhD studies. I would like to express my sincere gratitude to my supervisors Dr. Sveta Makovets and Dr. Sara Buonomo for the continuous support throughout my PhD studies. Besides my current supervisor, I would also like to thank my former supervisor, Dr. Irina Stancheva, who has helped me immensely during the first two years of my PhD studies. I would also like to show appreciation to my thesis committee member Dr. Bernard Ramsahoye and also to Dr. Philipp Voigt and Dr. Marcus Wilson for suggestions, input and advice. My sincere thanks also go to Dr. Kevin Hardwick and Dr. Caroline Proctor who have helped me during my transition from the Stancheva to Makovets/Buonomo lab. People from the Stancheva lab, particularly Burak Özkan, Simon Varzandeh, Natalia Torrea, Ilaria Amendola and Christian Belton were definitely responsible for all the fun stuff in and out of the lab. During the last 2 years of my PhD studies, I have been mostly indebted to people from the Buonomo lab, particularly Lynn Powell, Stefano Gnan, Eleonora Castelli, Naiming Chen, Elin Enervald and Sean Dunphy. Apologies if I have forgotten to mention everyone, but I would also like to thank all people from the Makovets, Buonomo and Voigt Labs for the help in day to day lab activities. Big love and hugs to my parents, in-laws and siblings who have supported me from Indonesia and have taken their time to visit me in the summer of 2018. Last but not least, I would like to thank my dearest wife Anggi Wulan, who has always been by my side since the start of my PhD studies and who gave birth to our beautiful daughter Freya here in Edinburgh in January 2018. Raising her together, far from our parents has been quite tough. But Freya's smile and laughter have always melted our hearts and brings love and joy to this little family.

Abbreviations

3D	Three-Dimensional
ALT	Alternative Lengthening of Telomeres
Amp	Ampicillin
BCA	Bicinchoninic Acid
bp	base pair
Blast	Blasticidin
BSA	Bovine Serum Albumin
bsr	Blasticidin-S resistance gene
CPD	Cumulative Population Doublings
CMV	Cytomegalovirus
Da	Dalton
kDa	kiloDalton
DAPI	4′,6-diamidino-2-phenylindole
DAT	Dissociates Activities of Telomerase
DD	Destabilising Domain
DDR	DNA Damage Response
DKC	Dyskeratosis Congenita
DNA	Deoxyribonucleic acid
cDNA	complementary DNA (synthesised from mRNA)
dsDNA	double-stranded DNA
dH_2O	Deionised water
DMEM	Dulbecco's Modified Eagle's Medium
DTT	Dithiotreitol
EDTA	Ethylenediaminetetraacetic acid
EdU	5-Ethynyl-2´-deoxyuridine
EtBr	Ethidium Bromide
FACS	Fluorescence-activated cell sorting
FBS	Foetal Bovine Serum
gDNA	Genomic DNA
GFP	Green Fluorescent Protein
HHS	Hoyeraal-Hreidarsson Syndrome

HR	Homologous Recombination
Hygro	Hygromycin
ICF	Immunodeficiency, Centromere instability and Facial anomalies
IF	Immunofluorescence
IPTG	Isopropyl β-D-1-thiogalactopyranoside
Kan	Kanamycin
Lab	Laboratory
LB	Lysogeny Broth
MEM	Minimum Essential Medium
MEF	Mouse Embryonic Fibroblasts
MMC	Mitomycin-C
mESCs	Mouse Embryonic Stem Cells
MOI	Multiplicity of infection
MRC-5	Medical Research Council cell strain 5
NEAA	Non-essential amino acids
Neo	Neomycin
NHEJ	Non-homologous End Joining
NMD	Nonsense-mediated mRNA decay
OD	Optical Density
OIS	Oncogene-induced Senescence
PAGE	Polyacrylamide Gel Electrophoresis
PBS	Phosphate Buffer Saline
PBS-T	PBS with Tween-20
PCR	Polymerase Chain Reaction
PD	Population Doublings
PFT-α	Pifithrin- α
PS	Premature Senescence
PSG	Penicillin Streptomycin Glutamine
Puro	Puromycin
RCF	Relative Centrifugal Force
RNA	Ribonucleic Acid
RNAi	RNA interference

mRNA	messenger RNA
RS	Replicative senescence
SA-β-gal	Senescence-associated β-galactosidase
SDS	Sodium Dodecyl Sulphate
SIPS	Stress-induced Premature Senescence
SADS	Senescence-associated Distension of Satellites
SEM	Standard Error of the Mean
shRNA	Short hairpin RNA
ssDNA	single-stranded DNA
SV40	Simian vacuolating virus 40
TAE	Tris Acetate EDTA
TBS	Tris Buffer Saline
TBS-T	TBS with Tween-20
TBE	Tris Borate EDTA
TE	Tris EDTA
TERRA	Telomeric Repeat-containing RNA
TERT	Telomerase reverse transcriptase
hTERT	human TERT
TRAP	Telomere Repeats Amplification Protocol
TRF	Telomere Restriction Fragment
TR	Telomerase RNA
hTR	human TR
UV	Ultraviolet
WT	Wild-Type
X-gal	5-bromo-4-chloro-3-indolyl-β-D-galactopyranoside

Table of Contents

List of Figures

List of Tables

Chapter 1 Introduction

1.1 Organisation and maintenance of linear chromosomal ends

Mammalian genomes are organised in linear chromosomes where each chromosome has two DNA ends, which are prone to end-to-end fusions and can potentially be a subject of DNA resection by endonucleases. As a countermeasure to avoid these detrimental processes, which could lead to genomic instability, linear chromosome ends are protected by DNA-protein complexes capping the DNA ends and called telomeres. Telomeres consist of repetitive non-coding DNA, which is bound by a set of proteins (shelterin) with the DNA binding specificity matching the telomeric repeat sequence. During normal cellular proliferation, the inability of the semi-conservative DNA replication machinery to copy linear DNA ends completely, colloquially termed the end-replication problem, could lead to a gradual shortening of telomeric DNA (Watson, 1972; Blackburn and Gall, 1978; Huffman et al., 2000; de Lange, 2002). When telomeres becomes critically short, they can no longer perform the capping function efficiently and the cell activates a DNA damage response (DDR) signalling at the telomeres which could initiate the senescence programme, if the DDR activation persists (de Lange, 2002; d'Adda di Fagagna et al., 2003). To overcome the end-replication problem, proliferating cells such as stem cells (embryonic and adult stem cells), male germ cells and activated lymphocytes, express telomerase, a ribonucleoprotein (RNP) which can elongate telomeres by adding telomeric repeats to the 3' end of the telomeres (Greider and Blackburn, 1985; Wright et al., 1996; Weinrich et al., 1997). Telomerase mainly consists of an RNA component (hTR or hTERC in humans) and a protein with a reverse transcriptase enzymatic activity (hTERT in humans). In human somatic cells, telomerase is either not expressed or expressed at a non-detectable level (Wright et al., 1996). On the other hand, approximately 80% of all cancers are known to express telomerase in order to allow infinite cell proliferation, by abrogating replicative senescence (Kim et al., 1994). While hTR is known to

be expressed in somatic tissues (Feng et al., 1995; Avilion et al., 1996), hTERT is generally repressed in normal differentiated cells (Kim et al., 1994). Ectopic expression of hTERT is sufficient to activate telomerase and immortalise several types of somatic cells (Bodnar et al., 1998; Counter et al., 1998; Vaziri and Benchimol, 1998). Mutations in telomerase, telomerase accessory proteins, shelterin components or proteins associated with telomere replication/elongation lead to abnormally short telomeres resulting in limited proliferation potential and have been associated with various human diseases, such as dyskeratosis congenita, aplastic anaemia, pulmonary fibrosis and pancytopenia (Heiss et al., 1998; Armanios et al., 2007; Tsangaris et al., 2008).

1.1.1 Structure and function of human telomeres

The natural ends of linear chromosomes were first defined as telomeres, from the greek words *telos* (end) and *meros* (part), in the 1930s by Herman Muller and later by Barbara McClintock, who studied these chromosomal ends in flies and corn respectively (Muller, 1938; McClintock, 1941). Human telomeres comprise of three main components: single stranded telomeric repeats, double stranded telomeric repeats and the shelterin protein complex. In humans, telomeric DNA is made of the tandem repetitive sequence 5'-TTAGGG(n), with a length of approximately 5 – 15 kb (Samassekou et al., 2010). The single stranded G-rich component of the telomere extends out of the 3'-end of the telomeric dsDNA to a size of approximately 50 - 200 bp (Makarov, Hirose and Langmore, 1997; McElligott and Wellinger, 1997; Wright et al., 1997). This single strand overhang of the telomere invades back into the double-stranded DNA portion to form a telomere loop (T-loop) (Figure 1.1 A) (Griffith et al., 1999; Cesare et al., 2003; Doksani et al., 2013). The shelterin complex consists of the six main protein components: TRF1, TRF2, TIN2, POT1, RAP1 and TPP1 (Figure 1.1 B). Binding of the shelterin complex to telomeric DNA is mediated by three proteins: TRF1, TRF2 and POT1. TRF1 and TRF2 bind to the dsDNA telomeric repeats via their Myb/SANT domain, which recognises the sequence 5'-TAGGGTT (Broccoli et al., 1997; Bianchi et al., 1997; Court et al., 2005). TRF1 and TRF2 form homodimers via their TRFH domains. The

dimer formation is known to be required for their telomeric DNA binding activity (Broccoli et al., 1997; Li, Oestreich and de Lange, 2000; Fairall et al., 2001). POT1 binds ssDNA telomeric repeats. This binding is mediated by its two OB-fold domains (OB1 & OB2) located at the N-terminus. POT1 recognises the sequence 5'-TTAGGGTTAG (Lei, Podell and Cech, 2004; Loayza et al., 2004). Unlike the three previously mentioned shelterin components, TIN2, TPP1 and RAP1 do not bind telomeric DNA directly. TIN2 is known to bind both TRF2 and TRF1, forming a bridge which connects both proteins. TIN2 binds TRF2 via its TRFH domain (Ye et al., 2004b). Furthermore, TIN2 also binds TRF1 via a C-terminal TRF1-specific binding domain (Ye et al., 2004b). TPP1 binds TIN2 through its TIN2-specific binding domain (Liu et al., 2004). Furthermore, TPP1 also binds POT1 through its POT1 binding domain, located downstream of its OB domain (Ye et al., 2004a). Together, this allowed tethering of POT1 to TIN2 via TPP1. Although RAP1 has a Myb domain similar to TRF1 and TRF2, it is understood that it is not capable of DNA binding but can play a role in protein-protein interactions and has been shown to be important for the binding of RAP1 to TRF2 (Hanaoka et al., 2001). However, another study suggests that human RAP1 can bind to telomeric DNA and that the binding of RAP1 to DNA is required for TRF2 localisation to telomeres (Arat and Griffith, 2012).

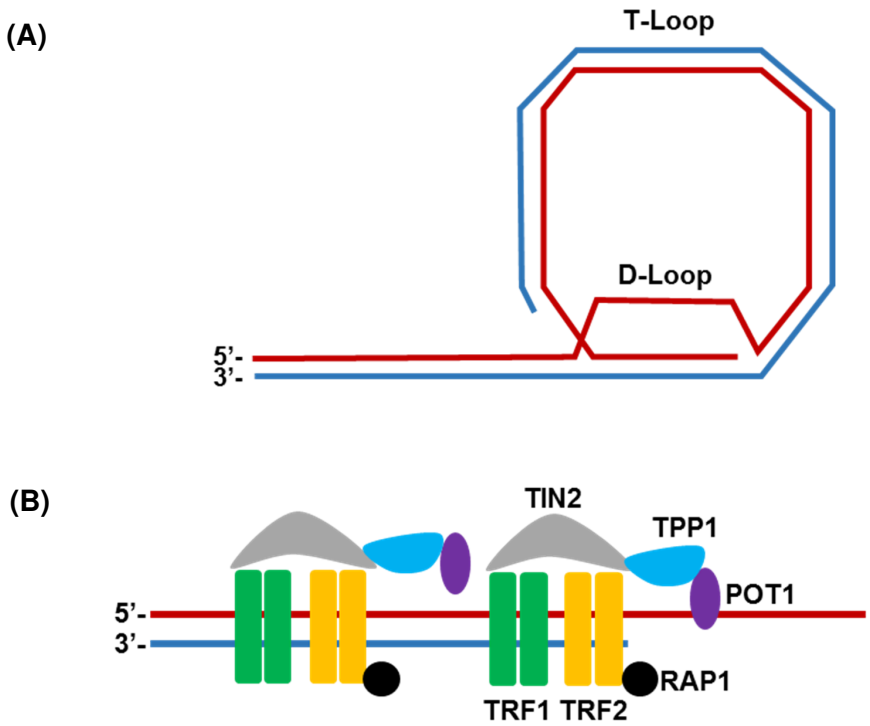

Figure 1.1 Mammalian telomere cap structure.
(A) The formation of the T-loop requires the invasion of the single-stranded DNA 3'-end of the telomere into its double-stranded DNA portion, which results in a displacement loop (D-loop). (B) Shelterin complex on telomeres.

The T-loop structure and the individual components of the shelterin complex are proposed to be important for the capping and protective function of the telomeres (Griffith et al., 1999; M.Stansel, Lange and Griffith, 2001; Karlseder, Smogorzewska and Lange, 2002; Van Ly et al., 2018). TRF2 and RAP1 have been shown to prevent both classical and alternative non-homologous end joining (NHEJ) repair activity on telomeres (Bae and Baumann, 2007; Doksani et al., 2013; Sfeir and De Lange, 2012). Furthermore, studies in mouse cells implicated POT1 together with RAP1 in preventing homology-directed repair (HDR) at telomeres (Palm et al., 2009; Sfeir et al., 2010). Together with the T-loop structure, these shelterin components prevent telomeric ends being

recognised as DSBs and processed by the DNA repair machineries resulting in telomeric end-to-end fusions. Interestingly, recent data in mice suggest that DSB repair can still operate at telomeres during the S-phase in a PARP1- and a Lig3-dependent manner (Doksani and de Lange, 2016). Although mouse and human telomeres have a high degree of structural similarity, they have very different responses to DNA damage signalling activated at telomeres, necessitating very careful interpretation of the data in the mouse model when superimposing it to the human telomere biology (Smogorzewska and de Lange, 2002).

1.1.2 DNA replication at telomeres

Yeast telomeres have been shown to replicate late during the S-phase (McCarroll and Fangman, 1988). Heterochromatic regions are generally late-replicating, and this was thought to be the reason for why telomeres replicate late. However, in human cells, replication of telomeres occurs sporadically throughout the cell cycle (Wright et al., 1999). A study using single molecule analysis of replicated DNA (SMARD) showed that the origins of replication exist at the sub-telomeric regions and that DNA replication could start from the sub-telomeric origins towards telomeres or originate from inside the telomeres themselves (Drosopoulos, Kosiyatrakul and Schildkraut, 2015).

Owing to its high GC content, the formation of G-quadruplex structures is rampant at telomeres and could trigger stalling of the DNA replication machinery. Therefore, the DNA replication machinery requires assistance from the helicases which can unwind G-quadruplex structures, such as RTEL1 and BLM, which are recruited to telomeres by PCNA as part of the DNA replication machinery and by TRF1 respectively, in order to increase the accessibility of the telomeric DNA during DNA replication (Vannier et al., 2012, 2013; Zimmermann et al., 2014; Drosopoulos, Kosiyatrakul and Schildkraut, 2015). As previously mentioned, telomeres shorten with each replication cycle. The rate of telomere shortening in human cells not expressing telomerase is approximately 50 – 200 bp per population doubling (Harley, Futcher and

Greider, 1990). Thus, in actively proliferating human cells, telomerase expression is required to prevent the shortening of the telomeres.

1.1.3 Telomerase structure and biogenesis

As briefly mentioned above, to counteract the telomere shortening with each DNA replication cycle, several types of human cells express telomerase. The core components of this RNP complex in human cells are the catalytic subunit hTERT and the RNA component hTR or hTERC, which have been shown to be sufficient for telomerase activity *in vitro* (Weinrich et al., 1997; Masutomi et al., 2000). The hTERT protein belongs to the family of reverse transcriptases and contains four main protein domains: a reverse transcriptase (RT) domain, a telomerase essential N-terminal (TEN) domain, telomerase RNA binding (TRBD) domain and a C-terminal extension (CTE) domain (Figure 1.2) (Nguyen et al., 2018). The RT domain of hTERT is known to be conserved across different species (Nakamura et al., 1997). Binding of TERT to TR is known to be mediated by the TRBD domain, which binds to the CR4/CR5 domain of TR (Lai, Mitchell and Collins, 2001). Other studies showed that the TRBD, RT and CTE domains form a ring-shaped structure (TERT ring) which is central to the catalytic activity of TERT (Gillis, Schuller and Skordalakes, 2008; Mitchell et al., 2010; Robart and Collins, 2011). Previously, it has been shown that a small region in the TEN domain called the N-terminal Dissociates Activity of Telomerase (N-DAT) domain/region was implicated in trafficking of telomerase to telomeres (Armbruster et al., 2001, 2004). More recent studies have shown that N-DAT is part of a region in telomerase necessary for its binding to the TPP1-POT1 heterodimer, thereby providing the recruitment of telomerase to telomeres (Schmidt, Dalby and Cech, 2014; Sexton et al., 2014). hTR is a 451 base long non-polyadenylated RNA, which is transcribed by the RNA polymerase II from the telomerase RNA gene called TERC located at chromosome 3q26.2, and belongs to a family of H/ACA RNA (Figure 1.3) (Feng et al., 1995; Mitchell, Cheng and Collins, 1999). The 3'-terminus of hTR contains an H/ACA motif which is prevalent in small nucleolar RNAs (sno-RNAs) and small Cajal body RNAs (Sca-RNAs) (Fu and Collins, 2003; Jády,

Bertrand and Kiss, 2004). During the hTR maturation process, the H/ACA motif is bound by the H/ACA pre-RNP complex, which consists of Dyskerin, NOP10, NHP2 and NAF1. This H/ACA motif is required for *in-vivo* accumulation and telomerase biogenesis (Mitchell, Cheng and Collins, 1999). The maturation of hTR occurs at nucleolus and is characterised by the substitution of NAF1 with GAR1 (Darzacq et al., 2006). hTERT is then bound to the pre-RNP complex to form a mature telomerase holoenzyme. The binding of hTERT to hTR is thought to be required for telomerase localisation to Cajal bodies (Tomlinson et al., 2008). A Cryo-EM structure of the human telomerase holoenzyme has been reported recently. It revealed a bi-lobal structure showing hTERT bound to one lobe and the telomerase accessory proteins at the other lobe (Nguyen et al., 2018) (Figure 1.4).

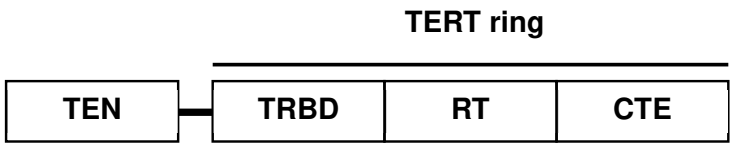

Figure 1.2 Domains of the hTERT protein
TEN domain at the N-terminus of hTERT is required for localisation of telomerase to telomeres. The TERT ring which encompasses the TRBD, RT and CTE domains is required for the catalytic activity of hTERT.

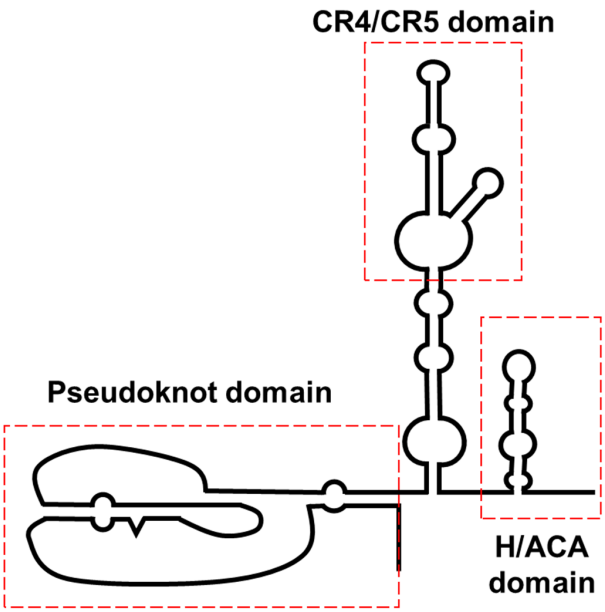

Figure 1.3 Domains of the hTR RNA

hTR can be sub-divided into three separate domains. The pseudoknot/template is the region containing the telomeric template 3'-CAAUCCCAAUC and is bound by hTERT, with its catalytic domain specifically located at the template. The CR4/CR5 also partially binds to the TRBD and CTE domains of hTERT. The H/ACA domain is bound by the telomerase accessory proteins.

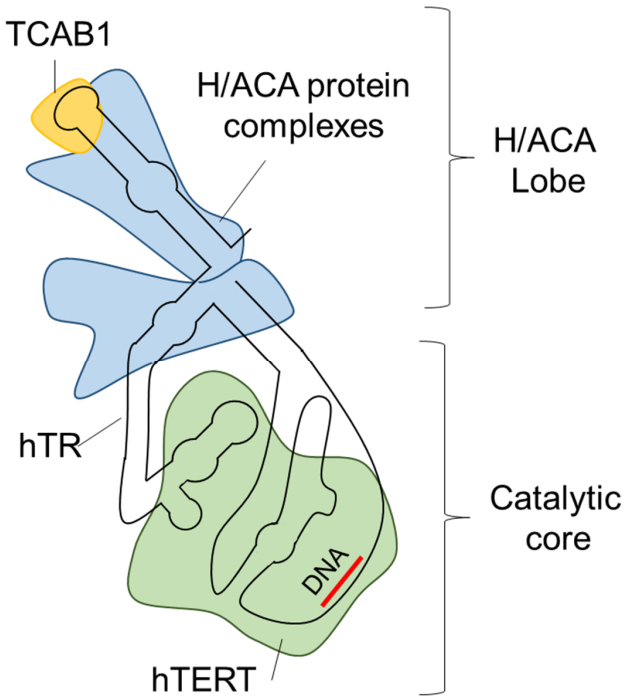

Figure 1.4 Structure of the human telomerase holoenzyme
The mature telomerase holoenzyme forms a bi-lobal structure. One lobe is called the catalytic core and consists of hTERT and the hTR telomeric substrate (shown in green). The other lobe is called the H/ACA lobe (blue and yellow), which consists of two complexes of H/ACA proteins: Dyskerin, NOP10, NHP2, GAR1 and 1 single TCAB1 binding to the CAB box. (Adapted from Nguyen et al., 2018)

1.1.4 Transcription regulation of hTERT

The human TERT gene is located at chromosome 5 (Genomic coordinate: 5p15.33), contains 16 exons and 15 introns which spans 40 kb in length (Cong, Wen and Bacchetti, 1999; Takakura et al., 1999; Wick, Zubov and Hagen, 1999; Bryce et al., 2000; Leem et al., 2002). The transcription regulatory region of *TERT* contains a single promoter which extends from 330 bp upstream of the translation start site (ATG) to 228 bp downstream of it and is characterised by high GC content, absence of TATA and CAAT boxes and presence of

multiple transcription response elements such as E-box and GC-box (Cong, Wen and Bacchetti, 1999; Horikawa et al., 1999; Takakura et al., 1999; Wick, Zubov and Hagen, 1999). Removal of E-boxes and E2F consensus motif in did not significantly affect *TERT* transcription suggesting that transcription factors that bind to these transcriptional response elements are either not required for *TERT* transcription in these cells or suggest a possible functional redundancy with other transcription factors (Cheng et al., 2017). Transcription factors can activate or repress transcription of a gene. c-Myc, HIF-1, NF-κB and β-catenin are a few of the transcription factors found to bind to the *TERT* promoter and activate transcription (Wu et al., 1999; Yatabe et al., 2004; Gizard et al., 2011; Hoffmeyer et al., 2012). On the other hand, WT1, Sp3 and CTCF were found to be repressors of *TERT* transcription (Oh et al., 1999; Wooten and Ogretmen, 2005; Renaud et al., 2007). *TERT* promoter mutations at position -146 (C228T) and -124 (C250T) have been reported in various cancers and were shown to form *de novo* binding sites for activator transcription factors ETS and GABPA respectively (Horn et al., 2013; Huang et al., 2013; Vinagre et al., 2013; Li et al., 2015; Stern et al., 2015). These mutations are implicated in de-repression of *TERT* in the majority of cancers which express telomerase (Huang et al., 2015). However, there are a subset of cancers such as Prostate cancer and Non-Hodgkin Lymphoma which express telomerase in the absence of these promoter mutations (Stoehr et al., 2015; Lam et al., 2016), indicating an alternative *TERT* regulatory mechanism, proposed to be epigenetic in nature. The *TERT* promoter is located in a CpG island (-1800 to +2200 of ATG), which imply that DNA methylation may play a role in epigenetic regulation of *TERT* transcription (Cong, Wen and Bacchetti, 1999). Methylation at CpG island promoters is generally thought to confer gene silencing (Aimee and Bird, 2011). Interestingly, a 433 bp region upstream of the transcription start site of the *TERT* promoter (–140 to –572, relative to the transcription start site) was discovered to be heavily methylated in cancer cells that express telomerase (Guilleret et al., 2002; Zinn et al., 2007; Castelo-Branco et al., 2013; Lee et al., 2019). This region is called *TERT* Hypermethylated Oncological Region (THOR) and molecular manipulations to

demethylate CpGs in this region significantly downregulate *TERT* expression (Lee et al., 2019).

1.1.5 Telomere length maintenance by telomerase

The catalytic core hTERT and the RNA component hTR are sufficient for telomerase activity *in vitro* (Weinrich et al., 1997; Masutomi et al., 2000). However, telomere elongation *in vivo* (cells) is a more complex process involving several telomerase accessory proteins which are involved in telomerase maturation and recruitment to telomeres. It is known that the action of telomerase at telomeres is restricted to the S-phase (Zhu et al., 1996; Jády et al., 2006; Tomlinson et al., 2006). This was thought to be due to the coupling of telomerase action to the conventional DNA replication. A study in yeast showed that telomeres are elongated by telomerase at the end of the S-phase (Marcand et al., 2000) and that replication fork passage through a telomere is required for this telomere being subjected to telomerase-dependent lengthening (Dionne and Wellinger, 1998). In human cancer cells and fibroblasts, telomere extension by telomerase occurs throughout the S-phase (Zhao et al., 2009; Chow et al., 2012). This is in agreement with the idea that telomerase-dependent telomere lengthening is coupled with the DNA replication, as telomeres are replicated throughout the S-phase in human cells (Arnoult et al., 2010). Interestingly, the C-strand fill-in process and the subsequent processing of the telomere occur late in the S-phase, subsequent to DNA replication (Zhao et al., 2009; Chow et al., 2012). It is known that the recruitment of telomerase to telomeres requires the action of the TPP1-POT1 heterodimer (Xin et al., 2007; Abreu et al., 2010). The Tel patch of the OB-fold domain of TPP1 is required for the binding to the TEN domain of hTERT (Nandakumar et al., 2012; Zhong et al., 2012). Furthermore, it has been reported that TPP1 undergoes an S-phase specific phosphorylation, which may indicate a potential telomerase restriction mechanism limiting it to the S-phase (Zhang et al., 2013). The action of telomerase at telomeres have been suggested to require its localisation to Cajal bodies (Jády et al., 2006). It is known that this requires TCAB1 and that TCAB1 is known to bind to the CAB

box of hTR at the G1/S boundary (Vogan and Collins, 2015). Therefore, both of these mechanisms might be important for the S-phase restrictions of the telomerase action at telomeres in human cells.

1.1.6 Role of TERRA in telomere length regulation

Telomeres contain repetitive sequences which are abundant in the heterochromatic histone mark H3K9me3, HP1 proteins and DNA methylation and therefore believed to be transcriptionally inert (Gonzalo et al., 2006; Benetti, García-Cao and Blasco, 2007). This is supported by studies where reporter genes inserted at sub-telomeric regions resulted in these genes to be repressed or silenced (Baur et al., 2001; Koering et al., 2002). However, later studies have shown that transcription occurs at telomeres which resulted in the production of long non-coding RNAs called Telomeric Repeat containing RNA (TERRA) (Azzalin et al., 2007; Schoeftner and Blasco, 2008). TERRA contains UUAGGG repeats at its 3'-end and is transcribed mainly by RNA Pol II, although it may also be transcribed by RNA Pol I/RNA Pol III in mammals (Luke et al., 2008; Schoeftner and Blasco, 2008; Déjardin and Kingston, 2009). TERRA is transcribed from two cryptic transcription start site (TSS) located around 100 bp and 1 kb into the subtelomeric region (Nergadze et al., 2009; Porro et al., 2014). The presence of two different TSS for TERRA may partially account for its variable length, which range in length from 100 – 9000 bp (Azzalin et al., 2007). Furthermore, location of TERRA transcription termination sites at telomeres is not known and may also explain this variable length feature. Abundance of TERRA at telomeres have been shown to be regulated by the Nonsense mediated decay (NMD) machinery (Azzalin et al., 2007). TERRA localisation studies showed that TERRA forms foci at telomeres which suggests that TERRA may play a role in telomere maintenance (Cusanelli, Romero and Chartrand, 2013).

As previously mentioned, telomeres shorten through each replication cycle and that telomere shortening can be counteracted by the telomere elongating enzyme telomerase. TERRA have been implicated in the negative regulation

of telomerase via direct complementary binding to telomerase RNA and may also inhibit telomerase catalytic subunit directly, as shown by experiments using TERRA-mimetic oligonucleotides and co-immunoprecipitation respectively (Schoeftner and Blasco, 2008; Redon, Reichenbach and Lingner, 2010). Contrastingly, TERRA does not seem to inhibit telomere elongation when overexpressed in a telomerase positive cancer cell line (Farnung et al., 2012). In the same study, knockout of DNMT1 and DNMT3B DNA methyltransferase was able to increase TERRA production but unable to inhibit telomerase activity and prevent telomere elongation (Farnung et al., 2012). It is known that methylation status in the subtelomeric region can influence TERRA transcription (Deng et al., 2009; Nergadze et al., 2009; Ng et al., 2009). Furthermore, telomerase reactivated in iPS cells derived from fibroblasts of patients with Immunodeficiency, Centromeric region stability, and Facial anomalies (ICF) syndrome which overexpress TERRA due to a loss of function DNMT3B mutation, was not inhibited and exhibit telomere elongation (Sagie et al., 2014). Therefore, these data suggest that TERRA is insufficient to act as an inhibitor of telomerase activity. In spite of this, it is still possible that TERRA may act on telomerase at specific time in the cell cycle. Expression of TERRA is known to be cell cycle dependent and is higher in G1 and G2-phase compared to S-phase of the cell cycle (Porro et al., 2010). This coincides with telomerase activity at telomeres which is known to be restricted to S-phase. Together with its direct association with telomerase, TERRA may play a role as a negative regulator of telomerase at specific times in the cell cycle and needs to be investigated further.

TERRA have also been shown to directly bind with telomeric repeats and form RNA:DNA hybrids or R-loops at telomeres (Luke et al., 2008; Xu, Kimura and Komiyama, 2008). Formation of RNA:DNA hybrid structure at telomeres may prevent telomerase access to telomeres. A study in the budding yeast *Saccharomyces cerevisiae* showed that TERRA can be degraded by the Rat1p 5’ – 3’ exonuclease which in turn promotes elongation of telomeres by telomerase (Luke et al., 2008). In the same study, a loss of function mutation

on Rat1p resulted in accumulation of TERRA at telomeres, formation of RNA:DNA hybrids and telomere shortening. This indicates that telomeric RNA:DNA hybrids may inhibit telomerase access to telomeres. Moreover, telomerase negative *S. cerevisiae* with short telomeres showed accumulation of R-loops at telomeres which promotes HR-based telomere elongation (Fallet et al., 2014; Yu, Kao and Lin, 2014). Whether this feature exist in human cells is not known, as homologous recombination is generally suppressed at telomeres of normal human cells (Wang, Smogorzewska and De Lange, 2004). Furthermore, RNA:DNA hybrid or R-loops formation can result in replication fork stalling, DSBs and loss of DNA sequence (Tuduri et al., 2009; Gan et al., 2011). As telomeres are difficult to replicate regions, presence of R-loops may increase replication fork stalling and collapse at telomeres which can lead to DSBs and telomere loss. Studies in fibroblasts derived from ICF patients showed increased formation of R-loops compared to fibroblasts from healthy control, which is attributed to increased TERRA expression as a result of DNMT3B deregulation and DNA hypomethylation at subtelomeric regions (Yehezkel et al., 2008; Sagie et al., 2017). Furthermore, this increased R-loops significantly correlates with short telomeres in ICF patient cells compared to control (Yehezkel et al., 2008). Therefore, these data suggest that formation of telomeric R-loops by TERRA, promote telomere shortening possibly via telomerase access inhibition and stochastic telomere loss due to telomeric replication fork collapse.

Although in general, TERRA is considered to be a negative regulator of telomerase and telomere length in the presence of telomerase, there are evidence in budding yeast which suggest the opposite. In *S. cerevisiae*, there is evidence that telomere shortening promote expression of TERRA (Cusanelli, Romero and Chartrand, 2013). Furthermore, TERRA was shown to colocalize with budding yeast telomerase RNA TLC1 and was suggested to act as a scaffold for the formation of telomerase recruitment clusters (T-recs), which recruit telomerase to the short telomere at early S-phase, from which TERRA was transcribed from (Gallardo et al., 2011; Cusanelli, Romero and

Chartrand, 2013). It is known that in budding yeast, there is a preference for telomerase to elongate the shortest telomere, which occur late in S-phase (Teixeira et al., 2004). This telomere elongation coincides with a reduction in TERRA molecules localisation at telomeres late in S-phase (Gallardo et al., 2011). In conclusion, these data suggest that in budding yeast, TERRA may act as a positive regulator of telomerase and may also suggest that TERRA have species specific telomeric functions.

1.1.7 Telomeropathies

Telomeropathies are genetic disorders of premature aging which is associated with abnormally short telomeres and/or telomere dysfunction (Armanios and Blackburn, 2012; Holohan, Wright and Shay, 2014). It is primarily caused by mutations in protein components of telomerase, shelterin and telomere maintenance pathway, which causes misregulation of the telomere maintenance mechanism and subsequently accelerated telomere shortening (Holohan, Wright and Shay, 2014). One of the earliest telomeropathy discovered was Dyskeratosis congenita (DKC), which was characterised by multiple phenotypes such as nail dystrophy, skin hyperpigmentation and oral leukoplakia, commonly called the “diagnostic triad” for DKC (Heiss et al., 1998; Mitchell, Cheng and Collins, 1999). DKC was initially found to be caused by mutations in the *DKC1* gene which encodes for Dyskerin, an H/ACA SnoRNP which binds to the H/ACA motif of hTR and is important for hTR processing and maturation (Mitchell, Cheng and Collins, 1999; Ballarino et al., 2005; Tseng et al., 2018; MacNeil, Lambert-Lanteigne and Autexier, 2019). Further studies showed that manifestations of DKC is very heterogenous, includes other symptoms not part of the diagnostic triad such as bone marrow failure, and have phenotype overlaps with other telomeropathies such as Hoyeraal-Hreidersson syndrome (HHS), Revesz syndrome and Coats plus syndrome (Tsangaris et al., 2008; Dokal, 2011; Young, 2012).

Mutation in *TINF2* gene which codes for the shelterin component TIN2 have been shown to be associated with HHS and Revesz syndrome (Savage et al.,

2008; Sasa et al., 2012; Vulliamy et al., 2012). Both HHS and Revesz syndrome have similar symptoms to DKC but with a more severe manifestation which includes prenatal growth retardation and cerebellar hypoplasia (Aalfs et al., 1995). Exudative retinopathy is a symptom which is observed only in Revesz syndrome and distinguishes it from HHS (Kajtar and Mehes, 1994). Symptoms of HHS have also been discovered in patients with mutations in *RTEL1* gene, which encodes for the helicase RTEL1, important for DNA replication through G4 structure rich telomeres and T-loop disassembly (Vannier et al., 2012, 2013; LeGuen et al., 2013). Furthermore, Mutation on TPP1 TEL-patch, which play a role in telomerase recruitment to telomere, have also been associated with HHS (Nandakumar et al., 2012; Kocak et al., 2014). Mutations in CTC1 gene, which encodes for CTC1, a member of the CST complex which play a role in telomere replication and end processing, have also been found in Patients with Coats plus syndrome (Anderson et al., 2012; Polvi et al., 2012; Walne et al., 2013). Mutations in hTR or hTERT can cause one of the following symptoms such as idiopathic pulmonary fibrosis, aplastic anemia and liver cirrhosis, particularly in adult patients (Fogarty et al., 2003; Armanios et al., 2007; Tsakiri et al., 2007). Other telomeropathy-associated mutations have also been found in NOP10, NHP2, TCAB1 and POT1 (Walne et al., 2007; Vulliamy et al., 2008; Zhong et al., 2011; Takai et al., 2016). Although telomeropathies have a very wide range of symptoms, many seems to overlap between distinct telomere disorders. Furthermore, compromised telomere maintenance seems to be the common fundamental mechanism between distinct telomere disorders. Thus, telomeropathies are currently considered to be a single spectrum of disorder caused by mutations in telomere maintenance associated genes, which manifests as cellular proliferation defect in various tissues (Dokal, 2011; Armanios and Blackburn, 2012; Holohan, Wright and Shay, 2014).

1.2 Cellular Senescence

1.2.1 Types of cellular senescence

In 1961, Hayflick and Moorhead described the finite proliferation capabilities of human fibroblasts in culture, which resulted in the onset of cellular senescence (Hayflick and Moorhead, 1961; Hayflick, 1965). The later studies in human fibroblasts have shown that cellular senescence is associated with telomere shortening and the telomeres have been proposed to act as a biological clock for cellular ageing (Harley, Futcher and Greider, 1990; Vaziri et al., 1994). However, other studies revealed that senescence can also be activated by other type of stress-inducing agents such as oncogene activation, reactive oxygen species (ROS) and DNA damaging agents (Reviewed in (Kuilman et al., 2010)). Therefore, cellular senescence was later classified into replicative senescence (RS) and premature senescence (PS), which were associated with telomere shortening and cell dysfunction/cellular ageing and cellular stress response, respectively. RS is activated by critically short telomeres, caused by the failure of the semi-conservative DNA replication machinery to replicate extreme ends of linear DNA, leading to DNA attrition every DNA replication cycle. Although the earlier discoveries suggest that short telomeres correlate with the onset of cellular senescence, it is not clearly understood how these short telomeres activate the senescence program. It has been proposed that short telomeres may have lost its T-loop conformation, presumably via loss of the 3' overhang, which in turn activates the DDR signalling required for the senescence program (Li et al., 2003; Stewart et al., 2003). However, in another report which uses a new overhang protection assay (Chai, Shay and Wright, 2005) in comparison to the telomere oligonucleotide ligation assay (T-OLA) used in previous reports (Cimino-Reale et al., 2001), showed that the size of the telomeric 3'-overhangs in senescent cells were similar to those in proliferating cells and the cells that bypassed the senescence via the expression of the HPV E6 and E7 oncoproteins, necessitating a re-think to this theory (Chai, Shay and Wright, 2005). Furthermore, the unfolding of the T-loop does not completely explain why the telomeres in senescent cells do not exhibit end-to-end fusions as observed in the cells undergoing crisis. It has

been suggested that the components of the shelterin complex, in particular TRF2, might still be bound to these short telomeres: this could be sufficient to prevent any end-to-end fusion (Reviewed in (Cesare and Karlseder, 2012)). TRF2 is known to be important for the formation of the T-loop (Doksani et al., 2013). A depletion of TRF2 is suggested to be the trigger of T-loop unfolding in senescent cells and this was supported by a study using a dominant negative TRF2 in mouse and human fibroblasts, which sequestrate TRF2 from binding to telomeres and activates a DDR response with similar characteristics to RS (Smogorzewska and de Lange, 2002). Therefore, although short telomeres are associated with RS, the RS might be activated by a state of a telomere in which the t-loop is unfolded resulting in an open telomere conformation, in the presence of limited amount of TRF2, rather than by telomere length *per se*.

On the other hand, as mentioned above PS could be triggered by various cellular stressors such as ROS and activation of oncogenes. Although RS and PS differ in the type of stimuli that activate them, there are some commonalities in terms of the maintenance of the senescence program and the biomarkers in both types of senescence (Figure 1.5). PS triggered by ROS have been implicated in accelerated shortening of telomeres (Richter and Zglinicki, 2007). Both RS and PS have been shown to require irreparable DNA damage which triggers a prolonged activation of the DDR (d'Adda di Fagagna et al., 2003; Fumagalli et al., 2012; Suram et al., 2012; Fumagalli et al., 2014). Interestingly, continuous DDR activation exists at telomeres in both types of senescence (Fumagalli et al., 2012; Suram et al., 2012). This suggests that DNA damage that occur at telomeres is maintained and required for the activation and maintenance of senescence (Fumagalli et al., 2014). Indeed, the presence of TRF2-RAP1 and POT1 at telomeres have been shown to prevent NHEJ and HDR respectively at telomeres, at least in human cells (Van Steensel, Smogorzewska and De Lange, 1998; Bae and Baumann, 2007; Denchi and de Lange, 2007; Palm et al., 2009; Sfeir and De Lange, 2012). Studying senescence reversal would possibly improve our understanding whether

damage at telomeres is required to maintain the senescence program or acts solely as the program trigger.

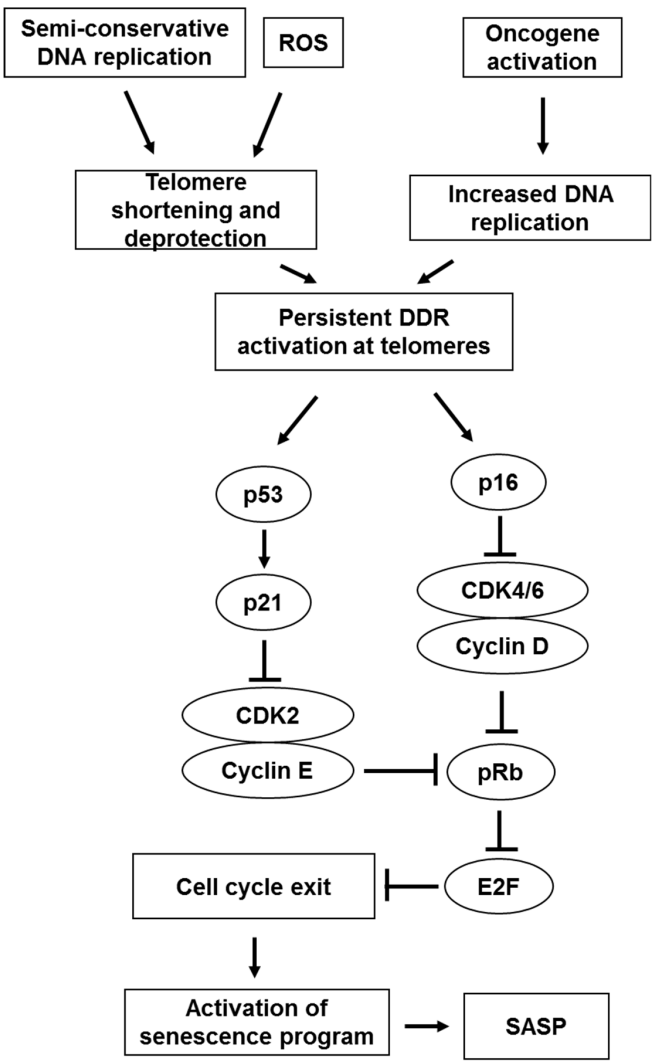

Figure 1.5 The senescence signalling pathway

Diagram showing pathways activating and maintaining senescence. The main pathways of senescence can be generally divided into the p53-p21 and p16-pRb pathways. It is also possible that these two pathways converge at pRb which inhibits entry into S-phase by inhibiting E2F at the G1/S boundary.

1.2.2 Stress-induced premature senescence and the role for telomeres

As previously mentioned, acute form of senescence not associated with chronological age of cells or telomere shortening is called premature senescence, which is triggered by various types of stressors. It can be activated in cells at early population doublings *in vitro*, hence the word premature (Brack et al., 2000). Premature senescence can be classified further into OIS which is triggered by the activation of oncogenes and stress induced premature senescence (SIPS), which is triggered by a diverse cell stress signals (Serrano et al., 1997; Brack et al., 2000). In general, depending on the level of cellular damage caused, cells can respond to cellular stress by either repairing the damage, commit to death via necrosis or apoptosis pathways or undergo senescence. It is now generally accepted that SIPS occur when cell stress is insufficient to induce cell death (sublethal), but sufficient to cause irreparable damage to the cell (Dumont et al., 2000; Toussaint, Medrano and Von Zglinicki, 2000). Fibroblasts undergoing SIPS exhibit similar features to RS cells such as a large and flattened morphology, increased SA-β-Galactosidase activity and upregulation of p16 (Toussaint, Medrano and Von Zglinicki, 2000). There is a great number of oxidative and DNA damaging cellular stressors that have been discovered in *in vitro* cell culture studies which can trigger SIPS such as hyperoxia, UVB, H_2O_2, tert-Butyl hydroperoxide (t-BHP), ionising radiation and antineoplastic agents (Bleomycin, Doxorubicin and Mitomycin C)(Rodemann, 1989; von Zglinicki et al., 1995; Von Zglinicki, Pilger and Sitte, 2000; Dumont et al., 2000; Chainiaux et al., 2002; Liu and Hornsby, 2007; Rodier et al., 2009; Bielak-Zmijewska et al., 2014). However, there are discrepancies surrounding the role of telomeres in SIPS.

Although SIPS, unlike RS, is thought to be independent of telomere length, studies on human fibroblasts undergoing hyperoxia (40% oxygen partial pressure) showed accelerated telomere shortening, due to oxidative DNA damage and formation of single strand breaks at telomeres (von Zglinicki et

al., 1995; Von Zglinicki, Pilger and Sitte, 2000). On the other hand, other oxidative damage inducer such as H_2O_2 showed contradicting result, where it showed significant accelerated telomere shortening in MRC-5 (Von Zglinicki, Pilger and Sitte, 2000) and 2BS (Duan et al., 2005) cells but not in IMR90 cells (Chen et al., 2001). Intriguingly, although accelerated telomere shortening was observed in WI-38 (von Zglinicki et al., 1995) and MRC-5 (Von Zglinicki, Pilger and Sitte, 2000) cells cultured under hyperoxic conditions, it was not the case with BJ (Lorenz et al., 2001) cells cultured under the similar conditions. Therefore, it is possible that there are cell specific differences which affect how these different SIPS-inducers stimulate telomere shortening. It is proposed that this may be due to the distinct antioxidative defence capacity of each cell type (Von Zglinicki, 2002). Furthermore, the dose (high vs low) and protocol (acute vs chronic) used to induce SIPS may also play a role in accelerated telomere shortening, as it may account for the difference in stress levels and possibly activate SIPS in a dose-dependent manner (Duan et al., 2005). The H_2O_2-induced SIPS study in IMR90 cells (Chen et al., 2001) utilised a more acute and higher dose protocol compared to a similar study in 2BS cells (Duan et al., 2005), which instead used a more chronic and lower dose protocol. An acute and high dose protocol may result in a faster growth arrest, which may prevent observation requiring cellular proliferation such as telomere shortening. Hence, aside from cell type specific antioxidative defence capacity, this difference between low and high stress induction may discriminate between telomere shortening dependent and independent SIPS, respectively. Interestingly, a more recent study showed that induction of SIPS by X-ray ionising radiation resulted in irreparable DNA damage and persistent DDR activation at telomeres in MRC-5 fibroblasts and MEFs regardless of telomerase expression, leading to telomere dysfunction and senescence, suggesting a different role for telomeres in SIPS (Hewitt et al., 2012). This persistent DDR activation at telomeres was also observed in oncogenic Ras-induced OIS in human BJ fibroblasts, irrespective of the presence of telomerase expression (Suram et al., 2012). It is possible that acute higher level of sublethal stress induced double strand breaks at telomeres rather than

single strand breaks as observed in chronic low-level stress. Thus, in chronic low stress SIPS, telomere shortening may play a role in its activation, while telomere dysfunction, but not telomere shortening is more important in acute high stress SIPS.

1.2.3 Cellular and molecular markers that define senescence

There are various morphological and molecular markers that could differentiate senescence from other cell cycle exit phenomena, such as quiescence and terminal differentiation. However, the variability of senescence stimuli and cellular responses in different types of cells have resulted in a lack of a universal cellular and molecular marker that could define senescence. Compared to its proliferating counterpart, a senescent cell exhibits a flattened, enlarged, vacuolated morphology and commonly shows multiple nuclei (Bowman, Meek and Daniel, 1975; Angello et al., 1987; Chen and Ames, 1994; Serrano et al., 1997; Denoyelle et al., 2006). Although not necessarily specific to senescent cells, the molecular markers for cell proliferation, such as Ki-67 expression and thymidine analogue (BrdU/EdU) incorporation, are also frequently used to characterise senescent cells. A particular staining method that could be considered as a gold standard for detecting almost all types of senescent cell, regardless of the activating stimuli, is the senescence-associated β-galactosidase staining/assay (SA-β-gal) (Dimri et al., 1995). Senescent cells are known to express high levels of lysosomal β-galactosidase, hence, specific staining of senescent cells could be achieved using X-gal as a chromogenic substrate for β-galactosidase at the sub-optimal detection pH of 6.0 (Lee et al., 2006). In contrast, the level of β-galactosidase enzyme activity in non-senescent cells is undetectable at this pH. Upregulation of the proteins involved in the molecular pathways associated with the activation and maintenance of the cell cycle arrest in senescence, such as p53, p16 and p21, have also been detected in multiple cell types during senescence (Serrano et al., 1997; Stein et al., 1999; Beauséjour et al., 2003). In addition, DDR foci formation, particularly at telomeres, which are associated with senescence have been previously detected utilising antibodies against γh2ax

or 53BP1 (d'Adda di Fagagna et al., 2003; Sedelnikova et al., 2004; Fumagalli et al., 2014). The downregulation of Lamin B1 have been implicated in IR-induced and oncogenic RAS-induced senescence (Freund et al., 2012). Telomere length is a marker ubiquitously employed in many replicative senescence studies. However, caution is required as sub-optimal culture conditions have been shown to induce senescence irrespective of telomere length (Ramirez et al., 2001). Formation of densely heterochromatic regions which could be detected via staining with a dsDNA-specific stain such as DAPI and an antibody to H3K9me3 and called senescence-associated heterochromatic foci (SAHF) have also been observed in senescent cells (Narita et al., 2003; Kosar et al., 2011). SAHF formation is thought to mediate gene silencing of proliferation genes via upregulation of H3K9me3 and HP1 (Narita et al., 2003). However, the use of SAHF is very limited as only specific senescence stimuli and type of cells, exhibit this feature (Kosar et al., 2011). Most importantly, senescent cells are known to secrete various cytokines, chemokines, growth factors and other factors highly associated with inflammation and cancer which is a phenomenon called Senescence-associated Secretory Phenotype (SASP) (Coppé et al., 2008).

1.2.4 Nuclear changes in senescence

During interphase of the cell cycle, chromatins are observed as loose bundles with a non-random and distinct separation between chromosomes called chromosomal territories (Cremer et al., 1982). High throughput whole genome conformation capture (Hi-C) studies have confirmed the idea of chromosome territories, in which intra-chromatin interactions tend to be stronger than inter-chromatin interactions, which the latter is also confirmed to be non-random (van Berkum et al., 2010; Sarnataro et al., 2017). It is thought that locality of a chromosome or chromosome neighbourhood may affect expression genes in that particular chromosome (Zhao et al., 2009). Furthermore, in normal cells, interphase chromatin are organised into specific compartments, in such a way that transcriptionally repressed heterochromatins are mostly associated with the nuclear lamina and nucleolus which are called Lamin-associated domains

(LADs) and Nucleolus-associated domains (NADs) respectively, while euchromatins fill the 3D space between these domains (Guelen et al., 2008; Németh et al., 2010). LADs have been shown to be a gene-poor region and largely transcriptionally silent (Guelen et al., 2008). Artificial tethering of transcriptionally active genes to the nuclear lamina have been shown to result in transcriptional downregulation, suggesting that the nuclear lamina is a transcriptionally repressive compartment (Finlan et al., 2008; Reddy et al., 2008). Together, it is clear that nuclear architecture can affect gene expression in a more global manner. Multiple studies have shown that senescent cells undergo various alterations to its nuclear architecture and morphology in the form of nuclear lamina depletion and deformation, senescence-associated heterochromatin foci (SAHF), and senescence associated distension of satellites (SADS), and these alterations may contribute to regulation of gene expression in senescent cells (Narita et al., 2003; Raz et al., 2008; Shimi et al., 2008; Swanson et al., 2013).

The nuclear lamina is located at the surface of the inner nuclear membrane and consists of A-type lamins (lamin A and C), B-type lamins (lamin B1 and B2) and lamin associated proteins (Gruenbaum and Foisner, 2015). The nuclear lamina provides mechanical support for the nuclear envelope and is known to be involved in chromatin organisation, DNA replication and cell division (Ottaviano and Gerace, 1985; Lammerding et al., 2004; Guelen et al., 2008; Shimi et al., 2008; Shumaker et al., 2008). As previously mentioned, the nuclear lamina interacts with heterochromatic regions of chromosomes called LADs. Downregulation of the components of the nuclear lamina, LMNA and Lamin B1 have been observed in cells undergoing RS or OIS (Shimi et al., 2011; Freund et al., 2012; Dou et al., 2015; Lenain et al., 2015). Furthermore, Ras oncogene activation was shown to trigger autophagy-mediated degradation of Lamin B1 via its binding with LC3 to induce nuclear export to cytoplasm for lysosomal protein degradation (Dou et al., 2015; Lenain et al., 2015). Induction of gene silencing to LMNB1 resulted in premature senescence and formation of Lamin A/C blebs characteristic of senescent and

progeroid cells (Goldman et al., 2004; Shimi et al., 2008, 2011; Shah et al., 2013; Adams et al., 2013). Furthermore, p53-induced Lamin A/C stabilisation have recently been shown to be the link between p53 and p16 induction during activation of cellular senescence through Lamin A/C mediated degradation of BMI-1 and MEL-18 (Yoon et al., 2019). Loss of Lamin B1 from the nuclear lamina was further showed to be responsible for the formation of SAHF, as it detaches heterochromatic LADs from the nuclear lamina (Sadaie et al., 2013). Lastly, Lamin B1 depletion significantly correlates with pericentromeric satellite DNA distention, suggesting for a role for Lamin B1 in SADS formation (Swanson et al., 2013).

As previously mentioned, certain senescent cells exhibit SAHF, a highly compacted chromatin domain observable by DAPI staining and is enriched in H3K27me3 and H3K9me3 marks, which are histone tail marks associated with facultative and constitutive heterochromatin respectively (Narita et al., 2003; Kosar et al., 2011; Chandra et al., 2012). It was one of the earliest known higher-order chromatin changes observed in senescent cells and is thought to mediate silencing of proliferation genes such as E2F target genes in a p16-pRb pathway-dependent manner, in order to enforce the permanent growth arrest of senescence (Narita et al., 2003). HP1, High mobility group A proteins (HMGA1 and HMGA2) and macroH2A histones are also known to be part of the SAHF structure (Zhang et al., 2005; Narita et al., 2006). Each SAHF focus is formed from a single chromosome, driven by the histone chaperones Histone Repressor A (HIRA) and Anti-silencing Function 1a (ASF1a) (Zhang et al., 2005; Ye et al., 2007; Zhang, Chen and Adams, 2007). Activity from both p53 and pRb senescence pathways are also required for SAHF formation, in parallel to HIRA and ASF1a (Narita et al., 2003; Zhang et al., 2005; Ye et al., 2007; Zhang, Chen and Adams, 2007). Later studies showed that the structure of SAHF is structured as H3K27me3-enriched outer layer which encapsulates an H3K9me3-enriched core (Chandra and Narita, 2013). SAHF have also been shown to be derived from LADs that have underwent spatial reorganisation, due to loss of heterochromatin attachment to the nuclear

lamina triggered by depletion of Lamin B1, a component of the nuclear lamina during senescence (Shimi et al., 2011; Freund et al., 2012; Sadaie et al., 2013). Hi-C analysis of OIS in WI-38 fibroblasts showed reduced local interactions of topologically associating domains associated with heterochromatin and increased long range interactions which represent the formation of SAHF by spatial clustering of heterochromatins (Chandra et al., 2015). Interestingly, formation of SAHF is consistently observed in OIS but not in RS or other SIPS in multiple fibroblastic cell lines (Narita et al., 2003; Di Micco et al., 2011). Furthermore, SAHF formation is cell type specific suggesting that SAHF may not be a universal feature of senescence (Kosar et al., 2011).

It is known that large arrays of tandem repeats called satellite DNA, prevalent in centromeres, form the bulk of the heterochromatin (Saksouk, Simboeck and Déjardin, 2015). Centromeric and Pericentromeric satellite DNA are normally constitutively repressed to maintain genomic stability. H3K18 deacetylation by SIRT6 have been shown to be required for satellite DNA transcriptional repression (Tasselli et al., 2016). It has been shown that centromeric and pericentromeric satellite DNA undergo decompaction shown as a distension of these satellites when observed by FISH and also DNA hypomethylation, in cells undergoing RS and OIS, in the absence of changes in heterochromatic marks H3K9me3 and H3K27me3 (Cruickshanks et al., 2013; De Cecco et al., 2013; Swanson et al., 2013; Criscione et al., 2016). This senescence-associated nuclear phenomenon is called senescence associated distension of satellites (SADS) and can be observed by 3D FISH (Swanson et al., 2013). Lamin B1 depletion, a marker of senescence, is proposed to be required for the formation of SADS. Interestingly, SADS was also present in fibroblasts derived from HGPS, suggesting a role for SADS in progeroid syndromes (Swanson et al., 2013). As a relatively recent discovery, it is currently unclear what role SADS play in the maintenance of senescence. It is proposed that SADS is an early event in the global chromatin alteration observed in

senescence and due to its location in the centromeres, it may also play a role in preventing cell division in senescent cells (Swanson et al., 2013).

1.2.5 Senescence in postmitotic cells

Postmitotic cells are cells that have exited the cell cycle and permanently cease cell division such as terminally differentiated cells. Postmitotic terminally differentiated cells are refractory to cellular proliferation stimuli and this was thought to be conferred by the action of pRb (Lipinski and Jacks, 1999). However, although most terminally differentiated cells are postmitotic, in exceptional cases such as during liver injury, terminally differentiated mature hepatocytes cells can re-enter the cell cycle and undergo cellular division for liver regeneration (Bisteau, Caldez and Kaldis, 2014). Senescence is traditionally associated with loss of proliferative capacity and therefore associated with actively cycling cells. Conversely, it is now generally accepted that cellular senescence is a stress response and a driver of organismal aging which hypothetically can affect all cells regardless of whether they are dividing or non-dividing. Most human cells that make up tissues of the human body are postmitotic and therefore it is interesting to observe whether these postmitotic cells can senesce in relation to the chronological age. Recent studies showed that terminally differentiated postmitotic cells, such as neurons, can undergo a senescent-like phenotype in mice, which correlate with old age (Jurk et al., 2012). Classical senescence markers such as persistent DDR activation, Elevated ROS production, SASP-associated IL-6 upregulation, positive SA-β-gal staining and SAHF-associated macroH2A histones accumulation have been observed in neurons from old mice, which was not observed in neurons of young mice (Jurk et al., 2012). As these cells are not cycling, cellular proliferation markers such as Ki-67 expression, PCNA expression and thymidine analogue incorporation are generally ineffective as a biomarker for senescence. Moreover, postmitotic cell senescence have also been shown to involve similar tumour suppressive pathway to cellular senescence in mitotic cells such as the p53-p21 and p16-pRb pathways (Farr et al., 2016; Oubaha et al., 2016; Musi et al., 2018). Several of these classical senescence markers

have also been observed in postmitotic cells of other tissues such as osteocytes, retinal cells, skeletal myofibers and cardiomyocytes, and osteocytes (Farr et al., 2016; Oubaha et al., 2016; Anderson et al., 2019). It is hypothesised that in the presence of debilitating cellular stressors, postmitotic cells may prefer senescence instead of apoptosis in order to maintain structural integrity of tissues (Sapieha and Mallette, 2018). Indeed, attempts at cell cycle re-entry in postmitotic cells have been shown to induce apoptosis instead of proliferation in neurons (Giovanni et al., 1999; Ino and Chiba, 2001). Ironically, senescent postmitotic cells also produce SASP which is implicated in the harmful aspects of senescence such as paracrine senescence and protumourigenic/ proinflammatory microenvironment (Coppé et al., 2008, 2010; Jurk et al., 2012; Oubaha et al., 2016; da Silva et al., 2019). Research into senescence of postmitotic cells is relatively new, therefore, further studies are required to help understand whether senescence in postmitotic cells are beneficial or detrimental for tissue integrity and function.

1.2.6 Mitochondria and senescence

Mitochondria, the cellular respiration organelles, play an essential role in producing chemical energy in the form of ATP for the cell and are present in most eukaryotic cells. However, mitochondria also emit hazardous by-products during molecular aerobic metabolism in the form of reactive oxygen species (ROS) (Boveris and Chance, 1973; Loschen et al., 1974; Turrens et al., 1982), which can induce oxidative stress damage to proteins, lipids and both mitochondrial and nuclear DNA (Richter, Park and Ames, 1988; Starke-Reed and Oliver, 1989; Rubbo et al., 1994). *In vitro* culture of mammalian cells is frequently carried out under atmospheric oxygen levels (~21% O_2) and have been shown to result in elevated ROS production and increased oxidative DNA damage (Turrens et al., 1982; Chen et al., 1995; Parrinello et al., 2003; Rai et al., 2009). Moreover, this increased ROS production can induce single strand DNA breaks to telomeric DNA (Petersen, Saretzki and Von Zglinicki, 1998; Von Zglinicki, Pilger and Sitte, 2000). G-rich telomeric DNA is prone to oxidative DNA damage and can also form 8-oxo-7,8-dihydro- 2′-

deoxyguanosine (8-oxodG) lesions (Kawanishi and Oikawa, 2004). ROS-induced single strand break formation at telomeres is difficult to repair which result in loss of telomeric sequence during subsequent DNA replication and is proposed to be the mechanism of ROS-induced accelerated telomere shortening, which increases the propensity for cells to undergo telomere dysfunction and senescence (von Zglinicki et al., 1995; Petersen, Saretzki and Von Zglinicki, 1998; Von Zglinicki, Pilger and Sitte, 2000; Coluzzi et al., 2014).

Thus, inhibiting ROS should theoretically prevent ROS-induced telomere shortening and possibly delay senescence. Indeed, treatment with the mitochondria targeted antioxidant MitoQ prevents accelerated telomere shortening in fibroblasts cultured in 40% oxygen partial pressure (Saretzki, Murphy and von Zglinicki, 2003). Furthermore, treatment of pre-senescent human endothelial cells with N-acetylcysteine antioxidant treatment was shown to decrease ROS formation and delay the onset of senescence (Haendeler et al., 2004). Similarly, uncoupling of mitochondria with 2,4-Dinitrophenol in MRC-5 fibroblasts also decreased telomere shortening rate and improved *in vitro* lifespan of the cells (Passos et al., 2007). Therefore, this reinforces the view that mitochondrial ROS overproduction is a major contributor of cellular senescence. The CDK inhibitor p21 is implicated in senescence-associated cell cycle arrest and overexpression of p21 have been shown to upregulate ROS, suggesting a link between senescence activation and ROS production (Macip et al., 2002). Moreover, chronic activation of p21 was also shown to activate a signalling cascade of GADD45 - p38MAPK - GRB2 - TGFBR2 - TGFβ which induce mitochondrial dysfunction and ROS production, resulting in a vicious cycle of ROS production and induction of persistent DDR activation, in order to maintain senescence in human fibroblasts (Passos et al., 2010). Together, these suggest that mitochondria play an important role in the activation and maintenance of cellular senescence through the production of ROS.

Aside from its role in ROS-dependent cellular senescence, mitochondria are also thought to play a role in SASP production, which the latter is thought to be activated by a persistent DNA damage associated with the activation and maintenance of senescence (Rodier et al., 2009). The transcription factors C/EBPβ and NF-κB have been shown to be involved in upregulation of proinflammatory cytokines IL-6 and IL-8 respectively during SASP (Kuilman et al., 2008; Acosta et al., 2013). In addition, the inflammasome is also implicated in the regulation of C/EBPβ and NF-κB during SASP production via IL-1 signalling upstream of these transcription factors, in a Caspase-1 dependent manner (Acosta et al., 2013). Mitochondria of senescent cells frequently exhibit increased mass, inefficient metabolism and elevated ROS production, suggesting impaired mitochondrial function (Lee et al., 2002; Passos et al., 2007; Moiseeva et al., 2009). In addition, retrograde signalling, a cellular response observed in dysfunctional mitochondria characterised by decreased membrane potential, Ca2+ signalling deregulation, metabolic readjustment, upregulation of antiapoptotic signalling and activation of mitochondrial biogenesis is also observed in senescent human fibroblast (Biswas et al., 1999; Butow and Avadhani, 2004; Passos et al., 2007). Mitochondria ablation in senescent fibroblasts showed reduction in multiple senescence markers including p21, p16 and SASP pro-inflammatory cytokines IL-6 and IL-8, suggesting that mitochondria play a role as a driver of the senescent phenotype (Correia-Melo et al., 2016). In the same study, DDR activation leads to a signalling cascade of ATM-Akt-mTORC1-PGC1β which increase mitochondrial mass. Moreover, inhibition of ATM or mTORC1 with an ATM inhibitor KU55933 or Rapamycin respectively, showed reduction in mitochondrial mass. This suggest that the DDR play a direct role in SASP maintenance via PGC1β-dependent mitochondrial biogenesis.

1.2.7 Irreversibility of senescence

In the 1960s, Leonard Hayflick and Patrick Moorhead discovered that following a certain number of population doublings, human diploid fibroblasts enter a state of cell cycle arrest called phase III growth phase, later termed as cellular

senescence, which can persist for a long time in culture and seems to be refractory to growth factor stimulation present in serum used in cell culture (Hayflick and Moorhead, 1961; Hayflick, 1965). This suggest that cellular senescence is a permanent endpoint to a cell's life cycle and possibly irreversible. It is thought that although p53-p21 pathway plays a role in activation of senescence in human fibroblasts, p16-pRb pathway seems to be the pathway associated with the persistent growth arrest phenotype, in a cell type dependent manner (Beauséjour et al., 2003). Furthermore, nuclear alterations observed in senescence such as SAHF and SADS, have been proposed to play a role in conferring the permanent growth arrest observed in senescent cells, by silencing of E2F gene targets and blocking cell division respectively (Narita et al., 2003; Swanson et al., 2013). However, there are evidence which suggest that reversal or escape from cellular senescence is possible under certain conditions. BJ fibroblasts which express low levels of p16 during senescence showed cellular proliferation following inhibition of p53 (Beauséjour et al., 2003). p53 inhibition was also sufficient to induce proliferation in senescent MEFs which maintains senescence in ARF and p53-dependent manner (Dirac and Bernards, 2003). This suggest that, escape or reversal from senescence is possible in cells where senescence is maintained by p53.

Findings in antineoplastic drug-induced cellular senescence suggest that it is a mechanism in which cancer survive from drug-induced cell death and may be reversed in certain conditions. Expression of senescence associated markers was observed in p16-negative HCT116 colorectal cancer cell line following low dose doxorubicin treatment (Sliwinska et al., 2009). A few cells were found to have escaped senescence growth arrest and exhibit aneuploidy (Sliwinska et al., 2009). However, it is possible that the absence of p16 may have resulted in a p53-dependent senescence maintenance, which was previously shown to be reversible following p53 inhibition (Beauséjour et al., 2003). Upregulation of CDK1 and its downstream target Survivin have also been observed in cells that have escaped ATM/ATR-dependent senescence

of H1299 cells induced with Camptotechin (Roberson et al., 2005; Wang et al., 2011). However, H1299 is a double p53 and p16 negative human lung cancer cell line, suggesting that other conditions may function as a prerequisite for senescence reversal. As previously mentioned, E2F targets required for cellular proliferation, is possibly silenced through heterochromatinization to maintain permanent cell cycle arrest of senescence. A recent report showed that depletion of Suv39h1 histone methyltransferase is sufficient to reverse the growth arrest phenotype of doxorubicin induced senescence in Eμ-Myc mouse cells with conditional Suv39h1 allele (Milanovic et al., 2018). It is also suggested that the constitutive heterochromatin mark H3K9me3 is constantly replenished in senescent cells by Suv39h1 histone methyltransferase to maintain silencing of E2F targets, suggesting a more dynamic nature of senescence (Braig et al., 2005; Milanovic et al., 2018).

Another aspect that confounds the study of the irreversibility of cellular senescence is its heterogenous nature. In a population of cultured cells, there are large differences in lifespan between individual cells, which could possibly be attributed to stochastic culture stress events, in particular oxidative stress (Smith and Whitney, 1980). In a report which studies single cell expression of SASP in IMR90 cells undergoing SIPS by bleomycin treatment, differing SASP expression was observed between cells (Wiley et al., 2017). Furthermore, RS cells have been shown to be more heterogenous in terms of cell to cell gene expression pattern than SIPS cells induced by IR damage (Tang et al., 2019). It is possible that the acute nature of SIPS may account for the observed relatively homogenous gene expression compared to RS cells where the senescence phenotype is developed over a long time in culture. Cellular senescence studies are often carried out using population of cells. This cell to cell variability in senescent phenotype may complicate analysis when trying to look for cellular alterations required for senescence reversal, as there is a possibility that these heterogeneity may reflect a subpopulation of cells which are arrested but not senescent or cells that are not fully senescent or cells are never senescent due to underlying genetic alteration which result in bypass of

senescence. Distinguishing between these technically non-senescent cells in a population of senescent cells would be crucial to specifically determine the genetic and epigenetic regulators which govern senescence.

1.2.8 Role of cellular senescence in organismal ageing

It has been long disputed whether cellular senescence contributes to organismal ageing. It has been previously suggested that cellular senescence is a process that only occurs during *ex-vivo* culturing of mammalian cells and consequently an artefact of cell culture (Rubin, 1997). However, observations in ageing mice and primate tissues showed significant correlation between old age and the build-up of senescent cells in the tissues (Jeyapalan et al., 2007; Lawless et al., 2010; Wang et al., 2009; Krishnamurthy et al., 2004). Furthermore, the importance of the accumulation of senescent cells during ageing is further highlighted in the studies which utilise biological or pharmacological (senolytics) approach to selectively deplete senescent cells. Targeting of senescent cells that express p16 for cell death in mice via an engineered construct called INK-ATTAC showed improvement of organ function and organismal fitness of these ageing mice, suggesting that the removal of senescent cells rescues these mice from the detrimental effects of ageing (Baker et al., 2011, 2016). Others have also seen similar effects using a class of small molecule inhibitors called senolytics which can specifically induce cell death in senescent cells (Chang et al., 2016; Yosef et al., 2016). Senolytics commonly target anti-apoptotic Bcl-2 family proteins such as Bcl-W and Bcl-XL and the inhibitors of p53 such as MDM2, which are upregulated in senescent cells (Reviewed in (van Deursen, 2019)). Overall, these reports suggest that cellular senescence plays an important role in organismal ageing and that the therapies targeting senescent cells could potentially increase the quality of life in humans during the old age.

1.2.9 Cellular senescence disorders: Progeroid syndromes

Progeroid syndromes is a terminology which corresponds to a group of genetic disorders associated with accelerated or premature aging. Progeroid

syndromes can be classified into lamina-associated and DNA repair-associated progeroid syndromes based on the affected molecular pathway (Carrero, Soria-Valles and López-Otín, 2016). Examples of lamina associated progeroid syndromes are Hutchinson-Gilford progeria syndrome (HGPS), progeria syndrome (NGPS) and atypical progeria syndromes (APS). While, Werner syndrome, Cockayne syndrome and Bloom syndrome are examples of DNA repair-associated progeroid syndromes which are caused by mutations in WRN, ERCC6/8 and BLM genes, respectively. One of the most extensively studied progeroid syndrome is HGPS which is the disease synonymous with the name Progeria. HGPS is caused by a C>T point mutation at position 1824 of the LMNA gene, which encodes for the precursor of Lamin A, one of the structural proteins of nuclear lamina (De Sandre-Giovannoli et al., 2003; Eriksson et al., 2003). This point mutation results in *de novo* formation of a spice site at exon 11 of the LMNA gene, which results in the production of a shorter mRNA transcript and translated pathologic protein called progerin (De Sandre-Giovannoli et al., 2003; Eriksson et al., 2003). Accumulation of progerin at the nuclear lamina can cause deformation of the nuclear envelope and this has been shown to cause DNA replication defects in HGPS cells (Gonzalo and Kreienkamp, 2015). Furthermore, a persistent activation of the DDR thought to be due to DNA repair problems on DNA damage sites have also been observed in HGPS cells suggesting a link between HGPS and SIPS (Liu et al., 2005, 2006). Indeed, p53 pathway activation is implicated in HGPS and was found to be triggered by progerin-induced replication fork stalling (Wheaton et al., 2017). Expression of progerin have been discovered in fibroblasts from old patients with age ranging from 81 – 96 years old, suggesting a role for Lamin A/progerin in normal aging (Scaffidi and Misteli, 2006). A study in cultured fibroblast from HGPS patients showed that treatment with the mTOR inhibitor rapamycin induced removal of progerin and restored nuclear membrane morphology and proper cellular functions, suggesting that the mTOR pathway is responsible in HGPS (Cao et al., 2011). Interestingly, mTOR has been recently shown to be involved in maintenance of DDR signalling in cellular senescence through mitochondrial biogenesis,

suggesting another feature cellular senescence that is replicated in premature aging syndromes (Correia-Melo et al., 2016).

The Werner syndrome, a DNA repair-associated progeroid syndrome, have also been extensively studied, as it showed similar accelerated aging features to HGPS but with a later onset which made it frequently called as adult progeria. It is caused by a spectrum of mutations on the WRN gene located at chromosome position 8p12, which encodes for a RecQ family helicase important in unwinding DNA during repair of DSBs by NHEJ or HR (Goto et al., 1992; Yu et al., 1996; Gray et al., 1997; Chen et al., 2003; Huang et al., 2006). Somatic cells derived from Werner syndrome patients exhibit various chromosomal aberrations such as translocations, inversions and large deletions in the genome suggesting genomic instability (Salk et al., 1981; Fukuchi et al., 1985; Fukuchi, Martin and Monnat, 1989). A study using DNA methylation markers as “epigenetic clocks”, showed that white blood cells of Werner syndrome patients displayed accelerated epigenetic aging as shown from increased DNA methylation at specific CpG sites (Maierhofer et al., 2017). Moreover, a gene expression microarray study showed similarity between gene expression pattern of fibroblasts of Werner syndrome patients and from old people, confirming the premature aging phenotype of patients with Werner syndrome (Kyng et al., 2003). The WRN helicase have also been implicated in telomere replication (Crabbe et al., 2004). Werner syndrome fibroblast showed reduced *in vitro* lifespan compared to normal fibroblasts, which can be rescued by telomerase expression, suggesting a role for telomere dysfunction in Werner syndrome (Martin, Sprague and Epstein, 1970; Wyllie et al., 2000). Loss of telomeric sequence from telomeres replicated by lagging strand synthesis was observed in fibroblasts lacking WRN, linking this progeroid syndrome to telomeropathies (Crabbe et al., 2004, 2007). Importantly, cellular feature overlaps are observed between telomeropathies and progeroid syndromes as both, in some of cases, prematurely activates the cellular senescence program (Davis et al., 2006, 2007; Deng et al., 2013; Lin, Mobasher and Alawi, 2014; Stockklausner et al., 2015; Wheaton et al., 2017).

1.3 Cellular senescence and cancer: Tumour suppression vs Tumour promotion

1.3.1 Structure and function of the tumour suppressor p53

The tumour suppressor protein p53 is a transcription factor which play multiple roles in cancer suppression such as DDR, DNA repair, apoptosis and senescence among others and due to these roles it is also known as the guardian of the genome (Yonish-Rouach et al., 1991; Shaw et al., 1992; Lane, 1992; el-Deiry et al., 1993; Waldman, Kinzler and Vogelstein, 1995; Offer et al., 1999; Saintigny et al., 1999; Lin et al., 2000; Amundson et al., 2002; Kortlever, Higgins and Bernards, 2006). p53 is frequently mutated in cancer and in Li Fraumeni syndrome which is characterised by early onset and increased susceptibility to multiple cancer formation (Baker et al., 1990; Malkin et al., 1990; Srivastava et al., 1990; Hussain and Harris, 1998). In humans, p53 is transcribed from the gene TP53, located at the genomic locus 17p13.1, which has 11+2 (β & γ) exons (2005). The gene has three known promoters; one located upstream of the first exon which is also a non-coding exon (P1) , a second one located at the first intron (P1') and a third one located at intron 4 (P2) (Reisman, Greenberg and Rotter, 1988; Bourdon et al., 2005). The full-length mRNA of the canonical p53 is transcribed from the P1 promoter, resulted in a 53 kDa protein following translation when analysed by SDS-PAGE, hence its name (Lane and Crawford, 1979; Linzer and Levine, 1979). mRNA transcription from the P2 promoter and multiple alternative splicing event can result in the formation of p53 isoforms (Joruiz and Bourdon, 2016). 12 different isoforms of human p53 have been discovered so far which include p53α (canonical p53), p53β, p53γ, Δ40p53α, Δ40p53β, Δ40p53γ, Δ133p53α, Δ133p53β, Δ133p53γ, Δ160p53α, Δ160p53β, Δ160p53γ. Although the function of these isoforms are mostly not known, p53β, Δ40p53 and Δ133p53α have been shown to be implicated in the regulation of cellular senescence (Fujita et al., 2009; Fujita, 2019). The main wild-type p53 gene product consist of 393 amino acids and has two N-terminal Transactivation domains (TAD1 & TAD2) followed by a Proline rich region (PRD), a core DNA binding domain (DBD), a

nuclear localisation signal domain (NLS), a tetramerization domain (TET) and a C-terminal basic domain (BD) (Figure 1.6). Residues encompassing TADI, TADII and PRD are known to be natively unfolded and undergoes folding when binding to another protein such as MDM2 (Dawson et al., 2003).

The p53 protein can only exert its function by binding to p53-response element as a tetramer to regulate expression of target genes (Halazonetis and Kandil, 1993; Warnock et al., 2008). The canonical p53 response element contains two repeats the motif "RRRCWWGYYY", where R represents Guanine / Adenine (purine) , W represents Adenine / Thymine and Y represents Cytosine / Thymine (pyrimidine), separated by a spacer of up to 13 nucleotides (El-Deiry et al., 1992; Funk et al., 1992; Farmer et al., 1992). The p53 tetramer is organised as a symmetric dimer of dimers and requires the tetramerization domain (TET) located at amino acid positions 325 – 356 (Jeffrey, Gorina and Pavletich, 1995). p53 tetramerization is also known to be required for effective ubiquitination of p53 by MDM2, p53 phosphorylation at S20 by Chk1/Chk2 and acetylation of p53 C-terminal lysine residues by p300 histone/lysine acetyltransferase (Maki, 1999; Shieh, 1999; Shieh et al., 2000; Mak, 2000; Itahana, Ke and Zhang, 2009). p53 is known to regulate expression of various genes such as *CDKN1A* (p21) and *BBC3* (PUMA) which play a role in cell cycle arrest and apoptosis respectively (El-Deiry et al., 1992; Shaw et al., 1992). Regulation of p53 activity mainly involves a negative feedback loop with the proteins MDM2 and MDM4/MDMX (Kubbutat, Jones and Vousden, 1997; Freedman, Wu and Levine, 1999; Stommel and Wahl, 2004). MDM2 is known to directly bind to the N-terminal transactivation domain of p53 and can also act as an E3 ubiquitin ligase for p53 and export p53 to the cytosol for degradation by the proteasome (Lin et al., 1994; Kussie et al., 1996; Honda, Tanaka and Yasuda, 1997; O'Keefe, Li and Zhang, 2003). Phosphorylation at Threonine residue 18 (Thr18) by Casein Kinase 1 (CK1) can release binding of MDM2 to p53 and this requires prior phosphorylation at Serine residue 15 (Ser15) (Dumaz, Milne and Meek, 1999; Lai et al., 2000; Sakaguchi et al., 2000; Schon et al., 2002). Ser15 residue is known to be phosphorylated by the

PI3K family kinases ATM and ATR in response to cellular stress such as DSB DNA damage (Nakagawa et al., 1999; Tibbetts et al., 1999). p53 Ser15 phosphorylation is required for p53 transactivation of p53 target genes and is known to precede any other phosphorylation at the transactivation domain (Sakaguchi et al., 1998; Dumaz, 1999; Dumaz, Milne and Meek, 1999; Saito et al., 2003). Therefore, this suggest that phosphorylation at Ser15 is the primary event in the activation and stabilisation of p53 and may be used as a general marker for p53 activation. Phosphorylation at Ser15 also play a role in the recruitment of the p53 coactivators p300/CBP to mediate acetylation of p53 at lysine sites in the DNA binding domain (DBD) and C-terminal basic domain (BD) which enhances p53 transactivation of target genes and increase stability of p53 by inhibiting MDM2-mediated ubiquitination of p53 (Lambert et al., 1998; Sakaguchi et al., 1998; Dumaz, 1999; Ito et al., 2001, 2002). Another transactivation domain phosphorylation site, Serine residue 20 (Ser20), is similarly important for p53 stabilisation and accumulation (Shieh, 1999).

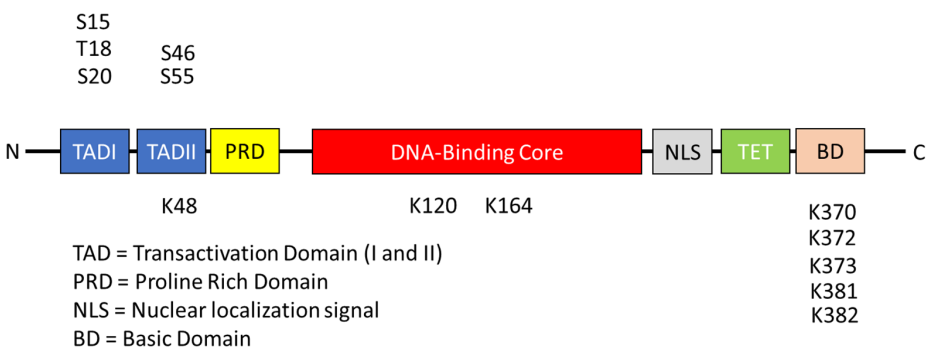

Figure 1.6 p53 functional domains and residues that can undergo posttranslational modifications.

1.3.2 Differences between tumour suppressor pathways in humans and mice

Mouse models have been used for a very long time to study cancer biology, owing to its ease in genetic manipulations and similarities to humans in terms of physiology, anatomy, and genetics. Thus, it is an indispensable tool in the quest to further understand cancer biology and discover future cancer therapies. However, it is also known that there are differences in tumour suppressor pathways between humans and mice (Wadhwa et al., 2002; Horvath et al., 2007; Jegga et al., 2008). Therefore, a cautious interpretation is required in order to be able to use data from mice to explain scientific findings in humans. This section will briefly describe these differences in order to understand how to interpret data taken from studies using mouse cells and animal models prior to extrapolating it to human cancer and senescence biology. This is important particularly as cellular senescence which is the main topic of this study, is a tumour suppressive mechanism and the tumour suppressor gene regulatory network plays an important role in the regulation of the senescence program (Alexander and Hinds, 2001; Beauséjour et al., 2003).

In 1977, Richard Peto postulated that bigger animals that live longer and have higher cell counts should have higher cancer incidence compared to smaller animals, due to increased risks of formation of oncogenic mutations from each cell division (Peto, 2015). However, he discovered that this was not the case as cancer incidence does not seem to correlate with the number of cells in an organism. For example, humans have 1000x more cells and live 30x longer than mice (Peto, Hiatt and Watson, 1977). However, probability of carcinogenesis induction in mice and humans by the end of the organism's life is similar at roughly 30% (Rangarajan and Weinberg, 2003). This simple observation is dubbed Peto's paradox and this spurred more research into how bigger animals can suppress cancer even with a very large number of cells and longer life expectancy. One factor that is thought to be able to explain this paradox is the difference in the components or regulation of tumour suppressor

pathway between species. Comparative cell culture studies in mice and humans have elucidated several distinctions in the molecular signalling of tumour suppressors which contribute to tumorigenic capacity *in vitro*. The first cell culture evidence which suggest that distinction was from a study which showed that spontaneous immortalisation, which is a hallmark of cancer, was observed in cultured murine but not human fibroblasts (Newbold, Overell and Connell, 1982). Further studies showed that p53-inactivating mutations were found in spontaneously immortalised mouse embryonic fibroblasts (MEF), suggesting a role for p53 in preventing immortalisation and activating senescence (Harvey and Levine, 1991). As telomerase is readily expressed in mice, it is thought that murine cells are readily immortalised, as long as the senescence pathway is inhibited via p53 inactivation. This idea was reinforced by experiments which showed that MEFs can bypass senescence and become immortal following p53 inactivation (Harvey et al., 1993; Dirac and Bernards, 2003). On the other hand, p53 alone is insufficient to bypass replicative senescence in human fibroblast which do not express telomerase (Shay, Pereira-Smith and Wright, 1991). In the same study, although cells can bypass senescence via ectopic expression of SV40 LT antigen or HPV E6/E7 viral oncoprotein which inhibit both p53 and pRb, this was not sufficient to induce immortalisation as the cells underwent crisis in the absence of telomerase expression. This suggest that, unlike in mice, both inactivation of p53 and pRb is required for cellular immortalisation in human cells. Lastly, a study which compared the requirement for cancer formation in both humans and mice showed that transformation of murine fibroblasts requires alteration in only two signalling pathways involving Raf and p53, compared to at least six in human fibroblasts, which involves p53, pRb, PI3K, telomerase, PP2A, Raf, and Ral-GEFs (Rangarajan et al., 2004). Overall, these data suggest an underlying difference in the regulation of tumour suppressor between the two species and could also explain the robustness of cancer suppression in humans.

1.3.3 Replicative senescence and crisis

It has been proposed that replicative senescence is a tumour-suppressive mechanism. p53, a principal component of the DDR and a tumour suppressor protein, is known to be inactivated in many cancer cells (Rivlin et al., 2011). Experimentally, inactivation of p53 and pRb via the expression of the SV40 LT antigen or the HPV E6-E7 oncoproteins results in a bypass of senescence which allows cells to continue proliferating until the cells reach a second proliferative barrier called crisis (Shay, Pereira-Smith and Wright, 1991). Unlike senescence, crisis is characterised by the end-to-end chromosomal fusions and genomic instability, which might be caused by the absence of all of the shelterin components required for telomere protection against the DNA repair machineries (Sfeir and De Lange, 2012). It is thought that genomic instability, arising from the breakage-fusion-bridge cycle and observed in the cells undergoing crisis may be sufficient to select for rare mutations which allow further uncontrollable proliferation (Shay and Wright, 1989; Wright, Pereira-Smith and Shay, 1989). Escape from the crisis may be accomplished by either reactivation of hTERT expression or by alternative lengthening of telomeres (ALT), which is a recombination-based telomere lengthening mechanism. Both routes lead to immortality and are a characteristic of cancer cells. Therefore, this suggests that senescence is a barrier that prevents carcinogenesis.

The idea that telomerase promotes cancer, came from studies showing that telomerase is expressed in the majority of cancers (Kim et al., 1994). However, this does not confirm whether telomerase is necessary early in oncogenesis. Indeed, telomerase expression alone does not confer phenotypical similarities to cancer in culture (Jiang et al., 1999; Morales et al., 1999). Studies in ageing mice have also shown that the over-expression of mouse TERT resulted in increased life expectancy without the tumour-inducing side effects (Bernardes de Jesus et al., 2012). Interestingly, although mice do express telomerase and have very long telomeres, this treatment surprisingly showed a decrease in

short telomeres suggesting that telomerase canonical function in telomere lengthening is required.

1.3.4 Reversal of senescence

Epigenetic evidence of the similarities between pre-cancer cells and senescent cells such as global hypomethylation and focal hypermethylation at promoters of genes linked to cancer, suggests that cancer cells may be derived from senescent cells that have escaped/reversed senescence (De Cecco et al., 2013; Cruickshanks et al., 2013; Sidler et al., 2014; Lowe et al., 2015). Although senescence is an important tumour suppressive mechanism, by limiting proliferation of old cells which have accumulated pathological mutations (RS) or cells which activated oncogenes (OIS – oncogene-induced senescence), it may paradoxically give rise to tumour-promoting cellular processes. Indeed, SASP have been proposed to produce a tumour-promoting microenvironment which could stimulate cell proliferation, epithelial to mesenchymal transition and invasion/metastasis capacity (Coppé et al., 2008). On the other hand, although some epigenetic changes and cellular processes of senescent cells are associated with cancer, it is unclear whether senescence escape/reversal is possible. Senescence bypass studies in human cells have shown that inhibition of both the p53-p21 and p16-pRb pathways is required to prevent cells from undergoing senescence, but insufficient to prevent cells from undergoing crisis (Shay, Pereira-Smith and Wright, 1991). Abrogation of senescence, once it has been established, has been shown possible in mice and certain human cells via the inhibition of p53 (Beauséjour et al., 2003; Dirac and Bernards, 2003). However, in human cells that upregulate p16, inhibition of both pathways is sufficient to abrogate cell cycle arrest but insufficient to allow cell division (Beauséjour et al., 2003). This suggests that senescence, at least RS, is irreversible in human cells expressing high levels of p16.

Activation of a single oncogene is generally insufficient to drive cancer formation. Furthermore, increased mutagenic signal from activated oncogenes

has been experimentally shown to trigger OIS, a subcategory of PS in various mouse and human cells, inhibiting the proliferation of pre-cancerous cells (Serrano et al., 1997; Suram et al., 2012). However, a study in BJ fibroblasts undergoing OIS showed a spontaneous escape from senescence associated with the upregulation of telomerase, thereby questioning the irreversibility of senescence (Patel et al., 2016). Interestingly, inhibition of p53 in BJ fibroblasts with RS was sufficient to reverse senescence (Beauséjour et al., 2003). Therefore, regardless of the senescence trigger, it is possible that irreversibility of senescence requires expression of p16.

1.4 Project aims

Cellular senescence is an important tumour suppressive mechanism and it has been suggested that cancer cells may be derived from the cells that escaped senescence. Therefore, this raises the question of whether senescence is truly permanent and therefore irreversible. This project aims to unravel potential ways in how RS cells might abrogate the proliferative arrests that governs their senescence by using telomerase. This project also aims to discover the requirements which might allow telomerase to elongate telomeres in senescent cells.

Chapter 2 Materials and methods

2.1 Cell culture conditions

MRC-5 Wild-Type (WT), hTERT and DD-hTERT cells were cultured in Gibco minimum essential medium (MEM) (Thermo Fisher Scientific, Waltham, MA, USA) supplemented with 10% HyClone foetal bovine serum (FBS) (GE Healthcare Life Sciences, Chicago, IL, USA), 1X Gibco penicillin-streptomycin-glutamine (PSG) solution (Thermo Fisher Scientific, Waltham, MA, USA), 1X Gibco non-essential amino acids (Thermo Fisher Scientific, Waltham, MA, USA), 1 mM Gibco sodium pyruvate (Thermo Fisher Scientific, Waltham, MA, USA). Shield-1 (Generon, Slough, UK) was added to the MRC-5 DD-hTERT cells at the concentration of 700 nM and replaced every four days. HEK293T packaging cells were cultured in Gibco Dulbecco's modified Eagle medium (DMEM) containing 3.7 g/l glucose, 4 mM glutamine, 1 mM sodium pyruvate (Thermo Fisher Scientific, Waltham, MA, USA) and supplemented with 10% HyClone FBS and 1X Gibco PSG solution. All cells were cultured in a 37 °C incubator with 5% CO_2. Proliferating cells were passaged every four days and re-seeded at 2.5 x 10^5, 7.5 x 10^5 or 1.75 x 10^6 cells per CELLSTAR 25 cm^2 (T25), 75 cm^2 (T75) or 175 cm^2 (T25) culture flasks (Greiner Bio-One, Kremsmünster, Austria) respectively.

2.2 Calculation of population doubling

Cells were manually counted using an improved Neubauer haemocytometer and the number of population doublings was calculated using the following formula: 3.32 (log UCY – log I) + X. Ultimate Cell Yield (UCY) corresponds to the cell number in the current passage, while Inoculum (I) is the number of the cells seeded in the previous passage and X is the population doubling number established at the previous passage (Patterson, 1979).

2.3 Genomic DNA extraction and quantification

Adherent cells were trypsinised and harvested by centrifuging at 300 RCF for 5 minutes. The supernatant was discarded, and the pellet was dissolved in 1 ml 1X PBS and transferred into a 2 ml microcentrifuge tube. This was followed by centrifugation at 300 RCF for 5 minutes. The resulting pellet was dissolved in 1 ml Tris-EDTA (TE) containing 0.1% SDS and 150 µg/ml Proteinase K, to lyse the cells overnight at 55 °C. 500 µl of Phenol:Chloroform:Isoamyl alcohol (25:24:1) solution was mixed with the lysed cells, followed by centrifugation for 5 minutes at 13,000 RPM, room temperature. The upper phase was then transferred into a fresh 2 ml microcentrifuge tube and 500 µl of chloroform was mixed with the upper phase solution. This was followed by centrifugation for 5 minutes at 13,000 RPM, room temperature. The Upper phase was transferred into a fresh 2 ml microcentrifuge tube. 100 µl of 3M sodium acetate and 1 ml of isopropanol were added to the upper phase solution. Genomic DNA was allowed to precipitate at -20 °C for at least 1 hour and as long as overnight. Following this, the genomic DNA was pelleted by centrifugation for 15 minutes at 13,000 RPM, 4 °C. The pellet was washed with ice-cold 70% ethanol and centrifuged for 5 minutes at 13,000 RPM, 4 °C. The DNA pellet was air-dried for 2 - 4 minutes and dissolved in 100 – 300 µl of the TE buffer, pH 8.0. 1 µl of RNAseA was added to the genomic DNA solution and the sample was incubated at 37 °C for 30 minutes to degrade contaminating RNA.

2.4 Western blotting

2.4.1 Protein extraction and quantification

1X RIPA buffer (25 mM Tris-HCl pH 7.6, 150 mM NaCl, 5 mM EDTA, either 1% NP-40 or 1% Triton X-100, 1% sodium deoxycholate and 0.1% SDS) supplemented with 1X cOmplete EDTA-free protease inhibitor cocktail (Roche Applied Science, Penzberg, Germany) and 1X Sigma phosphatase inhibitor cocktail 3 (Merck-Millipore, Burlington, MA, USA) was used to lyse mammalian cells that have been trypsinised and harvested by centrifugation. Following the cell resuspension in the RIPA buffer, the cell lysate was incubated on ice for

30 minutes and centrifuged at 8,000 RCF for 10 minutes at 4 °C, to pellet cell debris and clear up the lysate. Sigma bicinchoninic acid protein assay kit (Merck-Millipore, Burlington, MA, USA), was used to quantify proteins in the whole cell lysate according to the manufacturer's instructions, with 1 mg/ml BSA used for making a standard curve. Another method was also used in several western blots, where proteins were extracted from trypsinised cells by dissolving cell pellet in 2X Laemmli sample buffer at $1x10^4$ cells/µl of the sample buffer and boiling for 10 minutes at 100 °C on a heat block. 2X Laemmli sample buffer was prepared by diluting 4X Laemmli sample buffer containing 200 mM Tris-HCl pH 6.8, 8% SDS, 40 % glycerol, 0.04% Bromophenol blue and 400 mM DTT. The boiled whole cell lysate was passed through a 30G syringe needle 10 times to shear genomic DNA and reduce sample viscosity.

2.4.2 SDS-PAGE and protein transfer onto blotting membranes

For the cells lysed with the RIPA buffer, 30 to 50 µg of proteins were mixed with the 4X Laemmli sample buffer to a final concentration of 1X Laemmli, boiled for 5 minutes at 95 °C and then loaded into an SDS-PAGE gel in a vertical electrophoresis mini tank (Bio-Rad, Hercules, CA, USA) filled with 1X SDS-PAGE running buffer (25 mM Tris, 192 mM glycine, 0.1% (w/v) SDS) and run at 100 V for 2 hours or 180 V for 1 hour to separate the proteins by size. For cells directly lysed with 2X Laemmli buffer, 10 to 50 µl of whole cell extract (corresponding to $1x10^5$ to $5x10^5$ cells) was loaded into an SDS-PAGE gel and followed a similar electrophoresis setting as above. Following the SDS-PAGE, the proteins were transferred from the gel onto a Protran 0.45 µm NC nitrocellulose membrane (GE Healthcare Life Sciences, Chicago, IL, USA). The gel and the membrane were sandwiched between four blotting paper pieces (two on either side) and two fibre pads, which were all held together by a blotting cassette. The blotting sandwich was submerged completely in 1X transfer buffer (25 mM Tris, 192 mM glycine, 20% (v/v) methanol) in a mini blotting tank (Bio-Rad, Hercules, CA, USA) and protein transfer was run at 400 mA, 4°C for 1 hour or at 30 V, 4°C overnight.

2.4.3 Antibody probing and detection

Prior to antibody probing, western blot membranes were blocked in 4% skim milk dissolved in 1X TBS for 1 hour at room temperature. The membranes were then probed with primary antibodies diluted in 4% skim milk in 1X TBS and 0.1% Tween-20 (1X TBST) at the appropriate concentrations (Table 2.3). The incubations were carried out overnight at 4 °C. Following the primary antibody incubations, the membranes were washed with 1X TBST and probed for 1 hour at room temperature with a secondary antibody conjugated to either IRDye 680RD or IRDye 800CW (LI-COR, Lincoln, NE, USA) diluted at 1:15,000 in 4% skim milk in 1X TBST. The membranes were washed again with 1X TBST before detection of the proteins using a LI-COR Odyssey Imager (LI-COR, Lincoln, NE, USA) using either the 700 nm channel for IRDye 680RD secondary antibodies or the 800 nm channel for the IRDye 800CW secondary antibodies.

2.5 Telomere Repeat Amplification Protocol (TRAP)

Whole cell lysates for TRAP assays were made by re-suspending cell pellets in the NP-40 lysis buffer (10 mM Tris-HCl pH 8.0, 1 mM $MgCl_2$, 1 mM EDTA, 1% NP-40, 0.25 mM sodium deoxycholate, 10% glycerol, 150 mM NaCl, 5 mM β-mercaptoethanol, 1X Sigma P8340 protease inhibitor cocktail (Merck-Millipore, Burlington, MA, USA)). 1 µl of the buffer was used per 1,000 cells to lyse and the cell lysis samples were incubated on ice for 30 minutes. The cell lysates were diluted accordingly, using NP-40 lysis buffer and fluorescence-based TRAP assay was performed as described by Mender and Shay, with some modifications (Mender and Shay, 2015). MRC-5 WT and MRC-5 hTERT cells were used as negative and positive controls, respectively. The 5'-DY-782-labelled oligo TRAP-TS-IR was used as a synthetic template for telomerase. A mixture of 3 primers: ACX, TSNT and NT was also used in the TRAP reaction to function as a reverse primer for telomerase product, an internal control for the PCR reaction and a reverse primer for the internal control, respectively. The TRAP PCR reactions were setup in 50 µl reaction volumes, containing 1X

TRAP buffer (200 mM Tris-HCl pH 8.3, 15 mM MgCl2, 630 mM KCl, 0.5% v/v Tween-20 and 10 mM EGTA), 200 µM dNTPs, 0.2 mg/ml BSA, 2 ng/µl TRAP-TS-IR primer, 1X TRAP primer mix (0.1 µg/µl ACX primer 0.1 µg/µl NT primer and 0.01 pM TSNT primer), 2.5 U *Taq* polymerase and 1 µl of a tested sample or a cell lysate. The TRAP PCR reaction was initiated with a telomerase extension step at 30 °C for 40 minutes followed by an initial denaturation step at 95 °C for 5 minutes and 26 cycles of Denaturation, Annealing and Extension for 30 seconds at 95 °C, 30 seconds at 52 °C and 45 seconds at 72 °C respectively, before ending the PCR with a final extension step at 72 °C for 10 minutes. 10 µl of 6X Orange G DNA loading dye was added to 50 µl of the TRAP PCR products and 30 µl of the mixture was loaded into a pre-chilled 10% native polyacrylamide gel in 0.5 % TBE running buffer. The gel was run in a Biometra Model V.15.17 vertical electrophoresis apparatus (Analytik Jena, Jena, Germany) at 250 V, 4 °C for 2.5 hours. The whole gel was scanned using a LI-COR Odyssey Imager (LI-COR, Lincoln, NE, USA) using the IR800 channel. DNA markers were imaged separately by staining the gel with 0.5 µg/ml ethidium bromide (EtBr) for 15 minutes, followed by washing with distilled water for 15 minutes and scanning using a gel imaging system equipped with a UV transilluminator.

2.6 Telomere Restriction Fragment (TRF) Southern blotting (Teloblots)

2.6.1 Genomic DNA restriction digests

30 µg of genomic DNA was digested with the HinfI restriction enzyme (Thermo Fisher Scientific, Waltham, MA, USA) at 5 U/µg DNA in 1X buffer R at 37 °C in a water bath overnight. Following inactivation of HinfI at 65 °C for 20 minutes, HinfI-digested DNA was precipitated using either one volume of 100% isopropanol or three volumes of 100% ethanol, 1/10 volume of 3 M sodium acetate pH 5.2 and 100 µg/ml glycogen at -20 °C overnight. The precipitated DNA was pelleted by centrifugation at 17,000 g, 4 °C for 15 minutes. The DNA pellet was washed with 100 % ethanol, one volume of the initial genomic DNA digest, and centrifuged again as above for 5 minutes. The

supernatant was removed, and the pellet was allowed to dry before being resuspended in 100 µl of dH_2O. The HinfI-digested genomic DNA was further digested with the RsaI restriction enzyme (Thermo Fisher Scientific, Waltham, MA, USA) at 5 U/µg DNA in 1X Tango buffer at 37 °C in a water bath overnight. RsaI was inactivated by incubation at 80 °C (heatblock) for 20 minutes. HinfI-RsaI digested genomic DNA was precipitated, centrifuged, and washed according to the procedure described above for the HinfI-digested DNA. Air-dried HinfI-RsaI digested genomic DNA was dissolved in 20 µl of dH_2O and the DNA quantity was measured using Nanodrop 2000 (Thermo Fisher Scientific, Waltham, MA, USA).

2.6.2 DNA electrophoresis

20 µg of HinfI-RsaI digested genomic DNA was mixed with 1X Orange G DNA loading dye and loaded into the wells of a 0.8% agarose gel in 1X TAE buffer supplemented with 0.5 µg/ml EtBr. Agarose gel electrophoresis was run at 30 V for 1 hour and at 45 V for 16 hours using a Bio-Rad Sub-Cell GT tank (Inter-electrode distance = 29.5) (Bio-Rad, Hercules, CA, USA). Following the electrophoresis, the agarose gel was incubated sequentially in depurination solution (0.25 M HCl) for 30 minutes, in denaturing solution (1.5 M NaCl and 0.5 M NaOH) for 30 minutes and in neutralising solution (1.5 M NaCl, 0.5 M Tris-HCl pH 7.2 and 1 mM EDTA) for 40 minutes, with a single tap water rinse in between the incubations with the solutions above.

2.6.3 DNA transfer onto a membrane

3 mm filter paper and Hybond N+ charged nylon membrane (GE Healthcare Life Sciences, Chicago, IL, USA) were cut to the size of the gel and soaked in 20X SSC buffer (3M NaCl and 0.3 M Na citrate). The DNA was transferred from gel on to the membrane by capillary action through a Southern blot sandwich, for 8 hours at room temperature with 20X SSC buffer (Figure 2.1). Following the transfer, the nylon membrane was air dried and the DNA was cross-linked to the membrane using a 254 nm UV cross-linker at 120 mJoules/cm^2.

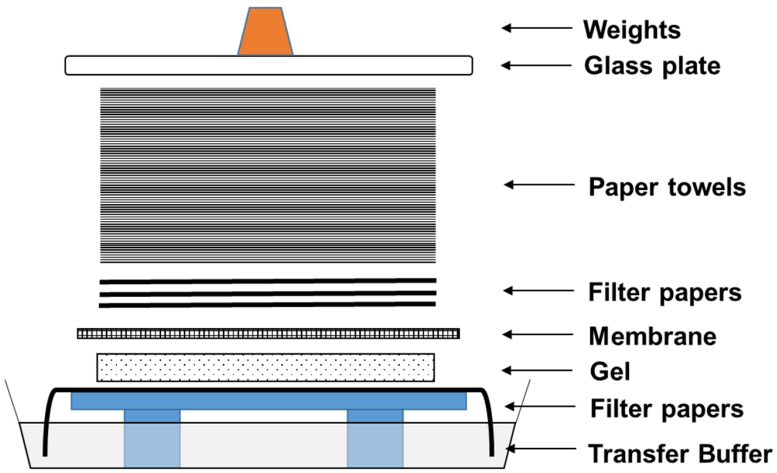

Figure 2.1 Southern blot sandwich.

2.6.4 TRF probe hybridization

The membrane was placed into a hybridization bottle containing ~17.5 ml of pre-warmed (50 °C) fresh hybridization solution (5X Denhardt's solution [0.1% w/v BSA Fraction V, 0.1% w/v Ficoll 400, 0.1% w/v Polyvinylpyrrolidone], 6X SSPE buffer [0.9 M NaCl, 60 mM NaH_2PO4 pH 7.4 and 6 mM EDTA] and 0.5% SDS). The membrane was pre-hybridized for 1 hour at 50 °C in a hybridization oven. 2 µl of 0.5 µg/µl DY-782-conjugated TRF probe (5'-DY-782-TTAGGGTTAGGGTTAGGG) was diluted with 100 µl of dH_2O, denatured for 2 minutes at 95 °C in a thermal cycler and cold shocked on ice. The denatured TRF probe was added to ~7.5 ml of pre-warmed (50 °C) hybridization solution. The pre-hybridization solution was replaced with the TRF probe solution and the membrane was hybridized overnight at 50 °C in the dark. Following the hybridization, the membrane was washed with 30 ml of pre-warmed washing buffer (1X SSPE and 0.1% SDS) at 50 °C, twice for 20 minutes and 15 minutes, respectively. The membrane was transferred to a clean container, rinsed with 1X SSPE buffer and stored in 1X SSPE buffer, dark until scanning.

2.6.5 Blot scanning

The membrane was placed on the glass scanning surface of a Li-COR Odyssey infrared imager, the DNA side down, and any bubbles formed were removed using a roller. The membrane was scanned at 800 nm, 169 µm resolution and medium image quality.

2.7 Senescence-associated β-galactosidase staining

Cells cultured in either 6-well or 24-well plate were washed with 1X PBS and fixed with 4% formaldehyde solution for 5 minutes at room temperature. Following the fixation, the cells were washed again with 1X PBS and then immersed in the SA-β-Gal staining solution (1 mg/ml X-gal, 40 mM citrate-phosphate buffer pH 6.0, 5 mM potassium ferricyanide, 5 mM potassium ferrocyanide, 150 mM NaCl, 2 mM $MgCl_2$). Cells were then incubated at 37 °C in the dark for 16 hours. Following the incubation, the cells were washed sequentially with 1X PBS for 5 minutes, dH_2O for 5 minutes and 100% methanol for 30 seconds at room temperature and left to dry in the dark before taking images of the cells using a bright-field microscope.

2.8 Immunofluorescence microscopy

Cells were cultured on acid-washed, poly-L-lysine coated coverslips and fixed for 10 minutes using 4% formaldehyde solution made fresh by dissolving paraformaldehyde in 1X PBS. The fixed cells were permeabilised by incubating in 0.2% Triton-X100 in 1X PBS at 37 °C for 10 minutes. 4% BSA in 1X PBS was used for blocking and diluting primary and secondary antibodies (See Table 2.3. for list of antibodies used in this study). After blocking and the incubations with primary and secondary antibodies, the cells were counterstained with DAPI di-lactate solution (5 mg/ml) diluted at 1:5,000 in 1X PBS for 10 minutes. Prolong Gold antifade mountant (Thermo Fisher Scientific, Waltham, MA, USA) was used to mount coverslips on superfrost microscope slides. The slides were imaged using a Zeiss AxioImager fluorescence microscope (Carl Zeiss Microscopy, Jena, Germany) and

µManager open source microscopy software (Open-Imaging, UCSF, San Francisco, CA, USA).

2.9 Quantification of Immunofluorescence signals

NIH ImageJ 1.51r software (Schneider, Rasband and Eliceiri, 2012) was used for semi-automatic quantification analysis of immunofluorescence microscopy images. Initially, 16-bit image stacks consisting of a DAPI channel image and a target protein channel image (defined by the secondary antibody fluorescent conjugate) were size calibrated and split into single images and converted into 8-bit grayscale images. These images were processed using the "Auto-threshold" function with the default setting, in order to highlight the cells. The images were then converted into the binary format, which allowed quantification of cells as particles of a certain size. The "watershed" function was used to cut cells that were merged together. False positives were removed by subtracting the target channel image with the DAPI channel image using the "Image Calculator" function. The "Analyze Particles" function was used to quantify cells in both DAPI channel and target protein channel, which corresponded to the total cell count and the positively stained cell count, respectively.

2.10 Cell proliferation assayed by EdU incorporation followed by flow cytometry

Cells were grown in a 10 cm culture dish to approximately 60% confluency. EdU was added dropwise to the cells at the final concentration of 10 µM and the cells were incubated for 24 hours in a 37 °C, 5% CO_2 incubator. Following the incubation, culture media were removed, cells were washed with 5 ml of cold 1X PBS and incubated with 2 ml Gibco 1X Trypsin-EDTA (Made from 10X Trypsin-EDTA containing no phenol red and diluted to 1X with 1X PBS)(Thermo Fisher Scientific, Waltham, MA, USA) at 37 °C to dislodge adherent cells. Trypsin-EDTA was quenched with 4 ml of media containing 10% FBS and the cells were dissociated by pipetting up and down. The cells were then pelleted by centrifugation at 300 RCF for 5 minutes and the pellet

was resuspended in 2.5 ml of ice-cold 1% FBS in 1X PBS. The cells were counted using Invitrogen Countess cell counter (Thermo Fisher Scientific, Waltham, MA, USA) and fixed by adding 7.5 ml of ice cold 100% ethanol, drop by drop while gently vortexing. 7.5 x 10^5 cells were transferred into a 2 ml microcentrifuge tube and centrifuged for 5 minutes at 500 RCF, 4 °C. The ethanol-fixed cells (as a pellet) were washed with 900 µl of 1X PBS and centrifuged for 5 minutes at 500 RCF, 4 °C. Click reaction cocktail was prepared by combining the following ingredients in the following order, for 1 reaction: 873 µl 1X PBS, 9 µl of 1 M sodium ascorbate, 0.45 µl of Alexa Fluor 647 Azide and 18 µl of 0.1 M $CuSO_4$. The cell pellet was resuspended in 900 µl of either the Click reaction cocktail (for protein staining) or 900 µl 1X PBS (for DAPI only and no staining controls) and incubated at room temperature/dark on a rotator for 30 minutes. Following the Click reaction, cells were centrifuged for 5 minutes at 500 g, room temperature. The cell pellet was then resuspended in 900 µl of 1% FBS and 0.5% Tween-20 in 1X PBS and incubated for 10 minutes at room temperature to permeabilise the cells. Following the cell permeabilisation, cells were centrifuged for 5 minutes at 500 RCF at room temperature and the pellet was resuspended in 300 µl of 1% FBS + 2.5 µg/ml DAPI in 1X PBS or 900 µl of 1% FBS in 1X PBS for Alexa 647 only and no staining controls, followed by incubation at room temperature for 1 hour. Cells were passed through a 40 µm cell strainer and analysed using an LSR II flow cytometer (BD Biosciences, Franklin Lakes, NJ, USA). Data were analysed using FlowJo software (FlowJo LLC., Ashland Oregon, USA) or Flowing software (Perttu Terho, University of Turku, Finland).

2.11 Cell proliferation assayed by EdU incorporation followed by immunofluorescence microscopy

Cells were seeded on coverslips overnight. Next day, EdU solution was added directly to the culture media to the final concentration of 10 µM. The EdU treated cells were incubated for 30 minutes in a 37 °C, 5% CO_2 incubator. Following the EdU treatment, cells were fixed with 4% formaldehyde solution in 1X PBS for 10 minutes in the dark at room temperature. The fixed cells were

washed with 1X PBS three times for 5 minutes each wash. Cells were then permeabilised by incubating in 0.5% Triton-X100 in 1X PBS for 10 minutes at 37 °C. The permeabilised cells were washed with 1X PBS twice for 1 minute each wash followed by a wash with 3% BSA in 1X PBS for 2 minutes. Invitrogen Click-iT EdU cell proliferation kit (Thermo Fisher Scientific, Waltham, MA, USA) was used to stain EdU positive cells. 500 µl of the Click Reaction cocktail (430 µl of 1X Click-iT reaction buffer, 20 µl of CuSO4, 1.2 µl Alexa Fluor 647 azide and 50 µl of 1X reaction buffer additive) was added onto the coverslips containing the fixed and permeabilised cells and incubated for 30 minutes in the dark at room temperature. This was followed by a 2-minute wash with 3% BSA in 1X PBS. Cells were then counterstained with 2 µg/ml DAPI in 1XPBS for 20 minutes in the dark at room temperature. Following two 5-minute washes with 1X PBS remove excess DAPI, cells on the coverslips were mounted on Superfrost microscope slides using Prolong Gold antifade mountant. Slides were imaged and quantified according to the immunofluorescence microscopy method described in the sections 2.8 and 2.9.

2.12 Lentiviral transduction

2.12.1 p53 and p16 shRNA constructs

p53 and p16 shRNA sequences (shp53 and shp16 respectively) were acquired from several publications and the RNAi consortium database (Table 2.4). An shRNA sequence to luciferase (shLuc) was used as a non-targeting shRNA control. Based on these sequences, custom DNA oligos corresponding to the shRNA sequences were designed; a 5' AgeI overhang (CCGG) and a 3' termination sequence (TTTTT) were added to the top oligo and a 5' EcoRI overhang (AATT) preceding the complementary sequence of the termination sequence (AAAAA) was included into the bottom oligo. These DNA oligos were custom made by Sigma-Aldrich and reconstituted in dH_2O. 11.25 µl of the top and bottom oligos were mixed with 2.5 µl of 10X annealing buffer (1 M NaCl and 100 mM Tris-HCl pH 7.4) and annealed using a thermal cycler by heating the mixture to 95 °C for 5 minutes, cooling to 25 °C at 0.1 °C/s followed

by 10 minute incubation at 25 °C. This produced a double stranded DNA ready for ligation into a vector digested with AgeI and EcoRI. These shRNA-corresponding sequences were diluted 1:400 in 0.5X annealing buffer and ligated with either a pLKO-IPTG-3XLacO or pLKO.1-hygro plasmids digested with AgeI and EcoRI before subsequent lentiviral packaging and transduction into target cells.

2.12.2 Cloning of the hPOT1-hTERT fusion into a lentiviral vector

The insert of the pBABE-Puro-hPOT1-hTERT plasmid, a gift from Christopher M. Counter (Armbruster et al., 2004), was PCR amplified using the primers with AttB1/B2 overhangs (Table 2.2) and Q5 high-fidelity DNA polymerase (New England Biolabs, Ipswich, MA, USA) to create the hPOT1-hTERT fusion sequence flanked by the AttB1 and AttB2 sites for cloning into a Gateway cloning-compatible plasmid according to the manufacturer's instructions (Table 2.1). The amplified fragment was run on a 0.8% agarose gel to confirm the size (5455 bp), excised from the gel and purified with a Qiaquick gel extraction kit according to the manufacturer's instructions (QIAGEN, Hilden, Germany). The amplified AttB1-hPOT1-hTERT-AttB2 insert was cloned into pDONR211 Gateway entry plasmid using the Gateway BP clonase II enzyme mix (Thermo Fisher Scientific, Waltham, MA, USA) according to the manufacturer's instructions, converting the pDONR211 into a pENTR-hPOT1-hTERT. The insert of the pENTR-hPOT1-hTERT plasmid was cloned into a pLENTI6/V5-DEST Gateway destination plasmid using Gateway LR clonase II enzyme mix (Thermo Fisher Scientific, Waltham, MA, USA) according to the manufacturer's instructions, converting the pDONR211 into a pLENTI6-hPOT1-hTERT plasmid ready for lentiviral packaging. The integrity of the inserts in pBABE-Puro-hPOT1-hTERT, pENTR-hPOT1-hTERT and pLENTI6-hPOT1-hTERT have been confirmed by Sanger sequencing.

Table 2.1 PCR conditions for AttB1-hPOT1-hTERT-AttB2 amplification

Step	Temperature	Time	Cycles
Initial denaturation	98 °C	1 minute	1
Denaturation	98 °C	10 seconds	
Annealing	66 °C	20 seconds	30
Extension	72 °C	1 minute and 30 seconds	
Final Extension	72 °C	2 minutes	1

2.12.3 Viral packaging and delivery of lentiviral constructs

2.5 x 10^6 HEK293T cells were seeded into 10 ml of the DMEM media in a 10-cm dish. 2-days after the seeding, the following plasmids were transfected into the HEK293T cells via the calcium phosphate method: 1 µg of pMD-HIV1-Gag/Pol plasmid, 1 µg of pRSV-Rev plasmid, 2 µg of pMD2.G-VSVG plasmid and 20 µg lentivector plasmid (e.g., pLKO-puro-shp53-1, pLENTI6-hPOT1-hTERT etc.). Following an overnight incubation, the medium containing the transfection reagent was replaced with a fresh medium and cells were incubated for another 24 hours for viral production. Virus-containing media were harvested and centrifuged at 300 RCF for 3 minutes at room temperature to remove any dislodged cells. The supernatant with the virus was filtered through a 0.45 µm polyethersulfone (PES) syringe filter, supplemented with 8 µg/ml Polybrene and directly transferred to a T75 culture flask containing the target cells which had its media removed. Fresh DMEM media were added back to HEK293T cells following the harvesting of the lentiviral supernatant. After the incubation for another 24 hours, the harvesting process and lentiviral transduction of the target cells was repeated one more time. Selection of the positive cells was performed by a treatment with either 2 µg/ml Puromycin, 5 µg/ml Blasticidin or 100 µg/ml Hygromycin, according to the mammalian antibiotic resistance marker of the lentivector plasmid used.

2.13 DNA oligonucletides

All DNA oligonucleotides were synthesized by Sigma-Genosys, Haverhill, United Kingdom unless otherwise stated.

Table 2.2 DNA oligonucleotides used in this study as primers

Primer	Description	Sequence 5' → 3'	Source
attB1-hPOT1-hTERT-F2	Primers with attB overhangs to amplify pBABE-Puro-hPOT1-hTERT insert	GGGGACAAGTTTGTACAAAAAAGC AGGCTTCGTGTGGTGGTACGTAGC TAGCATG	This study
attB2-hPOT1-hTERT-R		GGGGACCACTTTGTACAAGAAAGC TGGGTTTCAGTCCAGGATGGTCTT GAAGTC	This study
hPOT1-Seq-1-F		AAGTGGACGGAGCATCATTTC	This study
hPOT1-Seq-1-R		TTTGTAGCCGATGGATGTGAC	This study
hPOT1-Seq-2-F		TCAGTCTGTTAAACTTCATTGCCC	This study
hPOT1-Seq-2-R		ATGTGGAACTTCTTGCAGCAAATG	This study
hPOT1-Seq-3-F		AAATTGATGCATATCCGTGGTTGG	This study
hPOT1-Seq-3-R		ATGACTTGATGAAGCATTCCAACC	This study
hTERT-Seq-1-F	For sequencing of hPOT1-hTERT	TGCAGAGCGACTACTCCAGCTATG	This study
hTERT-Seq-1-R		AGGCTGTTCACCTGCAAATC	This study
hTERT-Seq-2-F		CTGAGCTGTACTTTGTCAAGGTGG	This study
hTERT-Seq-2-R		CTGGAGGTCTGTCAAGGTAGAG	This study
hTERT-Seq-3-F		GCTTCCTCAGGAACACCAAG	This study
hTERT-Seq-3-R		TTTGAAACGTGGTCTCCGTGAC	This study
hTERT-Seq-4-F		CTCCTTCCTACTCAGCTCTC	This study

hTERT-Seq-4-R		GCCTGGAACCCAGAAAGATG	This study
pLKO-shRNA-Seq-1	For sequencing of inserts of pLKO-puro-IPTG-3xLacO and pLKO.1-hygro plasmids	GGCAGGGATATTCACCATTATCGTTTCAGA	Dmitri Wiederschain
pLKO-shRNA-Seq-2		ACCCAGAGAGGGCCTATTTC	This study
pLKO-shRNA-Seq-3		CTCTGCTGTCCCTGTAATAAAC	This study
pLKO-shRNA-Seq-4		GGACTATCATATGCTTACCGTAAC	This study
pLKO-shRNA-Seq-5		TGGATGAATACTGCCATTTGTCTC	This study
pBABE-Seq-F	5' of the MCS of pBABE based vectors	CTTTATCCAGCCCTCAC	Robert Weinberg
pBABE-Seq-R	3' of the MCS of pBABE based vectors	ACCCTAACTGACACACATTCC	Robert Weinberg
M13 (-21)	M13 Forward primer	TGTAAAACGACGGCCAGT	Applied Biosystems
M13rev	M13 Reverse primer	GGAAACAGCTATGACCATG	Stratagene
hPOT1-hTERT-F1	hPOT1-hTERT genotyping primers	TGGACCTTTCAGCACCATTTCT	This study
hPOT1-hTERT-R1		GCATCTTGTCGTCATCGTCTTT	This study
BLAST-F1	Blasticidin resistance gene genotyping primers	GCCAAGCCTTTGTCTCAAGAAG	This study
BLAST-R1		ATAACCAGAGGGCAGCAATTCA	This study

Table 2.3 DNA oligonucleotides used in this study to make the constructs for shRNA expression

shRNA Oligo	Description	Target	Sequence 5' → 3'	Source
shp53-1-TOP	Type 1, Top oligo	p53	CCGGGACTCCAGTGGTAATCTACTTCAAGAGAGTAGATTACCACTGGAGTCTTTTT	Godar et al., 2008
shp53-1-BOT	Type 1, Bottom oligo		AATTAAAAAGACTCCAGTGGTAATCTACTCTCTTGAAGTAGATTACCACTGGAGTC	
shp53-2-TOP	Type 2, Top oligo		CCGGCACCATCCACTACAACTACATCTCGAGATGTAGTTGTAGTGGATGGTGTTTTT	Kim et al., 2007
shp53-2-BOT	Type 2, Bottom oligo		AATTAAAAACACCATCCACTACAACTACATCTCGAGATGTAGTTGTAGTGGATGGTG	
shp53-3-TOP	Type 3, Top oligo		CCGGGTCCAGATGAAGCTCCCAGAACTCGAGTTCTGGGAGCTTCATCTGGACTTTTT	Kim et al., 2007
shp53-3-BOT	Type 3, Bottom oligo		AATTAAAAAGTCCAGATGAAGCTCCCAGAACTCGAGTTCTGGGAGCTTCATCTGGAC	
shp53-4-TOP	Type 4, Top oligo		CCGGGACTCCAGTGGTAATCTACTGCTCGAGCAGTAGATTACCACTGGAGTCTTTTT	Masutomi et al., 2003
shp53-4-BOT	Type 4, Bottom oligo		AATTAAAAAGACTCCAGTGGTAATCTACTGCTCGAGCAGTAGATTACCACTGGAGTC	
shp16-1-TOP	Type 1, Top oligo	p16	CCGGGGAGCAGCATGGAGCCTTCGGAAGCTTCCGAAGGCTCCATGCTGCTCCTTTTT	Shin et al., 2004
shp16-1-BOT	Type 1, Bottom oligo		AATTAAAAAGGAGCAGCATGGAGCCTTCGGAAGCTTCCGAAGGCTCCATGCTGCTCC	
shp16-2-TOP	Type 2, Top oligo		CCGGGACCGTAACTATTCGGTGCGTTGGGCAGAAGCTTGTGCTCAACGCACCGAATAGTTGCGGTCTTTTT	Eric Campeau/ Christian Beausejour
shp16-2-BOT	Type 2, Bottom oligo		AATTAAAAAGACCGCAACTATTCGGTGCGTTGAGCACAAGCTTCTGCCCAACGCACCGAATAGTTACGGTC	
shp16-3-TOP	Type 3, Top oligo		CCGGGCGCTGCCCAACGCACCGAATCTCGAGATTCGGTGCGTTGGGCAGCGCTTTTT	The RNAi consortium

shp16-3-BOT	Type 3, Bottom oligo		AATTAAAAAGCGCTGCCCAACGCACCGAATCTCGAGATTCGGTGCGTTGGGCAGCGC	(TRCN0000039751)
shp16-4-TOP	Type 4, Top oligo		CCGGGCATGGAGCCTTCGGCTGACTCTCGAGAGTCAGCCGAAGGCTCCATGCTTTTT	The RNAi consortium (TRCN0000010482)
shp16-4-BOT	Type 4, Bottom oligo		AATTAAAAAGCATGGAGCCTTCGGCTGACTCTCGAGAGTCAGCCGAAGGCTCCATGC	
shLuc-TOP	Non-target control, Top oligo	Luciferase	CCGGATGTTTACTACACTCGGATATCTCGAGATATCCGAGTGTAGTAAACATTTTTT	The RNAi consortium (TRCN0000072254)
shLuc-BOT	Non-target control, Bottom oligo		AATTAAAAAATGTTTACTACACTCGGATATCTCGAGATATCCGAGTGTAGTAAACAT	

2.14 Antibodies

Table 2.4 Primary antibodies used in this study

Antigen	Host	Clone	Application	Dilution	Supplier	Catalog number
β-Tubulin	Mouse	TUB 2.1	WB	1:3000	Sigma-Aldrich	T4026
DYKDDDDK	Goat	Polyclonal	WB/IF	1:1000	Novus Biologicals	NB600-344
FLAG	Mouse	M2	WB	1:1000	Agilent	200472-21
GAPDH	Rabbit	Polyclonal	WB	1:3000	Abcam	ab9485
γH2AX (S139)	Mouse	JBW301	IF	1:1000	Millipore	05-636
FKBP12	Rabbit	Polyclonal	WB	1:1000	Thermo Fisher Scientific	PA1-026A
Ki-67	Rabbit	Polyclonal	IF	1:250	Novus Biologicals	NB-500-170
Lamin B1	Rabbit	Polyclonal	WB	1:1000	Abcam	ab16048
p53	Mouse	DO-1	WB	1:250	Santa Cruz Biotechnology	sc-126
p16	Mouse	G175-1239	WB	1:1000	BD Biosciences	554079
p21	Mouse	F5	WB	1:250	Santa Cruz Biotechnology	sc-6249
SMC1	Rabbit	Polyclonal	WB	1:1000	Bethyl Laboratories	A300-055A
TRF-2	Rabbit	Polyclonal	IF	1:250	Novus Biologicals	NB110-57130
TERT	Rabbit	Y182	WB	1:1000	Abcam	ab32020

2.15 Plasmid vectors

Table 2.5 Plasmid vectors

Plasmid name	Description	Source
pBABE-hPOT1-hTERT	Retroviral expression of hPOT1-hTERT	(Armbruster et al., 2004) (Christopher Counter)
pDONR221	Gateway™ donor plasmid	Invitrogen/Thermo-Fisher
pENTR-hPOT	hPOT1-hTERT Gateway™ entry plasmid	This study
pLENTI6/V5-DEST	Lentiviral expression vector Gateway™ destination plasmid	Invitrogen/Thermo-Fisher
pLENTI6-hPOT1-hTERT	Lentiviral expression of hPOT1-hTERT	This study
pLKO-puro-IPTG-3xLacO	IPTG-inducible shRNA expression plasmid	Invitrogen/Thermo-Fisher
pLKO-IPTG-shp53-1	IPTG-inducible expression of shRNA to knockdown p53 (type 1)	This study
pLKO-IPTG-shp53-2	IPTG-inducible expression of shRNA to knockdown p53 (type 2)	This study
pLKO-IPTG-shp16-1	IPTG-inducible expression of shRNA to knockdown p16 (type 1)	This study
pLKO-IPTG-shp16-2	IPTG-inducible expression of shRNA to knockdown p16 (type 2)	This study
pLKO-IPTG-shp16-3	IPTG-inducible expression of shRNA to knockdown p16 (type 3)	This study
pLKO-IPTG-shp16-4	IPTG-inducible expression of shRNA to knockdown p16 (type 4)	This study
pLKO.1 hygro	Constitutive shRNA expression plasmid	Bob Weinberg
pLKO.1-hygro-shp16-1	Constitutive shRNA expression to knockdown p16 (type 1)	This study
pLKO.1-hygro-shp16-2	Constitutive shRNA expression to knockdown p16 (type 2)	This study
pLKO.1-hygro-shp16-3	Constitutive shRNA expression to knockdown p16 (type 3)	This study
pLKO.1-hygro-shp16-4	Constitutive shRNA expression to knockdown p16 (type 4)	This study

pMDLg/pRRE	Lentiviral packaging plasmid for Gag, Pol and RRE expression	(Dull et al., 1998) (Didier Trono)
pMD2.G	VSV-G expressing envelope plasmid	Didier Trono
pRSV-Rev	Rev cDNA expressing plasmid	(Dull et al., 1998) (Didier Trono)

Chapter 3 Results - A cellular model of inducible-degradation of telomerase

3.1 Introduction

Telomerase plays an essential role during embryonic development and adulthood by maintaining the proliferative capacity of embryonic stem cells and adult/somatic stem cells respectively (Hiyama et al., 1996; Morrison et al., 1996; Wright et al., 1996; Amit et al., 2000; Xu et al., 2001; Wright et al., 2001). However, telomerase activity is significantly higher in embryonic stem cells compared to adult/somatic stem cells, resulting in a more limited proliferative capacity in the latter (Reviewed in (Hiyama and Hiyama, 2007)). On the other hand, somatic cells (not stem cells) do not express telomerase or have no detectable telomerase activity (Kim et al., 1994; Wright et al., 1996). These observations suggest a fine-tuning mechanism of telomerase expression regulation and suggest a linear relationship to proliferative capacity/self-renewal. Furthermore, although telomerase is expressed in ~90% of cancers, telomere length of primary cancer cells is shorter compared to the adjacent normal somatic cells (Shay and Bacchetti, 1997; Barthel et al., 2017). This suggests that telomerase expression in cancer cells is sufficient to counter but inadequate to overcome telomere shortening and therefore, maintain telomeres at a short length. In contrast, somatic stem and progenitor cells cannot maintain telomere lengths during cellular division despite having detectable levels of telomerase activity, eventually reaching to senescence as reported in cell culture studies (Harley, Futcher and Greider, 1990; Vaziri et al., 1994; Hiyama et al., 1996). Therefore, a cell model allowing precise tuning of telomerase levels would be very useful for studying the role of telomerase in various developmental and pathological disorders, involving variable telomerase protein levels. The following chapter will describe the characterisation of a human fibroblast cell line expressing telomerase whose protein levels can be controlled by fusing a destabilising domain to hTERT coding sequence. This cell line was used in this study to investigate the role of telomerase in senescence reversal, once senescence is established.

3.2 Establishment of MRC-5 cells expressing hTERT fused to a destabilising domain

To allow a tuneable and reversible control of hTERT protein, a destabilising domain (DD) tag derived from a F36V/L106P mutated FKBP12 protein (Banaszynski et al., 2006) was utilised by fusing the DD-tag to the N-terminus of hTERT. The DD-tag is inherently unstable due to protein misfolding and, when fused to another protein, can target it for degradation via the ubiquitin-proteasome pathway (Egeler et al., 2011). A small molecule ligand called Shield-1 could prevent the degradation of the DD-fusion protein by specifically binding to the DD-domain, allowing proper folding, and resulting in the stabilisation of the tagged protein (Figure 3.1). This process can be reversed by addition or removal of Shield-1. The cDNA encoding for the fusion protein DD-hTERT was cloned into a pBABE-Neo retroviral vector (pBABE-DDΔpthTERTNeo) and MRC-5 lung fibroblasts were transduced with the construct (Katrina Gordon, Unpublished).

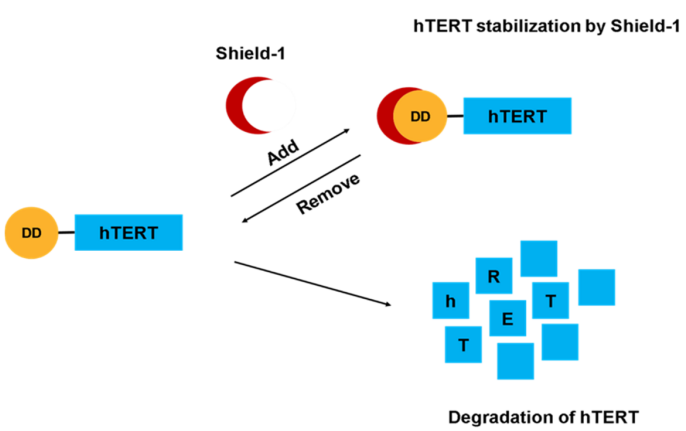

Figure 3.1 hTERT fused to a destabilising domain (DD).
Fusing hTERT to a DD-tag allows reversible stabilisation of hTERT in the presence of a Shield-1 ligand.

To measure if, in the cellular context, Shield-1 addition could stabilise enough DD-hTERT fusion protein to result in detectable telomerase activity, I performed a TRAP assay. MRC-5 DD-hTERT cells were cultured with and without 700 nM Shield-1 for 7 days prior to harvesting and analysis by TRAP assay (Figure 3.2). Previous observations had indicated that telomerase activity measured by TRAP assay reached a plateau above this concentration (Katrina Gordon, Stancheva lab, unpublished), suggesting that 700 nM Shield-1 is sufficient to achieve maximal stabilisation. Wild-Type MRC-5 (WT) cells, which do not express telomerase, and MRC-5 hTERT cells, which constitutively overexpress hTERT, were used as negative and positive controls, respectively. Whole cell extracts from control cells and MRC-5 DD-hTERT cells cultured with and without Shield-1 for 7 days were subjected to the TRAP assay and the resulting PCR products were analysed onto a 10% polyacrylamide gel (Figure 3.2.A). In agreement with absence of hTERT expression, WT cells showed no detectable TRAP ladder formation. On the other hand, MRC-5 hTERT showed strong TRAP ladder formation, as expected from high, constitutive overexpression. MRC-5 DD-hTERT cells cultured without Shield-1 showed a substantial reduction of telomerase activity to a level only detectable at the highest cell number used (2000 cells). In contrast, addition of 700 nM of Shield-1 resulted in a robust increase in telomerase activity, comparable to MRC-5 hTERT cells. To assess the rate of decrease in telomerase activity following removal of Shield-1, MRC-5 DD-hTERT cells were cultured without Shield-1 and were harvested at 0, 2, 4- and 8-days following Shield-1 removal (Figure 3.2.B). Removal of Shield-1 from the cell culture media showed progressive reduction in telomerase activity of MRC-5 DD-hTERT cells, which reached the lowest level on the eighth day. These data suggest (1) A negligible level of background expression of DD-hTERT in absence of Shield-1; (2) A slow turnover of the fusion protein once Shield-1 is removed from the culture media. One week of culture is indeed required to achieve to the lowest level of telomerase activity upon Shield-1 removal.

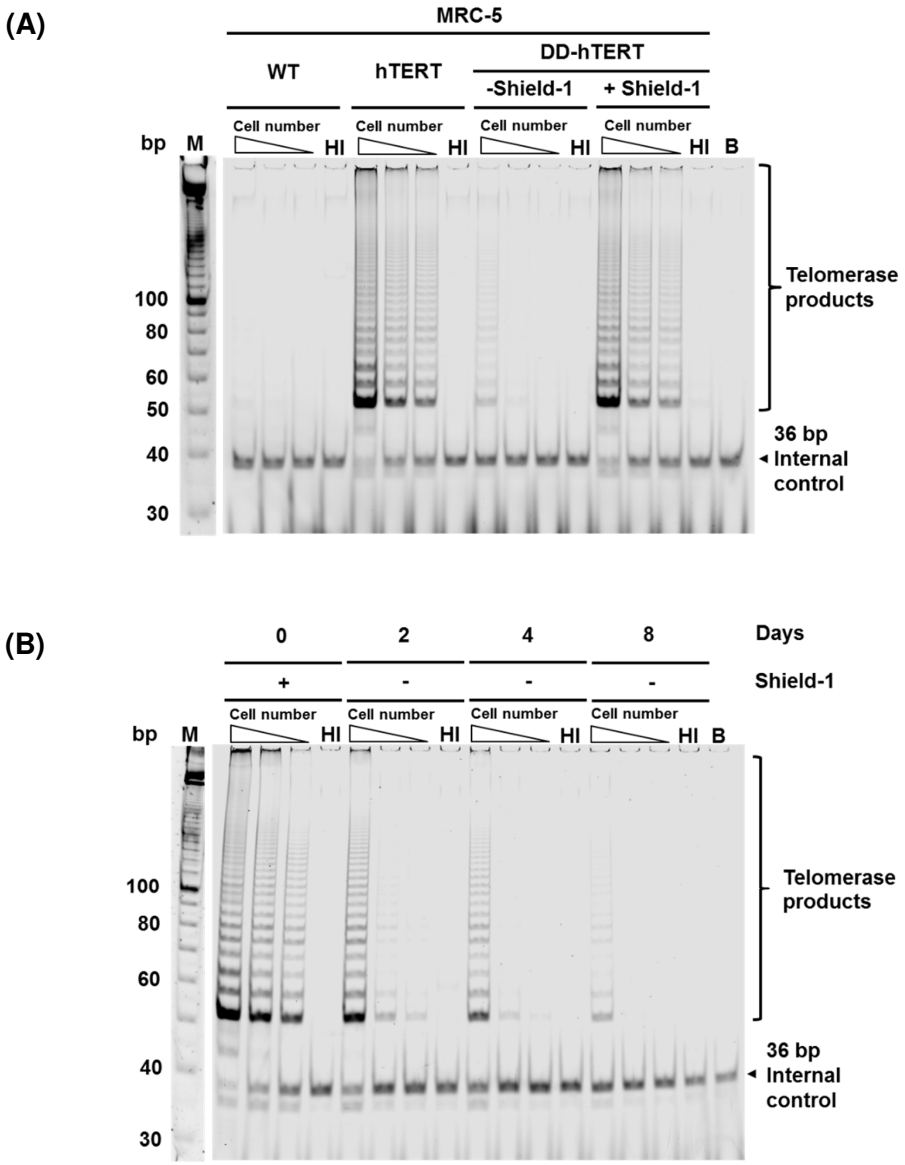

Figure 3.2 Telomerase activity can be modulated by Shield-1 treatment in MRC-5 DD-hTERT cells.

Whole cell extracts obtained from the equivalent of 2000, 400 and 80 cells, were used for TRAP assay, from the indicated cell lines. Whole cell extracts equivalent to 2000 cells, heated for 10 minutes at 80 °C were used as heat-inactivated controls “HI”, while buffer control “B” contains the entire reaction mix except the cell extract. 10 bp DNA ladder was used as a sizing marker and detected separately via EtBr staining. (A) MRC-5 DD-hTERT cells treated with Shield-1 for 7 days. (B) Telomerase activity measured in MRC-5 DD-hTERT cells following removal of Shield-1 for 2, 4 and 8 days.

To asses if prolonged period of culture could select for cells constitutively expressing hTERT, either via removal of the DD-tag or reactivation of endogenous hTERT gene, MRC-5 DD-hTERT cells were cultured with and without Shield-1 and harvested at passage 13, 24 and 33. Whole cell extracts were subjected to TRAP assay to assess telomerase activity at three different passage numbers (Figure 3.3). MRC-5 DD-hTERT cells cultured continuously with Shield-1 showed consistent telomerase activity in the three different passages tested, comparable to the positive control. This was also the case with MRC-5 DD-hTERT cells cultured continuously without Shield-1, where telomerase activity is consistently low with increasing passage number compared to the positive control. This result suggests that endogenous reactivation of telomerase or DD-tag inactivation did not occur following prolonged culture *in vitro*.

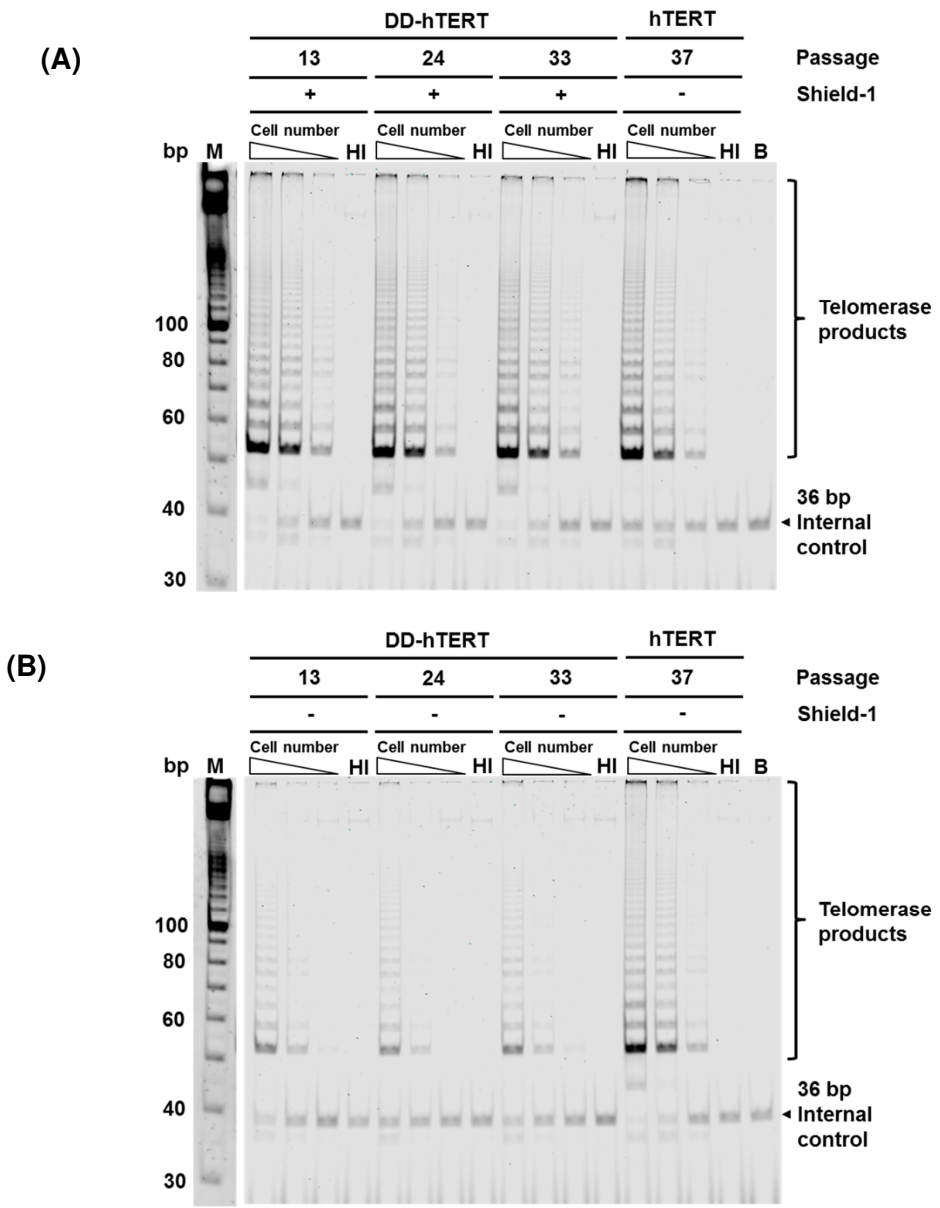

Figure 3.3 No selection for constitutive hTERT expression was observed in MRC-5 DD-hTERT cultured without Shield-1 following prolonged culture.

Whole cell extracts of MRC-5 DD-hTERT cells equivalent to 2000, 400 and 80 cells were used for TRAP assay. MRC-5 hTERT was used as positive control for telomerase activity. Heat-inactivated extract "HI" and lysis buffer only "B" were used as negative controls. Telomerase activity of MRC-5 DD-hTERT cells cultured with Shield-1 (A) and without Shield-1 (B) at passage 13, 24 and 33 is showed here.

3.3 MRC-5 DD-hTERT cells undergo senescence due to shortening of the telomeres

Although MRC-5 DD-hTERT cells continuously cultured without Shield-1 (MRC-5 DD-hTERT -Shield-1) show very low telomerase activity compared to MRC-5 DD-hTERT cells continuously cultured with Shield-1 (MRC-5 DD-hTERT +Shield-1), the TRAP assay detects persistent low-levels of hTERT activity in the former. As one of the aims of this project is to investigate whether telomerase reactivation could promote escape from cellular senescence, it was crucial to asses if the background level of DD-hTERT activity in absence of Shield-1 would be sufficient to prevent senesce. To investigate whether MRC-5 DD-hTERT -Shield-1 cells could undergo senescence, cumulative population doublings (CPD) was measured in MRC-5 DD-hTERT cells cultured with and without Shield-1 up to 190 days in three separate replicate cultures (Figure 3.4). MRC-5 DD-hTERT +Shield-1 cells showed a constant increase of CPD throughout the 190 days of culture, indicating that these cells do not undergo senescence. There is some variability in the rate of growth measured for the triplicate MRC-5 DD-hTERT cells + Shield-1 (Fig. 3.4). One possible explanation is that prolonged culture could have led to selection of a mutated, faster growing sub-clone, at least in one case. However, these cells become contaminated by mycoplasma during the prolonged culture. I treated them at different time points with BM-Cyclin (Roche, Basel, Switzerland) to eliminate the contamination without interrupting the experiment. However, this has introduced a variable that could explain the differences in growth rate. The two cultures that have slower growth rate, suffered from persistent mycoplasma infection, which require longer treatment compared to the faster growing culture. More importantly, however, MRC-5 DD-hTERT -Shield-1 cells showed a decrease in the rate of CPD compared to MRC-5 DD-hTERT +Shield-1 at approximately 35 PD. Furthermore, the population doubling curve showed a gradual flattening from 40 - 47 PD (~100-190 days in culture) which suggests that these cells were ceasing cell division.

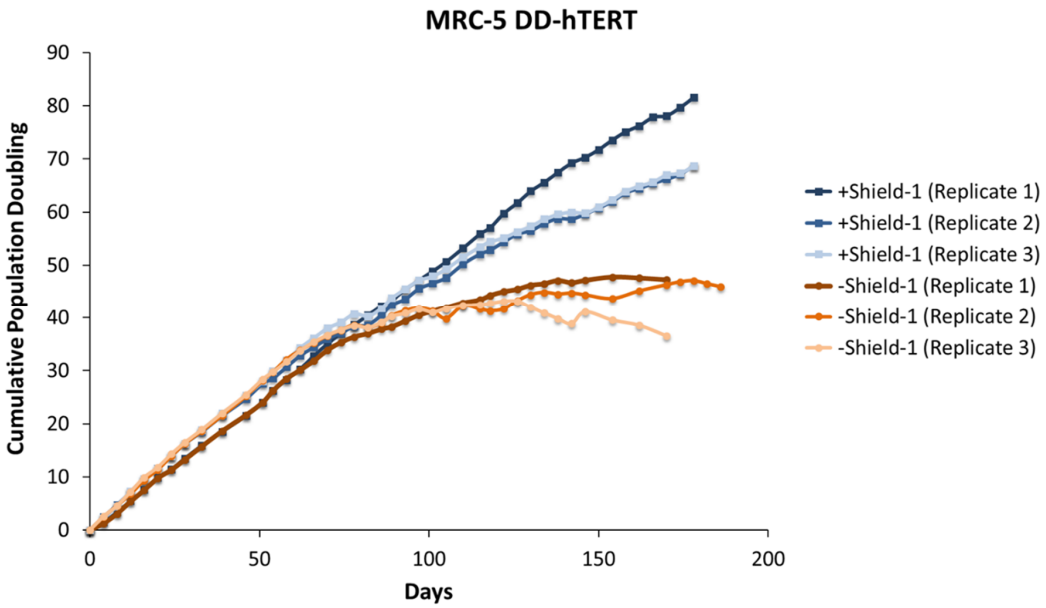

Figure 3.4 MRC-5 DD-hTERT cells cultured without Shield-1 undergo growth arrest at 40 - 47 PD.
Calculated cumulative population doublings of three replicates of MRC-5 DD-hTERT cells cultured with or without Shield-1 for 190 days.

To confirm that the growth arrest was due to replicative senescence, telomere length and senescence were examined in these cells by TRF Southern blot and senescence-associated β-galactosidase (SA-β-gal) staining, respectively. MRC-5 DD-hTERT cells were continuously cultured with and without Shield-1, harvested at 5, 15, 25 and 35 PD and subjected to TRF Southern blot (Figure 3.5). The results showed that +Shield-1 cells have a constant mean telomere size of 8 kb. In contrast, -Shield-1 cells showed decreasing mean telomere size, from 8 kb at 5 PD to 4.5 kb at 35 PD. MRC-5 hTERT control cells maintain a stable mean telomere length of 10 kb, while I could not measure telomere length in MRC-5 WT cells, presumably due to a very weak signal caused by high variability of telomere lengths. These results confirmed that telomere shortens with increasing population doublings in MRC-5 DD-hTERT cells cultured without Shield-1 but not in cells cultured with Shield-1, supporting the idea that growth arrest observed between 40 to 47 PD could be due to critically

short telomeres. From 25-35 PD, average size of telomeres of MRC-5 DD-hTERT -Shield-1 seems to have plateaued at ~4.5 kb. Therefore, due to this observation and technical consideration involved in obtaining sufficient DNA for the fluorescent TRF southern blotting (30 µg) in non-dividing cells, telomeres at 40-47 PD were not measured. To further verify the hypothesis that MRC-5 DD-hTERT -Shield-1 cells undergo senescence at 40-47 PD, I have quantified the fraction of the population that has entered senescence in MRC-5 DD-hTERT +/- Shield-1 cells at 70 and 47 PD respectively. Both of the MRC-5 DD-hTERT +/-Shield-1 have been cultured in parallel from the start and by the time -Shield-1 cells were fully arrested, the +Shield-1 cells have reached 70 PD. By measuring senescence-associated β-galactosidase activity (SA-β-Gal), it appears that 75% of -Shield-1 cells at 47 PD and 9% of +Shield-1at 70 PD have entered senescence (Figure 3.6). Together, telomere shortening and entry into senescence, suggest that growth arrest at ~40 PD of MRC-5 DD-hTERT cells -Shield-1 is due to the presence of enough critically short telomeres to trigger the DNA damage response and consequent growth arrest, consistent with previous reports (Bodnar et al., 1998; d'Adda di Fagagna et al., 2003).

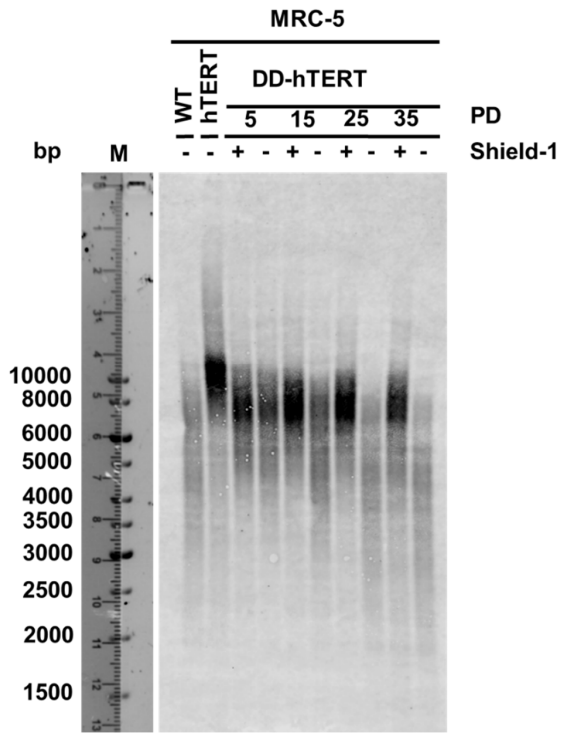

Figure 3.5 Telomeres of MRC-5 DD-hTERT cells shorten with each population doubling in the absence of Shield-1.
MRC-5 DD-hTERT cells cultured with or without Shield-1 were harvested at 5, 15, 25 and 35 population doublings (PD) and subjected to TRF Southern blot. MRC-5 WT and MRC-5 hTERT cells were used as controls for short and long telomeres, respectively. 1 Kb DNA ladder was used as size marker (M) and was stained with EtBr and detected separately by UV illumination.

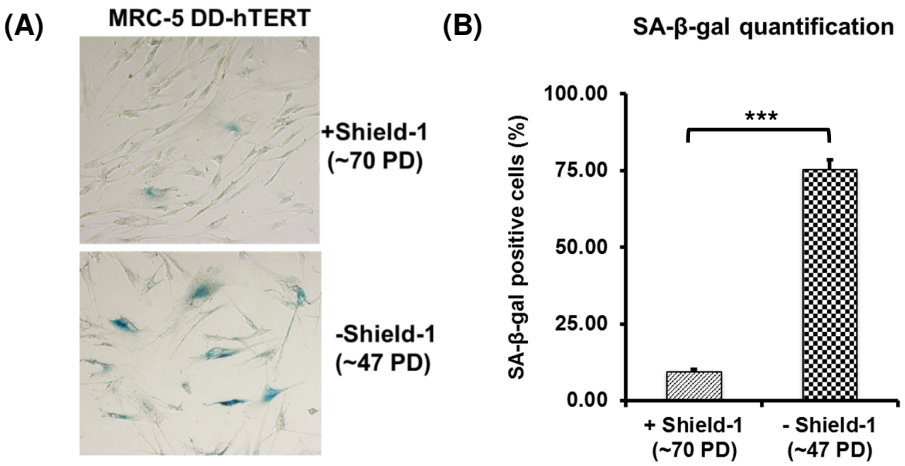

Figure 3.6 The majority of the cells in MRC-5 DD-hTERT -Shield-1 cultures have entered senescence by ~47 PD

Senescence was assayed by SA-β-gal assay in MRC-5 DD-hTERT +Shield-1 (~70 PD) and -Shield-1 (~47 PD) cells. (A) Representative images. (B) Quantification of SA-β-gal positive cells (mean of 3 experiments). Error bars represent SEM. p-value ≤ 0.0001 by unpaired student T-test.

3.4 Discussion

The results of the initial experiments presented above, aimed at characterising MRC-5 DD-hTERT cell line, support its suitability to investigate the role of telomerase in reversing entry into senescence. DD-hTERT fusion protein is fully functional, as indicated by the fact that MRC-5 DD-hTERT cells cultured with Shield-1 behaved similarly to MRC-5 hTERT, in that they are both capable of prolonged survival in culture, far surpassing the proliferation capability of MRC-5 WT cells. Moreover, fusing the DD domain to hTERT allows efficient control of hTERT levels, as shown by the fact that removal of Shield-1 from the culture media results progressive telomere shortening and cells undergoing senescence at 40-47 PD. Interestingly, the background levels of telomerase activity measured in MRC-5 DD-hTERT -Shield-1 cells could be similar to the low, basal levels of telomerase activity in some adult/ somatic

stem cells, which extend proliferation potential compared to somatic cells, but are insufficient to prevent cellular senescence (Kim et al., 1994; Hiyama et al., 1996). To investigate this further, MRC-5 DD-hTERT cells could be treated with varying concentrations of Shield-1 to test the correlation of telomerase activity with Shield-1 concentration and compare this to telomerase activity in various stem cells. This could also assist in elucidating the hTERT or telomerase cellular levels that is required for immortality in stem cells and cancers.

I have shown that 8 days of culture in the absence of Shield-1 is required to reach a low level of telomerase activity, comparable to the background. The slow kinetics of destabilisation of the fusion protein could be influenced by some Shield-1 remaining within the cell upon removal from the culture medium. Treating the cells with purified F36V DD protein would allow a more rapid removal of Shield-1 from the cells by competitive binding of Shield-1 ligands to F36V DD protein (Egeler et al., 2011). Although this approach could improve the kinetics of destabilisation, it would not solve the issue of residual DD-hTERT remaining in absence of Shield-1. In the original experiment where a YFP reporter protein was fused to the FKBP L106P DD domain, basal levels of YFP expression at 1-2% of DD-YFP in the absence of Shield-1 (Banaszynski et al., 2006) were also detected, indicating that it is not possible to get a complete removal of a target protein using this system. Others have also confirmed this observation of residual protein levels in the absence Shield-1 using the FKBP-based DD system (Maji et al., 2017; Qi et al., 2017). This could be a disadvantage when studying a protein which only require a small protein quantity in order to perform its cellular function. However, this does not appear to be the case for hTERT. There are other destabilising domains or degrons such as the ecDHFR DD (Iwamoto et al., 2010) and the Auxin-inducible Degron (AID) (Nishimura et al., 2009), which are based on engineered mutants of *Escherichia coli* dihydrofolate reductase and the *Arabidopsis thaliana* Auxin responsive protein IAA7 complemented with *Oryza sativa* TIR1 respectively, that could be used as an alternative to the FKBP-based DD system with

regards to the current protein and cell of interest. Latest improvements in these DD/Degron systems have made it possible to further minimise the basal protein levels in the absence of ligand (Shield-1 and Trimethoprim (TMP) for FKBP and ecDHFR DD respectively) (Kogenaru and Isalan, 2018) or the inefficient protein depletion in the presence of Auxin in the case with the AID system (Li et al., 2019).

Finally, my experiments show that MRC-5 DD-hTERT -Shield-1 cells undergo growth arrest ~15 PD later than MRC-5 WT cells (Gordon et al., 2014). This discrepancy is potentially explained by the fact that MRC-5 DD-hTERT are cultured in the presence of Shield-1 for ~23 PD prior to the start of the extended culture experiments. As a consequence, the average telomere length of MRC-5 DD-hTERT -Shield-1 at the start of the experiment would be longer than for MRC-5 WT cells. This hypothesis is confirmed by the TRF southern blot data (Figure 3.5) which showed that at 5 PD, the mean telomere length of MRC-5 DD-hTERT -Shield-1 cells was approximately 8 kb, similar to MRC-5 DD-hTERT +Shield-1 cells.

Chapter 4 Results - Reactivation of telomerase cannot induce escape from replicative senescence

4.1 Introduction

Critically short telomeres activate the senescence program as a consequence of the activation of the DNA damage response (DDR). The shortening of telomeric overhang and/or decreased quantity of TRF2 at telomeres can result in the loss of the T-loop protective structure, exposing telomere ends to be recognised as double strand breaks by the DDR (Li et al., 2003; Stewart et al., 2003; Takai, Smogorzewska and De Lange, 2003; Cesare et al., 2009). Accordingly, ectopic expression of the human telomerase catalytic subunit hTERT in various non-transformed human cells has been shown to prevent replicative senescence and induce immortalisation (Bodnar et al., 1998; Counter et al., 1998; Vaziri and Benchimol, 1998). However, it is unclear whether expressing telomerase in senescent cells could force them out of proliferation arrest, by elongating critically short telomeres and thus switching off the DDR. I therefore set out to investigate whether telomerase reactivation in MRC-5 DD-hTERT cells is sufficient to force proliferation once senescence is established.

4.2 Verification of reactivation of telomerase by Shield-1 treatment in senescent cells

I have previously shown that MRC-5 DD-hTERT cells cultured without Shield-1 undergo senescence at 40 - 47 PD (Figure 3.4). Furthermore, I have demonstrated that telomerase activity can be modulated by removal/addition of Shield-1 to MRC-5 DD-hTERT (Figure 3.2). To verify whether DD-hTERT stabilisation in senescent cells would lead to restoration of telomerase activity, pre-senescent (~35 PD) and senescent (~42 PD) MRC-5 DD-hTERT -Shield-1 cells were cultured with or without addition of Shield-1 for 7 days and telomerase activity was assessed by TRAP assay. MRC-5 DD-hTERT +Shield-1 (~35 and ~42 PD) and MRC-5 hTERT were used as positive controls

for telomerase activity. TRAP assay showed low telomerase activity in both pre-senescent and senescent MRC-5 DD-hTERT -Shield-1 cells compared to the positive controls (Figure 4.1). Furthermore, Shield-1 supplementation to both pre-senescent and senescent MRC-5 DD-hTERT -Shield-1 cells showed restoration of telomerase activity to both cells, comparable to the positive controls. This result confirmed that adding Shield-1 to senescent MRC-5 DD-hTERT cells could reactivate telomerase in senescent cells as well as in proliferating cells.

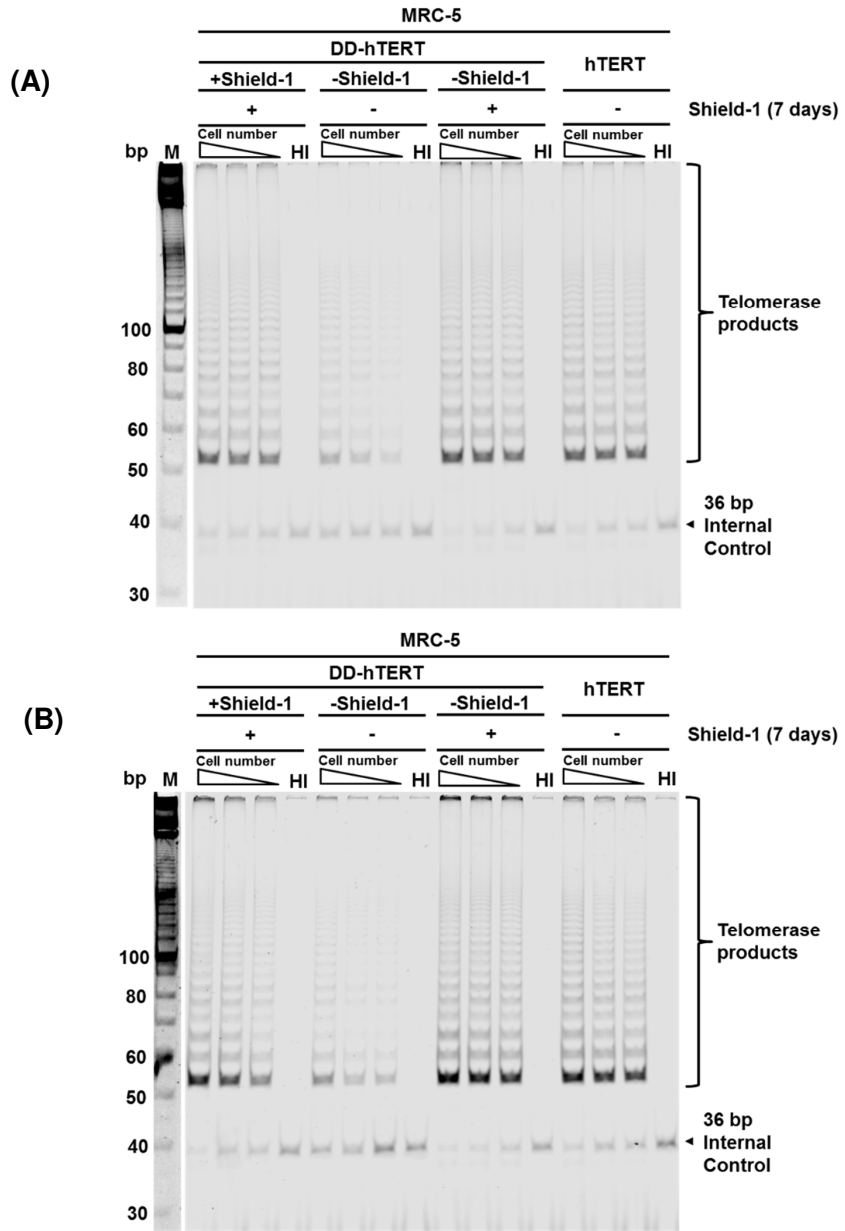

Figure 4.1 Telomerase activity is comparably restored upon Shield-1-mediated stabilisation of DD-hTERT in both pre- and senescent cells.
Whole cell extracts from (A) pre-senescent and (B) senescent MRC-5 DD-hTERT cells, equivalent to 2000, 400 and 80 cells, were subjected to TRAP assay and analysed as described previously. HI = heat-inactivated whole cell extracts. MRC-5 hTERT whole cell extract was used as a positive control. 10 bp DNA ladder was used as a sizing marker and detected separately via EtBr staining.

4.3 Senescent cells remain growth arrested following reactivation of telomerase by Shield-1 treatment

To investigate whether telomerase could reverse senescence, pre-senescent (~35 PD) and senescent (~42 PD) MRC-5 DD-hTERT -Shield-1 cells were re-supplemented with Shield-1 and cultured for 7 days. To assess senescence reversal, cell proliferation was measured by immunostaining for Ki-67, a proliferative marker (Gerdes et al., 1983; Bruno and Darzynkiewicz, 1992). MRC-5 DD-hTERT +Shield-1 cells, which were cultured continuously with Shield-1 and harvested at similar PD to the MRC-5 DD-hTERT -Shield-1, were used as a positive control for cellular proliferation. Quantification of Ki-67 positive cells showed that 70% of MRC-5 DD-hTERT +Shield-1 cells were proliferating at ~35 PD (Figure 4.2). On the other hand, at similar PD (equivalent to pre-senescent cells), the percentage of proliferating cells in MRC-5 DD-hTERT -Shield-1 culture was reduced to 60%. This might suggest that a small proportion of the cell population had already undergone proliferative arrest, possibly due to replicative senescence. Re-supplementation of Shield-1 to MRC-5 DD-hTERT -Shield-1 increased the proportion of proliferating cells to 64%. This suggest that reactivation of telomerase was able to prevent entry into senescence for a fraction of the pre-senescent cell population. At ~42 PD, the proportion of the population of MRC-5 DD-hTERT +Shield-1 cells proliferating (67%) was very similar to 35 PD (70%), indicating that continuous hTERT expression is sufficient to confer stable growth. On the contrary, only 3.4% of MRC-5 DD-hTERT -Shield-1 cells at ~42 PD were positive for Ki-67, irrespective of Shield-1 being added back to the culture medium or not (2.6%, Figure 4.2). This confirmed that the majority of cells cultured continuously without Shield-1 at ~42 PD were not dividing and possibly had entered senescence. Reactivation of telomerase by adding Shield-1 for 7 days to MRC-5 DD-hTERT -Shield-1 cells at ~42 PD did not affect the fraction of Ki-67 positive cells in the population. This result suggest that once senescence is established, telomerase reactivation could not force cells out of the arrest and therefore could not reverse senescence.

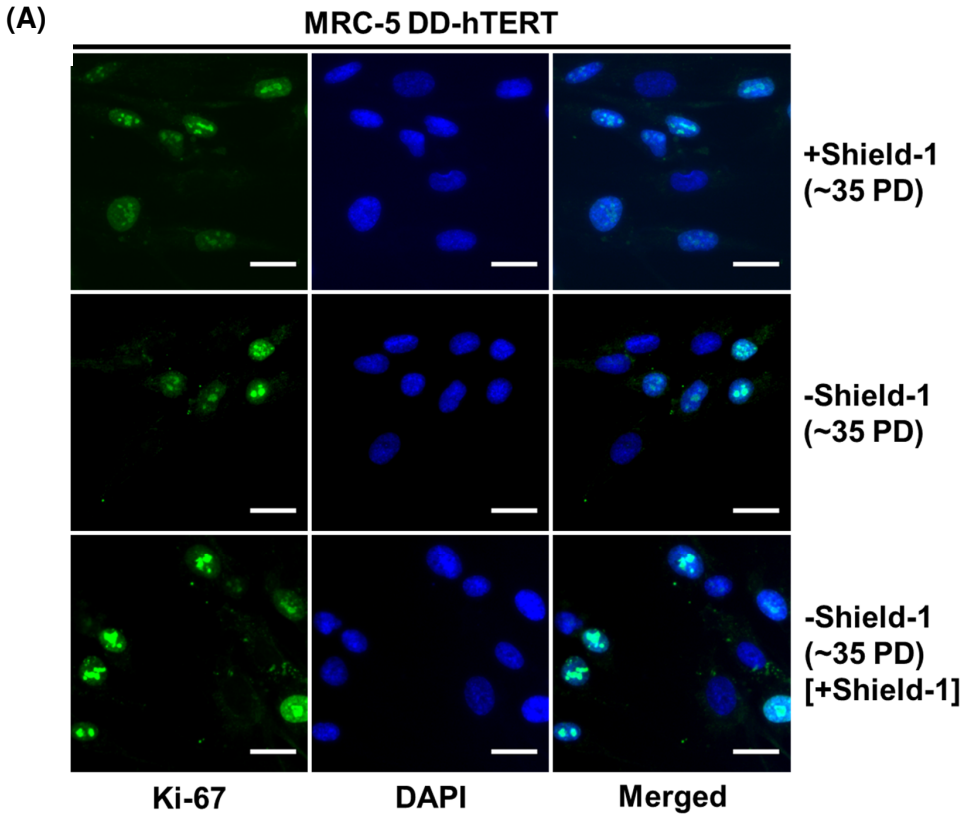

Figure 4.2 Stabilisation of hTERT can avoid entry into senescence for some pre-senescent cells.

(A) Representative images of Ki-67 immmunostaining (green) and DAPI (blue). Scale bar = 25 µm. (B) Mean number of Ki-67 positive cells. Error bars = SEM (n = 3).

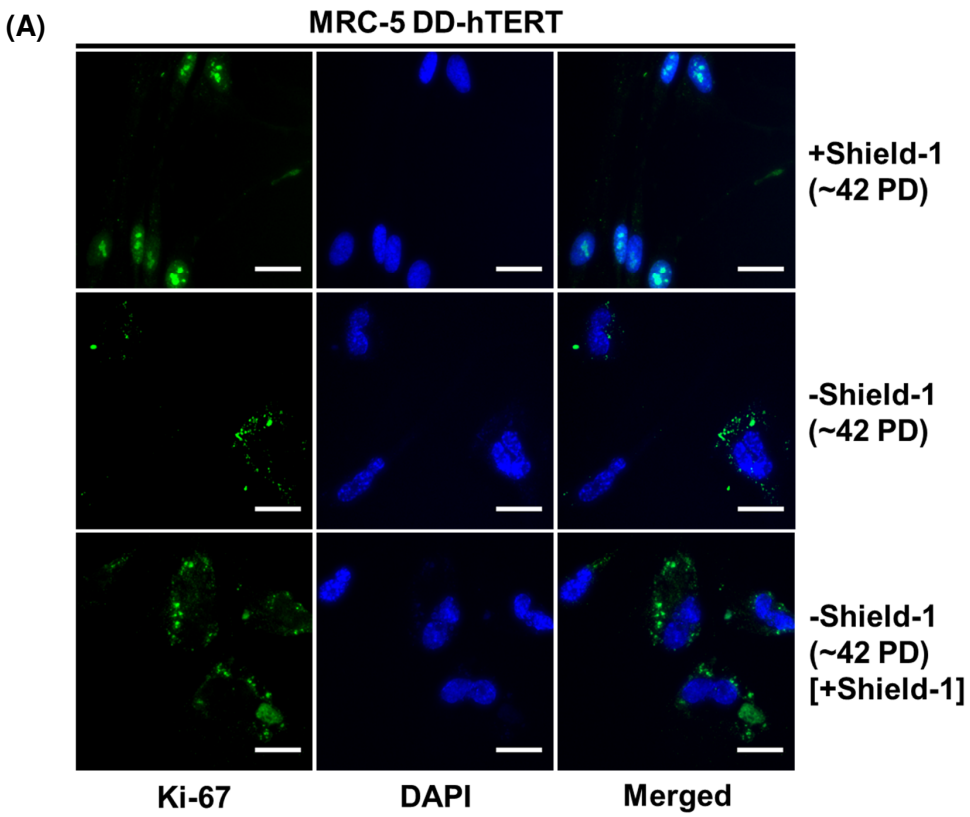

Figure 4.3 No proliferation was observed in senescent cells following telomerase reactivation for 7 days.

(A) Representative images of Ki-67 immmunostaining (green) and DAPI (blue). Scale bar = 25 µm. (B) Mean number of Ki-67 positive cells. Error bars = SEM (n = 3).

As an independent approach, I also quantified the number of proliferating cells in MRC-5 DD-hTERT cell population at ~35 and ~40 PD by flow cytometric analysis of EdU incorporation (Figure 4.4). EdU is a thymidine analogue incorporated into DNA during replication that can be labelled with Alexa Fluor 647 fluorophore via Click chemistry. In agreement with the data obtained by Ki67 immunostaining, in the pre-senescent -Shield-1 cells, there was a 6% increase in EdU positive cells following telomerase reactivation. On the other hand, no increase was observed in the senescent -Shield-1 cells following telomerase reactivation. Overall, the result of the EdU proliferation assay was in agreement with the Ki-67 immunostaining, confirming that telomerase is insufficient to abrogate senescence-associated proliferative arrest.

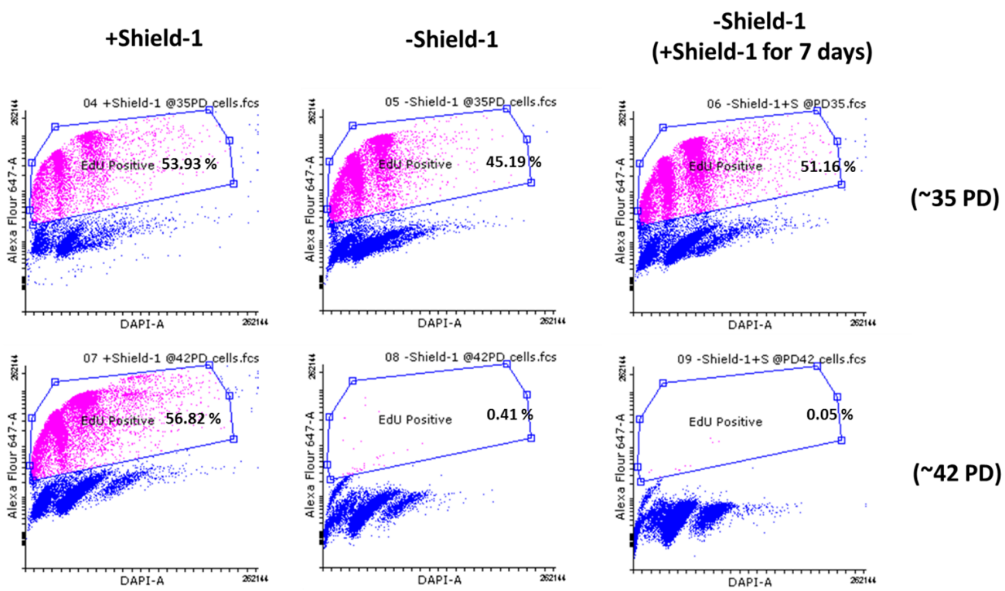

Figure 4.4 Senescent cells cannot be pushed back into proliferation by hTERT stabilization.
Upon treatment with Shield-1 as in Fig. 4.3, cells were pulsed with 10 µM EdU for 24 hours and ethanol-fixed. EdU was stained with Alexa Fluor 647 azide via click chemistry and DNA counterstained by DAPI. EdU incorporation subsequently quantified by flow cytometry.

4.4 Prolonged culture of senescent cells in Shield-1 did not affect proliferation

To rule out the possibility that the failure to reverse senescence could be due to insufficient time in Shield-1, MRC-5 DD-hTERT +Shield-1 cells, -Shield-1 cells and -Shield-1 cells re-supplemented with shield-1 (+S) were cultured for 26 days instead of 7, from ~35 PD (Pre-senescent -Shield-1 cells) and from ~42 PD (Senescent -Shield-1 cells). PD were tracked for both pre-senescent and senescent cells by determining the number of cells at seeding and at sub-culturing and calculating the PD using the formula in chapter 2.2. Cells were seeded constantly at 750,000 cells for each passage and passaged/sub-cultured at 90% confluency (every 3 – 5 days). After 10-days of culture, pre-senescent -Shield-1 cells showed a decline of PD rate as compared to immortal +Shield-1 cells, suggesting that a small proportion of the cell population entered growth arrest (Figure 4.5). Adding Shield-1 to reactivate telomerase in the pre-senescent cells was sufficient to avoid the decrease of PD rate (Figure 4.5). However, this was not the case when telomerase was reactivated in the senescent -Shield-1 cells. Similarly to what was observed for shorter culture, addition of Shield-1 and culture for 26 days were not sufficient to restore growth. These data suggest that pre-senescent but not senescent cells clearly responded to telomerase reactivation. Thus, I have confirmed that prolonged telomerase reactivation was unable to force cells to proliferate once the senescence program is established.

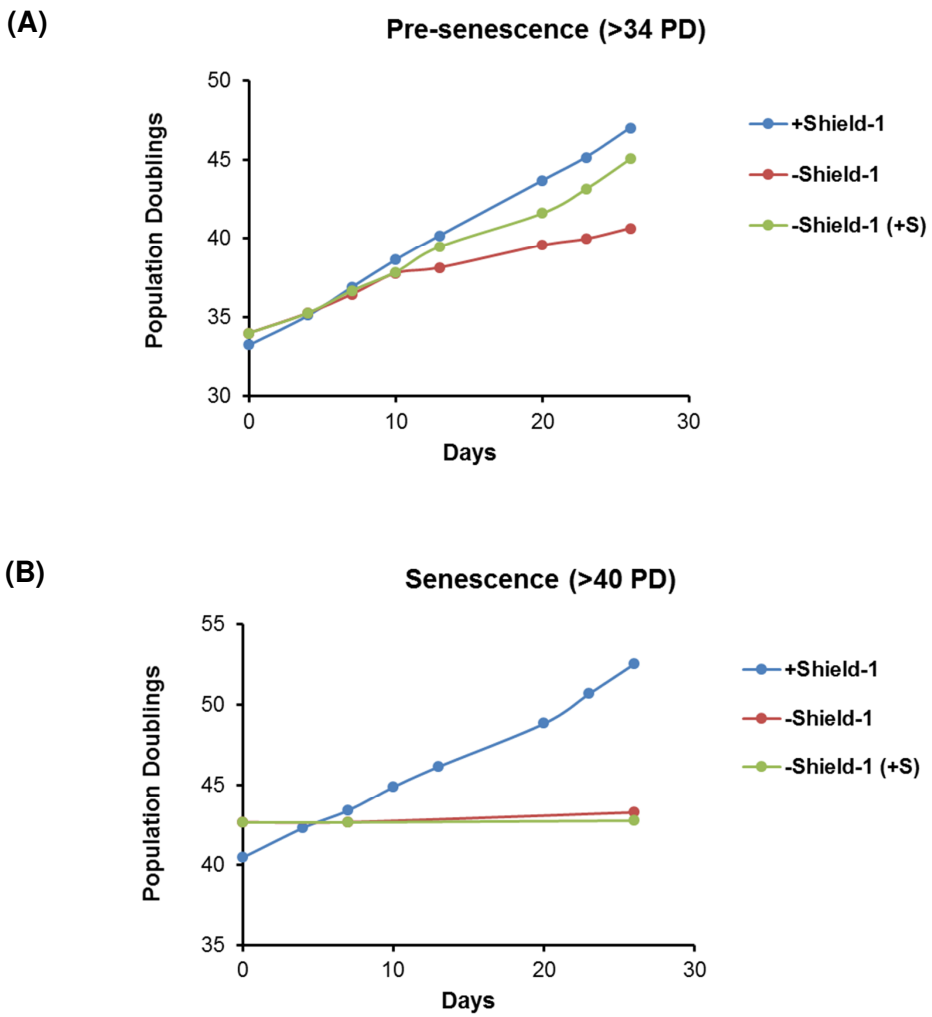

Figure 4.5 Prolonged culturing in presence of Shield-1 is not sufficient to restore proliferation of senescent cells.
MRC-5 DD-hTERT +Shield-1 was used as a positive control for proliferating cells. MRC-DD-hTERT continuously cultured without Shield-1 (-Shield-1) were cultured without or with Shield-1 (+S) for 26 days and the calculated PD is shown here for (A) pre-senescent -Shield-1 cells and (B) senescent -Shield-1 cells.

4.5 Effect of telomerase reactivation on pathways regulating senescence growth arrest

Lack of senesce reversal upon telomerase re-expression could be explained in two different ways. Stabilised DD-hTERT could be able to elongate critically short telomeres and shut down the DDR, but the cells could have reached a stable arrest, independent of the DDR. Alternatively, stabilised DD-hTERT cannot elongate critically short telomeres and therefore is unable to switch off the DDR. To distinguish between these hypotheses, I have analysed the expression of DDR components responsible for the induction of cell cycle arrest in senescent cells treated for 7 days with Shield-1. In general, p53 transcription factor and p16 cyclin dependent kinase inhibitor are associated with the activation and possibly maintenance of senescence. Senescent cells showed slightly lower p53 levels compared to proliferating cells, in agreement with the reduced levels of p53 downstream target p21. On the other hand, p16 levels were higher in senescent cells compared to proliferating cells. This suggests that proliferative arrest in MRC-5 DD-hTERT is mainly maintained by p16. In both proliferating and senescent cells, stabilisation of hTERT via Shield-1 treatment did not affect p53, p16 and p21 protein levels, suggesting that telomerase reactivation could not influence DDR signalling responsible for activation and maintenance of senescence. These data suggest that stabilised hTERT cannot elongate critically short telomeres in senescent cells or that telomere elongation is not sufficient to extinguish the DDR.

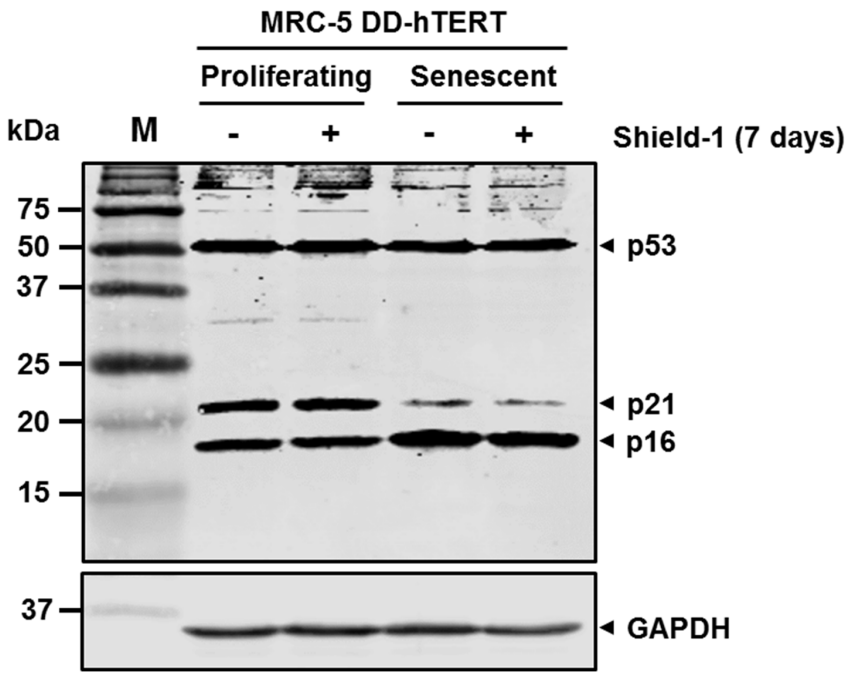

Figure 4.6 Telomerase reactivation does not affect p53, p21 and p16 levels.

Proliferating and senescent MRC-5 DD-hTERT cells cultured with and without Shield-1 were subjected to Western blot and probed with antibodies against p53 (53 kDa), p21 (16 kDa), p16 (16 kDa) and GAPDH (37 kDa). GAPDH was used as a loading control.

4.6 Discussion

One of the key hallmarks of cancer is cellular immortality. The importance of telomerase reactivation to achieve the indefinite proliferative potential of cancer cells is well recognised (Kim et al., 1994; Hanahan and Weinberg, 2011). Activation of telomerase has been shown to prevent replicative senescence and support proliferation of human endothelial and human primary colorectal carcinoma cells *in vitro* (Yang et al., 1999; Dalerba et al., 2005). Replicative senescence is defined as growth arrest resulting from DNA replication-induced telomere attrition. Therefore, telomerase should in theory be able to reverse replicative senescence by elongating telomeres. However, it has been previously reported that ectopic telomerase expression in replicatively senescent WI-38 and BJ fibroblasts is insufficient to rescue cell cycle arrest induced by the senescence program (Beauséjour et al., 2003). On the contrary, however, it has also been reported that telomerase expression could prevent oncogene induced senescence (OIS) in cells expressing oncogenic RAS and promotes reversal/escape from OIS (Suram et al., 2012; Patel et al., 2016). Although upregulation of telomerase was observed in cells that spontaneously escaped OIS, this does not prove that telomerase was responsible for bypassing the cell cycle arrest signalling associated with OIS.

p53-p21 and p16-pRb pathways have been shown to link the DDR to the induction of senescence (Shay, Pereira-Smith and Wright, 1991; Beauséjour et al., 2003). In my experiments, the inability of telomerase expression in senescent cells to reverse the growth arrest indicates that probably the DDR is still active, suggesting that telomeres are not being elongated (Figure 4.6). Moreover, aside from its role in telomere lengthening, it has also been suggested that TERT could have non-canonical roles in regulating cellular proliferation via Wnt/β-catenin or NFκB signalling pathways (Choi et al., 2008; Park et al., 2009; Ghosh et al., 2012; Ding et al., 2013). The results shown in this chapter suggest that hTERT stabilised in senescent cells was either unable of performing these non-canonical roles or that these functions are insufficient to abrogate senescence and restore cell proliferation.

The action of telomerase at telomeres has been known to be restricted to the S-phase of the cell cycle (Wright et al., 1999; Tomlinson et al., 2006; Jády et al., 2006). This was thought to be caused by increased accessibility of telomeres at S - G2/M phase of the cell cycle and association of telomerase activity at telomeres with the replication machinery required for telomeric C-rich strand replication (Verdun et al., 2005; Jády et al., 2006). Recent progress in the field have also shown that this was possibly due to the requirement of TCAB1-mediated G1/S recruitment of the telomerase holoenzyme complex to Cajal body, prior to trafficking to telomeres (Venteicher et al., 2009; Vogan and Collins, 2015). TPP1, which is known to recruit telomerase to telomeres, has been also shown to undergo S - G2/M specific phosphorylation at S111, potentially explaining the S-phase restriction of telomerase action at telomeres (Wang et al., 2007; Xin et al., 2007; Zaug et al., 2010; Zhang et al., 2013). Senescent cells have been shown to undergo cell cycle arrest predominantly in G1. Due to S-phase specific action of telomerase at telomeres, G1 cell cycle arrest in senescent cells could prevent telomerase to gain access to telomeres. Unfortunately, due to the unavailability of markers/tags for specific detection of DD-hTERT, I was unable to confirm the subcellular localisation of telomerase holoenzyme complex. As the TRAP assay indicates that DD-hTERT re-expressed in senescent cells is active, we can speculate that the telomerase complex is properly assembled, and is potentially localised in the nucleolus (Lee et al., 2014), as recruitment to Cajal bodies requires TCAB1 and is S-phase specific (Vogan and Collins, 2015). A TERT antibody (Abcam ab32020), which was successfully used for Western blots in this study could possibly be used to analyse DD-hTERT sub-cellular localisation. Alternatively, the TRAP assay results could be explained by the formation of an active telomerase complex *in vitro,* prior to assay. *In vitro* assembly of the telomerase holoenzyme has been previously reported (Weinrich et al., 1997; Masutomi et al., 2000), and lysing the cells may have abolished the distinct subnuclear localisation of hTR and hTERT, which prevent telomerase holoenzyme assembly in the senescent cells.

Chapter 5 Results - Pharmacological inhibition of p53 together with telomerase activation in senescent cells

5.1 Introduction

p53, also known as Tumour Protein 53 or TP53, is a tumour suppressor gene encoding for a transcription factor that acts as a crucial hub to control the activation of DDR, DNA repair, apoptosis (cell death) and senescence (permanent cell cycle arrest) genes. The DDR is a very complex molecular signalling cascade, initiated by sensor proteins detecting damaged DNA, such as the MRN complex and KU70/80, ATM, ATR and DNA-PK kinases that generate a diffusible signal, amplified by intermediate transducers such as CHK1 and CHK2, and effector proteins such as p53 and/or p16. These effectors have the role of coordinating the type of cellular responses, inducing a temporary or permanent cell cycle arrest, depending on the severity of the damaged cells (Reviewed in (Jackson and Bartek, 2009; Ciccia and Elledge, 2010)). A persistent activation of the DDR is required for the activation of cellular senescence and p53 plays an important role in senescence activation (Herbig et al., 2004; Fumagalli et al., 2012; Suram et al., 2012). p53 chronic activation leads to a persistent activation of the G1/S checkpoint, that blocks damaged cell from entry into S-phase. However, the role of p53 in maintenance of senescence is unclear. For example, inhibition of p53 using GSE-22 peptide is sufficient to abrogate senescence-associated cell cycle arrest and proliferation arrest in senescent BJ fibroblasts. However, WI38 fibroblasts cannot escape senescence upon p53 inhibition (Beauséjour et al., 2003). The differences in the response to p53 inhibition of these two cell lines is thought to be due to a cell-line intrinsic variability in the roles that the p53-p21 or p16-pRb pathways play in response to senescence-inducing stimuli. Interestingly, in MEFs, although both CDK inhibitors p21 and p16 are expressed during senescence, shRNA mediated knockdown of p53 is sufficient to abrogate senescence growth arrest (Dirac and Bernards, 2003). These reports confirm that there are variations in senescence maintenance pathways in cells with different genetic backgrounds. In the previous results

chapter, I have shown that the addition of Shield-1 to senescent MRC-5 DD-hTERT cells resulted in restoration of telomerase activity in these cells. However, this was insufficient to relief cell cycle arrest and reverse senescence. One of the reasons for this result could be that DD-hTERT cannot gain access to telomeres as cells do not enter S-phase due to persistent p53 signalling. In order to test this hypothesis, I decided to transiently inhibit p53, just enough to allow entry into S-phase. In order to set up a tightly controllable p53 inhibition, I choose to employ a p53 inhibitor Pifithrin-α, a compound initially discovered in a screening for inhibitors of p53-dependent transactivation of target genes, particularly in apoptosis (Komarov et al., 1999)(Figure 5.1).

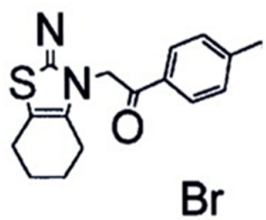

Figure 5.1 Chemical structure of Pifithrin-α.
Small molecule inhibitor of p53 [2-(2-imino-4,5,6,7-tetrahydrobenzothiazol-3-yl)-1-*p*-tolylethanone] or Pifithrin-α (Image taken from Komarov et al., 1999)

5.2 Pifithrin-α downregulates p53 and its downstream target p21

Pifithrin-α (PFT-α) is a small molecule inhibitor found to inhibit p53 and its downstream transcriptional target p21 (Komarov et al., 1999). To test PFT-α inhibition in MRC-5 WT and MRC-5 DD-hTERT, cells were cultured with 10 µM of PFT-α for 1, 24 and 72 hours (Komarov et al., 1999). Treated cells were harvested, lysed in RIPA buffer and protein extracts were analysed for p53 and p21 levels. In MRC-5 WT cells, no noticeable decrease of p53 protein

levels was observed from 1 to 72 hours of treatment. On the other hand, there was a clear reduction in p21 protein levels particularly after 72 hours of treatment in the WT cells. Reduction in basal p53 were much more evident in MRC-5 DD-hTERT compared to MRC-5 WT cells. This was possibly due to higher basal p53 protein expression in MRC-5 DD-hTERT cells. Although p21 is expected to decrease concomitant with decrease in p53 levels, it is unclear whether there is a decrease in p21 levels in MRC-5 DD-hTERT cells treated with PFT-α. Overall, these western blots showed that PFT-α was capable of inhibiting basal p53 or p21 protein expression in both cell lines used.

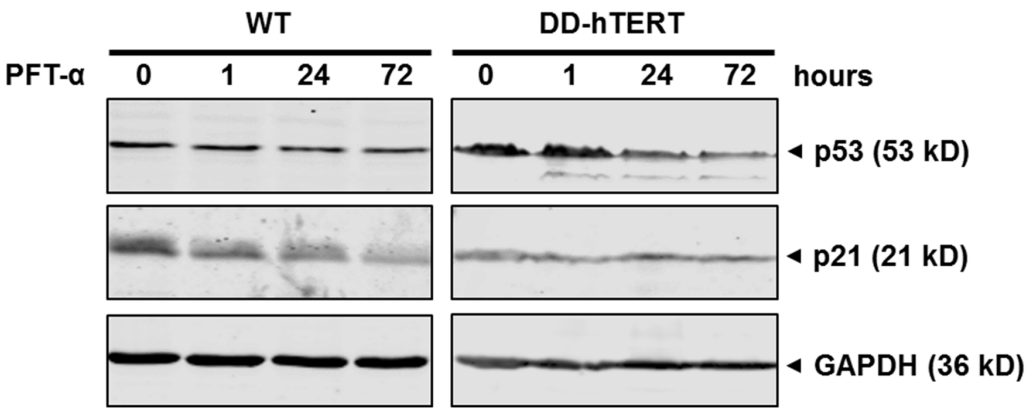

Figure 5.2 p53 and p21 downregulation was observed upon treatment with PFT-α for 72 hours.

MRC-5 WT and MRC-5 DD-hTERT cells were treated with 10 μM PFT-α and were subjected to Western blotting to detect p53, p21 and GAPDH (Loading control) proteins.

5.3 Senescent cells treated with Pifithrin-α remain growth arrested

Having validated PFT-α as a p53 inhibitor in my cells, I proceeded to test if PFT-α mediated inhibition of p53 in combination with telomerase reactivation can abrogate proliferation arrest and reverse senescence. Proliferating and senescent MRC-5 DD-hTERT cells at similar PD (~42 PD) were cultured for 7 days in the presence or absence of 10 μM PFT-α, in combination with 700 nM Shield-1. Media containing PFT-α plus Shield-1 or Shield-1 alone were replaced every 2 days to maintain the concentration of both chemicals in culture. SA-β-gal staining was used to assess the proportion of cells that have reversed senescence. In proliferating cells, no significant difference was observed in the small proportion (~ 1 %) of SA- β-gal positive stained cells in PFT-α treated compared to untreated cells (Figure 5.3). Similarly, treatment with PFT-α of senescent cells also did not affect the high proportion (~ 90%) of SA- β-gal positive stained cells in comparison with untreated cells. In a parallel experiment, I independently assessed reversion of senescence arrest by monitoring cell proliferation by cell count. Cells were cultured for 7 days in the presence or absence of 10 μM PFT-α, in combination with 700 nM Shield-1. Cells were counted at seeding (day 0), at day 4 and at day 7 for proliferating cells and at seeding and day 7 for senescent cells. This is to account for the differences in proliferation between both cell types. As expected, both proliferating cells, with and without PFT- α, showed increasing cell number across the 7-day time point (Figure 5.4). There was a slight increase in the number of cells counted at day 7 in the treated fraction. However, as this experiment was only performed once, I could not confirm whether the slight difference observed in the proliferating cells at day 7 was due to PFT-α treatment. However, both assays show that treatment of senescent cells with PFT-α is not sufficient to reverse senescence, irrespective of DD-hTERT stabilisation. In conclusion, these data suggest that PFT-α mediated p53 inhibition in combination with telomerase was unable to abrogate growth arrest and senescence in senescent MRC-5 DD-hTERT cells.

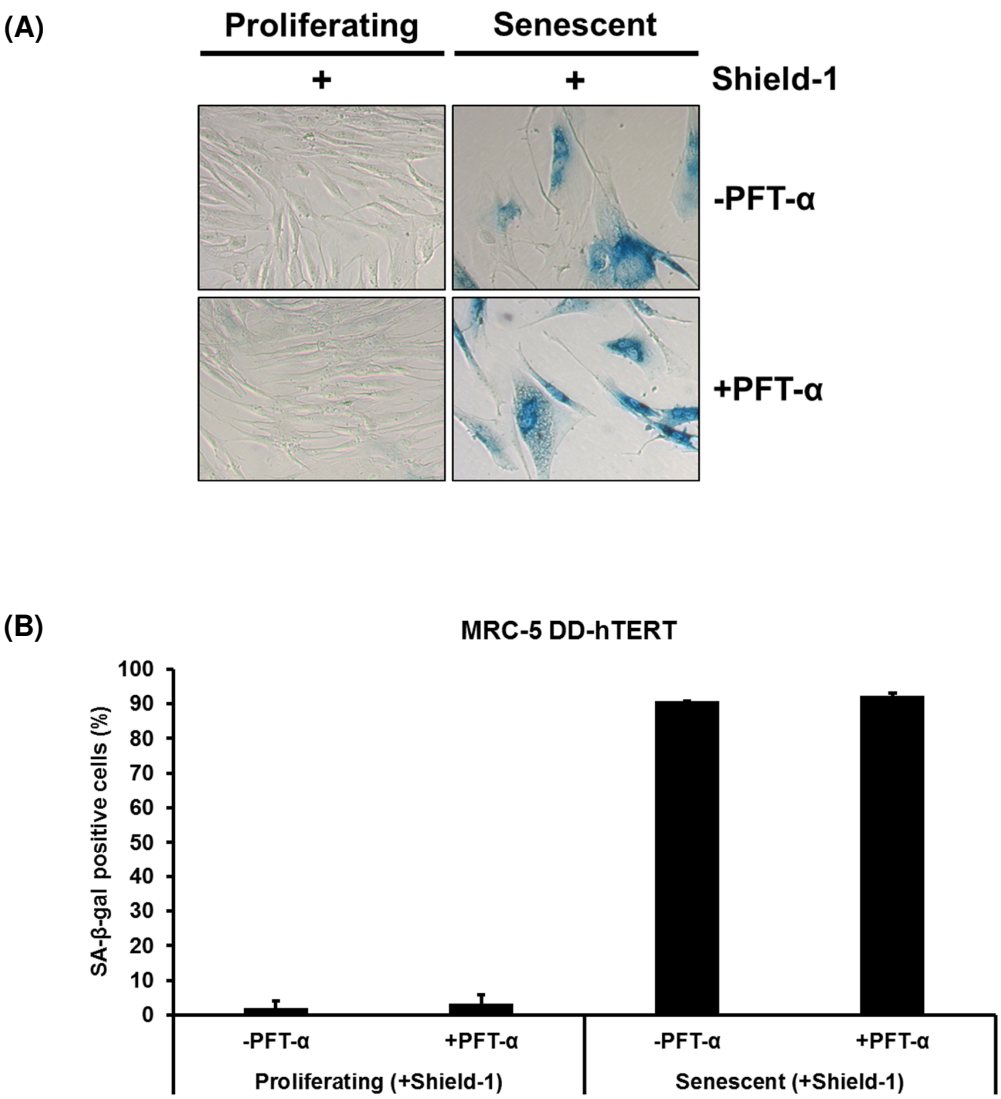

Figure 5.3 PFT-α in combination with telomerase-reactivation was unable to reverse senescence.

(A) Quantification of senescent cells in the population by SA-β-Gal staining. Representative images from brightfield microscopy are shown. (B) Quantification of SA-β-Gal positive MRC-5 DD-hTERT cells treated with and without 10 µM PFT-α in combination with 700 nM Shield-1 to re-activate telomerase. Data were shown as the mean ± SEM (n = 2).

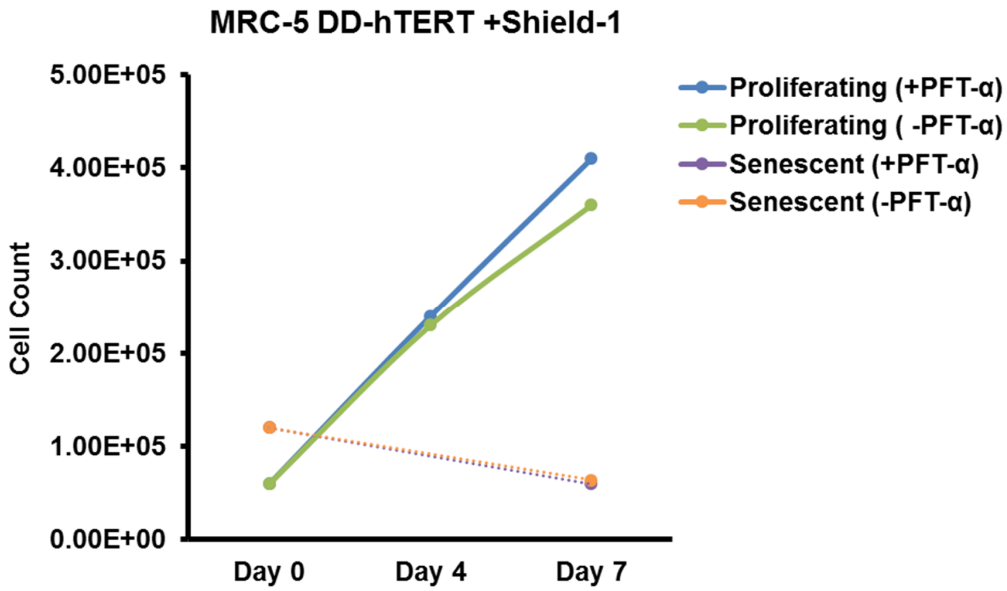

Figure 5.4 PFT-α in combination with telomerase-reactivation was unable to abrogate proliferation arrest of senescence MRC-5 DD-hTERT cells.

Proliferating and senescent MRC-5 DD-hTERT cells were both cultured in media containing Shield-1, in the presence or absence of PFT-α for 7 days. Cells were counted with a haemocytometer at day 0, 4 and 7 for proliferating cells and at day 0 and 7 for senescent cells.

5.4 Pifithrin-α was unable to inhibit p53 function in DNA damage response

The conclusion that p53 inhibition is insufficient to reverse senescence, even upon DD-hTERT stabilisation relies on the efficacy of PFT-α mediated p53 inhibition. However, a report from the same group that had discovered PFT-α has shown that PFT-α does not target p53 specifically (Komarova et al., 2003). As p53's role during induction of senescence is related to its function within the DDR, it is important to verify if PFT-α is in fact able inhibit p53 function in the context of DDR. I therefore treated MRC-5 WT or DD-hTERT cells with mitomycin-C (MMC) in the presence/absence of PFT-α. MMC is a DNA

crosslinking agent which activates the p53 DDR response and upregulate p21. Treatment with MMC increased p53 and p21 levels particularly in DD-hTERT cells. However, PFT-α was unable to prevent damage-dependent p53 upregulation, suggesting that PFT-α is does not efficiently inhibit p53 function during the DDR. This result suggests that PFT-α could inhibit p53 indirectly. Consequently, the inability of PFT-α treatment to reverse senescence in the experiments described in the previous paragraph is inconclusive, leaving open the possibility that direct p53 inhibition could achieve this effect.

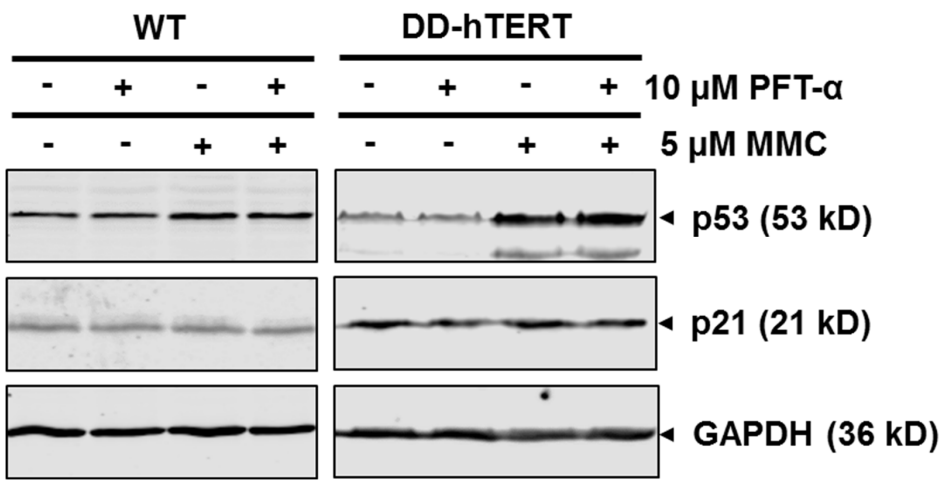

Figure 5.5 PFT-α was unable to inhibit p53 and p21 upregulation by the DDR pathway.

Western blot for p53 and p21 in MRC-5 WT and MRC-5 DD-hTERT cells treated with 5 μM of Mitomycin C in combination with 10 μM PFT-α. Treatment was done for 6 hours and 24 hours for MRC-5 WT and MRC-5 DD-hTERT respectively. GAPDH was used as a loading control.

5.5 Discussion

The experiments described in this chapter were aimed at investigating whether restoring entry into S-phase in senescent cells could be sufficient to grant stabilised DD-hTERT access to critically short telomeres. Elongation and restoration of functional telomeres could have led to shutting down of the DDR responsible for the maintenance of growth arrest. In order to allow entry into S-phase, I inhibited p53, which controls one of the two key pathways leading to the establishment of growth arrest during senescence. The results presented show that inhibition of p53 using PFT-α, with or without of Shield-1, in senescent MRC-5 DD-hTERT cells was not able to reverse senescence. I proposed that there are at least three possible explanations for this result: (1) PFT-α does not effectively inhibit p53, (2) PFT-α does not specifically target p53, (3) Inhibition of p53 alone is not sufficient to abrogate the senescence activated cell cycle arrest. I have shown that PFT-α does decrease p53 levels in proliferating MRC-5 DD-hTERT cells, ruling out that the inhibitor is generally ineffective. However, I have also shown that PFT-α is unable to prevent DNA damage-dependent p53 upregulation and therefore, presumably, ineffective at preventing p53-dependent DDR. As a consequence, as p53 function in the induction of senescence is tightly coupled with the role in the DDR, my results could indicate that PFT-α is not the right tool to manipulate p53 function in this context. The molecular basis of PFT-α dependent p53 inhibition is largely unknown and there are contrasting data in the literature about its efficacy and specificity, for example in the context of heat shock response (Komarova et al., 2003; Murphy et al., 2004). It was also proposed that PFT-α can act as an aryl hydrocarbon receptor agonist, similar to 2,3,7,8-tetrachlorodibenzo-p-dioxin (TCCD) but with much lower efficacy compared to TCCD (Hoagland, Hoagland and Swanson, 2005). Overall, these data render the interpretation of my results very difficult. Alternatives to pharmacological inhibition of p53 would be the inhibition of the upstream kinase ATM, using a well characterised, specific inhibitor, KU-55933 (Hickson et al., 2004), or p53 knockdown by shRNAs.

Chapter 6 Results - Transient knockdown of p53 or p16 and subsequent telomerase reactivation in senescent cells

6.1 Introduction

Several studies in human cells have shown that inhibition of both p53-p21 and p16-pRb pathways is required to bypass or prevent replicative senescence (Shay, Pereira-Smith and Wright, 1991; Smogorzewska and de Lange, 2002; Beauséjour et al., 2003). Although mouse cells do not undergo replicative senescence due to telomerase constitutive expression, they can be forced into senescence by expressing a dominant negative TRF2, that causes telomere uncapping and DDR activation (Smogorzewska and de Lange, 2002). Interestingly, inhibition of p53 prior to TRF2 knockdown is sufficient to avoid entry into senescence in cells expressing dominant negative TRF2, highlighting the differences in senescence signalling between mice and humans in which mouse cells do not require the p16-pRb pathway for entry into senescence. Several studies have focused on the bypass of senescence, inhibiting p53-p21 and p16-pRb pathways by multiple means, such as expression of viral proteins SV40 LT or HPV E6 + E7, dominant negative version of the target protein or via RNAi. However, very few studies have addressed whether inhibiting these pathways is sufficient to abrogate senescence once it is established (senescence reversal). As in the previous chapter, I have shown that PFT-α mediated inhibition of p53 in the context of DDR was ineffective. I therefore set out to test an alternative means to achieve the same goal, namely using IPTG-inducible shRNA constructs directed against p53 mRNA. Using the same strategy, I also tested the effect of p16 knock-down in combination with DD-hTERT stabilisation on senescence reversal.

6.2 p53 knockdown in MRC-5 DD-hTERT cells

Four p53-targeting shRNAs, compiled from published reports (See Table 2.4 for sequences and references) and the RNAi consortium database (http://www.broadinstitute.org/rnai/trc) were cloned into a pLKO-puro-IPTG-3xLacO backbone for lentiviral transduction and IPTG-inducible shRNA expression. However, only for two shRNA constructs (shp53-1 and shp53-2) DNA sequencing confirmed successful cloning, while for the other two constructs repeated attempts to obtain sequences failed. shRNA genes are notoriously difficult to sequence due to the very stable secondary structures formed after denaturation. Therefore, only the two sequenced shRNA constructs were carried forward, to test their ability to induce p53 knockdown. To this end, MRC-5 DD-hTERT +Shield-1 cells were infected with lentiviruses carrying either control shRNAs directed against Luciferase mRNA (shLuc), or either one of two p53-directed shRNAs (shp53-1 or shp53-2). shRNA expression was then induced by treating infected cells with 1 mM IPTG for 48 hours (Figure 6.1). The efficiency of knock-down was tested by analysing p53 levels in infected cells by western blotting. As expected, MRC-5 DD-hTERT cells transduced with shLuc showed no difference in the levels of p53 and its downstream target p21, with or without IPTG-induction. In contrast, both shp53-1 and shp53-2 cells showed a reduction of p53 and p21 levels following IPTG-induction. shp53-1 was substantially more efficient in knocking down p53 compared to shp53-2. The following experiments were therefore performed using shp53-1. I also verified that p53 knock-down did not affect the levels of p16 protein, in the presence or absence of Shield-1.

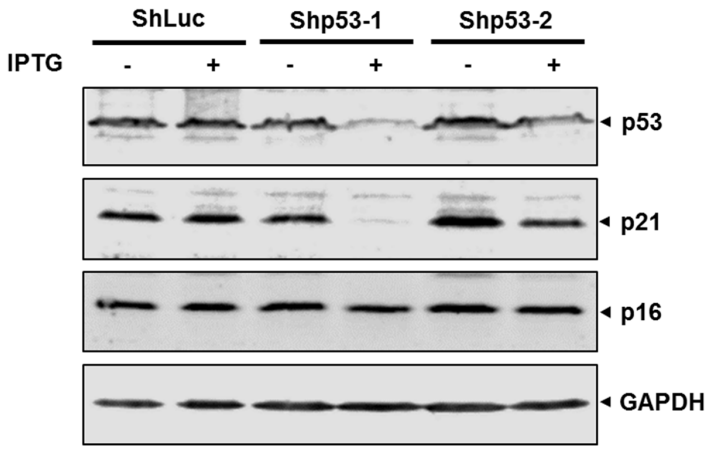

Figure 6.1 Knockdown of p53 by IPTG-inducible shRNAs in MRC-5 DD-hTERT cells.
Western blot quantification of p53 levels in MRC-5 DD-hTERT +Shield-1 cells lentivirally transduced with either shLuc, shp53-1 or shp53-2, with or without IPTG induction. The results obtained by using antibodies directed against p53, its downstream effector p21, p16 and GAPDH are shown. GAPDH was used as loading control.

My previous experiment with PFT-α have shown its inability to inhibit DNA damage-induced p53. To assess whether shp53-1 mediated p53 knock-down is capable of inhibiting p53 function in the context of the DDR, MRC-5 DD-hTERT +Shield-1 cells transduced with shp53-1 were cultured in the presence or absence of IPTG and exposed to 2 Gy of ionising radiation. The treatment was followed by 30 minutes EdU pulse at 1, 4, 8 and 24 hours prior to fixation with 4% formaldehyde. Fixed cells were analysed for EdU incorporation by Click-reaction mediated detection and fluorescence microscopy analysis. In response to ionising radiation induced double strand breaks, p53 triggers a sustained G1/S arrest, quantifiable as a decrease of the number of EdU-incorporating cells in the culture. In agreement with this, control cells showed a substantial drop in the proportion of cycling cells, irrespective of the IPTG treatment, following ionising radiations. In the absence of IPTG, cells

transduced with shp53-1 also showed a decline in EdU incorporation that is comparable to the control cells. In contrast, IPTG-induction of shp53-1 expression resulted in lack of sustained arrest in response to double strand break, measurable as an unchanged incorporation of EdU after irradiation. This response is typical of cells with defective G1/S checkpoint and is known as radio-resistant DNA synthesis (RDS). This result suggests that shp53-1 mediated knockdown of p53 efficiently inhibits p53 function in the DDR.

(A)

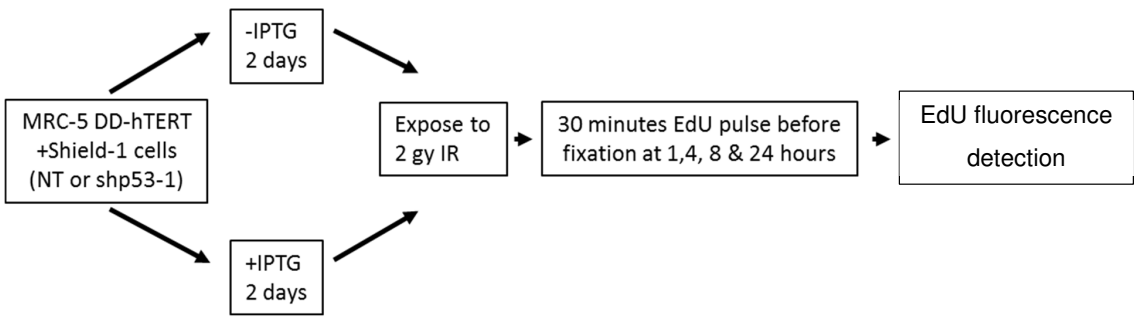

(B)

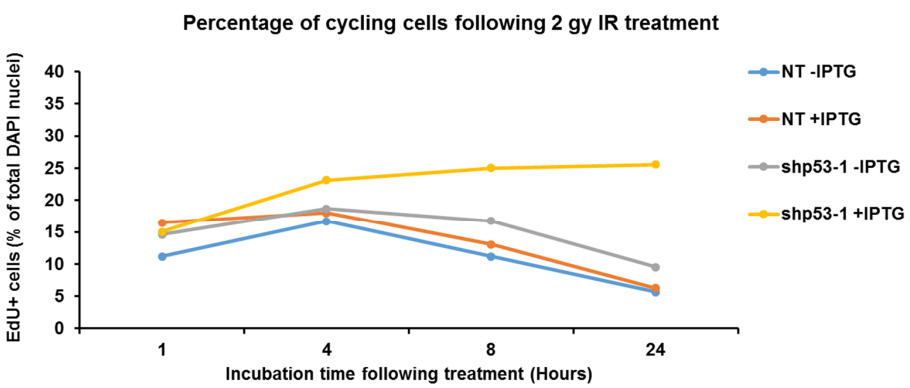

Figure 6.2 Knockdown of p53 by shp53-1 allowed cells to proliferate in the presence of ionising radiation-induced DNA damage.
(A) Experimental plan. (B) Graph showing percentage of EdU positive (Edu+) cells through the time course of the experiment in non-transduced (NT) and shp53-1 transduced MRC-5 DD-hTERT +Shield-1 cells, with or without IPTG treatment.

6.3 p53 knockdown alone could not abrogate senescence in MRC-5 DD-hTERT cells

To assess whether shRNA-mediated inhibition of p53 is sufficient to abrogate proliferation arrest in senescent MRC-5 fibroblasts, shLuc and shp53-1 transduced MRC-5 DD-hTERT cells were cultured with and without IPTG-induction. Proliferating control cells were also cultured with Shield-1 while senescent cells were cultured either in the presence or absence of Shield-1. Cells were counted 12-days following treatment to understand whether senescent cells can proliferate when p53 is knocked down by shRNA and telomerase is stabilised/reactivated by addition of Shield-1 (Figure 6.3). Proliferating shLuc and shp53-1 cells showed increased number of cells following culture for 12-days with and without IPTG-induction, whereas senescent cells showed a decrease in cell number at assay endpoint in the presence or absence of IPTG-induction. This suggest that p53 knockdown was insufficient to abrogate cell cycle arrest and force senescent cells to proliferate. Introducing telomerase in combination with p53 knockdown led to similar results, confirming that the cell cycle arrest abrogation, required for telomerase to act on telomeres was not achieved. Interestingly, proliferating cells (senescence (-)) transduced with shp53-1 showed more cell growth than the corresponding shLuc control cells. This result could be explained by the loss of G1/S checkpoint induced by p53 knock-down, and the consequent increase of cell proliferation. Occurrence of similar observation in non IPTG-induced shp53-1 cells may suggest leaky expression of shp53-1. However, I have only performed this assay once, therefore, more experimental replicates need to be done, to confirm whether this is a reproducible result.

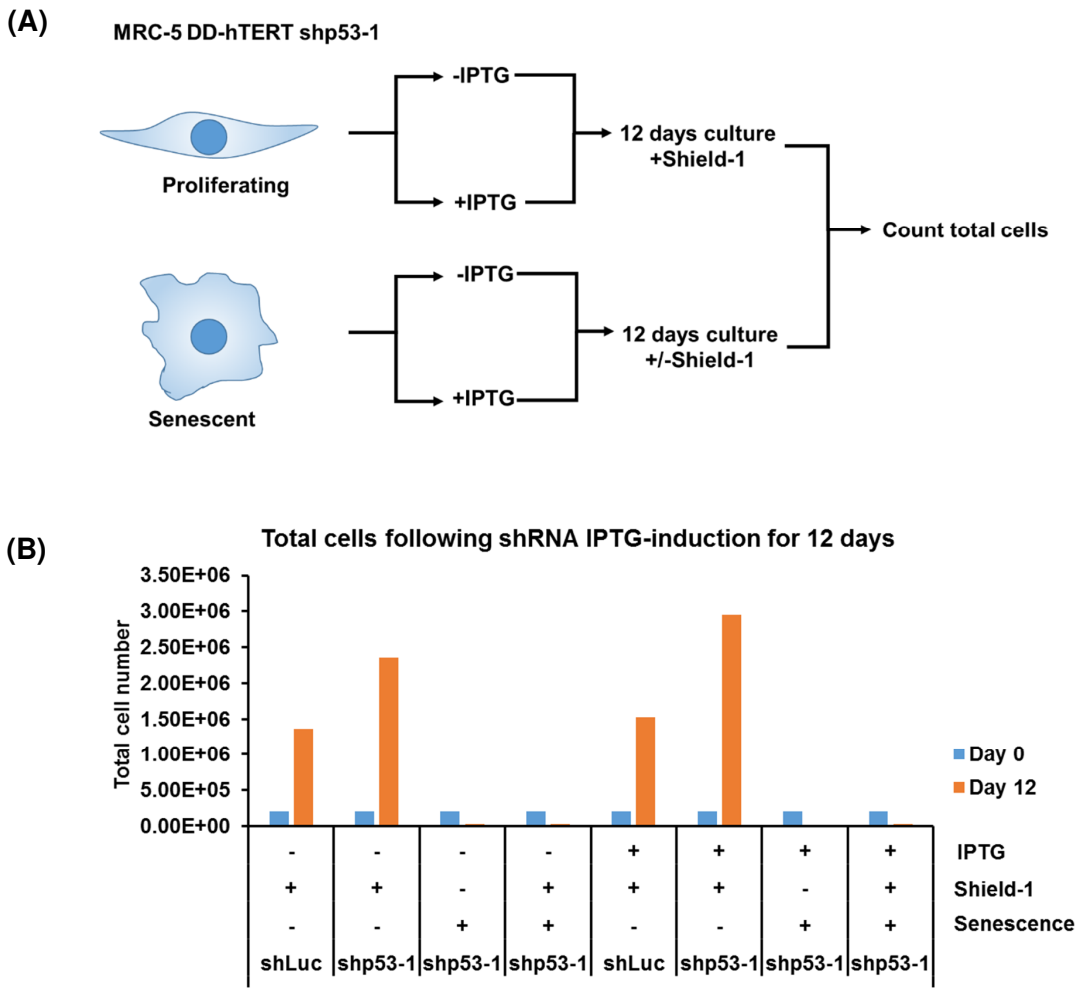

Figure 6.3 Knockdown of p53 by shp53-1 was unable to abrogate senescence enforced growth arrest.

(A) Experimental plan. (B) Quantification of cell proliferation by count at day 0 and 12. The seeding density was maintained the same for all treatments, 7.5 x 10^5 cells. Cells that reached 90% confluency were sub-cultured and re-seeded at 7.5 x 10^5 cells. In this case, cumulative cell number at endpoint (day 12) is shown.

Parallel to the cell counting experiment, I also analysed the proportion of the senescent population by SA-β-gal staining assay. Proliferating MRC-5 DD-hTERT shLuc or shp53-1 transduced cells, cultured with Shield-1 were used as negative controls. These control cells showed no SA-β-gal staining, as expected. On the other hand, senescent MRC-5 DD-hTERT +/- Shield-1 cells, infected with shp53-1 and untreated or treated with IPTG showed a similar proportion of senescent population. Together with the previous results, these data suggest that p53 knockdown, with or without telomerase reactivation was insufficient to reverse senescence.

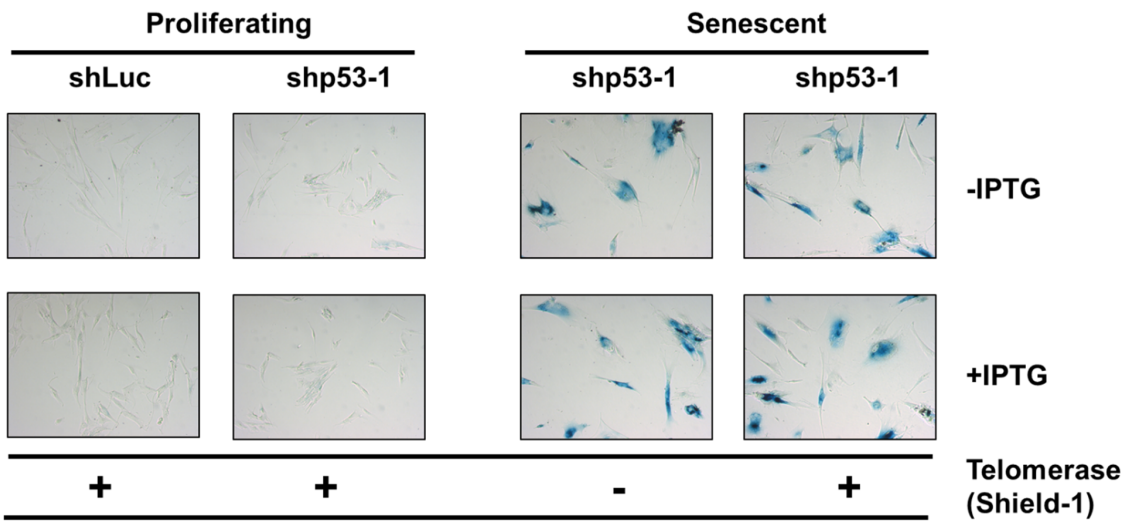

Figure 6.4 Knockdown of p53 alone by shp53-1 was unable to reverse senescence.

Brightfield microscopy images of SA-β-gal stained proliferating (left) and senescent (right) MRC-5 DD-hTERT transduced with IPTG-inducible shRNA to luciferase (shLuc) or p53 (shp53-1). IPTG induction was performed for 12 days and topped up every 2 days with 1 mM IPTG. Shield-1 treatment was performed similarly to the IPTG treatment, with 700 nM Shield-1.

6.4 Confirmation of p16 knockdown in MRC-5 DD-hTERT cells

The experiments above showed that knockdown of p53 alone is insufficient to abrogate senescence. It has been shown that cells that upregulate both p16 and p53 during senescence require inhibition of both pathways in order to bypass senescence associated proliferation arrest (Shay, Pereira-Smith and Wright, 1991; Smogorzewska and de Lange, 2002). Therefore, I have compiled four shRNA sequences (Shp16-1, Shp16-2, shp16-3 and Shp16-4) from published reports (See Table 2.4 for sequences and references) and the RNAi consortium database (http://www.broadinstitute.org/rnai/trc) and cloned them into a pLKO-puro-IPTG-3XLacO backbone, similarly to the shRNAs directed against p53. Following lentiviral infection of MRC-5 DD-hTERT +Shield-1 cells and antibiotic selection with puromycin, cells were cultured with and without IPTG for 48 hours, trypsinised and subjected to western blotting to analyse p16 levels. Western blot showed that p16 is expressed in all cells prior to IPTG induction. Surprisingly, IPTG-induction did not result in a visible decrease of p16 levels in all four shRNAs tested, compared to the shLuc control. One possible explanation for this result is the level of shRNA expression obtained by IPTG-induction are not high enough to effectively knock-down p16 mRNA levels. To verify this hypothesis, the four selected shRNA against p16 were cloned into pLKO.1-hygro backbone. This plasmid uses the same U6 promoter as pLKO-puro-IPTG-3xLacO minus the lac operon and therefore allows constitutive expression of the shRNA. Although all four shRNAs sequenced have been cloned into pLKO.1-hygro backbone, I was only able to confirm successful cloning for two (shp16-2 and shp16-3) out of the four shRNAs. Lentiviral particles containing either shp16-2 or shp16-3 were used to infect proliferating and senescent MRC-5 DD-hTERT at maximum MOI (undiluted viral supernatant). Infected cells were selected with hygromycin for 6 days and harvested for analysis of p16 levels by western blot. In both proliferating and senescent cells, shp16-2 but not shp16-3 showed substantial reduction of p16 protein levels compared to shLuc. It is interesting to note that senescent shLuc cells showed low levels of p21 and p53 compared to

proliferating cells which was also observed previously in MRC-5 DD-hTERT cells not lentivirally transduced with shRNA constructs (See chapter 4). Knockdown of p16 by Shp16-2 induced upregulation of p21 and p53, consistent with a previous observation in senescent WI-38 cells, where inhibition of p16 prior to senescence produced senescent cells which upregulates p21 (Beauséjour et al., 2003). Strangely, despite not showing a visible p16 knockdown, upregulation of p21 was also seen in senescent Shp16-3 cells. This upregulation of p21 was not observed in proliferating cells following p16 knockdown suggesting that this effect is specific to senescent cells and that this might correlate to p16 function during senescence. Shp16-2 was selected for further downstream applications.

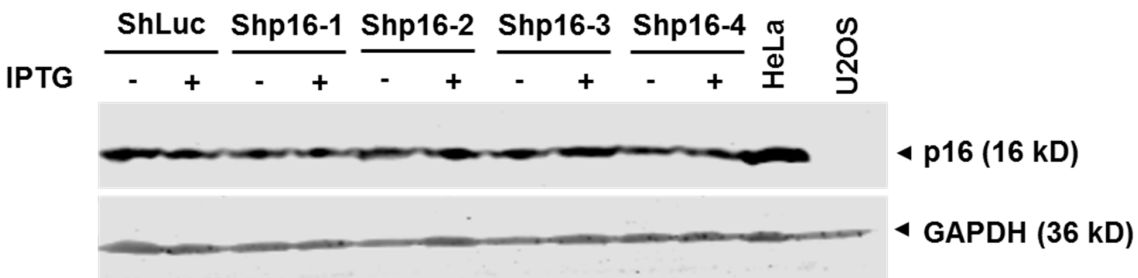

Figure 6.5 IPTG-inducible shRNA expression does not result in efficient knock-down of p16 levels.
Following 48 hours of IPTG-induction, proliferating MRC-5 DD-hTERT cells transduced with 4 different IPTG-inducible shRNAs to p16 were subjected to Western blot analysis to assess p16 knockdown. HeLa and U2OS cell lysates were used as positive and negative control respectively, for the presence of p16. GAPDH was used as loading control.

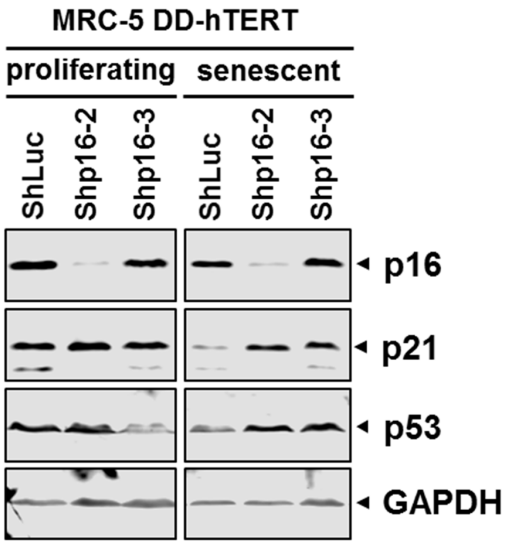

Figure 6.6 Constitutive Shp16-2 expression efficiently knocks down p16. Proliferating and senescent MRC-5 DD-hTERT cells infected with viruses carrying either ShLuc, Shp16-2 or Shp16-3 under the control of a constitutive U6 promoter, were tested for p16 levels by Western blot. p21 and p53 levels were also assessed. GAPDH was used as loading control.

6.5 Discussion

The aim of the work described in this chapter was to investigate potential routes to inhibit p53-p21 and p16-pRb pathways, to ultimately attempt reversing senescence in cells with stabilised telomerase. As briefly mentioned, both pathways are required for establishment and maintenance of senescence and inhibition of both of these pathways prior to senescence could prevent cells from entering senescence (senescence bypass) (Smogorzewska and de Lange, 2002). However, once senescence is established, abrogation of senescence (senescence reversal) have been reported to depend on the levels of p16 in the cells and that WI-38 fibroblasts expressing high levels of p16 at senescence cannot be forced to proliferate in spite of dual inhibition of

p53 and p16 (Beauséjour et al., 2003). However, in the same report, senescent cells that failed to proliferate following inhibition of p53 and p16 did undergo DNA replication. Therefore, this may suggest that there are factors preventing these cells to proceed to mitosis, possibly the DNA damage at telomeres which activates senescence in the first place. In this chapter, I have showed that knockdown of p53 alone was insufficient to abrogate growth arrest once senescence is established in my cells. Unfortunately, I have not been able to test whether dual knockdown of p53 and p16 can force cells to proceed to S-phase. There is a possibility that the result in MRC-5 cells may replicate previous result in WI-38 as mentioned above. However, to my knowledge, the effect of introducing telomerase following abrogation of cell cycle arrest by dual p53 and p16 knockdown in senescent cells has not been investigated. Telomerase expression have been shown to affect stability of OIS via clearance of DNA damage at telomeres (Suram et al., 2012). Therefore, telomerase reactivation following abrogation of senescence could potentially result in reversal of senescence by means of eliminating the DDR signals at telomeres that maintain senescence.

Although senescence is defined as a static proliferative arrest, it has been suggested that it is a more dynamic process than its definition suggest (Reviewed in (Van Deursen, 2014)). In human cells, p53 has been associated with the activation and maintenance of early or light senescence, while p16 is associated with late or deep senescence (Alcorta et al., 1996; Stein et al., 1999; Chen and Ozanne, 2006). I have showed in chapter 4 that the senescent MRC-5 DD-hTERT cells have higher levels of p16 compared to proliferating cells at relatively similar population doublings (Figure 4.6). Furthermore, it seems that there is always a basal level of p16 expression in proliferating MRC-5 DD-hTERT cells. Although p16 expression is highly associated with senescence, expression of p16 have also been reported in cultured human cells under sub-optimal culture conditions (Ramirez et al., 2001). This may partially explain the expression of p16 in the proliferating MRC-5 DD-hTERT cells. Furthermore, p53 and p21 levels are lower in the senescent cells

compared to proliferating cells (Figure 4.6 and 6.6). Downregulation of p53 and p21 in senescent cells have been previously reported and was linked to SCF^{FBXO22} upregulation which can ubiquitylate methylated p53 for proteasomal degradation (Stein et al., 1999; Bakkenist et al., 2004; Chen and Ozanne, 2006; Johmura et al., 2016).

As mentioned above, the proliferating MRC-5 cells have relatively high basal levels of p16, which I proposed to be due to sub-optimal culture conditions. This includes media formulations and O_2 levels in the cell culture incubator. Traditional CO_2 incubators have atmospheric O_2 levels which is approximately 21% O_2 partial pressure while *in vivo* physiological oxygen levels in tissues could range from 4 – 7.5% (McKeown, 2014). This suggest that the MRC-5 cells used in the study were cultured in relatively hyperoxic conditions, which does not reflect its normal environment *in vivo*. Mitochondrial ROS production have been shown to increase linearly with increase in oxygen concentration (Grivennikova, Kareyeva and Vinogradov, 2018). This imply that culturing the MRC-5 cells at relatively hyperoxic condition may result in excess ROS production which could lead to increased oxidative stress and possibly senescence or senescence-like phenotype in certain situations. It has been shown that fibroblast live longer *in vitro* when cultured at 10% O_2 compared to 20% (Richter, Sanford and Evans, 1972; Packer and Fuehr, 1977). Furthermore, physiological O_2 levels significantly delays cellular senescence and increase lifespan of MEFs compared to atmospheric O_2 levels (Parrinello et al., 2003). In addition, atmospheric O_2 levels and excess ROS production has been implicated in upregulation of p16 (Jenkins et al., 2011; Sasaki et al., 2014; Mas-Bargues et al., 2017; Lin et al., 2019). Hence, lowering O_2 levels is a clear benefit for replicative lifespan of mammalian cells *in vitro* and could possibly lower p16 levels in culture. To allow for reduced O_2 levels, a Tri-gas incubator can be used which allow injection of gaseous N_2 in parallel with CO_2 injection. Gaseous N_2 would displace O_2 and reduce its concentration to tissue physiological levels. However, as cells require constant re-plating every 3-4 days, it is very difficult to maintain O_2 levels when cells were taken outside of

the incubator and this requires further observation to see the effect of this acute change in O_2 levels when incubator O_2 concentration have been set to in physiological levels.

Non-specific antibody binding can also result in over representation of western blot data, which may explain the high basal p16 levels observed. The p16 antibody used in this study is a monoclonal antibody (clone G175-1239) from BD biosciences and have been validated in the lab by western blot using whole cell lysates of U2OS cells (p16 negative) and HeLa cells (p16 positive), which showed positive band of ~16 kDa in size in the HeLa lane but not in the U2OS lane (Figure 6.5). Furthermore, it has also been frequently used for western blot in other senescence-related studies (Ramirez et al., 2003; Takaoka et al., 2004; Zhang et al., 2009; Fischer et al., 2013). Thus, antibody specificity does not seem to be an issue in this case. Regarding other antibodies used in my western blot experiments, my p53 western blots may possibly benefit from adding p53 phosphorylation data, particularly p53 Ser15 phosphorylation which is the initial phosphorylation event required for p53 transactivation (Dumaz, 1999). It is known that following DDR-associated sequential phosphorylation of p53 at Ser15, Ser20 and Thr18 by upstream kinases ATM, Chk2 and CK1 respectively, MDM2 is dissociated from p53 leading to stabilisation of p53 protein (Jiang, Sheikh and Huang, 2010). This stabilisation can be observed as increased p53 protein levels in western blots. However, this increased p53 level is not a direct marker for p53 activity. Mutant p53 which have lost its transactivation capability is frequently showed to be constitutively highly expressed in cancer cells, when observed by western blot (Midgley and Lane, 1997). The inability of mutant p53 to transactivate its target genes resulted in the absence of the p53 negative feedback loop with MDM2, leading to chronic stabilisation of p53 (Midgley and Lane, 1997).Therefore, this imply that p53 levels is insufficient to be a surrogate marker for its function, supporting the benefit of adding p53 phosphorylation data for characterisation of p53 function.

It was also reported that replicatively senescent BJ fibroblasts showed an active DDR, as detected via 53BP1 and γH2AX foci formation, that is maintained upon prolonged culture (Fumagalli et al., 2014). On the contrary, in the same report, DDR activation in senescent WI-38 and IMR-90 cells diminished upon prolonged culture, possibly due to loss by death of the cells carrying the highest DNA damage burden. Similarly to the observation in WI-38 and IMR-90 cells, in my experiments senescent MRC-5 DD-hTERT cells showed a substantial reduction of cell numbers during serial passaging, suggesting the possible loss of cells with the highest DNA damage levels. Moreover, it is known that , like in the case of MRC-5 DD-hTERT cells, WI-38 but not BJ cells express high levels of p16 (Beausejour et al., 2003). Knockdown of p16 in senescent cells resulted in upregulation of p53 and p21 (Figure 6.6), suggesting a redundancy between p53-p21 and p16-pRb pathway in maintaining senescence, which was also previously reported (Stein and Dulic, 1998; Beauséjour et al., 2003). This might also explain the reliance of BJ fibroblasts on p53-p21 pathway for maintenance of senescence.

As mentioned above senescent BJ cells but not WI-38 and IMR-90 cells maintain higher viability in culture. It is possible that loss of viability of senescent WI-38 and IMR-90 cells in culture is linked to the targeted degradation of p53 by SCF^{FBXO22}. p21 has been implicated in maintenance of cell viability in senescent IMR90 fibroblasts induced by etoposide (Yosef et al., 2017), hence, cells that downregulate p53 and its downstream target p21 during senescence may not be able to maintain viability in culture. It would be interesting to test whether inhibition of p16, which upregulates p53 and p21 in RS-induced MRC-5 DD-hTERT cells could increase viability in culture. Together, these data suggest that in MRC-5 fibroblasts both pathways, p53 and p16 are possibly activated sequentially during senescence and support the hypothesis that some type of cells progress from light to deep senescence by downregulating p53 and upregulating p16.

Chapter 7 Results - The effect of forced localisation of telomerase at telomeres by fusion of hPOT1 to hTERT in senescent cells

7.1 Introduction

As briefly discussed previously, my failure to force senescent MRC-5 cells back into proliferation is possibly explained by the fact that telomerase localisation to telomeres and the consequent telomere elongation are normally restricted to S-phase (Ten Hagen et al., 1990; Wright et al., 1999; Jády et al., 2006; Tomlinson et al., 2006). I therefore reasoned that providing an S-phase independent mechanism to localise it to telomeres, could allow telomerase to inactivate DDR-dependent cell cycle arrest by elongating critically short telomeres. Currently, the molecular basis of the S-phase specific recruitment of telomerase to telomeres are only partially understood. However, it has been shown that mutations localised within hTERT Dissociates Activities of Telomerase (DAT) domain/region at the N-terminus result in loss of telomere elongation activity *in vivo* (in cells) but not *in vitro* (Armbruster et al., 2001; Banik et al., 2002; Armbruster et al., 2004). These data have been explained by the potential inability of DAT-mutant telomerase to localise to telomeres. To demonstrate this hypothesis, DAT-mutant hTERT was fused to POT1, a component of the shelterin complex which binds to the single-stranded telomeric overhang (Armbruster et al., 2004). Expression of the POT1-DAT mutant hTERT fusion protein was in fact able to rescue telomere elongation. It has been proposed that the signal to induce DDR-dependent replicative senescence is triggered by the depletion of shelterin components at critically short telomeres and by the shortening of the 3'-overhang, with the consequent loss the T-loop protective conformation (Li et al., 2003; Stewart et al., 2003; Takai, Smogorzewska and De Lange, 2003; Cesare et al., 2009). All these events effectively transform the end of the chromosome into a double strand break. I propose to use hPOT1-hTERT fusion to force hTERT localisation to telomeres in senescent MRC-5 cells. This could allow elongation of the

telomeric 3'-overhang, restore the T-loop conformation and reverse senescence by abolishing damage recognition at telomeres by the DDR.

7.2 Lentiviral transduction of hPOT1-hTERT to MRC-5 DD-hTERT cells

MRC-5 DD-hTERT cells were infected with lentiviruses carrying hPOT1-hTERT fusion. Following treatment with 5 µg/ml blasticidin to select a cell population carrying a stably integrated virus, genomic DNA (gDNA) was extracted and 1 µg of gDNA was subjected to PCR to confirm the presence of hPOT1-hTERT DNA sequence random integration into the MRC-5 DD-hTERT genome. PCR was performed using primers amplifying a 498 bp region spanning the 3'-end of hPOT1, the internal FLAG sequence and 4 bp into the 5'-end of the hTERT sequence. As internal control, a primer pair designed to amplify a 381 bp of the internal region of the Blasticidin-S resistance gene (*bsr*) was also used for PCR. 1 pg and 10 pg of plasmids were used as controls for the presence or absence *bsr* and *hPOT1-hTERT*, respectively. The result showed that the controls were working as expected (Figure 7.1). Both MRC-5 DD-hTERT transduced with vector only (pLENTI6/V5-DEST) and hPOT1-hTERT showed a clear amplified band for *bsr*. On the other hand, only MRC-5 DD-hTERT cells transduced with pLENTI6-hPOT1-hTERT showed ~500 bp band for *hPOT1-hTERT*. This result confirmed that MRC-5 DD-hTERT vector only and hPOT1-hTERT cells had successfully integrated the respective viral plasmids.

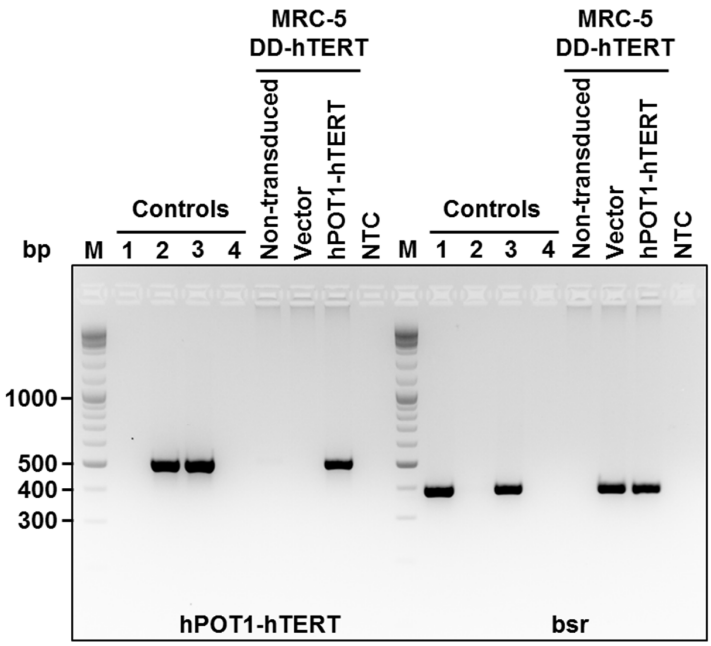

No.	Control plasmids	hPOT1-hTERT	bsr
1	pLENTI6/V5-DEST	-	+
2	pENTR-hPOT1-hTERT	+	-
3	pLENTI6-hPOT1-hTERT	+	+
4	pDONR221	-	-

Figure 7.1 Genotyping of hPOT1-hTERT in MRC-5 DD-hTERT following lentiviral transduction with pLENTI6-hPOT1-hTERT plasmid.

PCR was performed for 30 and 35 cycles for *bsr* (381 bp) and hPOT1-hTERT (498 bp) respectively. M = Marker (GeneRuler Ladder Mix). Blasticidin S-resistance gene (*bsr*). NTC = no template control. pDONR221 was used as negative and pLENTI6/V5-DEST as positive control for *bsr* amplification. pENTR-hPOT1-hTERT is the positive control for hPOT1-hTERT fusion gene.

In order to verify whether hPOT1-hTERT fusion protein is expressed in MRC-5 DD-hTERT the transduced cells, I performed immunostaining using a monoclonal FLAG (M2) antibody to detect the fusion protein. Indeed, both hPOT1 and hTERT are FLAG-tagged. As a positive control for FLAG immunostaining, mouse embryonic stem cells (mESCs) stably expressing a FLAG-tagged KAP1 protein were used (Lynn Powell, unpublished). Despite a clear signal was detected for FLAG-KAP-1, hPOT1-hTERT fusion protein could not be detected in the MRC-5 DD-hTERT cells infected with the lentivirus encoding for hPOT1-hTERT fusion protein (Figure 7.2). To verify this further, the expression of the fusion protein was also assayed by western blot. In this case, mouse embryonic stem cells (mESCs) expressing a FLAG-Cas9 fusion protein were used as positive control for FLAG-immunodetection (Naiming Chen, unpublished). Accordingly, while the 150 kDa FLAG-Cas9 fusion protein was readily detected by probing the western blot with anti-FLAG antibody, hPOT1-hTERT fusion protein band, expected to run approximately around 201kDa, could not be detected (Figure 7.3). Re-probing the same blot with mouse-anti-TERT antibody revealed strong bands at ~130 kDa which corresponds with stabilised DD-hTERT protein (139 kDa) in all samples except the FLAG-control cells and a very faint band only in which might be hPOT1-hTERT. This suggest that expression of hPOT1-hTERT might be extremely low, and the fusion protein possibly have lost the 5' FLAG-tag as well.

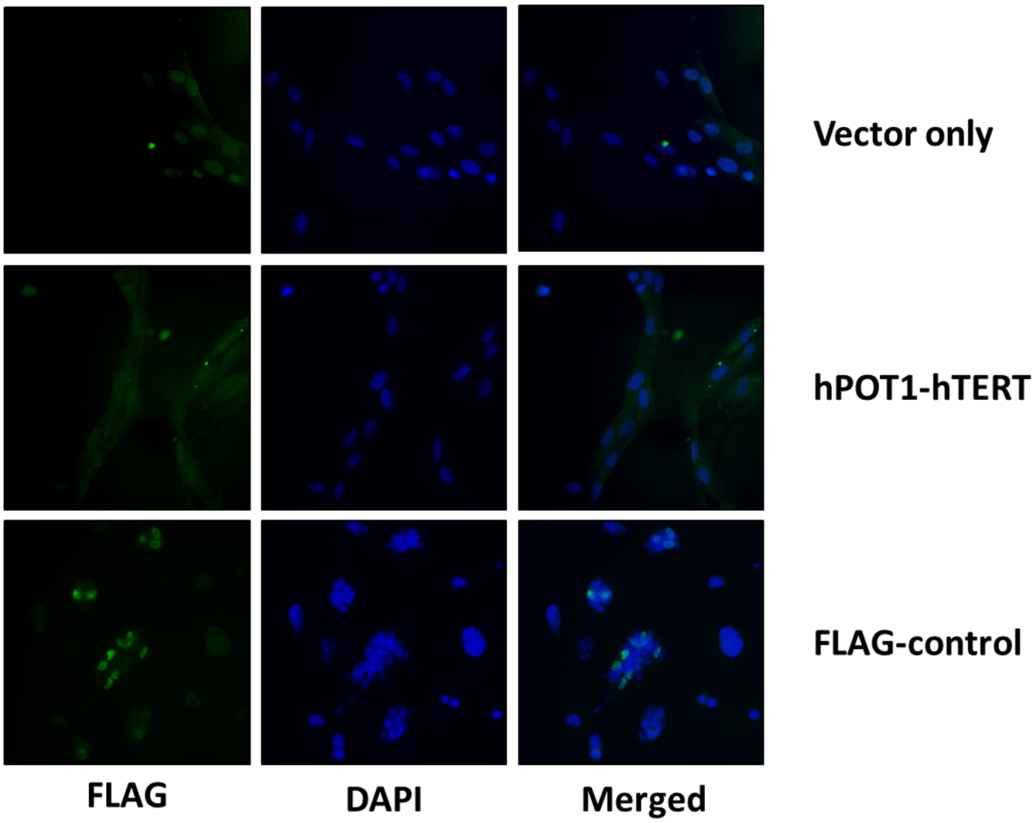

Figure 7.2 hPOT1-hTERT protein expression was not detected by immunostaining in MRC-5 DD-hTERT cells transduced with hPOT1-hTERT.

Images acquired at the fluorescence microscope, showing MRC-5 DD-hTERT cells infected with lentivirus carrying empty vector (vector only) or lentivirus encoding for hPOT1-hTERT. DNA was counterstained with DAPI. mESCs expressing FLAG-tagged KAP1 protein were used as positive control for FLAG immunostaining (FLAG-control).

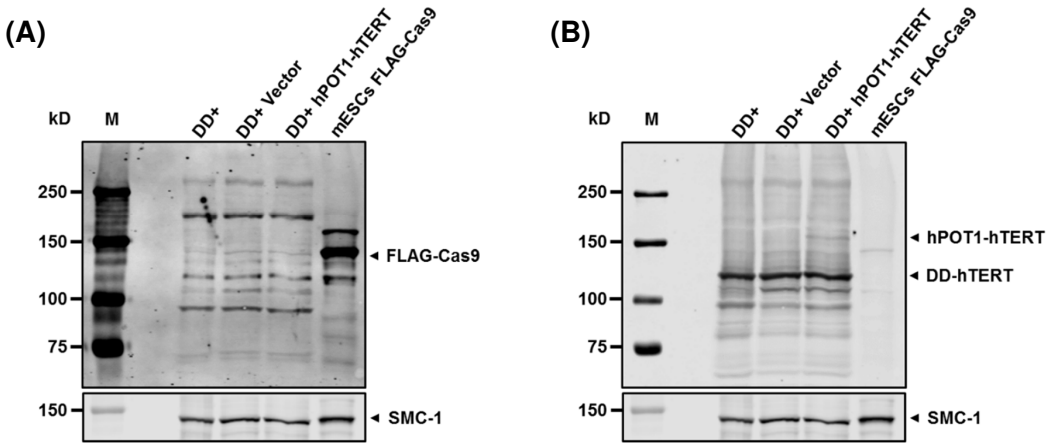

Figure 7.3 hPOT1-hTERT protein expression in MRC-5 DD-hTERT +Shield-1 cells.

Whole cell extracts of non-transduced MRC-5 DD-hTERT +Shield cells (DD+), transduced with vector only (DD+ Vector), with hPOT1-hTERT (DD+ hPOT1-hTERT) and of FLAG-control cells (mESCs FLAG-Cas9) were loaded onto 6% SDS-PAGE gel at 100000 cells/well and transferred onto nitrocellulose membranes, subsequently probed with antibodies directed against (A) FLAG tag, (B) TERT and SMC-1 (loading control). The expected sizes for FLAG-Cas9, DD-hTERT, hPOT1-hTERT and SMC-1 are 150 kDa, 139 kDa, 201 kDa and 145 kDa respectively.

Since the hPOT1-hTERT transgene expression is constitutively driven by the CMV promoter present in the lentiviral vector, telomerase activity of MRC-5 DD-hTERT cells expressing hPOT1-hTERT fusion protein should be high in the absence of Shield-1, compared to non-infected cells. Since, the fusion hPOT1-hTERT protein expression is not detectable by western blotting, I decided to try and detect it by taking advantage of the higher sensitivity of the TRAP assay, which measures telomerase enzymatic activity. MRC-5 DD-hTERT cells infected with control lentivirus (vector only) or the virus encoding for hPOT1-hTERT were cultured for 7 days without Shield-1 to reduce DD-hTERT activity to background level (Figure 7.4). This was followed by culture with or without Shield-1 for 24 hours, in order to compare basal and Shield-1 stabilised telomerase activity in the absence or presence of hPOT1-hTERT. Whole cell extract from these cells were subjected to TRAP assay. MRC-5 WT and hTERT were used as negative and positive controls for telomerase activity respectively. As expected, both vector control and hPOT1-hTERT transduced MRC-5 DD-hTERT cultured with Shield-1 showed high telomerase activity. On the other hand, although both vector only and hPOT1-hTERT transduced cells cultured without Shield-1 showed low telomerase activity if compared to cells cultured with Shield-1, hPOT1-hTERT cells - Shield-1 showed a slightly higher telomerase activity in comparison to the vector transduced cells in the same condition. This is visible as an increased laddering at the top end of the gel in the 1000 cells lane and one extra band at the bottom end in the 100 cells lane compared to vector cells in the absence of Shield-1 (Fig. 7.4B). This result suggests that albeit at very low levels, hPOT1-hTERT fusion protein is expressed and active.

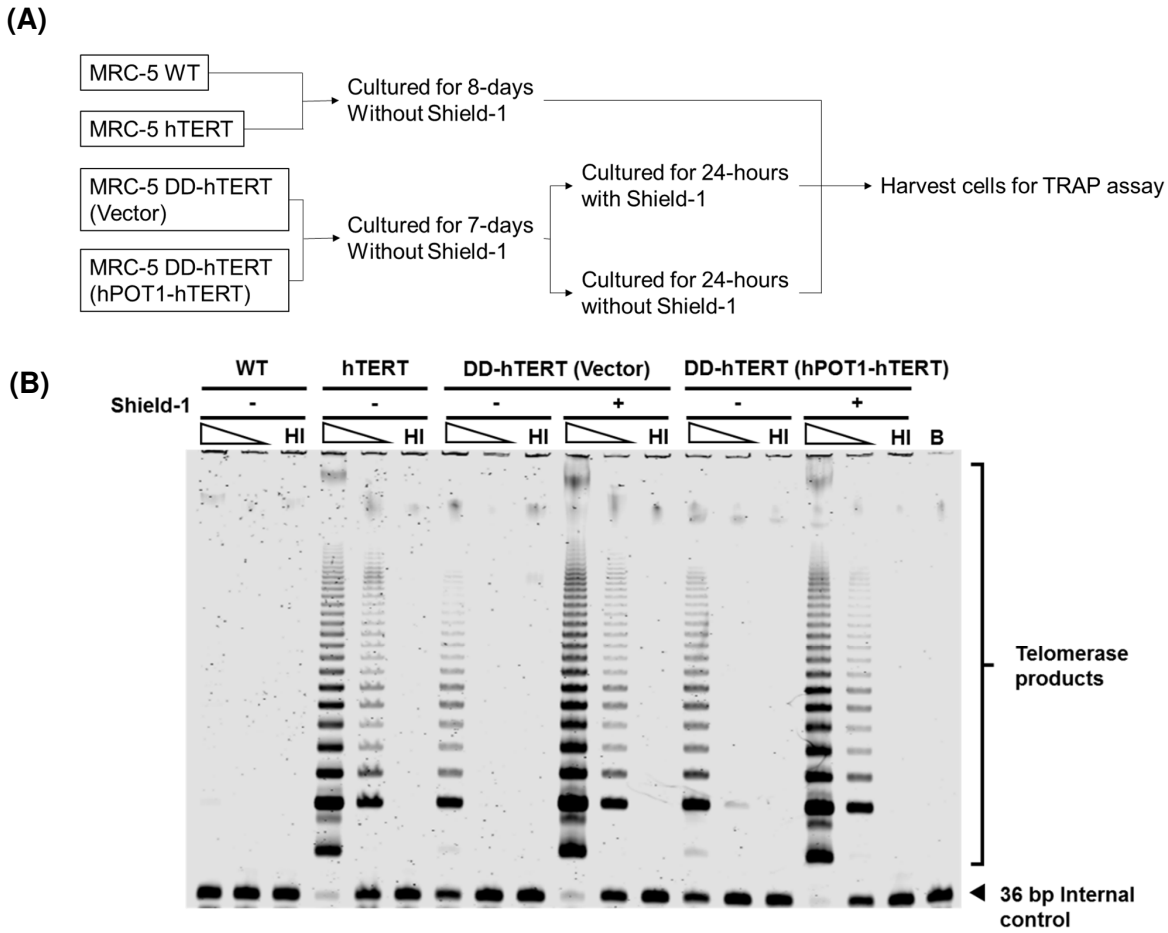

Figure 7.4 hPOT1-hTERT telomerase activity in MRC-5 DD-hTERT cells.
(A) Experimental plan. (B) TRAP assay electropherogram. Whole cell lysate obtained from MRC-5 WT, hTERT, DD-hTERT (Vector) and DD-hTERT (hPOT1-hTERT) equivalent to 1000 and 100 cells were subjected to TRAP assay and loaded into a 0.5X TBE polyacrylamide gel. The extent of 6-bp DNA laddering is proportional to telomerase activity in the cell population. HI = heat inactivated control. B = Lysis buffer only control.

The very low levels of expression hPOT1-hTERT fusion protein observed could be due to CMV promoter silencing in MRC-5 cells. This problem has been reported for the CMV promoter in various cell types (Teschendorf et al., 2002; Brooks et al., 2004; Meilinger et al., 2009; Qin et al., 2010). To verify this hypothesis, I tested whether higher expression levels of hPOT1-hTERT fusion protein could be obtained in a different cell type, namely 293T cells. Cells were transfected with pLENTI6-hPOT1-hTERT using calcium phosphate method and harvested 2-days post-transfection for western blot analysis. pLENTI6-hPOT1-hTERT transfected 293T cells showed a band at the expected size for hPOT1-hTERT (~201 kDa, Figure 7.5). No bands were observed at the same size in the lanes for vector-only and mock transfected cells. This suggests that hPOT1-hTERT expression driven by the CMV promoter is not silenced in 293T cells but possibly silenced or cannot drive high expression of hPOT1-hTERT in MRC-5 cells.

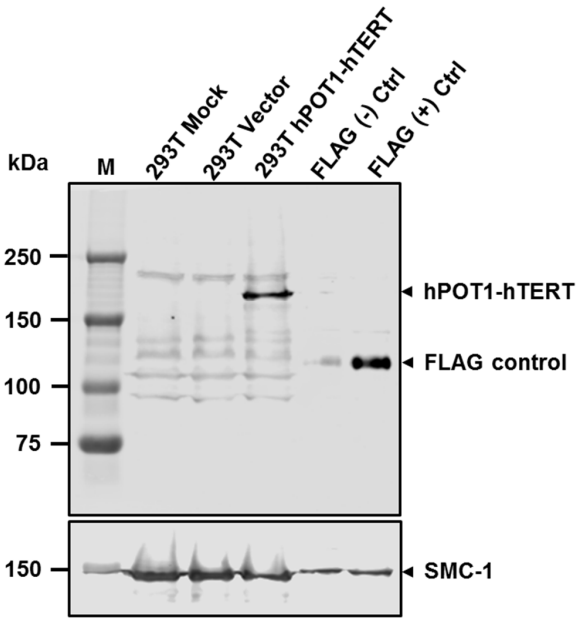

Figure 7.5 hPOT1-hTERT expression in 293T cells is detectable.
Whole cell extracts obtained from HEK293T cells (293T) either mock transfected or transfected with pLENTI6/V5-DEST plasmid (Vector) or pLENTI6-hPOT1-hTERT plasmid (hPOT1-hTERT) were subjected to western blotting and probed with anti-FLAG antibody. Wild type mESCs (FLAG (-) Ctrl) or mESCs expressing FLAG-KAP1 (FLAG (+) Ctrl) were used as negative and positive control, respectively. SMC-1 was used as a loading control.

7.3 Discussion

The main aim of the work described in this chapter was to test whether artificially localising/tethering telomerase to telomeres via expression of hPOT1-hTERT fusion protein is sufficient to abrogate replicative senescence. I have successfully introduced hPOT1-hTERT into MRC-5 DD-hTERT cells as confirmed by genotyping PCR. However, I have not been able to obtain good levels of expression of the fusion protein using a lentiviral vector (pLENTI6/V5-DEST). Due to this technical difficulty and time constraints, I was also unable to confirm localisation of hPOT1-hTERT to telomeres. However, by

troubleshooting, I found that the poor levels of expression of hPOT1-hTERT fusion proteins are due to the CMV promoter present in the lentivector, which is perhaps silenced or too weak to drive detectable expression of hPOT1-hTERT in MRC-5 cells. A previous report testing five different gene promoters to drive expression of GFP in various human cell lines frequently used in laboratory experiments has demonstrated that chicken β-actin promoter coupled with cytomegalovirus early enhancer (CAG), human elongation factor 1α promoter (EF1A) and Simian vacuolating virus 40 promoter (SV40) but not cytomegalovirus immediate early promoter (CMV), mouse phosphoglycerate kinase 1 promoter (PGK) and human ubiquitin C promoter (UBC) can drive high expression of GFP in MRC-5 cells (Qin et al., 2010). This is in agreement with my results showing that the same CMV promoter is insufficient to drive the expression of hPOT1-hTERT in MRC-5 cells but able to give good levels of expression in 293T cells. Treatment with 5-Aza-2'-deoxycytidine, has been shown to reverse CMV silencing and restore expression of LacZ (β-galactosidase) gene driven by a CMV promoter previously silenced (Radhakrishnan et al., 2008). By using this treatment on my cells, I could further verify my hypothesis. However, the most crucial part is to solve the low expression levels in MRC-5 DD-hTERT cells transduced with hPOT1-hTERT. To this end I am currently planning to replace the CMV with a CAG promoter.

Alternatively, I could introduce a DD-tag to the N-terminus of hPOT1-hTERT and obtain stable cell lines using pre-senescent MRC-5 DD-hTERT -Shield-1 cells. Since expression of DD-hPOT1-hTERT would not result in an active telomerase in the absence of Shield-1, MRC-5 DD-hTERT -Shield-1 cells encoding for DD-hPOT1-hTERT will senesce. Only in the presence of Shield-1 would these cells stabilise hPOT1-hTERT fusion protein, allowing hTERT localisation to telomeres in senescent cells. I have constructed the pLENTI6-DD-hPOT1-hTERT plasmid and have tried to transfect MRC-5 cells using Lipofectamine 3000. However, I encountered high level of cell death following transfection. Therefore, the transfection conditions require further optimisations. To validate the localisation of hPOT1-hTERT in senescent cells,

dual immunostaining with anti-FLAG and anti-TRF2 antibody will be performed, to detect hPOT1-hTERT and telomeres, respectively. Proliferation and senescence will be measured in hPOT1-expressing senescent cells by quantifying EdU incorporation and by SA-β-gal staining. In order to verify if reactivation and localisation of telomerase can switch off the DDR induced by critically short telomeres, it would also be interesting to measure the DDR at telomeres following hPOT1-hTERT expression by monitoring the presence/absence of γH2AX foci at telomeres.

There are two of potential obstacles that could prevent hPOT1-hTERT fusion protein from localising to telomeres in the absence of proliferation. Although POT1 has a DNA binding domain (OB fold domain), it has been shown to be insufficient for its localisation at telomeres and requires TPP1 (ACD/PTOP) for its recruitment to telomeres (Liu et al., 2004). This indirect recruitment of POT1 to telomeres is potentially the mechanism used by hPOT1-hTERT fusion protein to localise to telomeres. TPP1 and POT1 have been shown to exist in an approximately 1:1 ratio in the cell and this is possibly due to TPP1 conferring stability to POT1 via formation of a heterodimer in the cell (Loayza and De Lange, 2003; Hockemeyer et al., 2007; Xin et al., 2007; Takai et al., 2010). As TPP1 abundance in the cell is not in excess to POT1 and because POT1 requires TPP1 for stabilisation, the stability of hPOT1-hTERT may also be compromised due to this factor. Thus, the successful localisation of hPOT1-hTERT in senescent cells hinges on TPP1's abundance and ability to confer protein stabilisation to hPOT1-hTERT and its recruitment to telomeres in the absence of proliferation.

Chapter 8 Conclusion and future work

Senescence is generally seen as a static cell cycle arrest resulting from cellular stress that could not be overcome by the cell. Unlike apoptosis, which is also a cellular response to irreparable cellular or DNA damage, senescent cells remain viable and can be maintained for months in culture, as this study have shown. However, it is proposed that senescence is a more dynamic process and that temporal epigenetic and transcriptional alterations occur in senescent cells maintained in culture. Although epigenetic studies suggest that senescent cells may be derived from the cells that have escaped senescence, very few studies have truly addressed whether these senescent cells can escape from or reverse senescence. In this study, I have attempted to test the possible ways that can be utilised to reverse senescence using RS-induced MRC-5 fibroblasts. Using a different fibroblast cell line and telomerase activation method, I have currently confirmed a previous observation (Beauséjour et al., 2003) that telomerase reactivation alone cannot induce the escape from RS. Using the DD-hTERT reversible telomerase activation system, I have also shown that low basal telomerase activity was insufficient to prevent telomere shortening and senescence. Further work is required to compare the telomerase activity of MRC-5 DD-hTERT cells and other telomerase-expressing cells to understand how telomerase activity levels affect immortality in different human cells. A previous study in WI-38 fibroblasts, which are also derived from foetal lung fibroblasts similar to MRC-5 fibroblasts, showed that cellular division was not observed following a knockdown of p16 with shRNA and an inhibition of p53 via a p53 dominant negative peptide (Beauséjour et al., 2003). However, in that particular study, the role of telomerase was not tested following the inhibition of p53 and p16. Therefore, experimental evidence needs to be acquired to test whether knockdown of p53 and p16 with telomerase reactivation can reverse senescence.

Studies using BJ cells showed that OIS and RS can be abrogated. BJ cells do not upregulate p16 and are thought to maintain senescence via p53. Inhibition of p53 but not telomerase expression is sufficient in overcoming the

proliferation arrest in the senescent BJ cells (Beauséjour et al., 2003). Furthermore, the BJ cells that escaped OIS upregulate telomerase and this was concomitant with diminished DDR foci at telomeres (Patel et al., 2016). The fact that telomerase was unable to abrogate RS but possibly abrogate OIS in the same type of cells can mean two things. Firstly, in the case with the spontaneous escape from OIS, p53 inhibition possibly precedes telomerase reactivation. Secondly, the response to telomerase reactivation may be different in OIS compared to RS. Therefore, it would be interesting to test whether telomerase reactivation could result in senescence reversal of BJ cells undergoing OIS and RS. This might suggest that in cases where senescence is maintained by p53 only, telomerase reactivation may be sufficient to reverse the senescence in certain scenarios. It will also be interesting to pursue further the factors associated with the p16 dominance in proliferation arrest over p53 in senescent cells.

Due to technical difficulties encountered, I have not been able to test the potential of tethering of telomerase to telomeres using the hPOT1-hTERT fusion construct in the context of senescence. Therefore, further work is still required to test whether hPOT1-hTERT could force the localisation of telomerase to telomeres and elongate telomeres in senescent cells, in the absence of DNA replication. Further work is also required to study the tethering of telomerase to short telomeres, potentially by fusing TPP1 or TCAB1 to hTERT to complement the hPOT1-hTERT study. Overall, this work provides an insight into the understanding of how human cells can reverse senescence and the role of telomerase in the process of senescence reversal.

References

Aalfs, C. M. et al. (1995). The Hoyeraal-Hreidarsson syndrome: The fourth case of a separate entity with prenatal growth retardation, progressive pancytopenia and cerebellar hypoplasia. *European Journal of Pediatrics*, 154 (4), pp.304–308. [Online]. Available at: doi:10.1007/BF01957367.

Abreu, E. et al. (2010). TIN2-tethered TPP1 recruits human telomerase to telomeres in vivo. *Molecular and cellular biology*, 30 (12), pp.2971–2982. [Online]. Available at: doi:10.1128/MCB.00240-10.

Acosta, J. C. et al. (2013). A complex secretory program orchestrated by the inflammasome controls paracrine senescence. *Nature Cell Biology*, 15 (8), pp.978–990. [Online]. Available at: doi:10.1038/ncb2784.

Adams, P. D. et al. (2013). Lysosome-mediated processing of chromatin in senescence. *Journal of Cell Biology*, 202 (1), pp.129–143. [Online]. Available at: doi:10.1083/jcb.201212110.

Alcorta, D. A. et al. (1996). Involvement of the cyclin-dependent kinase inhibitor p16 (INK4a) in replicative senescence of normal human fibroblasts. *Proceedings of the National Academy of Sciences of the United States of America*, 93 (24), pp.13742–13747. [Online]. Available at: doi:10.1073/pnas.93.24.13742.

Alexander, K. and Hinds, P. W. (2001). Requirement for p27KIP1 in Retinoblastoma Protein-Mediated Senescence. *Molecular and Cellular Biology*, 21 (11), pp.3616–3631. [Online]. Available at: doi:10.1128/mcb.21.11.3616-3631.2001.

Amit, M. et al. (2000). Clonally derived human embryonic stem cell lines maintain pluripotency and proliferative potential for prolonged periods of culture. *Developmental Biology*, 227 (2), pp.271–278. [Online]. Available at: doi:10.1006/dbio.2000.9912.

Amundson, S. A. et al. (2002). A nucleotide excision repair master-switch: p53

regulated coordinate induction of global genomic repair genes. *Cancer Biology and Therapy*, 1 (2), pp.145–149. [Online]. Available at: doi:10.4161/cbt.59.

Anderson, B. H. et al. (2012). Mutations in CTC1, encoding conserved telomere maintenance component 1, cause Coats plus. *Nature Genetics*, 44 (3), pp.338–342. [Online]. Available at: doi:10.1038/ng.1084.

Anderson, R. et al. (2019). Length-independent telomere damage drives post-mitotic cardiomyocyte senescence. *The EMBO Journal*, 38 (5). [Online]. Available at: doi:10.15252/embj.2018100492.

Angello, J. C. et al. (1987). Proliferative potential of human fibroblasts: An inverse dependence on cell size. *Journal of Cellular Physiology*, 132 (1), pp.125–130. [Online]. Available at: doi:10.1002/jcp.1041320117.

Arat, N. Ö. and Griffith, J. D. (2012). Human Rap1 interacts directly with telomeric DNA and regulates TRF2 localization at the telomere. *Journal of Biological Chemistry*, 287 (50), pp.41583–41594. [Online]. Available at: doi:10.1074/jbc.M112.415984.

Armanios, M. and Blackburn, E. H. (2012). The telomere syndromes. *Nature reviews. Genetics*, 13 (10), pp.693–704. [Online]. Available at: doi:10.1038/nrg3246.

Armanios, M. Y. et al. (2007). Telomerase mutations in families with idiopathic pulmonary fibrosis. *New England Journal of Medicine*, 356 (13), pp.1317–1326. [Online]. Available at: doi:10.1056/NEJMoa066157.

Armbruster, B. N. et al. (2001). N-Terminal Domains of the Human Telomerase Catalytic Subunit Required for Enzyme Activity in Vivo. *Molecular and Cellular Biology*, 21 (22), pp.7775–7786. [Online]. Available at: doi:10.1128/mcb.21.22.7775-7786.2001.

Armbruster, B. N. et al. (2004). Rescue of an hTERT mutant defective in telomere elongation by fusion with hPot1. *Molecular and cellular biology*, 24 (8), pp.3552–3561. [Online]. Available at: doi:10.1128/mcb.24.8.3552-

3561.2004.

Arnoult, N. et al. (2010). Replication Timing of Human Telomeres Is Chromosome Arm–Specific, Influenced by Subtelomeric Structures and Connected to Nuclear Localization. Haber, J. E. (Ed). *PLoS Genetics*, 6 (4), p.e1000920. [Online]. Available at: doi:10.1371/journal.pgen.1000920.

Avilion, A. A. et al. (1996). Human telomerase RNA and telomerase activity in immortal cell lines and tumor tissues. *Cancer research*, 56 (3), pp.645–650. [Online]. Available at: http://www.ncbi.nlm.nih.gov/pubmed/8564985.

Azzalin, C. M. et al. (2007). Telomeric repeat-containing RNA and RNA surveillance factors at mammalian chromosome ends. *Science*, 318 (5851), pp.798–801. [Online]. Available at: doi:10.1126/science.1147182.

Bae, N. S. and Baumann, P. (2007). A RAP1/TRF2 Complex Inhibits Nonhomologous End-Joining at Human Telomeric DNA Ends. *Molecular Cell*, 26 (3), pp.323–334. [Online]. Available at: doi:10.1016/j.molcel.2007.03.023.

Baker, D. J. et al. (2011). Clearance of p16 Ink4a-positive senescent cells delays ageing-associated disorders. *Nature*, 479 (7372), pp.232–236. [Online]. Available at: doi:10.1038/nature10600.

Baker, D. J. et al. (2016). Naturally occurring p16 Ink4a-positive cells shorten healthy lifespan. *Nature*, 530 (7589), pp.184–189. [Online]. Available at: doi:10.1038/nature16932.

Baker, S. J. et al. (1990). Suppression of human colorectal carcinoma cell growth by wild-type p53. *Science*, 249 (4971), pp.912–915. [Online]. Available at: doi:10.1126/science.2144057.

Bakkenist, C. J. et al. (2004). Disappearance of the telomere dysfunction-induced stress response in fully senescent cells. *Cancer Research*, 64 (11), pp.3748–3752. [Online]. Available at: doi:10.1158/0008-5472.CAN-04-0453.

Ballarino, M. et al. (2005). The Cotranscriptional Assembly of snoRNPs

Controls the Biosynthesis of H/ACA snoRNAs in Saccharomyces cerevisiae. *Molecular and Cellular Biology*, 25 (13), pp.5396–5403. [Online]. Available at: doi:10.1128/mcb.25.13.5396-5403.2005.

Banaszynski, L. A. et al. (2006). A Rapid, Reversible, and Tunable Method to Regulate Protein Function in Living Cells Using Synthetic Small Molecules. *Cell*, 126 (5), pp.995–1004. [Online]. Available at: doi:10.1016/J.CELL.2006.07.025.

Banik, S. S. R. et al. (2002). C-Terminal Regions of the Human Telomerase Catalytic Subunit Essential for In Vivo Enzyme Activity. *Molecular and Cellular Biology*, 22 (17), pp.6234–6246. [Online]. Available at: doi:10.1128/mcb.22.17.6234-6246.2002.

Barthel, F. P. et al. (2017). Systematic analysis of telomere length and somatic alterations in 31 cancer types. *Nature Genetics*, 49 (3), pp.349–357. [Online]. Available at: doi:10.1038/ng.3781.

Baur, J. A. et al. (2001). Telomere position effect in human cells. *Science*, 292 (5524), pp.2075–2077. [Online]. Available at: doi:10.1126/science.1062329.

Beauséjour, C. M. et al. (2003). Reversal of human cellular senescence: roles of the p53 and p16 pathways. *The EMBO journal*, 22 (16), pp.4212–4222. [Online]. Available at: doi:10.1093/emboj/cdg417.

Benetti, R., García-Cao, M. and Blasco, M. A. (2007). Telomere length regulates the epigenetic status of mammalian telomeres and subtelomeres. *Nature Genetics*, 39 (2), pp.243–250. [Online]. Available at: doi:10.1038/ng1952.

van Berkum, N. L. et al. (2010). Hi-C: A method to study the three-dimensional architecture of genomes. *Journal of Visualized Experiments*, (39). [Online]. Available at: doi:10.3791/1869.

Bernardes de Jesus, B. et al. (2012). Telomerase gene therapy in adult and old mice delays aging and increases longevity without increasing cancer.

EMBO Molecular Medicine, 4 (8), pp.691–704. [Online]. Available at: doi:10.1002/emmm.201200245.

Bianchi, A. et al. (1997). TRF1 is a dimer and bends telomeric DNA. *EMBO Journal*, 16 (7), pp.1785–1794. [Online]. Available at: doi:10.1093/emboj/16.7.1785.

Bielak-Zmijewska, A. et al. (2014). A comparison of replicative senescence and doxorubicin-induced premature senescence of vascular smooth muscle cells isolated from human aorta. *Biogerontology*, 15 (1), pp.47–64. [Online]. Available at: doi:10.1007/s10522-013-9477-9.

Bisteau, X., Caldez, M. J. and Kaldis, P. (2014). The complex relationship between liver cancer and the cell cycle: A story of multiple regulations. *Cancers*, 6 (1), Multidisciplinary Digital Publishing Institute (MDPI)., pp.79–111. [Online]. Available at: doi:10.3390/cancers6010079.

Biswas, G. et al. (1999). Retrograde Ca2+ signaling in C2C12 skeletal myocytes in response to mitochondrial genetic and metabolic stress: A novel mode of inter-organelle crosstalk. *EMBO Journal*, 18 (3), pp.522–533. [Online]. Available at: doi:10.1093/emboj/18.3.522.

Blackburn, E. H. and Gall, J. G. (1978). A tandemly repeated sequence at the termini of the extrachromosomal ribosomal RNA genes in Tetrahymena. *Journal of Molecular Biology*, 120 (1), pp.33–53. [Online]. Available at: doi:10.1016/0022-2836(78)90294-2.

Bodnar, A. G. et al. (1998). Extension of Life-Span by Introduction of Telomerase into Normal Human Cells. *Science*, 279 (5349), pp.349–352. [Online]. Available at: doi:10.1126/SCIENCE.279.5349.349.

Bourdon, J. C. et al. (2005). p53 isoforms can regulate p53 transcriptional activity. *Genes and Development*, 19 (18), pp.2122–2137. [Online]. Available at: doi:10.1101/gad.1339905.

Boveris, A. and Chance, B. (1973). The mitochondrial generation of hydrogen

peroxide. General properties and effect of hyperbaric oxygen. *Biochemical Journal*, 134 (3), pp.707–716. [Online]. Available at: doi:10.1042/bj1340707.

Bowman, P. D., Meek, R. L. and Daniel, C. W. (1975). Aging of human fibroblasts in vitro. Correlations between DNA synthetic ability and cell size. *Experimental Cell Research*, 93 (1), pp.184–190. [Online]. Available at: doi:10.1016/0014-4827(75)90438-3.

Brack, C. et al. (2000). EMBO WORKSHOP REPORT: Molecular and cellular gerontology Serpiano, Switzerland, September 18-22, 1999. *The EMBO journal*, 19 (9), pp.1929–1934. [Online]. Available at: doi:10.1093/emboj/19.9.1929.

Braig, M. et al. (2005). Oncogene-induced senescence as an initial barrier in lymphoma development. *Nature*, 436 (7051), pp.660–665. [Online]. Available at: doi:10.1038/nature03841.

Broccoli, D. et al. (1997). Human telomeres contain two distinct Myb–related proteins, TRF1 and TRF2. *Nature Genetics*, 17 (2), pp.231–235. [Online]. Available at: doi:10.1038/ng1097-231.

Brooks, A. R. et al. (2004). Transcriptional silencing is associated with extensive methylation of the CMV promoter following adenoviral gene delivery to muscle. *The Journal of Gene Medicine*, 6 (4), pp.395–404. [Online]. Available at: doi:10.1002/jgm.516.

Bruno, S. and Darzynkiewicz, Z. (1992). Cell cycle dependent expression and stability of the nuclear protein detected by Ki-67 antibody in HL-60 cells. *Cell Proliferation*, 25 (1), pp.31–40. [Online]. Available at: doi:10.1111/j.1365-2184.1992.tb01435.x.

Bryce, L. A. et al. (2000). Mapping of the gene for the human telomerase reverse transcriptase, hTERT, to chromosome 5p15.33 by fluorescence in situ hybridization. *Neoplasia*, 2 (3), pp.197–201. [Online]. Available at: doi:10.1038/sj.neo.7900092.

Butow, R. A. and Avadhani, N. G. (2004). Mitochondrial signaling: The retrograde response. *Molecular Cell*, 14 (1), pp.1–15. [Online]. Available at: doi:10.1016/S1097-2765(04)00179-0.

Cao, K. et al. (2011). Rapamycin reverses cellular phenotypes and enhances mutant protein clearance in Hutchinson-Gilford progeria syndrome cells. *Science Translational Medicine*, 3 (89), pp.89ra58-89ra58. [Online]. Available at: doi:10.1126/scitranslmed.3002346.

Carrero, D., Soria-Valles, C. and López-Otín, C. (2016). Hallmarks of progeroid syndromes: Lessons from mice and reprogrammed cells. *DMM Disease Models and Mechanisms*, 9 (7), Company of Biologists Ltd., pp.719–735. [Online]. Available at: doi:10.1242/dmm.024711.

Castelo-Branco, P. et al. (2013). Methylation of the TERT promoter and risk stratification of childhood brain tumours: An integrative genomic and molecular study. *The Lancet Oncology*, 14 (6), pp.534–542. [Online]. Available at: doi:10.1016/S1470-2045(13)70110-4.

De Cecco, M. et al. (2013). Genomes of replicatively senescent cells undergo global epigenetic changes leading to gene silencing and activation of transposable elements. *Aging Cell*, 12 (2), pp.247–256. [Online]. Available at: doi:10.1111/acel.12047.

Cesare, A. J. et al. (2003). Telomere looping in P. sativum (common garden pea). *Plant Journal*, 36 (2), pp.271–279. [Online]. Available at: doi:10.1046/j.1365-313X.2003.01882.x.

Cesare, A. J. et al. (2009). Spontaneous occurrence of telomeric DNA damage response in the absence of chromosome fusions. *Nature Structural & Molecular Biology*, 16 (12), pp.1244–1251. [Online]. Available at: doi:10.1038/nsmb.1725.

Cesare, A. J. and Karlseder, J. (2012). A three-state model of telomere control over human proliferative boundaries. *Current Opinion in Cell Biology*, 24 (6),

pp.731–738. [Online]. Available at: doi:10.1016/j.ceb.2012.08.007.

Chai, W., Shay, J. W. and Wright, W. E. (2005). Human telomeres maintain their overhang length at senescence. *Molecular and cellular biology*, 25 (6), pp.2158–2168. [Online]. Available at: doi:10.1128/MCB.25.6.2158-2168.2005.

Chainiaux, F. et al. (2002). UVB-induced premature senescence of human diploid skin fibroblasts. *International Journal of Biochemistry and Cell Biology*, 34 (11), pp.1331–1339. [Online]. Available at: doi:10.1016/S1357-2725(02)00022-5.

Chandra, T. et al. (2012). Independence of Repressive Histone Marks and Chromatin Compaction during Senescent Heterochromatic Layer Formation. *Molecular Cell*, 47 (2), pp.203–214. [Online]. Available at: doi:10.1016/j.molcel.2012.06.010.

Chandra, T. et al. (2015). Global reorganization of the nuclear landscape in senescent cells. *Cell Reports*, 10 (4), pp.471–483. [Online]. Available at: doi:10.1016/j.celrep.2014.12.055.

Chandra, T. and Narita, M. (2013). High-order chromatin structure and the epigenome in SAHFs. *Nucleus (United States)*, 4 (1), pp.23–28. [Online]. Available at: doi:10.4161/nucl.23189.

Chang, J. et al. (2016). Clearance of senescent cells by ABT263 rejuvenates aged hematopoietic stem cells in mice. *Nature Medicine*, 22 (1), pp.78–83. [Online]. Available at: doi:10.1038/nm.4010.

Chen, J. H. and Ozanne, S. E. (2006). Deep senescent human fibroblasts show diminished DNA damage foci but retain checkpoint capacity to oxidative stress. *FEBS Letters*, 580 (28–29), pp.6669–6673. [Online]. Available at: doi:10.1016/j.febslet.2006.11.023.

Chen, L. et al. (2003). WRN, the protein deficient in Werner syndrome, plays a critical structural role in optimizing DNA repair. *Aging Cell*, 2 (4), pp.191–199. [Online]. Available at: doi:10.1046/j.1474-9728.2003.00052.x.

Chen, Q. et al. (1995). Oxidative DNA damage and senescence of human diploid fibroblast cells. *Proceedings of the National Academy of Sciences of the United States of America*, 92 (10), pp.4337–4341. [Online]. Available at: doi:10.1073/pnas.92.10.4337.

Chen, Q. and Ames, B. N. (1994). Senescence-like growth arrest induced by hydrogen peroxide in human diploid fibroblast F65 cells. *Proceedings of the National Academy of Sciences of the United States of America*, 91 (10), pp.4130–4134. [Online]. Available at: doi:10.1073/pnas.91.10.4130.

Chen, Q. M. et al. (2001). Uncoupling the senescent phenotype from telomere shortening in hydrogen peroxide-treated fibroblasts. *Experimental Cell Research*, 265 (2), pp.294–303. [Online]. Available at: doi:10.1006/excr.2001.5182.

Cheng, D. et al. (2017). Regulation of human and mouse telomerase genes by genomic contexts and transcription factors during embryonic stem cell differentiation. *Scientific Reports*, 7 (1). [Online]. Available at: doi:10.1038/s41598-017-16764-w.

Choi, J. et al. (2008). TERT promotes epithelial proliferation through transcriptional control of a Myc- and Wnt-related developmental program. *PLoS Genetics*, 4 (1), pp.0124–0138. [Online]. Available at: doi:10.1371/journal.pgen.0040010.

Chow, T. T. et al. (2012). Early and late steps in telomere overhang processing in normal human cells: The position of the final RNA primer drives telomere shortening. *Genes and Development*, 26 (11), pp.1167–1178. [Online]. Available at: doi:10.1101/gad.187211.112.

Ciccia, A. and Elledge, S. J. (2010). The DNA Damage Response: Making It Safe to Play with Knives. *Molecular Cell*, 40 (2), pp.179–204. [Online]. Available at: doi:10.1016/j.molcel.2010.09.019.

Cimino-Reale, G. et al. (2001). The length of telomeric G-rich strand 3′-

overhang measured by oligonucleotide ligation assay. *Nucleic Acids Research*, 29 (7).

Coluzzi, E. et al. (2014). Oxidative stress induces persistent telomeric DNA damage responsible for nuclear morphology change in mammalian cells. *PLoS ONE*, 9 (10). [Online]. Available at: doi:10.1371/journal.pone.0110963.

Cong, Y.-S., Wen, J. and Bacchetti, S. (1999). The Human Telomerase Catalytic Subunit hTERT: Organization of the Gene and Characterization of the Promoter. *Human Molecular Genetics*, 8 (1), pp.137–142. [Online]. Available at: doi:10.1093/hmg/8.1.137.

Coppé, J.-P. et al. (2008). Senescence-Associated Secretory Phenotypes Reveal Cell-Nonautonomous Functions of Oncogenic RAS and the p53 Tumor Suppressor. Downward, J. (Ed). *PLoS Biology*, 6 (12), p.e301. [Online]. Available at: doi:10.1371/journal.pbio.0060301.

Coppé, J.-P. et al. (2010). The Senescence-Associated Secretory Phenotype: The Dark Side of Tumor Suppression. *Annual Review of Pathology: Mechanisms of Disease*, 5 (1), pp.99–118. [Online]. Available at: doi:10.1146/annurev-pathol-121808-102144.

Correia-Melo, C. et al. (2016). Mitochondria are required for pro-ageing features of the senescent phenotype. *The EMBO Journal*, 35 (7), pp.724–742. [Online]. Available at: doi:10.15252/embj.201592862.

Counter, C. M. et al. (1998). Telomerase activity is restored in human cells by ectopic expression of hTERT (hEST2), the catalytic subunit of telomerase. *Oncogene*, 16 (9), pp.1217–1222. [Online]. Available at: doi:10.1038/sj.onc.1201882.

Court, R. et al. (2005). How the human telomeric proteins TRF1 and TRF2 recognize telomeric DNA: A view from high-resolution crystal structures. *EMBO Reports*, 6 (1), pp.39–45. [Online]. Available at: doi:10.1038/sj.embor.7400314.

Crabbe, L. et al. (2004). Defective telomere lagging strand synthesis in cells lacking WRN helicase activity. *Science*, 306 (5703), pp.1951–1953. [Online]. Available at: doi:10.1126/science.1103619.

Crabbe, L. et al. (2007). Telomere dysfunction as a cause of genomic instability in Werner syndrome. *Proceedings of the National Academy of Sciences of the United States of America*, 104 (7), pp.2205–2210. [Online]. Available at: doi:10.1073/pnas.0609410104.

Cremer, T. et al. (1982). Analysis of chromosome positions in the interphase nucleus of Chinese hamster cells by laser-UV-microirradiation experiments. *Human Genetics*, 62 (3), pp.201–209. [Online]. Available at: doi:10.1007/BF00333519.

Criscione, S. W. et al. (2016). Biomolecules: Reorganization of chromosome architecture in replicative cellular senescence. *Science Advances*, 2 (2). [Online]. Available at: doi:10.1126/sciadv.1500882.

Cruickshanks, H. A. et al. (2013). Senescent Cells Harbour Features of the Cancer Epigenome. *Nature Cell Biology*, 15 (12), pp.1495–1506. [Online]. Available at: doi:10.1038/ncb2879.

Cusanelli, E., Romero, C. A. P. and Chartrand, P. (2013). Telomeric Noncoding RNA TERRA Is Induced by Telomere Shortening to Nucleate Telomerase Molecules at Short Telomeres. *Molecular Cell*, 51 (6), pp.780–791. [Online]. Available at: doi:10.1016/j.molcel.2013.08.029.

d'Adda di Fagagna, F. et al. (2003). A DNA damage checkpoint response in telomere-initiated senescence. *Nature*, 426 (6963), pp.194–198. [Online]. Available at: doi:10.1038/nature02118.

Dalerba, P. et al. (2005). Reconstitution of human telomerase reverse transcriptase expression rescues colorectal carcinoma cells from in vitro senescence: Evidence against immortality as a constitutive trait of tumor cells. *Cancer Research*, 65 (6), pp.2321–2329. [Online]. Available at:

doi:10.1158/0008-5472.CAN-04-3678.

Darzacq, X. et al. (2006). Stepwise RNP assembly at the site of H/ACA RNA transcription in human cells. *Journal of Cell Biology*, 173 (2), pp.207–218. [Online]. Available at: doi:10.1083/jcb.200601105.

Davis, T. et al. (2006). Prevention of accelerated cell aging in the werner syndrome. In: *Annals of the New York Academy of Sciences*. 1067 (1). 2006. Blackwell Publishing Inc. pp.243–247. [Online]. Available at: doi:10.1196/annals.1354.031.

Davis, T. et al. (2007). The role of cellular senescence in Werner syndrome: Toward therapeutic intervention in human premature aging. In: *Annals of the New York Academy of Sciences*. 1100 (1). 1 April 2007. Blackwell Publishing Inc. pp.455–469. [Online]. Available at: doi:10.1196/annals.1395.051.

Dawson, R. et al. (2003). The N-terminal domain of p53 is natively unfolded. *Journal of Molecular Biology*, 332 (5), pp.1131–1141. [Online]. Available at: doi:10.1016/j.jmb.2003.08.008.

Déjardin, J. and Kingston, R. E. (2009). Purification of Proteins Associated with Specific Genomic Loci. *Cell*, 136 (1), pp.175–186. [Online]. Available at: doi:10.1016/j.cell.2008.11.045.

Denchi, E. L. and de Lange, T. (2007). Protection of telomeres through independent control of ATM and ATR by TRF2 and POT1. *Nature*, 448 (7157), pp.1068–1071. [Online]. Available at: doi:10.1038/nature06065.

Deng, Z. et al. (2009). TERRA RNA Binding to TRF2 Facilitates Heterochromatin Formation and ORC Recruitment at Telomeres. *Molecular Cell*, 35 (4), pp.403–413. [Online]. Available at: doi:10.1016/j.molcel.2009.06.025.

Deng, Z. et al. (2013). Inherited mutations in the helicase RTEL1 cause telomere dysfunction and Hoyeraal-Hreidarsson syndrome. *Proceedings of the National Academy of Sciences of the United States of America*, 110 (36),

p.E3408. [Online]. Available at: doi:10.1073/pnas.1300600110.

Denoyelle, C. et al. (2006). Anti-oncogenic role of the endoplasmic reticulum differentially activated by mutations in the MAPK pathway. *Nature Cell Biology*, 8 (10), pp.1053–1063. [Online]. Available at: doi:10.1038/ncb1471.

van Deursen, J. M. (2019). Senolytic therapies for healthy longevity. *Science*, 364 (6441), American Association for the Advancement of Science., pp.636–637. [Online]. Available at: doi:10.1126/science.aaw1299.

Van Deursen, J. M. (2014). The role of senescent cells in ageing. *Nature*, 509 (7501), Nature Publishing Group., pp.439–446. [Online]. Available at: doi:10.1038/nature13193.

Dimri, G. P. et al. (1995). A biomarker that identifies senescent human cells in culture and in aging skin in vivo. *Proceedings of the National Academy of Sciences of the United States of America*, 92 (20), pp.9363–9367. [Online]. Available at: doi:10.1073/pnas.92.20.9363.

Ding, D. et al. (2013). Human telomerase reverse transcriptase regulates MMP expression independently of telomerase activity *via* NF-κB-dependent transcription. *The FASEB Journal*, 27 (11), pp.4375–4383. [Online]. Available at: doi:10.1096/fj.13-230904.

Dionne, I. and Wellinger, R. J. (1998). Processing of telomeric DNA ends requires the passage of a replication fork. *Nucleic Acids Research*, 26 (23), pp.5365–5371. [Online]. Available at: doi:10.1093/nar/26.23.5365.

Dirac, A. M. G. and Bernards, R. (2003). Reversal of senescence in mouse fibroblasts through lentiviral suppression of p53. *The Journal of biological chemistry*, 278 (14), pp.11731–11734. [Online]. Available at: doi:10.1074/jbc.C300023200.

Dokal, I. (2011). Dyskeratosis congenita. *Hematology / the Education Program of the American Society of Hematology. American Society of Hematology. Education Program*, 2011, pp.480–486. [Online]. Available at:

doi:10.1182/asheducation-2011.1.480.

Doksani, Y. et al. (2013). Super-Resolution Fluorescence Imaging of Telomeres Reveals TRF2-Dependent T-loop Formation. *Cell*, 155 (2), pp.345–356. [Online]. Available at: doi:10.1016/J.CELL.2013.09.048.

Doksani, Y. and de Lange, T. (2016). Telomere-Internal Double-Strand Breaks Are Repaired by Homologous Recombination and PARP1/Lig3-Dependent End-Joining. *Cell Reports*, 17 (6), pp.1646–1656. [Online]. Available at: doi:10.1016/J.CELREP.2016.10.008.

Dou, Z. et al. (2015). Autophagy mediates degradation of nuclear lamina. *Nature*, 527 (7576), pp.105–109. [Online]. Available at: doi:10.1038/nature15548.

Drosopoulos, W. C., Kosiyatrakul, S. T. and Schildkraut, C. L. (2015). BLM helicase facilitates telomere replication during leading strand synthesis of telomeres. *The Journal of cell biology*, 210 (2), pp.191–208. [Online]. Available at: doi:10.1083/jcb.201410061.

Duan, J. et al. (2005). Irreversible cellular senescence induced by prolonged exposure to H 2O2 involves DNA-damage-and-repair genes and telomere shortening. *International Journal of Biochemistry and Cell Biology*, 37 (7), pp.1407–1420. [Online]. Available at: doi:10.1016/j.biocel.2005.01.010.

Dull, T. et al. (1998). A third-generation lentivirus vector with a conditional packaging system. *Journal of virology*, 72 (11), pp.8463–8471. [Online]. Available at: http://www.ncbi.nlm.nih.gov/pubmed/9765382.

Dumaz, N. (1999). Serine15 phosphorylation stimulates p53 transactivation but does not directly influence interaction with HDM2. *The EMBO Journal*, 18 (24), pp.7002–7010. [Online]. Available at: doi:10.1093/emboj/18.24.7002.

Dumaz, N., Milne, D. M. and Meek, D. W. (1999). Protein kinase CK1 is a p53-threonine 18 kinase which requires prior phosphorylation of serine 15. *FEBS Letters*, 463 (3), pp.312–316. [Online]. Available at: doi:10.1016/S0014-

5793(99)01647-6.

Dumont, P. et al. (2000). Induction of replicative senescence biomarkers by sublethal oxidative stresses in normal human fibroblast. *Free Radical Biology and Medicine*, 28 (3), pp.361–373. [Online]. Available at: doi:10.1016/S0891-5849(99)00249-X.

Egeler, E. L. et al. (2011). Ligand-switchable substrates for a ubiquitin-proteasome system. *The Journal of biological chemistry*, 286 (36), pp.31328–31336. [Online]. Available at: doi:10.1074/jbc.M111.264101.

el-Deiry, W. S. et al. (1993). WAF1, a potential mediator of p53 tumor suppression. *Cell*, 75 (4), pp.817–825. [Online]. Available at: doi:10.1016/0092-8674(93)90500-p.

El-Deiry, W. S. et al. (1992). Definition of a consensus binding site for p53. *Nature Genetics*, 1 (1), pp.45–49. [Online]. Available at: doi:10.1038/ng0492-45.

Eriksson, M. et al. (2003). Recurrent de novo point mutations in lamin A cause Hutchinson-Gilford progeria syndrome. *Nature*, 423 (6937), pp.293–298. [Online]. Available at: doi:10.1038/nature01629.

Fairall, L. et al. (2001). Structure of the TRFH dimerization domain of the human telomeric proteins TRF1 and TRF2. *Molecular cell*, 8 (2), pp.351–361. [Online]. Available at: doi:10.1016/s1097-2765(01)00321-5.

Fallet, E. et al. (2014). Length-dependent processing of telomeres in the absence of telomerase. *Nucleic Acids Research*, 42 (6), pp.3648–3665. [Online]. Available at: doi:10.1093/nar/gkt1328.

Farmer, G. et al. (1992). Wild-type p53 activates transcription in vitro. *Nature*, 358 (6381), pp.83–86. [Online]. Available at: doi:10.1038/358083a0.

Farnung, B. O. et al. (2012). Telomerase Efficiently Elongates Highly Transcribing Telomeres in Human Cancer Cells. Lustig, A. J. (Ed). *PLoS ONE*,

7 (4), p.e35714. [Online]. Available at: doi:10.1371/journal.pone.0035714.

Farr, J. N. et al. (2016). Identification of Senescent Cells in the Bone Microenvironment. *Journal of Bone and Mineral Research*, 31 (11), pp.1920–1929. [Online]. Available at: doi:10.1002/jbmr.2892.

Feng, J. et al. (1995). The RNA component of human telomerase. *Science*, 269 (5228), pp.1236–1241. [Online]. Available at: doi:10.1126/science.7544491.

Finlan, L. E. et al. (2008). Recruitment to the Nuclear Periphery Can Alter Expression of Genes in Human Cells. Reik, W. (Ed). *PLoS Genetics*, 4 (3), p.e1000039. [Online]. Available at: doi:10.1371/journal.pgen.1000039.

Fischer, B. M. et al. (2013). Increased expression of senescence markers in cystic fibrosis airways. *American Journal of Physiology - Lung Cellular and Molecular Physiology*, 304 (6), p.L394. [Online]. Available at: doi:10.1152/ajplung.00091.2012.

Fogarty, P. F. et al. (2003). Late presentation of dyskeratosis congenita as apparently acquired aplastic anaemia due to mutations in telomerase RNA. *Lancet*, 362 (9396), pp.1628–1630. [Online]. Available at: doi:10.1016/S0140-6736(03)14797-6.

Freedman, D. A., Wu, L. and Levine, A. J. (1999). Functions of the MDM2 oncoprotein. *Cellular and Molecular Life Sciences*, 55 (1), pp.96–107. [Online]. Available at: doi:10.1007/s000180050273.

Freund, A. et al. (2012). Lamin B1 loss is a senescence-associated biomarker. *Molecular Biology of the Cell*, 23 (11), pp.2066–2075. [Online]. Available at: doi:10.1091/mbc.E11-10-0884.

Fu, D. and Collins, K. (2003). Distinct Biogenesis Pathways for Human Telomerase RNA and H/ACA Small Nucleolar RNAs. *Molecular Cell*, 11 (5), pp.1361–1372. [Online]. Available at: doi:10.1016/S1097-2765(03)00196-5.

Fujita, K. et al. (2009). p53 isoforms Δ133p53 and p53β are endogenous regulators of replicative cellular senescence. *Nature Cell Biology*, 11 (9), pp.1135–1142. [Online]. Available at: doi:10.1038/ncb1928.

Fujita, K. (2019). P53 isoforms in cellular senescence-and ageing-associated biological and physiological functions. *International Journal of Molecular Sciences*, 20 (23), MDPI AG. [Online]. Available at: doi:10.3390/ijms20236023.

Fukuchi, K. ichiro et al. (1985). Elevated spontaneous mutation rate in SV40-transformed werner syndrome fibroblast cell lines. *Somatic Cell and Molecular Genetics*, 11 (3), pp.303–308. [Online]. Available at: doi:10.1007/BF01534688.

Fukuchi, K., Martin, G. M. and Monnat, R. J. (1989). Mutator phenotype of Werner syndrome is characterized by extensive deletions. *Proceedings of the National Academy of Sciences of the United States of America*, 86 (15), pp.5893–5897. [Online]. Available at: doi:10.1073/pnas.86.15.5893.

Fumagalli, M. et al. (2012). Telomeric DNA damage is irreparable and causes persistent DNA-damage-response activation. *Nature Cell Biology*, 14 (4), pp.355–365. [Online]. Available at: doi:10.1038/ncb2466.

Fumagalli, M. et al. (2014). Stable Cellular Senescence Is Associated with Persistent DDR Activation. Marcu, K. B. (Ed). *PLoS ONE*, 9 (10), p.e110969. [Online]. Available at: doi:10.1371/journal.pone.0110969.

Funk, W. D. et al. (1992). A transcriptionally active DNA-binding site for human p53 protein complexes. *Molecular and Cellular Biology*, 12 (6), pp.2866–2871. [Online]. Available at: doi:10.1128/mcb.12.6.2866.

Gallardo, F. et al. (2011). Live cell imaging of telomerase RNA dynamics reveals cell cycle-dependent clustering of telomerase at elongating telomeres. *Molecular Cell*, 44 (5), pp.819–827. [Online]. Available at: doi:10.1016/j.molcel.2011.09.020.

Gan, W. et al. (2011). R-loop-mediated genomic instability is caused by impairment of replication fork progression. *Genes and Development*, 25 (19), pp.2041–2056. [Online]. Available at: doi:10.1101/gad.17010011.

Gerdes, J. et al. (1983). Production of a mouse monoclonal antibody reactive with a human nuclear antigen associated with cell proliferation. *International Journal of Cancer*, 31 (1), pp.13–20. [Online]. Available at: doi:10.1002/ijc.2910310104.

Ghosh, A. et al. (2012). Telomerase directly regulates NF-B-dependent transcription. *Nature Cell Biology*, 14 (12), pp.1270–1281. [Online]. Available at: doi:10.1038/ncb2621.

Gillis, A. J., Schuller, A. P. and Skordalakes, E. (2008). Structure of the Tribolium castaneum telomerase catalytic subunit TERT. *Nature*, 455 (7213), pp.633–637. [Online]. Available at: doi:10.1038/nature07283.

Giovanni, A. et al. (1999). Involvement of cell cycle elements, cyclin-dependent kinases, pRB, and E2F·DP, in B-amyloid-induced neuronal death. *Journal of Biological Chemistry*, 274 (27), pp.19011–19016. [Online]. Available at: doi:10.1074/jbc.274.27.19011.

Gizard, F. et al. (2011). Telomerase activation in atherosclerosis and induction of telomerase reverse transcriptase expression by inflammatory stimuli in macrophages. *Arteriosclerosis, Thrombosis, and Vascular Biology*, 31 (2), pp.245–252. [Online]. Available at: doi:10.1161/ATVBAHA.110.219808.

Goldman, R. D. et al. (2004). Accumulation of mutant lamin A progressive changes in nuclear architecture in Hutchinson-Gilford progeria syndrome. *Proceedings of the National Academy of Sciences of the United States of America*, 101 (24), pp.8963–8968. [Online]. Available at: doi:10.1073/pnas.0402943101.

Gonzalo, S. et al. (2006). DNA methyltransferases control telomere length and telomere recombination in mammalian cells. *Nature Cell Biology*, 8 (4),

pp.416–424. [Online]. Available at: doi:10.1038/ncb1386.

Gonzalo, S. and Kreienkamp, R. (2015). DNA repair defects and genome instability in Hutchinson-Gilford Progeria Syndrome. *Current Opinion in Cell Biology*, 34, Elsevier Ltd., pp.75–83. [Online]. Available at: doi:10.1016/j.ceb.2015.05.007.

Gordon, K. et al. (2014). Immortality, but not oncogenic transformation, of primary human cells leads to epigenetic reprogramming of DNA methylation and gene expression. *Nucleic Acids Research*, 42 (6), pp.3529–3541. [Online]. Available at: doi:10.1093/nar/gkt1351.

Goto, M. et al. (1992). Genetic linkage of Werner's syndrome to five markers on chromosome 8. *Nature*, 355 (6362), pp.735–738. [Online]. Available at: doi:10.1038/355735a0.

Gray, M. D. et al. (1997). The Werner syndrome protein is a DNA helicase. *Nature Genetics*, 17 (1), pp.100–103. [Online]. Available at: doi:10.1038/ng0997-100.

Greider, C. W. and Blackburn, E. H. (1985). Identification of a specific telomere terminal transferase activity in tetrahymena extracts. *Cell*, 43 (2), pp.405–413. [Online]. Available at: doi:10.1016/0092-8674(85)90170-9.

Griffith, J. D. et al. (1999). Mammalian Telomeres End in a Large Duplex Loop. *Cell*, 97 (4), pp.503–514. [Online]. Available at: doi:10.1016/S0092-8674(00)80760-6.

Grivennikova, V. G., Kareyeva, A. V. and Vinogradov, A. D. (2018). Oxygen-dependence of mitochondrial ROS production as detected by Amplex Red assay. *Redox Biology*, 17, pp.192–199. [Online]. Available at: doi:10.1016/j.redox.2018.04.014.

Gruenbaum, Y. and Foisner, R. (2015). Lamins: Nuclear Intermediate Filament Proteins with Fundamental Functions in Nuclear Mechanics and Genome Regulation. *Annual Review of Biochemistry*, 84 (1), pp.131–164. [Online].

Available at: doi:10.1146/annurev-biochem-060614-034115.

Guelen, L. et al. (2008). Domain organization of human chromosomes revealed by mapping of nuclear lamina interactions. *Nature*, 453 (7197), pp.948–951. [Online]. Available at: doi:10.1038/nature06947.

Guilleret, I. et al. (2002). Hypermethylation of the human telomerase catalytic subunit (hTERT) gene correlates with telomerase activity. *International Journal of Cancer*, 101 (4), pp.335–341. [Online]. Available at: doi:10.1002/ijc.10593.

Haendeler, J. et al. (2004). Antioxidants Inhibit Nuclear Export of Telomerase Reverse Transcriptase and Delay Replicative Senescence of Endothelial Cells. *Circulation Research*, 94 (6), pp.768–775. [Online]. Available at: doi:10.1161/01.RES.0000121104.05977.F3.

Ten Hagen, K. G. et al. (1990). Replication timing of DNA sequences associated with human centromeres and telomeres. *Molecular and Cellular Biology*, 10 (12), pp.6348–6355. [Online]. Available at: doi:10.1128/mcb.10.12.6348.

Halazonetis, T. D. and Kandil, A. N. (1993). Conformational shifts propagate from the oligomerization domain of p53 to its tetrameric DNA binding domain and restore DNA binding to select p53 mutants. *The EMBO Journal*, 12 (13), pp.5057–5064. [Online]. Available at: doi:10.1002/j.1460-2075.1993.tb06199.x.

Hanahan, D. and Weinberg, R. A. (2011). Hallmarks of Cancer: The Next Generation. *Cell*, 144 (5), pp.646–674. [Online]. Available at: doi:10.1016/J.CELL.2011.02.013.

Hanaoka, S. et al. (2001). NMR structure of the hRap1 Myb motif reveals a canonical three-helix bundle lacking the positive surface charge typical of Myb DNA-binding domains. *Journal of Molecular Biology*, 312 (1), pp.167–175. [Online]. Available at: doi:10.1006/jmbi.2001.4924.

Harley, C. B., Futcher, A. B. and Greider, C. W. (1990). Telomeres shorten

during ageing of human fibroblasts. *Nature*, 345 (6274), pp.458–460. [Online]. Available at: doi:10.1038/345458a0.

Harvey, D. M. and Levine, A. J. (1991). p53 alteration is a common event in the spontaneous immortalization of primary BALB/c murine embryo fibroblasts. *Genes and Development*, 5 (12 PART B), pp.2375–2385. [Online]. Available at: doi:10.1101/gad.5.12b.2375.

Harvey, M. et al. (1993). In vitro growth characteristics of embryo fibroblasts isolated from p53-deficient mice. *Oncogene*, 8 (9), pp.2457–2467.

Hayflick, L. (1965). The limited in vitro lifetime of human diploid cell strains. *Experimental Cell Research*, 37 (3), pp.614–636. [Online]. Available at: doi:10.1016/0014-4827(65)90211-9.

Hayflick, L. and Moorhead, P. S. (1961). The serial cultivation of human diploid cell strains. *Experimental Cell Research*, 25 (3), pp.585–621. [Online]. Available at: doi:10.1016/0014-4827(61)90192-6.

Heiss, N. S. et al. (1998). X-linked dyskeratosis congenita is caused by mutations in a highly conserved gene with putative nucleolar functions. *Nature Genetics*, 19 (1), pp.32–38. [Online]. Available at: doi:10.1038/ng0598-32.

Herbig, U. et al. (2004). Telomere shortening triggers senescence of human cells through a pathway involving ATM, p53, and p21CIP1, but not p16INK4a. *Molecular Cell*, 14 (4), pp.501–513. [Online]. Available at: doi:10.1016/S1097-2765(04)00256-4.

Hewitt, G. et al. (2012). Telomeres are favoured targets of a persistent DNA damage response in ageing and stress-induced senescence. *Nature Communications*, 3 (1), p.708. [Online]. Available at: doi:10.1038/ncomms1708.

Hickson, I. et al. (2004). Identification and characterization of a novel and specific inhibitor of the ataxia-telangiectasia mutated kinase ATM. *Cancer Research*, 64 (24), pp.9152–9159. [Online]. Available at: doi:10.1158/0008-

5472.CAN-04-2727.

Hiyama, E. et al. (1996). Telomerase activity in human intestine. *International Journal of Oncology*, 9 (3), pp.453–458. [Online]. Available at: doi:10.3892/ijo.9.3.453.

Hiyama, E. and Hiyama, K. (2007). Telomere and telomerase in stem cells. *British Journal of Cancer*, 96 (7), pp.1020–1024. [Online]. Available at: doi:10.1038/sj.bjc.6603671.

Hoagland, M. S., Hoagland, E. M. and Swanson, H. I. (2005). The p53 inhibitor pifithrin-alpha is a potent agonist of the aryl hydrocarbon receptor. *The Journal of pharmacology and experimental therapeutics*, 314 (2), pp.603–610. [Online]. Available at: doi:10.1124/jpet.105.084186.

Hockemeyer, D. et al. (2007). Telomere protection by mammalian Pot1 requires interaction with Tpp1. *Nature Structural and Molecular Biology*, 14 (8), pp.754–761. [Online]. Available at: doi:10.1038/nsmb1270.

Hoffmeyer, K. et al. (2012). Wnt/β-catenin signaling regulates telomerase in stem cells and cancer cells. *Science*, 336 (6088), pp.1549–1554. [Online]. Available at: doi:10.1126/science.1218370.

Holohan, B., Wright, W. E. and Shay, J. W. (2014). Telomeropathies: An emerging spectrum disorder. *Journal of Cell Biology*, 205 (3), Rockefeller University Press., pp.289–299. [Online]. Available at: doi:10.1083/jcb.201401012.

Honda, R., Tanaka, H. and Yasuda, H. (1997). Oncoprotein MDM2 is a ubiquitin ligase E3 for tumor suppressor p53. *FEBS Letters*, 420 (1), pp.25–27. [Online]. Available at: doi:10.1016/S0014-5793(97)01480-4.

Horikawa, I. et al. (1999). Cloning and Characterization of the Promoter Region of Human Telomerase Reverse Transcriptase Gene. *Cancer Research*, 59 (4), pp.826 LP – 830. [Online]. Available at: http://cancerres.aacrjournals.org/content/59/4/826.abstract.

Horn, S. et al. (2013). TERT promoter mutations in familial and sporadic melanoma. *Science*, 339 (6122), pp.959–961. [Online]. Available at: doi:10.1126/science.1230062.

Horvath, M. M. et al. (2007). Divergent evolution of human p53 binding sites: Cell cycle versus apoptosis. *PLoS Genetics*, 3 (7), pp.1284–1295. [Online]. Available at: doi:10.1371/journal.pgen.0030127.

Huang, D. S. et al. (2015). Recurrent TERT promoter mutations identified in a large-scale study of multiple tumour types are associated with increased TERT expression and telomerase activation. *European Journal of Cancer*, 51 (8), pp.969–976. [Online]. Available at: doi:10.1016/j.ejca.2015.03.010.

Huang, F. W. et al. (2013). Highly recurrent TERT promoter mutations in human melanoma. *Science*, 339 (6122), pp.957–959. [Online]. Available at: doi:10.1126/science.1229259.

Huang, S. et al. (2006). The spectrum of *WRN* mutations in Werner syndrome patients. *Human Mutation*, 27 (6), pp.558–567. [Online]. Available at: doi:10.1002/humu.20337.

Huffman, K. E. et al. (2000). Telomere shortening is proportional to the size of the G-rich telomeric 3'-overhang. *The Journal of biological chemistry*, 275 (26), pp.19719–19722. [Online]. Available at: doi:10.1074/jbc.M002843200.

Hussain, S. P. and Harris, C. C. (1998). Molecular epidemiology of human cancer: Contribution of mutation spectra studies of tumor suppressor genes. *Cancer Research*, 58 (18), American Association for Cancer Research., pp.4023–4037.

Ino, H. and Chiba, T. (2001). Cyclin-dependent kinase 4 and cyclin D1 are required for excitotoxin-induced neuronal cell death in vivo. *Journal of Neuroscience*, 21 (16), pp.6086–6094. [Online]. Available at: doi:10.1523/JNEUROSCI.21-16-06086.2001.

Itahana, Y., Ke, H. and Zhang, Y. (2009). p53 oligomerization is essential for

its C-terminal lysine acetylation. *Journal of Biological Chemistry*, 284 (8), pp.5158–5164. [Online]. Available at: doi:10.1074/jbc.M805696200.

Ito, A. et al. (2001). p300/CBP-mediated p53 acetylation is commonly induced by p53-activating agents and inhibited by MDM2. *EMBO Journal*, 20 (6), pp.1331–1340. [Online]. Available at: doi:10.1093/emboj/20.6.1331.

Ito, A. et al. (2002). MDM2-HDAC1-mediated deacetylation of p53 is required for its degradation. *EMBO Journal*, 21 (22), pp.6236–6245. [Online]. Available at: doi:10.1093/emboj/cdf616.

Iwamoto, M. et al. (2010). A general chemical method to regulate protein stability in the mammalian central nervous system. *Chemistry and Biology*, 17 (9), pp.981–988. [Online]. Available at: doi:10.1016/j.chembiol.2010.07.009.

Jackson, S. P. and Bartek, J. (2009). The DNA-damage response in human biology and disease. *Nature*, 461 (7267), pp.1071–1078. [Online]. Available at: doi:10.1038/nature08467.

Jády, B. E. et al. (2006). Cell cycle-dependent recruitment of telomerase RNA and Cajal bodies to human telomeres. *Molecular biology of the cell*, 17 (2), pp.944–954. [Online]. Available at: doi:10.1091/mbc.e05-09-0904.

Jády, B. E., Bertrand, E. and Kiss, T. (2004). Human telomerase RNA and box H/ACA scaRNAs share a common Cajal body-specific localization signal. *Journal of Cell Biology*, 164 (5), pp.647–652. [Online]. Available at: doi:10.1083/jcb.200310138.

Jeffrey, P. D., Gorina, S. and Pavletich, N. P. (1995). Crystal structure of the tetramerization domain of the p53 tumor suppressor at 1.7 angstroms. *Science*, 267 (5203), pp.1498–1502. [Online]. Available at: doi:10.1126/science.7878469.

Jegga, A. G. et al. (2008). Functional evolution of the p53 regulatory network through its target response elements. *Proceedings of the National Academy of Sciences of the United States of America*, 105 (3), pp.944–949. [Online].

Available at: doi:10.1073/pnas.0704694105.

Jenkins, N. C. et al. (2011). The p16 INK4A tumor suppressor regulates cellular oxidative stress. *Oncogene*, 30 (3), pp.265–274. [Online]. Available at: doi:10.1038/onc.2010.419.

Jeyapalan, J. C. et al. (2007). Accumulation of senescent cells in mitotic tissue of aging primates. *Mechanisms of Ageing and Development*, 128 (1), pp.36–44. [Online]. Available at: doi:10.1016/j.mad.2006.11.008.

Jiang, L., Sheikh, M. S. and Huang, Y. (2010). Decision making by p53: Life versus death. *Molecular and Cellular Pharmacology*, 2 (2), pp.69–77. [Online]. Available at: doi:10.4255/mcpharmacol.10.10.

Jiang, X. R. et al. (1999). Telomerase expression in human somatic cells does not induce changes associated with a transformed phenotype. *Nature Genetics*, 21 (1), pp.111–1114. [Online]. Available at: doi:10.1038/5056.

Johmura, Y. et al. (2016). SCF Fbxo22-KDM4A targets methylated p53 for degradation and regulates senescence. *Nature Communications*, 7. [Online]. Available at: doi:10.1038/ncomms10574.

Joruiz, S. M. and Bourdon, J. C. (2016). P53 isoforms: Key regulators of the cell fate decision. *Cold Spring Harbor Perspectives in Medicine*, 6 (8). [Online]. Available at: doi:10.1101/cshperspect.a026039.

Jurk, D. et al. (2012). Postmitotic neurons develop a p21-dependent senescence-like phenotype driven by a DNA damage response. *Aging Cell*, 11 (6), pp.996–1004. [Online]. Available at: doi:10.1111/j.1474-9726.2012.00870.x.

Kajtar, P. and Mehes, K. (1994). Bilateral Coats retinopathy associated with aplastic anaemia and mild dyskeratotic signs. *American Journal of Medical Genetics*, 49 (4), pp.374–377. [Online]. Available at: doi:10.1002/ajmg.1320490404.

Karlseder, J., Smogorzewska, A. and Lange, T. de. (2002). Senescence Induced by Altered Telomere State, Not Telomere Loss. *Science*, 295 (5564), pp.2446–2449. [Online]. Available at: doi:10.1126/SCIENCE.1069523.

Kawanishi, S. and Oikawa, S. (2004). Mechanism of telomere shortening by oxidative stress. In: *Annals of the New York Academy of Sciences*. 1019 (1). 1 June 2004. New York Academy of Sciences. pp.278–284. [Online]. Available at: doi:10.1196/annals.1297.047.

Kim, N. W. et al. (1994). Specific association of human telomerase activity with immortal cells and cancer. *Science (New York, N.Y.)*, 266 (5193), pp.2011–2015. [Online]. Available at: doi:10.1126/science.7605428.

Kocak, H. et al. (2014). Hoyeraal-Hreidarsson syndrome caused by a germline mutation in the TEL patch of the telomere protein TPP1. *Genes and Development*, 28 (19), pp.2090–2102. [Online]. Available at: doi:10.1101/gad.248567.114.

Koering, C. E. et al. (2002). Human telomeric position effect is determined by chromosomal context and telomeric chromatin integrity. *EMBO reports*, 3 (11), pp.1055–1061. [Online]. Available at: doi:10.1093/embo-reports/kvf215.

Kogenaru, M. and Isalan, M. (2018). Drug-Inducible Control of Lethality Genes: A Low Background Destabilizing Domain Architecture Applied to the Gal4-UAS System in Drosophila. *ACS Synthetic Biology*, 7 (6), pp.1496–1506. [Online]. Available at: doi:10.1021/acssynbio.7b00302.

Komarov, P. G. et al. (1999). A Chemical Inhibitor of p53 That Protects Mice from the Side Effects of Cancer Therapy. *Science*, 285 (5434), pp.1733 LP – 1737. [Online]. Available at: http://science.sciencemag.org/content/285/5434/1733.abstract.

Komarova, E. A. et al. (2003). p53 inhibitor pifithrin alpha can suppress heat shock and glucocorticoid signaling pathways. *The Journal of biological chemistry*, 278 (18), pp.15465–15468. [Online]. Available at:

doi:10.1074/jbc.C300011200.

Kortlever, R. M., Higgins, P. J. and Bernards, R. (2006). Plasminogen activator inhibitor-1 is a critical downstream target of p53 in the induction of replicative senescence. *Nature Cell Biology*, 8 (8), pp.878–884. [Online]. Available at: doi:10.1038/ncb1448.

Kosar, M. et al. (2011). Senescence-associated heterochromatin foci are dispensable for cellular senescence, occur in a cell type- and insult-dependent manner and follow expression of p16 ^{ink4a}. *Cell Cycle*, 10 (3), pp.457–468. [Online]. Available at: doi:10.4161/cc.10.3.14707.

Krishnamurthy, J. et al. (2004). Ink4a/Arf expression is a biomarker of aging. *Journal of Clinical Investigation*, 114 (9), pp.1299–1307. [Online]. Available at: doi:10.1172/JCI22475.

Kubbutat, M. H. G., Jones, S. N. and Vousden, K. H. (1997). Regulation of p53 stability by Mdm2. *Nature*, 387 (6630), pp.299–303. [Online]. Available at: doi:10.1038/387299a0.

Kuilman, T. et al. (2008). Oncogene-Induced Senescence Relayed by an Interleukin-Dependent Inflammatory Network. *Cell*, 133 (6), pp.1019–1031. [Online]. Available at: doi:10.1016/j.cell.2008.03.039.

Kuilman, T. et al. (2010). The essence of senescence. *Genes and Development*, 24 (22), pp.2463–2479. [Online]. Available at: doi:10.1101/gad.1971610.

Kussie, P. H. et al. (1996). Structure of the MDM2 oncoprotein bound to the p53 tumor suppressor transactivation domain. *Science*, 274 (5289), pp.948–953. [Online]. Available at: doi:10.1126/science.274.5289.948.

Kyng, K. J. et al. (2003). Gene expression profiling in Werner syndrome closely resembles that of normal aging. *Proceedings of the National Academy of Sciences of the United States of America*, 100 (21), pp.12259–12264. [Online]. Available at: doi:10.1073/pnas.2130723100.

Lai, C. K., Mitchell, J. R. and Collins, K. (2001). RNA binding domain of telomerase reverse transcriptase. *Molecular and cellular biology*, 21 (4), pp.990–1000. [Online]. Available at: doi:10.1128/MCB.21.4.990-1000.2001.

Lai, Z. et al. (2000). Thermodynamics of p53 binding to hdm2(1-126): Effects of phosphorylation and p53 peptide length. *Archives of Biochemistry and Biophysics*, 381 (2), pp.278–284. [Online]. Available at: doi:10.1006/abbi.2000.1998.

Lam, G. et al. (2016). Lack of TERT promoter mutations in human B-cell non-Hodgkin lymphoma. *Genes*, 7 (11). [Online]. Available at: doi:10.3390/genes7110093.

Lambert, P. F. et al. (1998). Phosphorylation of p53 serine 15 increases interaction with CBP. *Journal of Biological Chemistry*, 273 (49), pp.33048–33053. [Online]. Available at: doi:10.1074/jbc.273.49.33048.

Lammerding, J. et al. (2004). Lamin A/C deficiency causes defective nuclear mechanics and mechanotransduction. *Journal of Clinical Investigation*, 113 (3), pp.370–378. [Online]. Available at: doi:10.1172/jci19670.

Lane, D. P. (1992). p53, guardian of the genome. *Nature*, 358 (6381), pp.15–16. [Online]. Available at: doi:10.1038/358015a0.

Lane, D. P. and Crawford, L. V. (1979). T antigen is bound to a host protein in SY40-transformed cells [19]. *Nature*, 278 (5701), Nature Publishing Group., pp.261–263. [Online]. Available at: doi:10.1038/278261a0.

de Lange, T. (2002). Protection of mammalian telomeres. *Oncogene*, 21 (4), pp.532–540. [Online]. Available at: doi:10.1038/sj.onc.1205080.

Lawless, C. et al. (2010). Quantitative assessment of markers for cell senescence. *Experimental Gerontology*, 45 (10), pp.772–778. [Online]. Available at: doi:10.1016/j.exger.2010.01.018.

Lee, B. Y. et al. (2006). Senescence-associated β-galactosidase is lysosomal

β-galactosidase. *Aging Cell*, 5 (2), pp.187–195. [Online]. Available at: doi:10.1111/j.1474-9726.2006.00199.x.

Lee, D. D. et al. (2019). DNA hypermethylation within TERT promoter upregulates TERT expression in cancer. *The Journal of Clinical Investigation*, 129 (1), pp.223–229. [Online]. Available at: doi:10.1172/JCI121303.

Lee, H. C. et al. (2002). Increase in mitochondrial mass in human fibroblasts under oxidative stress and during replicative cell senescence. *Journal of Biomedical Science*, 9 (6), pp.517–526. [Online]. Available at: doi:10.1007/BF02254978.

Lee, J. H. et al. (2014). Catalytically active telomerase holoenzyme is assembled in the dense fibrillar component of the nucleolus during S phase. *Histochemistry and Cell Biology*, 141 (2), pp.137–152. [Online]. Available at: doi:10.1007/s00418-013-1166-x.

Leem, S. H. et al. (2002). The human telomerase gene: Complete genomic sequence and analysis of tandem repeat polymorphisms in intronic regions. *Oncogene*, 21 (5), pp.769–777. [Online]. Available at: doi:10.1038/sj.onc.1205122.

LeGuen, T. et al. (2013). Human RTEL1 deficiency causes hoyeraal-hreidarsson syndrome with short telomeres and genome instability. *Human Molecular Genetics*, 22 (16), pp.3239–3249. [Online]. Available at: doi:10.1093/hmg/ddt178.

Lei, M., Podell, E. R. and Cech, T. R. (2004). Structure of human POT1 bound to telomeric single-stranded DNA provides a model for chromosome end-protection. *Nature Structural and Molecular Biology*, 11 (12), pp.1223–1229. [Online]. Available at: doi:10.1038/nsmb867.

Lenain, C. et al. (2015). Autophagy-mediated degradation of nuclear envelope proteins during oncogene-induced senescence. *Carcinogenesis*, 36 (11), pp.1263–1274. [Online]. Available at: doi:10.1093/carcin/bgv124.

Li, B., Oestreich, S. and de Lange, T. (2000). Identification of Human Rap1: Implications for Telomere Evolution. *Cell*, 101 (5), pp.471–483. [Online]. Available at: doi:10.1016/S0092-8674(00)80858-2.

Li, G.-Z. et al. (2003). Evidence that exposure of the telomere 3' overhang sequence induces senescence. *Proceedings of the National Academy of Sciences of the United States of America*, 100 (2), pp.527–531. [Online]. Available at: doi:10.1073/pnas.0235444100.

Li, S. et al. (2019). An efficient auxin-inducible degron system with low basal degradation in human cells. *Nature Methods*, 16 (9), pp.866–869. [Online]. Available at: doi:10.1038/s41592-019-0512-x.

Li, Y. et al. (2015). Non-canonical NF-κB signalling and ETS1/2 cooperatively drive C250T mutant TERT promoter activation. *Nature Cell Biology*, 17 (10), pp.1327–1338. [Online]. Available at: doi:10.1038/ncb3240.

Lin, J. et al. (1994). Several hydrophobic amino acids in the p53 amino-terminal domain are required for transcriptional activation, binding to mdm-2 and the adenovirus 5 E1B 55-kD protein. *Genes and Development*, 8 (10), pp.1235–1246. [Online]. Available at: doi:10.1101/gad.8.10.1235.

Lin, P., Mobasher, M. E. and Alawi, F. (2014). Acute dyskerin depletion triggers cellular senescence and renders osteosarcoma cells resistant to genotoxic stress-induced apoptosis. *Biochemical and Biophysical Research Communications*, 446 (4), pp.1268–1275. [Online]. Available at: doi:10.1016/j.bbrc.2014.03.114.

Lin, X. et al. (2000). p53 Interacts with the DNA mismatch repair system to modulate the cytotoxicity and mutagenicity of hydrogen peroxide. *Molecular Pharmacology*, 58 (6), American Society for Pharmacology and Experimental Therapy., pp.1222–1229. [Online]. Available at: doi:10.1124/mol.58.6.1222.

Lin, Y. et al. (2019). Normoxia is not favorable for maintaining stemness of human endothelial progenitor cells. *Stem Cell Research*, 38, p.101464.

[Online]. Available at: doi:10.1016/j.scr.2019.101464.

Linzer, D. I. H. and Levine, A. J. (1979). Characterization of a 54K Dalton cellular SV40 tumor antigen present in SV40-transformed cells and uninfected embryonal carcinoma cells. *Cell*, 17 (1), pp.43–52. [Online]. Available at: doi:10.1016/0092-8674(79)90293-9.

Lipinski, M. M. and Jacks, T. (1999). The retinoblastoma gene family in differentiation and development. *Oncogene*, 18 (55), Nature Publishing Group., pp.7873–7882. [Online]. Available at: doi:10.1038/sj.onc.1203244.

Liu, B. et al. (2005). Genomic instability in laminopathy-based premature aging. *Nature Medicine*, 11 (7), pp.780–785. [Online]. Available at: doi:10.1038/nm1266.

Liu, D. et al. (2004). PTOP interacts with POT1 and regulates its localization to telomeres. *Nature Cell Biology*, 6 (7), pp.673–680. [Online]. Available at: doi:10.1038/ncb1142.

Liu, D. and Hornsby, P. J. (2007). Senescent human fibroblasts increase the early growth of xenograft tumors via matrix metalloproteinase secretion. *Cancer Research*, 67 (7), pp.3117–3126. [Online]. Available at: doi:10.1158/0008-5472.CAN-06-3452.

Liu, Y. et al. (2006). DNA damage responses in progeroid syndromes arise from defective maturation of prelamin A. *Journal of Cell Science*, 119 (22), pp.4644–4649. [Online]. Available at: doi:10.1242/jcs.03263.

Loayza, D. et al. (2004). DNA binding features of human POT1: a nonamer 5'-TAGGGTTAG-3' minimal binding site, sequence specificity, and internal binding to multimeric sites. *The Journal of biological chemistry*, 279 (13), pp.13241–13248. [Online]. Available at: doi:10.1074/jbc.M312309200.

Loayza, D. and De Lange, T. (2003). POT1 as a terminal transducer of TRF1 telomere length control. *Nature*, 423 (6943), pp.1013–1018. [Online]. Available at: doi:10.1038/nature01688.

Lorenz, M. et al. (2001). BJ fibroblasts display high antioxidant capacity and slow telomere shortening independent of hTERT transfection. *Free Radical Biology and Medicine*, 31 (6), pp.824–831. [Online]. Available at: doi:10.1016/S0891-5849(01)00664-5.

Loschen, G. et al. (1974). Superoxide radicals as precursors of mitochondrial hydrogen peroxide. *FEBS Letters*, 42 (1), pp.68–72. [Online]. Available at: doi:10.1016/0014-5793(74)80281-4.

Lowe, R. et al. (2015). The senescent methylome and its relationship with cancer, ageing and germline genetic variation in humans. *Genome Biology*, 16 (1), p.194. [Online]. Available at: doi:10.1186/s13059-015-0748-4.

Luke, B. et al. (2008). The Rat1p 5′ to 3′ Exonuclease Degrades Telomeric Repeat-Containing RNA and Promotes Telomere Elongation in Saccharomyces cerevisiae. *Molecular Cell*, 32 (4), pp.465–477. [Online]. Available at: doi:10.1016/j.molcel.2008.10.019.

Van Ly, D. et al. (2018). Telomere Loop Dynamics in Chromosome End Protection. *Molecular Cell*, 71 (4), pp.510-525.e6. [Online]. Available at: doi:10.1016/j.molcel.2018.06.025.

M.Stansel, R., Lange, T. de and Griffith, J. D. (2001). T-loop assembly in vitro involves binding of TRF2 near the 3' telomeric overhang. *The EMBO Journal*, 20 (19), pp.5532–5540. [Online]. Available at: doi:10.1093/emboj/20.19.5532.

Macip, S. et al. (2002). Inhibition of p21-mediated ROS accumulation can rescue p21-induced senescence. *EMBO Journal*, 21 (9), pp.2180–2188. [Online]. Available at: doi:10.1093/emboj/21.9.2180.

MacNeil, D. E., Lambert-Lanteigne, P. and Autexier, C. (2019). N-terminal residues of human dyskerin are required for interactions with telomerase RNA that prevent RNA degradation. *Nucleic acids research*, 47 (10), pp.5368–5380. [Online]. Available at: doi:10.1093/nar/gkz233.

Maierhofer, A. et al. (2017). Accelerated epigenetic aging in Werner syndrome.

Aging, 9 (4), pp.1143–1152. [Online]. Available at: doi:10.18632/aging.101217.

Maji, B. et al. (2017). Multidimensional chemical control of CRISPR-Cas9. *Nature Chemical Biology*, 13 (1), pp.9–11. [Online]. Available at: doi:10.1038/nchembio.2224.

Mak, T. W. (2000). DNA damage-induced activation of p53 by the checkpoint kinase Chk2. *Science*, 287 (5459), pp.1824–1827. [Online]. Available at: doi:10.1126/science.287.5459.1824.

Makarov, V. L., Hirose, Y. and Langmore, J. P. (1997). Long G tails at both ends of human chromosomes suggest a C strand degradation mechanism for telomere shortening. *Cell*, 88 (5), pp.657–666. [Online]. Available at: doi:10.1016/S0092-8674(00)81908-X.

Maki, C. G. (1999). Oligomerization is required for p53 to be efficiently ubiquitinated by MDM2. *Journal of Biological Chemistry*, 274 (23), pp.16531–16535. [Online]. Available at: doi:10.1074/jbc.274.23.16531.

Malkin, D. et al. (1990). Germ line p53 mutations in a familial syndrome of breast cancer, sarcomas, and other neoplasms. *Science*, 250 (4985), pp.1233–1238. [Online]. Available at: doi:10.1126/science.1978757.

Marcand, S. et al. (2000). Cell cycle restriction of telomere elongation. *Current Biology*, 10 (8), pp.487–490. [Online]. Available at: doi:10.1016/S0960-9822(00)00450-4.

Martin, G. M., Sprague, C. A. and Epstein, C. J. (1970). Replicative life-span of cultivated human cells. Effects of donor's age, tissue, and genotype. *Laboratory Investigation*, 23 (1), pp.86–92. [Online]. Available at: https://pubmed.ncbi.nlm.nih.gov/5431223/?dopt=Abstract.

Mas-Bargues, C. et al. (2017). Role of p16INK4a and BMI-1 in oxidative stress-induced premature senescence in human dental pulp stem cells. *Redox Biology*, 12, pp.690–698. [Online]. Available at:

doi:10.1016/j.redox.2017.04.002.

Masutomi, K. et al. (2000). Telomerase activity reconstituted in vitro with purified human telomerase reverse transcriptase and human telomerase RNA component. *The Journal of biological chemistry*, 275 (29), pp.22568–22573. [Online]. Available at: doi:10.1074/jbc.M000622200.

McCarroll, R. M. and Fangman, W. L. (1988). Time of replication of yeast centromeres and telomeres. *Cell*, 54 (4), pp.505–513. [Online]. Available at: doi:10.1016/0092-8674(88)90072-4.

McClintock, B. (1941). The Stability of Broken Ends of Chromosomes in Zea Mays. *Genetics*, 26 (2), pp.234–282. [Online]. Available at: http://www.ncbi.nlm.nih.gov/pubmed/17247004.

McElligott, R. and Wellinger, R. J. (1997). The terminal DNA structure of mammalian chromosomes. *EMBO Journal*, 16 (12), pp.3705–3714. [Online]. Available at: doi:10.1093/emboj/16.12.3705.

McKeown, S. R. (2014). Defining normoxia, physoxia and hypoxia in tumours - Implications for treatment response. *British Journal of Radiology*, 87 (1035), British Institute of Radiology. [Online]. Available at: doi:10.1259/bjr.20130676.

Meilinger, D. et al. (2009). Np95 interacts with de novo DNA methyltransferases, Dnmt3a and Dnmt3b, and mediates epigenetic silencing of the viral CMV promoter in embryonic stem cells. *EMBO Reports*, 10 (11), pp.1259–1264. [Online]. Available at: doi:10.1038/embor.2009.201.

Mender, I. and Shay, J. W. (2015). Telomerase Repeated Amplification Protocol (TRAP). *Bio-protocol*, 5 (22). [Online]. Available at: http://www.ncbi.nlm.nih.gov/pubmed/27182535.

Di Micco, R. et al. (2011). Interplay between oncogene-induced DNA damage response and heterochromatin in senescence and cancer. *Nature Cell Biology*, 13 (3), pp.292–302. [Online]. Available at: doi:10.1038/ncb2170.

Midgley, C. A. and Lane, D. P. (1997). P53 protein stability in tumour cells is not determined by mutation but is dependent on Mdm2 binding. *Oncogene*, 15 (10), pp.1179–1189. [Online]. Available at: doi:10.1038/sj.onc.1201459.

Milanovic, M. et al. (2018). Senescence-associated reprogramming promotes cancer stemness. *Nature*, 553 (7686), pp.96–100. [Online]. Available at: doi:10.1038/nature25167.

Mitchell, J. R., Cheng, J. and Collins, K. (1999). A Box H/ACA Small Nucleolar RNA-Like Domain at the Human Telomerase RNA 3′ End. *Molecular and Cellular Biology*, 19 (1), pp.567–576. [Online]. Available at: doi:10.1128/mcb.19.1.567.

Mitchell, M. et al. (2010). Structural basis for telomerase catalytic subunit TERT binding to RNA template and telomeric DNA. *Nature Structural and Molecular Biology*, 17 (4), pp.513–518. [Online]. Available at: doi:10.1038/nsmb.1777.

Moiseeva, O. et al. (2009). Mitochondrial Dysfunction Contributes to Oncogene-Induced Senescence. *Molecular and Cellular Biology*, 29 (16), pp.4495–4507. [Online]. Available at: doi:10.1128/mcb.01868-08.

Morales, C. P. et al. (1999). Absence of cancer-associated changes in human fibroblasts immortalized with telomerase. *Nature Genetics*, 21 (1), pp.115–118. [Online]. Available at: doi:10.1038/5063.

Morrison, S. J. et al. (1996). Telomerase activity in hematopoietic cells is associated with self-renewal potential. *Immunity*, 5 (3), pp.207–216. [Online]. Available at: doi:10.1016/S1074-7613(00)80316-7.

Muller, H. J. (1938). The remaking of chromosomes. *Collecting net*, 13, pp.181–198.

Murphy, P. J. M. et al. (2004). Pifithrin-α inhibits p53 signaling after interaction of the tumor suppressor protein with hsp90 and its nuclear translocation. *Journal of Biological Chemistry*, 279 (29), pp.30195–30201. [Online]. Available

at: doi:10.1074/jbc.M403539200.

Musi, N. et al. (2018). Tau protein aggregation is associated with cellular senescence in the brain. *Aging Cell*, 17 (6). [Online]. Available at: doi:10.1111/acel.12840.

Nakagawa, K. et al. (1999). Requirement of ATM in Phosphorylation of the Human p53 Protein at Serine 15 following DNA Double-Strand Breaks. *Molecular and Cellular Biology*, 19 (4), pp.2828–2834. [Online]. Available at: doi:10.1128/mcb.19.4.2828.

Nakamura, T. M. et al. (1997). Telomerase catalytic subunit homologs from fission yeast and human. *Science*, 277 (5328), pp.955–959. [Online]. Available at: doi:10.1126/science.277.5328.955.

Nandakumar, J. et al. (2012). The TEL patch of telomere protein TPP1 mediates telomerase recruitment and processivity. *Nature*, 492 (7428), pp.285–289. [Online]. Available at: doi:10.1038/nature11648.

Narita, M. et al. (2003). Rb-mediated heterochromatin formation and silencing of E2F target genes during cellular senescence. *Cell*, 113 (6), pp.703–716. [Online]. Available at: doi:10.1016/S0092-8674(03)00401-X.

Narita, M. et al. (2006). A Novel Role for High-Mobility Group A Proteins in Cellular Senescence and Heterochromatin Formation. *Cell*, 126 (3), pp.503–514. [Online]. Available at: doi:10.1016/j.cell.2006.05.052.

Németh, A. et al. (2010). Initial genomics of the human nucleolus. *PLoS Genetics*, 6 (3). [Online]. Available at: doi:10.1371/journal.pgen.1000889.

Nergadze, S. G. et al. (2009). CpG-island promoters drive transcription of human telomeres. *RNA*, 15 (12), pp.2186–2194. [Online]. Available at: doi:10.1261/rna.1748309.

Newbold, R. F., Overell, R. W. and Connell, J. R. (1982). Induction of immortality is an early event in malignant transformation of mammalian cells

by carcinogens. *Nature*, 299 (5884), pp.633–635. [Online]. Available at: doi:10.1038/299633a0.

Ng, L. J. et al. (2009). Telomerase activity is associated with an increase in DNA methylation at the proximal subtelomere and a reduction in telomeric transcription. *Nucleic acids research*, 37 (4), pp.1152–1159. [Online]. Available at: doi:10.1093/nar/gkn1030.

Nguyen, T. H. D. et al. (2018). Cryo-EM structure of substrate-bound human telomerase holoenzyme. *Nature*, 557 (7704), pp.190–195. [Online]. Available at: doi:10.1038/s41586-018-0062-x.

Nishimura, K. et al. (2009). An auxin-based degron system for the rapid depletion of proteins in nonplant cells. *Nature Methods*, 6 (12), pp.917–922. [Online]. Available at: doi:10.1038/nmeth.1401.

O'Keefe, K., Li, H. and Zhang, Y. (2003). Nucleocytoplasmic Shuttling of p53 Is Essential for MDM2-Mediated Cytoplasmic Degradation but Not Ubiquitination. *Molecular and Cellular Biology*, 23 (18), pp.6396–6405. [Online]. Available at: doi:10.1128/mcb.23.18.6396-6405.2003.

Offer, H. et al. (1999). Direct involvement of p53 in the base excision repair pathway of the DNA repair machinery. *FEBS Letters*, 450 (3), pp.197–204. [Online]. Available at: doi:10.1016/S0014-5793(99)00505-0.

Oh, S. et al. (1999). The Wilms' tumor 1 tumor suppressor gene represses transcription of the human telomerase reverse transcriptase gene. *Journal of Biological Chemistry*, 274 (52), pp.37473–37478. [Online]. Available at: doi:10.1074/jbc.274.52.37473.

Ottaviano, Y. and Gerace, L. (1985). Phosphorylation of the nuclear lamins during interphase and mitosis. *Journal of Biological Chemistry*, 260 (1), pp.624–632. [Online]. Available at: https://pubmed.ncbi.nlm.nih.gov/3965465/.

Oubaha, M. et al. (2016). Senescence-associated secretory phenotype contributes to pathological angiogenesis in retinopathy. *Science Translational*

Medicine, 8 (362). [Online]. Available at: doi:10.1126/scitranslmed.aaf9440.

Packer, L. and Fuehr, K. (1977). Low oxygen concentration extends the lifespan of cultured human diploid cells [13]. *Nature*, 267 (5610), Nature Publishing Group., pp.423–425. [Online]. Available at: doi:10.1038/267423a0.

Palm, W. et al. (2009). Functional Dissection of Human and Mouse POT1 Proteins. *Molecular and Cellular Biology*, 29 (2), pp.471–482. [Online]. Available at: doi:10.1128/mcb.01352-08.

Park, J.-I. et al. (2009). Telomerase modulates Wnt signalling by association with target gene chromatin. *Nature*, 460 (7251), pp.66–72. [Online]. Available at: doi:10.1038/nature08137.

Parrinello, S. et al. (2003). Oxygen sensitivity severely limits the replicative lifespan of murine fibroblasts. *Nature Cell Biology*, 5 (8), pp.741–747. [Online]. Available at: doi:10.1038/ncb1024.

Passos, J. F. et al. (2007). Mitochondrial dysfunction accounts for the stochastic heterogeneity in telomere-dependent senescence. De Lange, T. (Ed). *PLoS Biology*, 5 (5), pp.1138–1151. [Online]. Available at: doi:10.1371/journal.pbio.0050110.

Passos, J. F. et al. (2010). Feedback between p21 and reactive oxygen production is necessary for cell senescence. *Molecular Systems Biology*, 6 (1), p.347. [Online]. Available at: doi:10.1038/msb.2010.5.

Patel, P. L. et al. (2016). Derepression of hTERT gene expression promotes escape from oncogene-induced cellular senescence. *Proceedings of the National Academy of Sciences of the United States of America*, 113 (34), pp.E5024–E5033. [Online]. Available at: doi:10.1073/pnas.1602379113.

Patterson, M. K. (1979). Measurement of growth and viability of cells in culture. *Methods in Enzymology*, 58 (C), pp.141–152. [Online]. Available at: doi:10.1016/S0076-6879(79)58132-4.

Petersen, S., Saretzki, G. and Von Zglinicki, T. (1998). Preferential accumulation of single-stranded regions in telomeres of human fibroblasts. *Experimental Cell Research*, 239 (1), pp.152–160. [Online]. Available at: doi:10.1006/excr.1997.3893.

Peto, R. (2015). Quantitative implications of the approximate irrelevance of mammalian body size and lifespan to lifelong cancer risk. *Philosophical Transactions of the Royal Society B: Biological Sciences*, 370 (1673). [Online]. Available at: doi:10.1098/rstb.2015.0198.

Peto, R., Hiatt, H. H. and Watson, J. D. (1977). Origins of human cancer. In: *Book C*. Cold Spring Harbor Laboratory New York. pp.1403–1437.

Polvi, A. et al. (2012). Mutations in CTC1, encoding the CTS telomere maintenance complex component 1, cause cerebroretinal microangiopathy with calcifications and cysts. *American Journal of Human Genetics*, 90 (3), pp.540–549. [Online]. Available at: doi:10.1016/j.ajhg.2012.02.002.

Porro, A. et al. (2010). Molecular Dissection of Telomeric Repeat-Containing RNA Biogenesis Unveils the Presence of Distinct and Multiple Regulatory Pathways. *Molecular and Cellular Biology*, 30 (20), pp.4808–4817. [Online]. Available at: doi:10.1128/mcb.00460-10.

Porro, A. et al. (2014). Functional characterization of the TERRA transcriptome at damaged telomeres. *Nature Communications*, 5. [Online]. Available at: doi:10.1038/ncomms6379.

Qi, Z. et al. (2017). An optimized, broadly applicable *piggyBac* transposon induction system. *Nucleic Acids Research*, p.gkw1290. [Online]. Available at: doi:10.1093/nar/gkw1290.

Qin, J. Y. et al. (2010). Systematic Comparison of Constitutive Promoters and the Doxycycline-Inducible Promoter. Hansen, I. A. (Ed). *PLoS ONE*, 5 (5), p.e10611. [Online]. Available at: doi:10.1371/journal.pone.0010611.

Radhakrishnan, P. et al. (2008). Cell type-specific activation of the

cytomegalovirus promoter by dimethylsulfoxide and 5-Aza-2′-deoxycytidine. *International Journal of Biochemistry and Cell Biology*, 40 (9), pp.1944–1955. [Online]. Available at: doi:10.1016/j.biocel.2008.02.014.

Rai, P. et al. (2009). Continuous elimination of oxidized nucleotides is necessary to prevent rapid onset of cellular senescence. *Proceedings of the National Academy of Sciences of the United States of America*, 106 (1), pp.169–174. [Online]. Available at: doi:10.1073/pnas.0809834106.

Ramirez, R. D. et al. (2001). Putative telomere-independent mechanisms of replicative aging reflect inadequate growth conditions. *Genes and Development*, 15 (4), pp.398–403. [Online]. Available at: doi:10.1101/gad.859201.

Ramirez, R. D. et al. (2003). Bypass of telomere-dependent replicative senescence (M1) upon overexpression of Cdk4 in normal human epithelial cells. *Oncogene*, 22 (3), pp.433–444. [Online]. Available at: doi:10.1038/sj.onc.1206046.

Rangarajan, A. et al. (2004). Species- and cell type-specific requirements for cellular transformation. *Cancer Cell*, 6 (2), pp.171–183. [Online]. Available at: doi:10.1016/j.ccr.2004.07.009.

Rangarajan, A. and Weinberg, R. A. (2003). Comparative biology of mouse versus human cells: Modelling human cancer in mice. *Nature Reviews Cancer*, 3 (12), European Association for Cardio-Thoracic Surgery., pp.952–959. [Online]. Available at: doi:10.1038/nrc1235.

Raz, V. et al. (2008). The nuclear lamina promotes telomere aggregation and centromere peripheral localization during senescence of human mesenchymal stem cells. *Journal of Cell Science*, 121 (24), pp.4018–4028. [Online]. Available at: doi:10.1242/jcs.034876.

Reddy, K. L. et al. (2008). Transcriptional repression mediated by repositioning of genes to the nuclear lamina. *Nature*, 452 (7184), pp.243–247. [Online].

Available at: doi:10.1038/nature06727.

Redon, S., Reichenbach, P. and Lingner, J. (2010). The non-coding RNA TERRA is a natural ligand and direct inhibitor of human telomerase. *Nucleic Acids Research*, 38 (17), pp.5797–5806. [Online]. Available at: doi:10.1093/nar/gkq296.

Reisman, D., Greenberg, M. and Rotter, V. (1988). Human p53 oncogene contains one promoter upstream of exon 1 and a second, stronger promoter within intron 1. *Proceedings of the National Academy of Sciences of the United States of America*, 85 (14), pp.5146–5150. [Online]. Available at: doi:10.1073/pnas.85.14.5146.

Renaud, S. et al. (2007). Dual role of DNA methylation inside and outside of CTCF-binding regions in the transcriptional regulation of the telomerase hTERT gene. *Nucleic Acids Research*, 35 (4), pp.1245–1256. [Online]. Available at: doi:10.1093/nar/gkl1125.

Richter, A., Sanford, K. K. and Evans, V. J. (1972). Influence of oxygen and culture media on plating efficiency of some mammalian tissue cells. *Journal of the National Cancer Institute*, 49 (6), pp.1705–1712. [Online]. Available at: doi:10.1093/jnci/49.6.1705.

Richter, C., Park, J. W. and Ames, B. N. (1988). Normal oxidative damage to mitochondrial and nuclear DNA is extensive. *Proceedings of the National Academy of Sciences of the United States of America*, 85 (17), pp.6465–6467. [Online]. Available at: doi:10.1073/pnas.85.17.6465.

Richter, T. and Zglinicki, T. von. (2007). A continuous correlation between oxidative stress and telomere shortening in fibroblasts. *Experimental Gerontology*, 42 (11), pp.1039–1042. [Online]. Available at: doi:10.1016/j.exger.2007.08.005.

Rivlin, N. et al. (2011). Mutations in the p53 tumor suppressor gene: Important milestones at the various steps of tumorigenesis. *Genes and Cancer*, 2 (4),

pp.466–474. [Online]. Available at: doi:10.1177/1947601911408889.

Robart, A. R. R. and Collins, K. (2011). Human Telomerase Domain Interactions Capture DNA for TEN Domain-Dependent Processive Elongation. *Molecular Cell*, 42 (3), pp.308–318. [Online]. Available at: doi:10.1016/j.molcel.2011.03.012.

Roberson, R. S. et al. (2005). Escape from therapy-induced accelerated cellular senescence in p53-null lung cancer cells and in human lung cancers. *Cancer Research*, 65 (7), pp.2795–2803. [Online]. Available at: doi:10.1158/0008-5472.CAN-04-1270.

Rodemann, H. P. (1989). Differential degradation of intracellular proteins in human skin fibroblasts of mitotic and mitomycin-C (MMC)-induced postmitotic differentiation states in vitro. *Differentiation*, 42 (1), pp.37–43. [Online]. Available at: doi:10.1111/j.1432-0436.1989.tb00605.x.

Rodier, F. et al. (2009). Persistent DNA damage signalling triggers senescence-associated inflammatory cytokine secretion. *Nature Cell Biology*, 11 (8), pp.973–979. [Online]. Available at: doi:10.1038/ncb1909.

Rubbo, H. et al. (1994). Nitric oxide regulation of superoxide and peroxynitrite-dependent lipid peroxidation. Formation of novel nitrogen-containing oxidized lipid derivatives. *Journal of Biological Chemistry*, 269 (42), pp.26066–26075.

Rubin, H. (1997). Cell aging in vivo and in vitro. *Mechanisms of Ageing and Development*, 98 (1), pp.1–35. [Online]. Available at: doi:10.1016/S0047-6374(97)00067-5.

Sadaie, M. et al. (2013). Redistribution of the Lamin B1 genomic binding profile affects rearrangement of heterochromatic domains and SAHF formation during senescence. *Genes and Development*, 27 (16), pp.1800–1808. [Online]. Available at: doi:10.1101/gad.217281.113.

Sagie, S. et al. (2014). Induced pluripotent stem cells as a model for telomeric abnormalities in ICF type I syndrome. *Human molecular genetics*, 23 (14),

pp.3629–3640. [Online]. Available at: doi:10.1093/hmg/ddu071.

Sagie, S. et al. (2017). Telomeres in ICF syndrome cells are vulnerable to DNA damage due to elevated DNA:RNA hybrids. *Nature Communications*, 8 (1), pp.1–12. [Online]. Available at: doi:10.1038/ncomms14015.

Saintigny, Y. et al. (1999). Mutant p53 proteins stimulate spontaneous and radiation-induced intrachromosomal homologous recombination independently of the alteration of the transactivation activity and of the G1 checkpoint. *Oncogene*, 18 (24), pp.3553–3563. [Online]. Available at: doi:10.1038/sj.onc.1202941.

Saito, S. et al. (2003). Phosphorylation site interdependence of human p53 post-translational modifications in response to stress. *Journal of Biological Chemistry*, 278 (39), pp.37536–37544. [Online]. Available at: doi:10.1074/jbc.M305135200.

Sakaguchi, K. et al. (1998). DNA damage activates p53 through a phosphorylation-acetylation cascade. *Genes and Development*, 12 (18), pp.2831–2841. [Online]. Available at: doi:10.1101/gad.12.18.2831.

Sakaguchi, K. et al. (2000). Damage-mediated phosphorylation of human p53 threonine 18 through a cascade mediated by a casein 1-like kinase. Effect on MDM2 binding. *Journal of Biological Chemistry*, 275 (13), pp.9278–9283. [Online]. Available at: doi:10.1074/jbc.275.13.9278.

Saksouk, N., Simboeck, E. and Déjardin, J. (2015). Constitutive heterochromatin formation and transcription in mammals. *Epigenetics and Chromatin*, 8 (1), BioMed Central Ltd., pp.1–17. [Online]. Available at: doi:10.1186/1756-8935-8-3.

Salk, D. et al. (1981). Cytogenet Genome Res of Werner’s syndrome cultured skin fibroblasts: variegated translocation mosaicism. *Cytogenetic and Genome Research*, 30 (2), pp.92–107. [Online]. Available at: doi:10.1159/000131596.

Samassekou, O. et al. (2010). Sizing the ends: Normal length of human telomeres. *Annals of Anatomy*, 192 (5), pp.284–291. [Online]. Available at: doi:10.1016/j.aanat.2010.07.005.

De Sandre-Giovannoli, A. et al. (2003). Lamin A truncation in Hutchinson-Gilford progeria. *Science*, 300 (5628), p.2055. [Online]. Available at: doi:10.1126/science.1084125.

Sapieha, P. and Mallette, F. A. (2018). Cellular Senescence in Postmitotic Cells: Beyond Growth Arrest. *Trends in Cell Biology*, 28 (8), Elsevier Ltd., pp.595–607. [Online]. Available at: doi:10.1016/j.tcb.2018.03.003.

Saretzki, G., Murphy, M. P. and von Zglinicki, T. (2003). MitoQ counteracts telomere shortening and elongates lifespan of fibroblasts under mild oxidative stress. *Aging cell*, 2 (2), pp.141–143. [Online]. Available at: doi:10.1046/j.1474-9728.2003.00040.x.

Sarnataro, S. et al. (2017). Structure of the human chromosome interaction network. *PLoS ONE*, 12 (11). [Online]. Available at: doi:10.1371/journal.pone.0188201.

Sasa, G. S. et al. (2012). Three novel truncating TINF2 mutations causing severe dyskeratosis congenita in early childhood. *Clinical Genetics*, 81 (5), pp.470–478. [Online]. Available at: doi:10.1111/j.1399-0004.2011.01658.x.

Sasaki, M. et al. (2014). Reactive oxygen species promotes cellular senescence in normal human epidermal keratinocytes through epigenetic regulation of p16INK4a. *Biochemical and Biophysical Research Communications*, 452 (3), pp.622–628. [Online]. Available at: doi:10.1016/j.bbrc.2014.08.123.

Savage, S. A. et al. (2008). TINF2, a Component of the Shelterin Telomere Protection Complex, Is Mutated in Dyskeratosis Congenita. *American Journal of Human Genetics*, 82 (2), pp.501–509. [Online]. Available at: doi:10.1016/j.ajhg.2007.10.004.

Scaffidi, P. and Misteli, T. (2006). Lamin A-dependent nuclear defects in human aging. *Science*, 312 (5776), pp.1059–1063. [Online]. Available at: doi:10.1126/science.1127168.

Schmidt, J. C., Dalby, A. B. and Cech, T. R. (2014). Identification of human TERT elements necessary for telomerase recruitment to telomeres. *eLife*, 3. [Online]. Available at: doi:10.7554/elife.03563.

Schneider, C. A., Rasband, W. S. and Eliceiri, K. W. (2012). NIH Image to ImageJ: 25 years of image analysis. *Nature methods*, 9 (7), pp.671–675. [Online]. Available at: http://www.ncbi.nlm.nih.gov/pubmed/22930834.

Schoeftner, S. and Blasco, M. A. (2008). Developmentally regulated transcription of mammalian telomeres by DNA-dependent RNA polymerase II. *Nature Cell Biology*, 10 (2), pp.228–236. [Online]. Available at: doi:10.1038/ncb1685.

Schon, O. et al. (2002). Molecular mechanism of the interaction between MDM2 and p53. *Journal of Molecular Biology*, 323 (3), pp.491–501. [Online]. Available at: doi:10.1016/S0022-2836(02)00852-5.

Sedelnikova, O. A. et al. (2004). Senescing human cells and ageing mice accumulate DNA lesions with unrepairable double-strand breaks. *Nature Cell Biology*, 6 (2), pp.168–170. [Online]. Available at: doi:10.1038/ncb1095.

Serrano, M. et al. (1997). Oncogenic ras Provokes Premature Cell Senescence Associated with Accumulation of p53 and p16INK4a. *Cell*, 88 (5), pp.593–602. [Online]. Available at: doi:10.1016/S0092-8674(00)81902-9.

Sexton, A. N. et al. (2014). Genetic and molecular identification of three human TPP1 functions in telomerase action: recruitment, activation, and homeostasis set point regulation. *Genes & development*, 28 (17), pp.1885–1899. [Online]. Available at: doi:10.1101/gad.246819.114.

Sfeir, A. et al. (2010). Loss of Rap1 induces telomere recombination in the absence of NHEJ or a DNA damage signal. *Science*, 327 (5973), pp.1657–

1661. [Online]. Available at: doi:10.1126/science.1185100.

Sfeir, A. and De Lange, T. (2012). Removal of shelterin reveals the telomere end-protection problem. *Science*, 336 (6081), pp.593–597. [Online]. Available at: doi:10.1126/science.1218498.

Shah, P. P. et al. (2013). Lamin B1 depletion in senescent cells triggers large-scale changes in gene expression and the chromatin landscape. *Genes and Development*, 27 (16), pp.1787–1799. [Online]. Available at: doi:10.1101/gad.223834.113.

Shaw, P. et al. (1992). Induction of apoptosis by wild-type p53 in a human colon tumor-derived cell line. *Proceedings of the National Academy of Sciences of the United States of America*, 89 (10), pp.4495–4499. [Online]. Available at: doi:10.1073/pnas.89.10.4495.

Shay, J. W. and Bacchetti, S. (1997). A survey of telomerase activity in human cancer. *European Journal of Cancer Part A*, 33 (5), pp.787–791. [Online]. Available at: doi:10.1016/S0959-8049(97)00062-2.

Shay, J. W., Pereira-Smith, O. M. and Wright, W. E. (1991). A role for both RB and p53 in the regulation of human cellular senescence. *Experimental Cell Research*, 196 (1), pp.33–39. [Online]. Available at: doi:10.1016/0014-4827(91)90453-2.

Shay, J. W. and Wright, W. E. (1989). Quantitation of the frequency of immortalization of normal human diploid fibroblasts by SV40 large T-antigen. *Experimental Cell Research*, 184 (1), pp.109–118. [Online]. Available at: doi:10.1016/0014-4827(89)90369-8.

Shieh, S.-Y. (1999). DNA damage-inducible phosphorylation of p53 at N-terminal sites including a novel site, Ser20, requires tetramerization. *The EMBO Journal*, 18 (7), pp.1815–1823. [Online]. Available at: doi:10.1093/emboj/18.7.1815.

Shieh, S. Y. et al. (2000). The human homologs of checkpoint kinases Chk1

and Cds1 (Chk2) phosphorylate, p53 at multiple DNA damage-inducible sites. *Genes and Development*, 14 (3), pp.289–300.

Shimi, T. et al. (2008). The A- and B-type nuclear lamin networks: Microdomains involved in chromatin organization and transcription. *Genes and Development*, 22 (24), pp.3409–3421. [Online]. Available at: doi:10.1101/gad.1735208.

Shimi, T. et al. (2011). The role of nuclear lamin B1 in cell proliferation and senescence. *Genes and Development*, 25 (24), pp.2579–2593. [Online]. Available at: doi:10.1101/gad.179515.111.

Shumaker, D. K. et al. (2008). The highly conserved nuclear lamin Ig-fold binds to PCNA: Its role in DNA replication. *Journal of Cell Biology*, 181 (2), pp.269–280. [Online]. Available at: doi:10.1083/jcb.200708155.

Sidler, C. et al. (2014). WI-38 senescence is associated with global and site-specific hypomethylation. *Aging*, 6 (7), pp.564–574. [Online]. Available at: doi:10.18632/aging.100679.

da Silva, P. F. L. et al. (2019). The bystander effect contributes to the accumulation of senescent cells in vivo. *Aging Cell*, 18 (1). [Online]. Available at: doi:10.1111/acel.12848.

Sliwinska, M. A. et al. (2009). Induction of senescence with doxorubicin leads to increased genomic instability of HCT116 cells. *Mechanisms of Ageing and Development*, 130 (1–2), pp.24–32. [Online]. Available at: doi:10.1016/j.mad.2008.04.011.

Smith, J. R. and Whitney, R. G. (1980). Intraclonal variation in proliferative potential of human diploid fibroblasts: stochastic mechanism for cellular aging. *Science*, 207 (4426), pp.82–84. [Online]. Available at: doi:10.1126/science.7350644.

Smogorzewska, A. and de Lange, T. (2002). Different telomere damage signaling pathways in human and mouse cells. *The EMBO journal*, 21 (16),

pp.4338–4348. [Online]. Available at: doi:10.1093/EMBOJ/CDF433.

Srivastava, S. et al. (1990). Germ-line transmission of a mutated p53 gene in a cancer-prone family with Li-Fraumeni syndrome. *Nature*, 348 (6303), pp.747–749. [Online]. Available at: doi:10.1038/348747a0.

Starke-Reed, P. E. and Oliver, C. N. (1989). Protein oxidation and proteolysis during aging and oxidative stress. *Archives of Biochemistry and Biophysics*, 275 (2), pp.559–567. [Online]. Available at: doi:10.1016/0003-9861(89)90402-5.

Van Steensel, B., Smogorzewska, A. and De Lange, T. (1998). TRF2 protects human telomeres from end-to-end fusions. *Cell*, 92 (3), pp.401–413. [Online]. Available at: doi:10.1016/S0092-8674(00)80932-0.

Stein, G. H. et al. (1999). Differential Roles for Cyclin-Dependent Kinase Inhibitors p21 and p16 in the Mechanisms of Senescence and Differentiation in Human Fibroblasts. *Molecular and Cellular Biology*, 19 (3), pp.2109–2117. [Online]. Available at: doi:10.1128/mcb.19.3.2109.

Stein, G. H. and Dulic, V. (1998). Molecular mechanisms for the senescent cell cycle arrest. In: *Journal of Investigative Dermatology Symposium Proceedings*. 3 (1). 1998. Blackwell Publishing Inc. pp.14–18. [Online]. Available at: doi:10.1038/jidsymp.1998.5.

Stern, J. L. et al. (2015). Mutation of the TERT promoter, switch to active chromatin, and monoallelic TERT expression in multiple cancers. *Genes and Development*, 29 (21), pp.2219–2224. [Online]. Available at: doi:10.1101/gad.269498.115.

Stewart, S. A. et al. (2003). Erosion of the telomeric single-strand overhang at replicative senescence. *Nature Genetics*, 33 (4), pp.492–496. [Online]. Available at: doi:10.1038/ng1127.

Stockklausner, C. et al. (2015). A novel autosomal recessive TERT T1129P mutation in a dyskeratosis congenita family leads to cellular senescence and

loss of CD34+ hematopoietic stem cells not reversible by mTOR-inhibition. *Aging*, 7 (11), pp.911–927. [Online]. Available at: doi:10.18632/aging.100835.

Stoehr, R. et al. (2015). Frequency of TERT Promoter Mutations in Prostate Cancer. *Pathobiology*, 82 (2), pp.53–57. [Online]. Available at: doi:10.1159/000381903.

Stommel, J. M. and Wahl, G. M. (2004). Accelerated MDM2 auto-degradation induced by DNA-damage kinases is required for p53 activation. *EMBO Journal*, 23 (7), pp.1547–1556. [Online]. Available at: doi:10.1038/sj.emboj.7600145.

Suram, A. et al. (2012). Oncogene-induced telomere dysfunction enforces cellular senescence in human cancer precursor lesions. *The EMBO journal*, 31 (13), pp.2839–2851. [Online]. Available at: doi:10.1038/emboj.2012.132.

Swanson, E. C. et al. (2013). Higher-order unfolding of satellite heterochromatin is a consistent and early event in cell senescence. *Journal of Cell Biology*, 203 (6), pp.929–942. [Online]. Available at: doi:10.1083/jcb.201306073.

Takai, H. et al. (2016). A POT1 mutation implicates defective telomere end fill-in and telomere truncations in coats plus. *Genes and Development*, 30 (7), pp.812–826. [Online]. Available at: doi:10.1101/gad.276873.115.

Takai, H., Smogorzewska, A. and De Lange, T. (2003). DNA damage foci at dysfunctional telomeres. *Current Biology*, 13 (17), pp.1549–1556. [Online]. Available at: doi:10.1016/S0960-9822(03)00542-6.

Takai, K. K. et al. (2010). In vivo stoichiometry of shelterin components. *Journal of Biological Chemistry*, 285 (2), pp.1457–1467. [Online]. Available at: doi:10.1074/jbc.M109.038026.

Takakura, M. et al. (1999). Cloning of human telomerase catalytic subunit (hTERT) gene promoter and identification of proximal core promoter sequences essential for transcriptional activation in immortalized and cancer

cells. *Cancer Research*, 59 (3), pp.551–557.

Takaoka, M. et al. (2004). Ha-RasG12V induces senescence in primary and immortalized human esophageal keratinocytes with p53 dysfunction. *Oncogene*, 23 (40), pp.6760–6768. [Online]. Available at: doi:10.1038/sj.onc.1207923.

Tang, H. et al. (2019). *Single senescent cell sequencing reveals heterogeneity in senescent cells induced by telomere erosion*. 10 (5), Higher Education Press., pp.370–375. [Online]. Available at: doi:10.1007/s13238-018-0591-y.

Tasselli, L. et al. (2016). SIRT6 deacetylates H3K18ac at pericentric chromatin to prevent mitotic errors and cellular senescence. *Nature Structural and Molecular Biology*, 23 (5), pp.434–440. [Online]. Available at: doi:10.1038/nsmb.3202.

Teixeira, M. T. et al. (2004). Telomere length homeostasis is achieved via a switch between telomerase- extendible and -nonextendible states. *Cell*, 117 (3), pp.323–335. [Online]. Available at: doi:10.1016/S0092-8674(04)00334-4.

Teschendorf, C. et al. (2002). Comparison of the EF-1α and the CMV promoter for engineering stable tumor cell lines using recombinant adeno-associated virus. *Anticancer Research*, 22 (6 A), pp.3325–3330.

Tibbetts, R. S. et al. (1999). A role for ATR in the DNA damage-induced phosphorylation of p53. *Genes and Development*, 13 (2), pp.152–157. [Online]. Available at: doi:10.1101/gad.13.2.152.

Tomlinson, R. L. et al. (2006). Cell cycle-regulated trafficking of human telomerase to telomeres. *Molecular biology of the cell*, 17 (2), pp.955–965. [Online]. Available at: doi:10.1091/mbc.e05-09-0903.

Tomlinson, R. L. et al. (2008). Telomerase reverse transcriptase is required for the localization of telomerase RNA to cajal bodies and telomeres in human cancer cells. *Molecular biology of the cell*, 19 (9), pp.3793–3800. [Online]. Available at: doi:10.1091/mbc.e08-02-0184.

Toussaint, O., Medrano, E. E. and Von Zglinicki, T. (2000). Cellular and molecular mechanisms of stress-induced premature senescence (SIPS) of human diploid fibroblasts and melanocytes. *Experimental Gerontology*, 35 (8), Pergamon., pp.927–945. [Online]. Available at: doi:10.1016/S0531-5565(00)00180-7.

Tsakiri, K. D. et al. (2007). Adult-onset pulmonary fibrosis caused by mutations in telomerase. *Proceedings of the National Academy of Sciences of the United States of America*, 104 (18), pp.7552–7557. [Online]. Available at: doi:10.1073/pnas.0701009104.

Tsangaris, E. et al. (2008). Ataxia and pancytopenia caused by a mutation in TINF2. *Human Genetics*, 124 (5), pp.507–513. [Online]. Available at: doi:10.1007/s00439-008-0576-7.

Tseng, C. K. et al. (2018). The H/ACA complex disrupts triplex in hTR precursor to permit processing by RRP6 and PARN. *Nature Communications*, 9 (1). [Online]. Available at: doi:10.1038/s41467-018-07822-6.

Tuduri, S. et al. (2009). Topoisomerase I suppresses genomic instability by preventing interference between replication and transcription. *Nature Cell Biology*, 11 (11), pp.1315–1324. [Online]. Available at: doi:10.1038/ncb1984.

Turrens, J. F. et al. (1982). The effect of hyperoxia on superoxide production by lung submitochondrial particles. *Archives of Biochemistry and Biophysics*, 217 (2), pp.401–410. [Online]. Available at: doi:10.1016/0003-9861(82)90518-5.

Vannier, J. B. et al. (2012). RTEL1 dismantles T loops and counteracts telomeric G4-DNA to maintain telomere integrity. *Cell*, 149 (4), pp.795–806. [Online]. Available at: doi:10.1016/j.cell.2012.03.030.

Vannier, J. B. et al. (2013). RTEL1 is a replisome-associated helicase that promotes telomere and genome-wide replication. *Science*, 342 (6155), pp.239–242. [Online]. Available at: doi:10.1126/science.1241779.

Vaziri, H. et al. (1994). Evidence for a mitotic clock in human hematopoietic stem cells: Loss of telomeric DNA with age. *Proceedings of the National Academy of Sciences of the United States of America*, 91 (21), pp.9857–9860. [Online]. Available at: doi:10.1073/pnas.91.21.9857.

Vaziri, H. and Benchimol, S. (1998). Reconstitution of telomerase activity in normal human cells leads to elongation of telomeres and extended replicative life span. *Current Biology*, 8 (5), pp.279–282. [Online]. Available at: doi:10.1016/S0960-9822(98)70109-5.

Venteicher, A. S. et al. (2009). A human telomerase holoenzyme protein required for Cajal body localization and telomere synthesis. *Science (New York, N.Y.)*, 323 (5914), pp.644–648. [Online]. Available at: doi:10.1126/science.1165357.

Verdun, R. E. et al. (2005). Functional human telomeres are recognized as DNA damage in G2 of the cell cycle. *Molecular cell*, 20 (4), pp.551–561. [Online]. Available at: doi:10.1016/j.molcel.2005.09.024.

Vinagre, J. et al. (2013). Frequency of TERT promoter mutations in human cancers. *Nature Communications*, 4. [Online]. Available at: doi:10.1038/ncomms3185.

Vogan, J. M. and Collins, K. (2015). Dynamics of human telomerase holoenzyme assembly and subunit exchange across the cell cycle. *Journal of Biological Chemistry*, 290 (35), pp.21320–21335. [Online]. Available at: doi:10.1074/jbc.M115.659359.

Vulliamy, T. et al. (2008). Mutations in the telomerase component NHP2 cause the premature ageing syndrome dyskeratosis congenita. *Proceedings of the National Academy of Sciences of the United States of America*, 105 (23), pp.8073–8078. [Online]. Available at: doi:10.1073/pnas.0800042105.

Vulliamy, T. et al. (2012). Telomere length measurement can distinguish pathogenic from non-pathogenic variants in the shelterin component, TIN2.

Clinical Genetics, 81 (1), pp.76–81. [Online]. Available at: doi:10.1111/j.1399-0004.2010.01605.x.

Wadhwa, R. et al. (2002). A major functional difference between the mouse and human ARF tumor suppressor proteins. *Journal of Biological Chemistry*, 277 (39), pp.36665–36670. [Online]. Available at: doi:10.1074/jbc.M203222200.

Waldman, T., Kinzler, K. W. and Vogelstein, B. (1995). p21 Is Necessary for the p53-mediated G1 Arrest in Human Cancer Cells. *Cancer Research*, 55 (22), pp.5187–5190.

Walne, A. J. et al. (2007). Genetic heterogeneity in autosomal recessive dyskeratosis congenita with one subtype due to mutations in the telomerase-associated protein NOP10. *Human Molecular Genetics*, 16 (13), pp.1619–1629. [Online]. Available at: doi:10.1093/hmg/ddm111.

Walne, A. J. et al. (2013). Mutations in the telomere capping complex in bone marrow failure and related syndromes. *Haematologica*, 98 (3), pp.334–338. [Online]. Available at: doi:10.3324/haematol.2012.071068.

Wang, C. et al. (2009). DNA damage response and cellular senescence in tissues of aging mice. *Aging Cell*, 8 (3), pp.311–323. [Online]. Available at: doi:10.1111/j.1474-9726.2009.00481.x.

Wang, F. et al. (2007). The POT1-TPP1 telomere complex is a telomerase processivity factor. *Nature*, 445 (7127), pp.506–510. [Online]. Available at: doi:10.1038/nature05454.

Wang, Q. et al. (2011). Survivin and escaping in therapy-induced cellular senescence. *International Journal of Cancer*, 128 (7), pp.1546–1558. [Online]. Available at: doi:10.1002/ijc.25482.

Wang, R. C., Smogorzewska, A. and De Lange, T. (2004). Homologous recombination generates t-loop-sized deletions at human telomeres. *Cell*, 119 (3), pp.355–368. [Online]. Available at: doi:10.1016/j.cell.2004.10.011.

Warnock, L. J. et al. (2008). Influence of tetramerisation on site-specific post-translational modifications of p53: Comparison of human and murine p53 tumour suppressor protein. *Cancer Biology and Therapy*, 7 (9), pp.1481–1489. [Online]. Available at: doi:10.4161/cbt.7.9.6473.

Watson, J. D. (1972). Origin of concatemeric T7 DNA. *Nature New Biology*, 239 (94), pp.197–201. [Online]. Available at: doi:10.1038/newbio239197a0.

Weinrich, S. L. et al. (1997). *Reconstitution of human telomerase with the template RNA component hTR and the catalytic protein subunit hTRT*. [Online]. Available at: http://www.nature.com/naturegenetics.

Wheaton, K. et al. (2017). Progerin-Induced Replication Stress Facilitates Premature Senescence in Hutchinson-Gilford Progeria Syndrome. *Molecular and Cellular Biology*, 37 (14). [Online]. Available at: doi:10.1128/mcb.00659-16.

Wick, M., Zubov, D. and Hagen, G. (1999). Genomic organization and promoter characterization of the gene encoding the human telomerase reverse transcriptase (hTERT). *Gene*, 232 (1), pp.97–106. [Online]. Available at: doi:10.1016/S0378-1119(99)00108-0.

Wiley, C. D. et al. (2017). Analysis of individual cells identifies cell-to-cell variability following induction of cellular senescence. *Aging Cell*, 16 (5), pp.1043–1050. [Online]. Available at: doi:10.1111/acel.12632.

Wooten, L. G. and Ogretmen, B. (2005). Sp1/Sp3-dependent regulation of human telomerase reverse transcriptase promoter activity by the bioactive sphingolipid ceramide. *Journal of Biological Chemistry*, 280 (32), pp.28867–28876. [Online]. Available at: doi:10.1074/jbc.M413444200.

Wright, D. L. et al. (2001). Characterization of telomerase activity in the human oocyte and preimplantation embryo. *Molecular Human Reproduction*, 7 (10), pp.947–955. [Online]. Available at: doi:10.1093/molehr/7.10.947.

Wright, W. E. et al. (1996). Telomerase activity in human germline and

embryonic tissues and cells. *Developmental Genetics*, 18 (2), pp.173–179. [Online]. Available at: doi:10.1002/(SICI)1520-6408(1996)18:2<173::AID-DVG10>3.0.CO;2-3.

Wright, W. E. et al. (1997). Normal human chromosomes have long G-rich telomeric overhangs at one end. *Genes and Development*, 11 (21), pp.2801–2809. [Online]. Available at: doi:10.1101/gad.11.21.2801.

Wright, W. E. et al. (1999). Normal Human Telomeres Are Not Late Replicating. *Experimental Cell Research*, 251 (2), pp.492–499. [Online]. Available at: doi:10.1006/EXCR.1999.4602.

Wright, W. E., Pereira-Smith, O. M. and Shay, J. W. (1989). Reversible cellular senescence: implications for immortalization of normal human diploid fibroblasts. *Molecular and Cellular Biology*, 9 (7), pp.3088–3092. [Online]. Available at: doi:10.1128/mcb.9.7.3088.

Wu, K. J. et al. (1999). Direct activation of TERT transcription by c-MYC. *Nature Genetics*, 21 (2), pp.220–224. [Online]. Available at: doi:10.1038/6010.

Wyllie, F. S. et al. (2000). Telomerase prevents the accelerated cell ageing of Werner syndrome fibroblasts. *Nature Genetics*, 24 (1), pp.16–17. [Online]. Available at: doi:10.1038/71630.

Xin, H. et al. (2007). TPP1 is a homologue of ciliate TEBP-β and interacts with POT1 to recruit telomerase. *Nature*, 445 (7127), pp.559–562. [Online]. Available at: doi:10.1038/nature05469.

Xu, C. et al. (2001). Feeder-free growth of undifferentiated human embryonic stem cells. *Nature Biotechnology*, 19 (10), pp.971–974. [Online]. Available at: doi:10.1038/nbt1001-971.

Xu, Y., Kimura, T. and Komiyama, M. (2008). Human telomere RNA and DNA form an intermolecular G-quadruplex. *Nucleic acids symposium series (2004)*, (52), pp.169–170. [Online]. Available at: doi:10.1093/nass/nrn086.

Yang, J. et al. (1999). Human endothelial cell life extension by telomerase expression. *Journal of Biological Chemistry*, 274 (37), pp.26141–26148. [Online]. Available at: doi:10.1074/jbc.274.37.26141.

Yatabe, N. et al. (2004). HIF-1-mediated activation of telomerase in cervical cancer cells. *Oncogene*, 23 (20), pp.3708–3715. [Online]. Available at: doi:10.1038/sj.onc.1207460.

Ye, J. Z.-S. et al. (2004a). POT1-interacting protein PIP1: a telomere length regulator that recruits POT1 to the TIN2/TRF1 complex. *Genes & development*, 18 (14), pp.1649–1654. [Online]. Available at: doi:10.1101/gad.1215404.

Ye, J. Z.-S. et al. (2004b). TIN2 binds TRF1 and TRF2 simultaneously and stabilizes the TRF2 complex on telomeres. *The Journal of biological chemistry*, 279 (45), pp.47264–47271. [Online]. Available at: doi:10.1074/jbc.M409047200.

Ye, X. et al. (2007). Definition of pRB- and p53-Dependent and -Independent Steps in HIRA/ASF1a-Mediated Formation of Senescence-Associated Heterochromatin Foci. *Molecular and Cellular Biology*, 27 (7), pp.2452–2465. [Online]. Available at: doi:10.1128/mcb.01592-06.

Yehezkel, S. et al. (2008). Hypomethylation of subtelomeric regions in ICF syndrome is associated with abnormally short telomeres and enhanced transcription from telomeric regions. *Human molecular genetics*, 17 (18), pp.2776–2789. [Online]. Available at: doi:10.1093/hmg/ddn177.

Yonish-Rouach, E. et al. (1991). Wild-type p53 induces apoptosis of myeloid leukaemic cells that is inhibited by interleukin-6. *Nature*, 352 (6333), pp.345–347. [Online]. Available at: doi:10.1038/352345a0.

Yoon, M.-H. H. et al. (2019). *p53 induces senescence through Lamin A/C stabilization-mediated nuclear deformation*. 10 (2). [Online]. Available at: doi:10.1038/s41419-019-1378-7.

Yosef, R. et al. (2016). Directed elimination of senescent cells by inhibition of BCL-W and BCL-XL. *Nature Communications*, 7. [Online]. Available at: doi:10.1038/ncomms11190.

Yosef, R. et al. (2017). p21 maintains senescent cell viability under persistent DNA damage response by restraining JNK and caspase signaling . *The EMBO Journal*, 36 (15), pp.2280–2295. [Online]. Available at: doi:10.15252/embj.201695553.

Young, N. S. (2012). Bone marrow failure and the new telomere diseases: Practice and research. *Hematology*, 17 (SUPPL. 1). [Online]. Available at: doi:10.1179/102453312X13336169155132.

Yu, C. E. et al. (1996). Positional cloning of the Werner's syndrome gene. *Science*, 272 (5259), pp.258–262. [Online]. Available at: doi:10.1126/science.272.5259.258.

Yu, T. Y., Kao, Y. W. and Lin, J. J. (2014). Telomeric transcripts stimulate telomere recombination to suppress senescence in cells lacking telomerase. *Proceedings of the National Academy of Sciences of the United States of America*, 111 (9), pp.3377–3382. [Online]. Available at: doi:10.1073/pnas.1307415111.

Zaug, A. J. et al. (2010). Functional interaction between telomere protein TPP1 and telomerase. *Genes & development*, 24 (6), pp.613–622. [Online]. Available at: doi:10.1101/gad.1881810.

von Zglinicki, T. et al. (1995). Mild Hyperoxia Shortens Telomeres and Inhibits Proliferation of Fibroblasts: A Model for Senescence? *Experimental Cell Research*, 220 (1), pp.186–193. [Online]. Available at: doi:10.1006/excr.1995.1305.

Von Zglinicki, T. (2002). Oxidative stress shortens telomeres. *Trends in Biochemical Sciences*, 27 (7), Elsevier Current Trends., pp.339–344. [Online]. Available at: doi:10.1016/S0968-0004(02)02110-2.

Von Zglinicki, T., Pilger, R. and Sitte, N. (2000). Accumulation of single-strand breaks is the major cause of telomere shortening in human fibroblasts. *Free Radical Biology and Medicine*, 28 (1), pp.64–74. [Online]. Available at: doi:10.1016/S0891-5849(99)00207-5.

Zhang, R. et al. (2005). Formation of macroH2A-containing senescence-associated heterochromatin foci and senescence driven by ASF1a and HIRA. *Developmental Cell*, 8 (1), pp.19–30. [Online]. Available at: doi:10.1016/j.devcel.2004.10.019.

Zhang, R., Chen, W. and Adams, P. D. (2007). Molecular Dissection of Formation of Senescence-Associated Heterochromatin Foci. *Molecular and Cellular Biology*, 27 (6), pp.2343–2358. [Online]. Available at: doi:10.1128/mcb.02019-06.

Zhang, Y. et al. (2009). Premature senescence of highly proliferative endothelial progenitor cells is induced by tumor necrosis factor-α *via* the p38 mitogen-activated protein kinase pathway. *The FASEB Journal*, 23 (5), pp.1358–1365. [Online]. Available at: doi:10.1096/fj.08-110296.

Zhang, Y. et al. (2013). Phosphorylation of TPP1 regulates cell cycle-dependent telomerase recruitment. *Proceedings of the National Academy of Sciences of the United States of America*, 110 (14), pp.5457–5462. [Online]. Available at: doi:10.1073/pnas.1217733110.

Zhao, Y. et al. (2009). Telomere Extension Occurs at Most Chromosome Ends and Is Uncoupled from Fill-In in Human Cancer Cells. *Cell*, 138 (3), pp.463–475. [Online]. Available at: doi:10.1016/J.CELL.2009.05.026.

Zhong, F. et al. (2011). Disruption of telomerase trafficking by TCAB1 mutation causes dyskeratosis congenita. *Genes and Development*, 25 (1), pp.11–16. [Online]. Available at: doi:10.1101/gad.2006411.

Zhong, F. L. et al. (2012). TPP1 OB-Fold Domain Controls Telomere Maintenance by Recruiting Telomerase to Chromosome Ends. *Cell*, 150 (3),

pp.481–494. [Online]. Available at: doi:10.1016/J.CELL.2012.07.012.

Zhu, X. et al. (1996). Cell cycle-dependent modulation of telomerase activity in tumor cells. *Proceedings of the National Academy of Sciences of the United States of America*, 93 (12), pp.6091–6095. [Online]. Available at: doi:10.1073/PNAS.93.12.6091.

Zimmermann, M. et al. (2014). TRF1 negotiates TTAGGG repeatassociated replication problems by recruiting the BLM helicase and the TPP1/POT1 repressor of ATR signaling. *Genes and Development*, 28 (22), pp.2477–2491. [Online]. Available at: doi:10.1101/gad.251611.114.

Zinn, R. L. et al. (2007). hTERT is expressed in cancer cell lines despite promoter DNA methylation by preservation of unmethylated DNA and active chromatin around the transcription start site. *Cancer Research*, 67 (1), pp.194–201. [Online]. Available at: doi:10.1158/0008-5472.CAN-06-3396.

Appendix A Optimisation of Biotinylated-CxxC Affinity Purification (Bio-CAP)

A.1 Introduction

A.1.1 DNA methylation

DNA methylation at the 5-carbon position of cytosine (5-mC) is a heritable epigenetic DNA modification, which occurs primarily at CpG dinucleotides in mammals (Holliday and Pugh, 1975; Riggs, 1975). An early discovery have identified DNA methylation at gene regulatory regions being associated with gene repression (Riggs, 1975). More recent studies have shown that DNA methylation is present not only at promoter regions but also at gene bodies and that its function changes depending on the location of the DNA methylation in the genome (Larsen, Solheim and Prydz, 1993; Robertson and Jones, 1998; Illingworth et al., 2010; Hahn et al., 2011; Laurent et al., 2010). Most CpG sequences in human DNA are methylated (70-80% of total CpGs) and the remaining unmethylated CpGs (20-30% of total CpGs) are mostly clustered together at short CpG rich regions called CpG Islands (CGIs), which are prevalent at the 5'-end regions of various genes (Bird, 1987; Saxonov, Berg and Brutlag, 2006).

A.1.2 hTERT-immortalisation and DNA methylation

Several groups have shown that ectopic hTERT expression is sufficient to immortalise several types of cells in *in vitro* culture (Bodnar et al., 1998; Counter et al., 1998; Vaziri and Benchimol, 1998). It is widely accepted that cellular immortality is a hallmark of cancer, which is achieved by re-activation of telomerase in 80% of cancers (Blasco, 2005; Hanahan and Weinberg, 2011). However, hTERT-immortalised cells showed no cancer-associated phenotypes such as lack of contact-inhibition and anchorage-independent growth (Jiang et al., 1999; Morales et al., 1999). In addition, hTERT-immortalised cells maintain a normal karyotype and long telomeres, which are advantageous properties for an *in vitro* model of normal cells. In contrast, more recent discoveries suggests that there are genetic and epigenetic changes

which could discriminate normal primary cells and their hTERT-immortalised counterparts (Gordon et al., 2014; Landan et al., 2012; Milyavsky et al., 2003). Furthermore, the DNA methylation patterns in hTERT-immortalised cells have been shown to mimic the patterns in pre-cancerous cells (Gordon et al., 2014) suggesting that telomerase might play a role in DNA methylation reprogramming during carcinogenesis. Previously, published results from the Stancheva laboratory have showed that hTERT-immortalised MRC-5 fibroblasts accumulate DNA methylation at gene promoters similar to MRC-5 cells transformed with Simian Vacuolating Virus 40 T-Antigen (SV40 T-Ag) and oncogenic HRAS (Gordon et al., 2014). This suggests that oncogenes may not play a leading role in the formation of aberrant DNA methylation pattern present in pre-cancerous cells. However, it is also currently not known whether telomerase is required for this observed *de novo* DNA methylation events following the hTERT-induced immortalisation. On the other hand, cells undergoing senescence showed hypomethylation in late-replicating, normally heterochromatic areas of the genome, which is similar to cancers (Cruickshanks et al., 2013). Therefore, this brings into question whether the methylation profiles of senescent and immortalised cells are signs of pre-malignancy and whether both cellular events have common players, which would be interesting to investigate further.

A.1.3 Whole genome DNA methylation analysis by Bio-CAP sequencing.

The advancement in high-throughput sequencing technology have made it possible to study genome-wide DNA methylation changes. The current gold standard technique to analyse whole genome DNA methylation is bisulphite conversion in combination with high throughput sequencing (Lister et al., 2009). This technique requires a treatment of genomic DNA with sodium bisulphite which converts non-methylated cytosines to uracils but leaves methylated cytosines unaltered, thereby allowing DNA methylation analysis at a single base-pair resolution (Hayatsu, Wataya and Kazushige, 1970; Shapiro, Servis and Welcher, 1970; Frommer et al., 1992). However, the bisulphite

conversion process is not error-free as non-methylated cytosines can fail to convert to uracil and cytosine can be incorrectly converted to thymine, which could give rise to an incorrect interpretation of the analysis (Genereux et al., 2008). Furthermore, the whole genome bisulphite sequencing is prohibitively expensive due to the high sequencing costs associated with the required sequencing depths for the accurate sequencing analysis. With the current bioinformatics tools available, it is possible to cost-effectively acquire a whole genome DNA methylation profile using non-methylated or methylated DNA capture/enrichment methods, which would allow analysis of a smaller proportion of the genome to infer a whole genome DNA methylation profile (Li et al., 2010; Trimarchi et al., 2012; Xu et al., 2018). Some examples of these non-methylated/methylated DNA enrichment techniques include methylated DNA immunoprecipitation (MeDIP), methyl-CpG binding domain (MBD) protein capture, and CxxC Affinity Purification (CAP) (Weber et al., 2005; Illingworth et al., 2008; Serre, Lee and Ting, 2009). A development of the CAP technique called Biotinylated-CxxC Affinity Purification (Bio-CAP) was published in 2012 (Blackledge et al., 2012). It employs a non-methylated CpG binding CxxC zinc finger domain of the human KDM2B protein, fused to a His6-tag containing six histidine residues at the N-terminus, an Avi-tag (GLNDIFEAQKIEWHE) at the C-terminus and a Tobacco Etch Virus (TEV) protease cleavage site (ELNYFQS) between the His6-tag and the CxxC domain (His6-CxxC-Avi). The His6-tag permits purification of the protein using immobilized metal affinity chromatography (IMAC) with Nickel-charged resins. The Avi-tag allows the CxxC protein to be immobilised to an Avidin-based support for further application in purifying non-methylated DNA, once the tag has been biotinylated by a recombinant *E. coli* BirA enzyme. Prior to the binding of the CxxC protein to the Avidin-based beads, the His-tag is removed by a TEV protease cleavage at the TEV site mentioned above. Removal of the His6-tag has been shown to increase binding capability of the CxxC domain protein to the non-methylated CpG (Blackledge et al., 2012). The full workflow of Bio-CxxC production, the biotinylated version of CxxC-Avi protein, is described in Figure A.1. During the first year of my PhD project, I established

and optimised the Bio-CAP technique while in the Stancheva laboratory. The following chapters describe the detailed optimisations and verifications necessary for the fully working order of the technique. Unfortunately, due to time constraints and changes in the direction of the project, the method was not utilised in any experiments detailed in the main text of my thesis and therefore was only included as part of the appendix here.

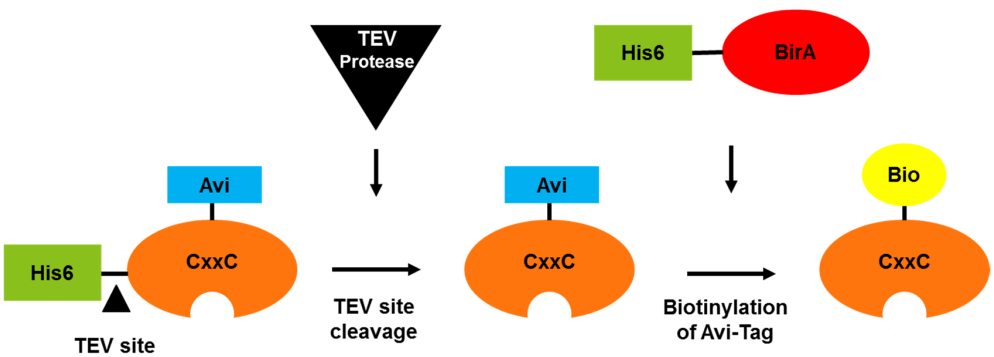

Figure A.1 Bio-CxxC protein production workflow required for the Bio-CAP technique

Purified His6-CxxC-Avi was cleaved with TEV protease to remove the His6-tag and form CxxC-Avi. CxxC-Avi was further modified by *in vitro* enzymatic biotinylation at the Avi-tag using a purified His6-BirA enzyme, to form the final product required for the Bio-CAP technique - Bio-CxxC.

A.2 Materials and Methods

A.2.1 Protein expression and purification of His6-BirA and His6-CxxC-Avi proteins

Plasmids for protein expression of His6-BirA (pET21a-BirA) and His6-CxxC-Avi (pNIC28-hKdm2b-CxxC-PHD) were transformed into BL21 codon-plus RIL *E. coli* expression strain, in separate experiments and plated on LB (Luria-Berthani) agar with ampicillin 100 µg/ml or kanamycin 50 µg/ml. Plates were incubated at 37 °C overnight. For the His6-BirA and His6-CxxC-Avi protein expression, one positive colony from a corresponding plate was inoculated into 25 ml of LB broth supplemented with either 100 µg/ml ampicillin or 50 µg/ml kanamycin respectively and cultured overnight. 10 ml of an overnight culture was diluted into 4 x 1 L LB broth and grown to an OD600 of 0.4 – 0.6 at 37 °C with 200 RPM shaking. The culture was then transferred into a 25 °C shaking incubator and the expression was induced by the addition of 0.5 mM IPTG. After 5 hours of incubation, the culture was pelleted by centrifugation at 6,000 RCF, 4 °C for 10 minutes. The supernatant was removed, and the pellet was resuspended in 1X PBS buffer, transferred into a clean 50 ml conical tube and pelleted again by centrifugation at 5,000 RCF, 4 °C for 10 minutes. Cell pellets were stored at -80 °C prior to protein extraction. Cells expressing His6-BirA and His6-CxxC-Avi proteins were lysed using sonication and French press respectively. Soluble and insoluble protein fractions were separated by centrifugation at 20,000 RCF, 4 °C for 20 minutes. Both His6-BirA and His6-CxxC-Avi proteins were purified by IMAC using Novagen Ni-NTA His-Bind resin (Merck-Millipore, Burlington, MA, USA) in gravity-flow columns. His6-tagged proteins bound to Ni-charged beads were washed sequentially with a low salt wash buffer (50 mM Tris pH 8.0, 300 mM NaCl, 10 mM Imidazole, 0.1% Triton-X100 and 1 mM PMSF) and a high salt wash buffer (50 mM Tris pH 8.0, 1000 mM NaCl and 1 mM PMSF) and eluted with the elution buffer (50 mM Tris pH 8.0, 300 mM NaCl, 300 mM Imidazole and 1 mM PMSF). For His6-BirA, only the low salt wash buffer was used for the washes and both wash and elution buffers were supplemented with 1 mM DTT. Peak elution fractions were pooled and dialysed overnight at 4 °C with the dialysis buffer containing

50 mM Tris pH 8.0, 300 mM NaCl and 0.5 mM PMSF to remove imidazole. Purified and dialysed His6-BirA protein sample was supplemented with 10% glycerol, aliquoted at 50 µl in 200 µl tubes, snap frozen in liquid N_2 and stored at -80 °C until further use. Purified and dialysed His6-CxxC-Avi protein samples were concentrated using Amicon Ultra-15 centrifugal filter units (Merck-Millipore, Burlington, MA, USA) before the TEV protease cleavage performed overnight at 4 °C and *in vitro* biotinylation by His6-BirA. Prior to the *in vitro* biotinylation, the His6-CxxC-Avi samples were dialysed to a buffer containing 10 mM Tris, pH 8.0 and 250 mM potassium glutamate. The *in vitro* biotinylation was carried out by adding the His6-BirA enzyme supplemented with 10 mM ATP, 10 mM magnesium acetate and 50 µM D-biotin to the CxxC-Avi proteins and incubating the reactions overnight on a tube rotator at 4 °C. The biotinylation reaction was re-applied to the Ni-NTA column to remove the His6-BirA enzyme and yield pure Bio-CxxC protein. Lastly, Bio-CxxC proteins were dialysed to 20 mM HEPES pH 7.0, 150 mM KCl, 0.5 mM DTT and 10% Glycerol. The dialysed Bio-CxxC protein samples were snap frozen in liquid N_2 and stored at -80 °C as 100 µl aliquots at the concentration of 1 mg/ml.

A.2.2 Protein quantification and gel electrophoresis

Sigma Bicinchoninic Acid (BCA) Assay kit (Merck-Millipore, Burlington, MA, USA) was used to quantify total protein concentration by following the manufacturer's instructions. 15% SDS-PAGE gel in 1X SDS-PAGE running buffer (25 mM Tris, 192 mM glycine, 0.1% SDS) was utilised to assess the purified proteins by size. Specific concentration of proteins was also assessed by quantifying the signal of Coomassie blue (R-250) stained protein bands of SDS-PAGE gels on IR700 channel of Li-Cor Odyssey near-infrared imager (LI-COR, Lincoln, NE, USA). The fluorescence intensity of bands of the proteins with an unknown concentration were interpolated to a standard curve plot based on the fluorescence intensity data of the BSA protein standards with known protein concentrations.

A.2.3 Optimisation of the His6-tag cleavage of His6-CxxC-Avi by TEV protease

Optimisation of the His6-tag removal via the TEV protease cleavage was accomplished by incubating 150 µg of His6-CxxC-Avi with 0, 2 and 4 µg of TEV protease in the reaction buffer (50 mM Tris pH 8.0 and 300 mM NaCl), with or without 0.5 mM DTT. The reaction mix was applied to a gravity column loaded with Novagen Ni-NTA His Bind resin (Merck-Millipore, Burlington, MA, USA) to remove the His6-tag. Input, Flow-through and Eluate fractions were saved and the proteins were separated by size on a 15% SDS-PAGE gel, stained with Coomassie blue and scanned on a Li-Cor Odyssey near-infrared scanner using the IR700 channel.

A.2.4 Optimisation of the enzymatic biotinylation of CxxC-Avi

To assess the extent of biotinylation of the CxxC-Avi protein by His6-BirA, three biotinylation reactions containing 25 µg of the CxxC-Avi protein for each reaction were incubated overnight at 4 °C with 0, 0.5 and 1 µg of the His6-BirA protein respectively, in the biotinylating buffer (10 mM Tris pH 8.0 and 250 mM potassium glutamate) supplemented with 10 mM ATP, 10 mM magnesium acetate and 50 µM D-biotin. The three biotinylation reactions were purified from the excess of free biotin using a Microcon YM-10 mini centrifugal filter unit (Merck-Millipore, Burlington, MA, USA) and the purified biotinylation reactions were subsequently incubated with streptavidin agarose beads at 4 °C for 1 hour (manufactured by Pierce, Thermo Fisher Scientific, Waltham, MA, USA), at 10 µl of resin per approximately 10 µg of the biotinylated protein. Following the binding reaction to streptavidin, the supernatant (flow-through) was collected centrifuged samples. Two subsequent washes of the resin with 1X PBS were also collected. Total proteins from the untreated CxxC-Avi, Input, Flow-through, Wash and Beads fractions from the three biotinylation reactions were resolved on 15% SDS-PAGE gel, stained with Coomassie blue and scanned on a Li-Cor Odyssey near-infrared imager at IR800 channel for further analysis.

A.2.5 Electrophoretic Mobility Shift Assay (EMSA)

EMSA was carried out using the EMSA buffer containing 6% glycerol, 20 mM HEPES, 150 mM KCl, 0.5 mM DTT, 25 ng/µl Poly dI-dC, 0.25% Tween-20 and DY-782 labelled methylated or unmethylated oligonucleotides. The oligonucleotides came as two complementary DNA sequences which were annealed together by heating a mixture of each pair to 95 °C and slowly cooling it down to room temperature. Two fluorescently labelled double-stranded oligonucleotides with the identical DNA sequence containing 3 non-methylated and 3 methylated CpGs respectively, at 1 µM concentration were mixed with 0, 25, 50, 75 and 100 µM Bio-CxxC in EMSA buffer. Bio-CxxC was incubated with the labelled oligonucleotides in the EMSA buffer at room temperature for 25 minutes before the samples were loaded onto a 10% non-denaturing polyacrylamide gel with the acrylamide to bis-acrylamide ratio of 19:1 in 1X TBE buffer containing 89 mM Tris-base, 89 mM Boric acid and 2 mM EDTA. The gels were pre-run at 150 V, 4 °C for 30 minutes before being loaded with samples. Loaded gels were run at 150 V, 4 °C for 2 hours. The gels were scanned on a Li-Cor Odyssey imager at IR800 channel.
The oligonucleotides used for EMSA are as follow:

3CG-Unmethylated-F:

5'-DY-782-GAGTCTCACTCACGCGCATTCCATTCCATCAGATACTAGTACGGTCAG

3CG-Unmethylated-R:

5'-CTGACCGTACTAGTATCTGATGGAATGGAATGCGCGTGAGTGAGACTC

3CG-Methylated-F:

5'-DY-782-GAGTCTCACTCAXGXGCATTCCATTCCATCAGATACTAGTAXGGTCAG

3CG-Methylated-R:

5'-CTGACXGTACTAGTATCTGATGGAATGGAATGXGXGTGAGTGAGACTC

A.2.6 Cell Culture

Mouse Embryonic Fibroblasts (MEFs) were cultured in DMEM (Sigma) supplemented with 10% Gibco Fetal Bovine Serum (FBS) (Thermo Fisher Scientific, Waltham, MA, USA) and 1X Gibso PSG (292 µg/ml L-glutamine,

100 U/ml Penicillin, 100 µg/ml Streptomycin) (Thermo Fisher Scientific, Waltham, MA, USA). MEFs were grown in a 37 °C incubator with 5.0% CO_2.

A.2.7 DNA extraction and purification

Genomic DNA (gDNA) for the Bio-CAP experiments was isolated from MEFs. Cell pellets were dissolved in 1X TE buffer containing 0.1% SDS and 200 µg/ml proteinase K and incubated overnight at 55 °C. Phenol: chloroform: isoamyl alcohol (25: 24: 1) followed by 100% chloroform were used to extract genomic DNA. 1X volume of 100% isopropanol and 0.3 M sodium acetate pH 5.2 were used to precipitate the DNA at -20 °C for 1 hour. The DNA was pelleted by centrifugation at 17,000 RCF, 4 °C for 15 minutes. DNA pellets were washed with 70% ethanol and air dried for 10 minutes. The air-dried pellets were dissolved in 1X TE buffer containing 10 mM Tris (pH 8.0) and 1 mM EDTA. Any contaminating RNA was digested by incubating the samples with RNAse A for 30 minutes at 37°C.

A.2.8 DNA Sonication

Purified gDNA for the Bio-CAP experiments was sonicated using Diagenode Bioruptor Twin sonicator (Diagenode, Liège, Belgium). The DNA was diluted in 1xTE at 80 ng/µl and 0.1% SDS was added to the samples prior to the sonication.The gDNA samples were sonicated for 120 cycles of 30 seconds on and 30 seconds off at 4 °C.

A.2.9 Bio-CAP

50 µl of 0.5 µg/µl biotinylated-CxxC protein (Bio-CxxC) was added to 25 µl packed volume of magnetic Speedbeads Neutravidin beads (GE Healthsciences, Chicago, IL, USA) in a siliconised 1.5 ml microtube and incubated for 1 hour at 4 °C on a tube rotator to produce CxxC beads. 500 µl of sonicated gDNA at 17.5 ng/µl was incubated with the CxxC beads for 1 hour at 4 °C on a tube rotator. Beads were collected with an Invitrogen Dynamag-2 magnetic tube rack (Thermo Fisher Scientific, Waltham, MA, USA) and the supernatant (flow-through) was saved for further analysis. The CxxC beads

were washed twice with the CAP100 buffer containing 20 mM HEPES-KOH pH 7.9, 0.1% Triton X-100, 12.5% Glycerol and 100 mM NaCl. gDNA was eluted from the CxxC beads using 2x 50 µl of a series of elution buffers containing 5 different NaCl concentrations: 300 mM, 500 mM, 700 mM and 1,000 mM of NaCl, for CAP300, CAP500, CAP700 and CAP1000 elution buffers respectively. 100 µl of input, flow-through, CAP300, CAP500, CAP700 and CAP1000 fractions were purified using Invitrogen Purelink PCR purification kit (Thermo Fisher Scientific, Waltham, MA, USA), according to the manufacturer's instructions.

A.2.10 PCR-amplification of the DNA pulled down in the Bio-CAP experiments

PCR reactions using Bio-CAP fractions as templates were carried out using 1 U of in-house made *Taq* polymerase, 0.2 mM dNTPs, 1X PCR Buffer, 3 mM $MgCl_2$, 10 nM forward and reverse primers, 1 µl purified Bio-CAP fractions in 25 µl reactions. Input and flow-through fractions were diluted 1:10 with dH_2O, while elution fractions were used undiluted. The PCR conditions used are as follow: Initial denaturation for 5 minutes at 95 °C followed by 35 cycles of denaturation for 30 seconds at 95 °C, annealing for 30 seconds at 58 or 60 °C (depending on primers used) and extension for 30 seconds at 72 °C and then followed by a final extension step at 72 °C for 10 minutes. The PCR products were separated by size using DNA electrophoresis in a 2% agarose gel made with 1X TAE buffer containing 40 mM Tris pH 8.0, 20 mM acetic acid and 1 mM EDTA and run at 14 V/cm for 30 minutes.

A.2.11 Bio-CAP PCR Primers

Mouse gene promoters can be divided into three groups based on the observed/expected CpG ratio (CpG o/e) calculated in 500 bp windows: Low CpG density promoters (LCP) or non-CGI promoters (CpG o/e <0.45), Intermediate CpG density promoters (ICP) or weak CGI promoters (CpG o/e 0.4-0.6) and High CpG density promoters HCP or strong CGI promoters (CpG o/e >0.6; High density) (Mohn et al., 2008). Based on this gene promoter

classification and the previous promoter DNA methylation data generated in the Stancheva laboratory for mouse embryonic fibroblasts (MEFs) (Myant et al., 2011), primers for the PCR were designed to test the efficacy of Bio-CAP in capturing non-methylated DNA corresponding to specific promoters. In addition, primers for *Actb* (β-actin) and *Rhox6* gene promoter regions were also included as controls for unmethylated and methylated promoters, respectively. I have also designed primers to amplify the imprinting control regions (ICR) which are differentially methylated regions located near imprinted genes and known to regulate their transcription in *cis* (Reviewed in (Bartolomei and Ferguson-Smith, 2011)). Sequences of primers used for PCR of DNA from purified Bio-CAP fractions are as follow:

Primer name	**Target**	**Sequence**
GEN-FABP7-Pr-F	Fabp7 promoter	5'-ATTGGCTTTTTGCCCGCTTC
GEN-FABP7-Pr-R	Fabp7 promoter	5'-AACTGGAGGAACTCGGGTCT
GEN-UTS2-Pr-F	Uts2 promoter	5'-AAGTTCTCCAGAGCAGACGC
GEN-UTS2-Pr-R	Uts2 promoter	5'-GTCACCTCACCTGGAAGCTG
GEN-MSN-Pr-F	Msn promoter	5'-GGGGTTTGTAAAGTCGTGGC
GEN-MSN-Pr-R	Msn promoter	5'-TTTGGCTGGAAACTGTCGGG
GEN-USP44-Pr-F	Usp44 promoter	5'-CGAAAGCCTAGCAGACGGTA
GEN-USP44-Pr-R	Usp44 promoter	5'-CCCTCATCAGCGGATTCTCC
Actb-DIP-F	Actb promoter	5'-ATGAAGAGTTTTGGCGATGG
Actb-DIP-R	Actb promoter	5'-GATGCTGACCCTCATCCACT
ChIP-Rhox6-F2	Rhox6 promoter	5'-CCATGTTGCTCAGGTCTTTATCTC
ChIP-Rhox6-R2	Rhox6 promoter	5'-GAGCGAGCCAGTTCAGTACAAG
Zac1 qPCR F	Zac1 ICR	5'-GCATCTGCGATTTGTCACTC
Zac1 qPCR R	Zac1 ICR	5'-CTTGCTCTCCAGTCCCGATA
Snrpn qPCR F	Snrpn ICR	5'-CAGGACATTCCGGTCAGAG
Snrpn qPCR R	Snrpn ICR	5'-TACTAGAATCCACAAGCCCAG
Nespas qPCR F	Nespas ICR	5'-CCGGACACTTTGAACTTTGG
Nespas qPCR R	Nespas ICR	5'-GCATCCTTGATTGGCGTGAC

A.3 Results

A.3.1 Expression and purification of His6-BirA and His6-CxxC-Avi proteins for establishment of Bio-CAP technique

Both bacterial expression plasmids (pET21a and pNIC28) used to express His6-CxxC-Avi and His6-BirA proteins requires IPTG, a non-hydrolysable allolactose analogue, to induce expression of the cloned target genes under the control of T7 promoter. IPTG relieves binding of *lac* repressor to the *lac* operator, which is located between the T7 promoter and the target gene in the bacterial expression plasmid, to allow transcription of target genes by T7 RNA polymerase. 0.5 and 0.4 mM IPTG were used to induce expression of His6-CxxC-Avi and His6-BirA respectively in *E. coli* strain BL21-CodonPlus-RIL. Induction was done at 25 °C for 6 hours and 4 hours for His6-CxxC-Avi and His6-BirA respectively. To check for recombinant protein expression, 15 µl of bacterial culture (uninduced and IPTG-induced) were mixed with 5 µl 4X SDS-PAGE sample buffer, boiled at 100 °C for 15 minutes and subjected to SDS-PAGE. Coomassie blue stained SDS-PAGE gels showed good expression of His6-CxxC-Avi (19 kDa) and His6-BirA (36 kDa) proteins in *E. coli* strain BL21-CodonPlus-RIL following induction with 0.5 and 0.4 mM IPTG respectively (Figure A.2).

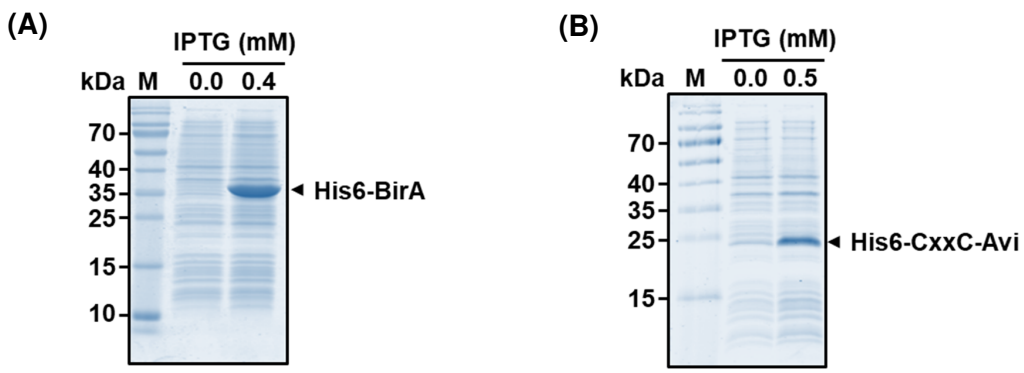

Figure A.2 Expression of His6-BirA and His6-CxxC-Avi proteins Coomassie blue staining of SDS-PAGE gels showed expression of (A) His6-BirA and (B) His6-CxxC-Avi recombinant proteins in *E. coli* strain BL21-CodonPlus-RIL following IPTG induction.

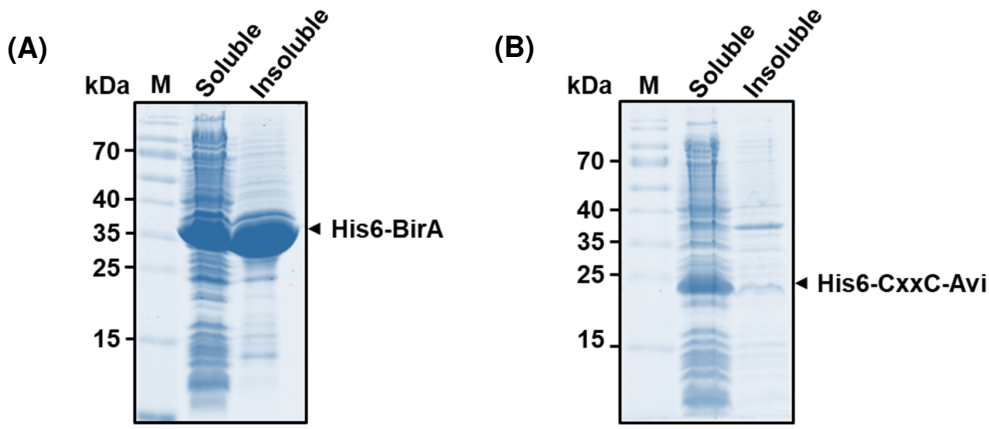

Figure A.3 His6-BirA and His6-CxxC-Avi protein extraction from *E. coli* strain BL21-Codonplus-RIL.
(A) His6-BirA and (B) His6-CxxC-Avi proteins were extracted from *E. coli* and soluble fraction (supernatant) was separated from insoluble fraction (pellet) by centrifugation and both fractions were analysed by SDS-PAGE and Coomassie blue staining.

Following protein induction, proteins were extracted from cells using methods mentioned in the materials and methods section. Coomassie blue stained SDS-PAGE gels of soluble and insoluble fractions showed that a large proportion of proteins, including target recombinant proteins, were found in the soluble fraction, which suggests a good level of protein extraction using the chosen methods (Figure A.3). To purify His6-BirA and His6-CxxC-Avi, soluble fractions were applied to IMAC columns. SDS-PAGE analysis of the collected IMAC fractions showed that both proteins bind to the nickel-charged resin and that 300 mM imidazole was sufficient to elute both proteins (Figure A.4). Elution fractions containing the highest amount of target proteins were pooled (Elution fractions 2-4 for His6-BirA and 2-3 for His6-CxxC-Avi) and dialysed to suitable buffers for storage (His6-BirA) and further downstream processing (His6-CxxC-Avi). The IMAC purification yields 6 mg of His6-BirA protein from 400 ml bacterial culture and 12 mg of His6-CxxC-Avi protein from 4000 ml bacterial culture.

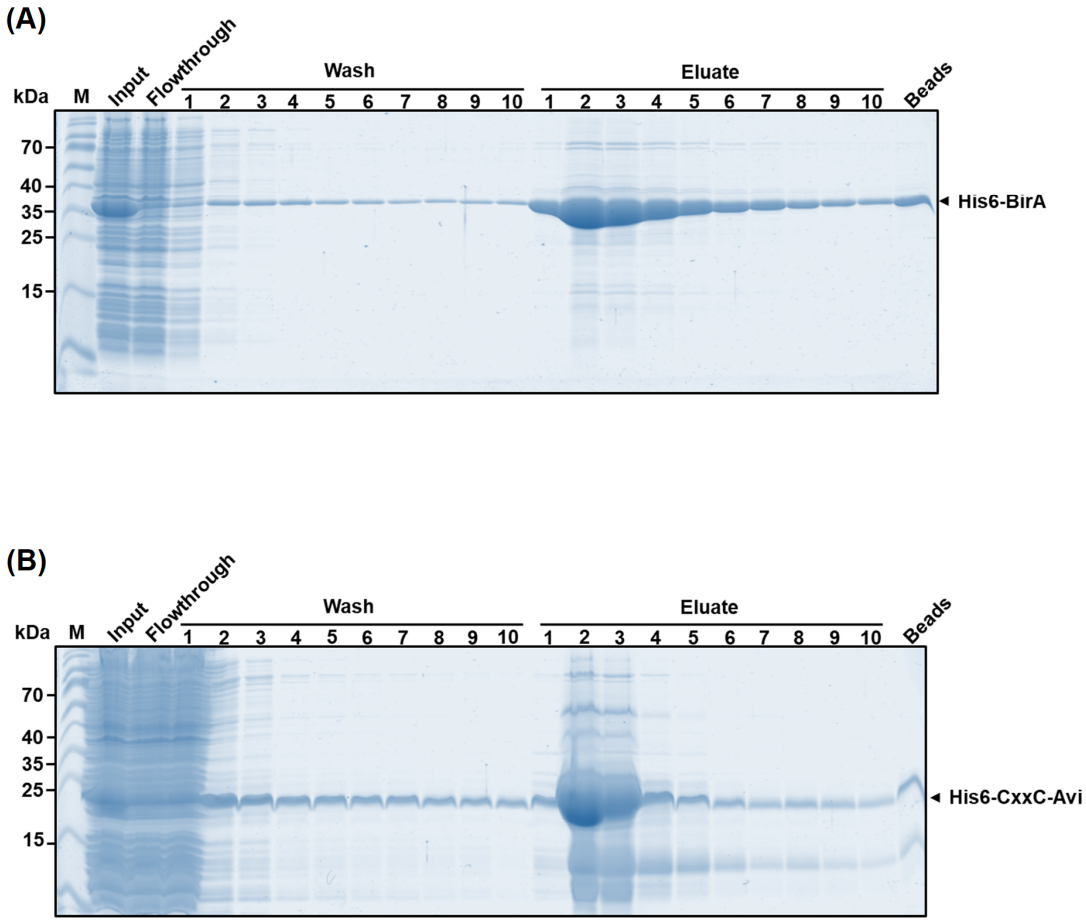

Figure A.4 Purification of His6-BirA and His6-CxxC-Avi protein by IMAC
(A) His6-BirA and (B) His6-CxxC-Avi soluble fractions were loaded into Ni-charged IMAC gravity column, washed with wash buffer containing 10 mM imidazole and eluted with elution buffer containing 300 mM imidazole. Input, Flow-through, Wash and Eluate fractions were collected and 15 µl of each fractions were analysed by SDS-PAGE and the SDS-PAGE gel was stained with Coomassie blue.

As briefly mentioned in the introduction section, removal of the His6-tag can increase the efficiency of CxxC domain binding to non-methylated CpG. Between the His6-tag and the N-terminus of the CxxC domain there is a TEV protease-recognition site. Incubation of His6-CxxC with TEV protease can therefore free the CxxC domain from the His6-tag. To optimise this procedure, 2 and 4 µg of His6-TEV protease (Simon Varzandeh, Richardson Laboratory, University of Edinburgh) were added to 150 µg His6-CxxC-Avi in separate reactions, with or without 0.5 mM DTT and incubated overnight at 4 °C. The reaction mix was applied to an IMAC column to bind the cleaved His6-tag. IMAC collected fractions were analysed by SDS-PAGE to observe the efficiency of His6-tag cleavage. The result showed that both 2 and 4 µg of TEV protease exhibit similar activity as shown from the intensity of the smaller CxxC-Avi band (18.9 kDa) in the flow-through fractions (Figure A.5). Furthermore, His6-CxxC-Avi (21.4 kDa) band was not detected in the flow-through fractions of both 2 and 4 µg TEV protease reactions supplemented with 0.5 mM DTT, suggesting that the addition of DTT resulted in complete digestion of the His6-tag from His6-CxxC-Avi protein. Therefore, it can be concluded that 1 µg His6-TEV protease is sufficient to efficiently cleave His6-tag from 75 µg of His6-CxxC-Avi protein.

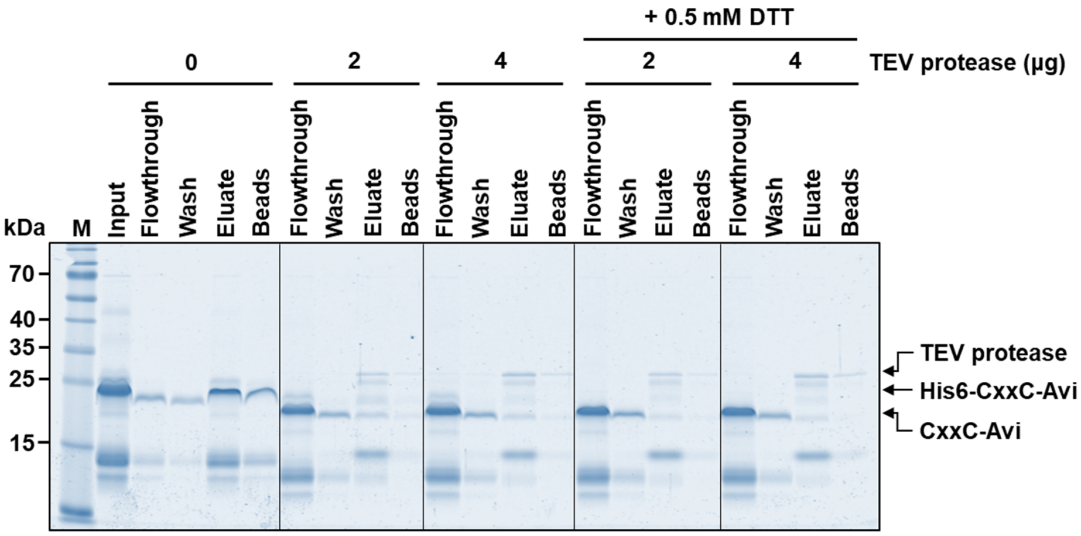

Figure A.5 Optimisation of His6-tag removal from His6-CxxC-Avi by TEV protease
Coomassie blue stained SDS-PAGE gel of IMAC fractions of His6-CxxC-Avi protein cleaved by TEV protease with or without 0.5 mM DTT. His6-TEV protease size is 28 kDa.

A.3.2 Biotinylation of CxxC-Avi protein by His6-BirA

In order to be able to pool down CxxC-Avi protein and associated DNA with streptavidin beads, CxxC-Avi protein was biotinylated *in-vitro* at the C-terminus on the Avi-tag, using His6-BirA enzyme. To assess the extent of biotinylation of the CxxC-Avi protein by His6-BirA enzyme, three biotinylation reactions containing 25 µg CxxC-Avi protein each were incubated with 0, 0.5 and 1 µg His6-BirA enzyme, respectively. Subsequently, CxxC-Avi proteins were mixed with streptavidin beads and input, flow-through, wash and beads fractions were collected and analysed by SDS-PAGE. Analysis of Coomassie blue stained SDS-PAGE gel showed that CxxC-Avi treated with 1 µg His6-BirA enzyme displayed the highest fraction of protein binding to streptavidin beads, as indicated by the band intensity of the beads fraction (Figure A.6). In agreement with this, CxxC-Avi treated with 1 µg His6-BirA showed the lowest protein loss in the flow-through compared to 0 and 0.5 µg His6-BirA. Increasing

Hi6-BirA enzyme quantity to 1.5 µg for 25 µg CxxC-Avi protein did not increase the amount of biotinylated CxxC-Avi bound to the beads (data not shown). These results suggest that 1 µg His6-BirA for 25 µg CxxC-Avi is the most efficient condition to maximise CxxC-Avi protein biotinylatation.

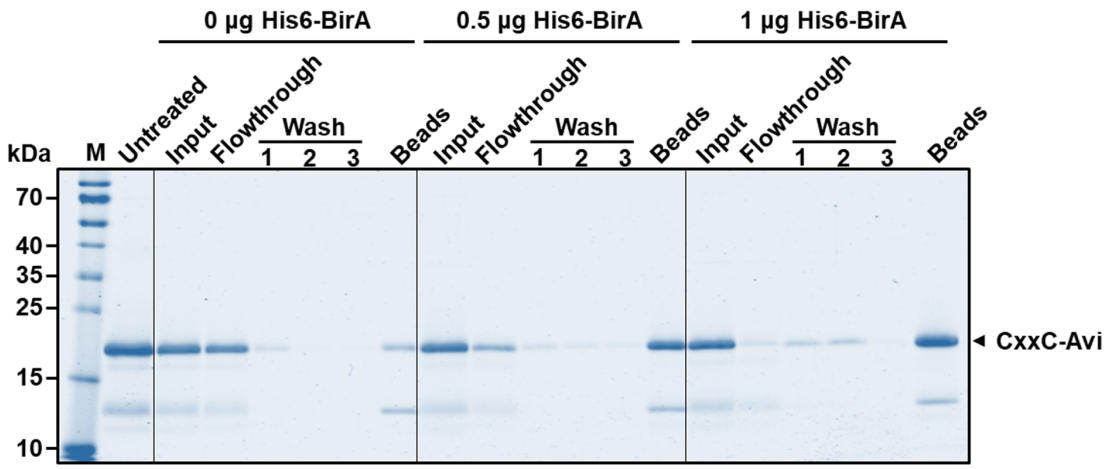

Figure A.6 Optimisation of CxxC-Avi protein biotinylation by His6-BirA CxxC-Avi protein treated with 0, 0.5 and 1 µg His6-BirA biotinylating enzyme was incubated with streptavidin beads. Input, biotinylated protein bound to the beads (beads) and protein not bound to the beads (flowthrough) were analysed by SDS-PAGE. CxxC-Avi treated with 1 µg His6-BirA showed the highest amount of CxxC-Avi protein binding to beads.

A.3.3 Bio-CxxC protein preferentially binds to non-methylated DNA

To assess the ability and specificity of Bio-CxxC protein (the biotinylated version of CxxC-Avi protein) binding to non-methylated CpG DNA, I carried out an electrophoretic mobility shift assay (EMSA) (Figure A.7). The results showed that Bio-CxxC has a much higher affinity for non-methylated CpG, showing an efficient band shift already at at 1:50 DNA:Protein molar ratio. Only at the highest DNA:protein ratio used Bio-CxxC protein showed some binding to methylated DNA. This suggests that Bio-CxxC preferentially binds to DNA

containing unmethylated CpGs and that non-specific binding occurs minimally and only at very high protein concentration. These results are in agreement with the data showing that KDM2B/FBXL10, from which the CxxC domain of Bio-CxxC protein was derived, binds specifically to non-methylated CpGs (Farcas et al., 2012; Koyama-Nasu, David and Tanese, 2007).

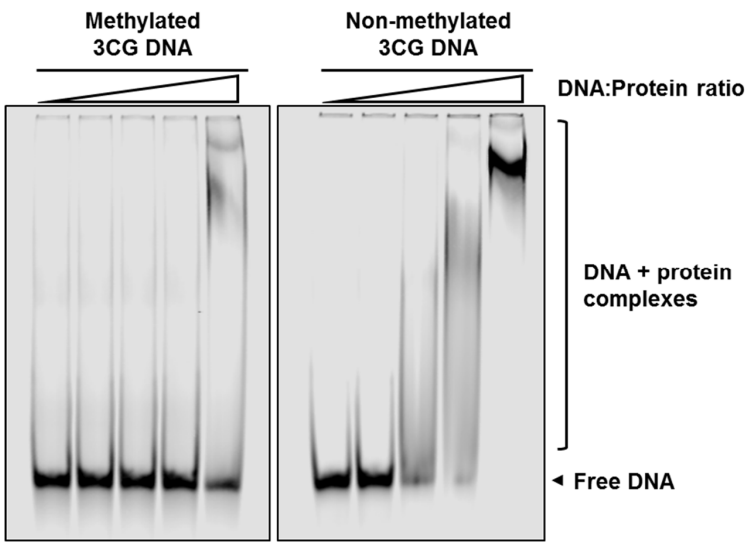

Figure A.7 Bio-CxxC protein showed preferential binding to non-methylated DNA

Two fluorescently labelled double-stranded oligonucleotides with identical DNA sequence containing 3 non-methylated and 3 methylated CpGs, respectively, at 1 µM concentration, were mixed with 0, 25, 50, 75 and 100 µM Bio-CxxC in EMSA buffer and loaded to a non-denaturing polyacrylamide in increasing DNA:Protein ratio for EMSA analysis.

A.3.4 Optimisation of Bio-CAP PCR

Bio-CAP can be carried out using avidin conjugated to agarose or magnetic beads. Magnetic beads were selected over agarose due to lower unspecific DNA binding and ease of handling (no centrifugation required). DNA polled down by Bio-CAP was purified over spin-columns and analysed by PCR using specific primers, designed to amplify candidate promoters of known CG

content and methylation status (Table A.1). Ideally, we would have liked to test Bio-CAP on known and well characterised CGIs. However, presumably due to the high GC content, these region could not be PCR-amplified. Addition of DMSO or GC-rich specific PCR reagents and the use of Phusion polymerase (NEB, Ipswich, MA, USA) did not solve the problem (data not shown). Therefore, the primers for CGI promoters (*Cog8* and *Smarca5*) were excluded from the analysis. PCR-analysis of DNA purified by Bio-CAP showed enrichment of unmethylated promoters (*Fabp7*, *Msn*, *Actb*) (Figure A.8.). *Fabp7* promoter was amplified in the low salt (CAP300) fraction, while *Msn* and *Actb* promoters were amplified in the high salt fractions (CAP 700 and CAP1000), suggesting that CpG density affects the strength of CxxC protein binding to unmethylated DNA. On the other hand, none of the primers detecting methylated promoters (*Uts2*, *Usp44* and *Rhox6*) were able to amplify DNA, in either low or high salt Bio-CAP purified fractions. The results were consistent across three different concentrations of input DNA, suggesting that Bio-CAP can be carried out with amount of input DNA as low as 350 ng, without significantly losing specificity.

Analysis of mouse imprinting control regions (ICRs) by Bio-CAP would be very interesting. Each ICR is present in each cell in two states, where one allele is methylated while the other is not, depending on the parent-of-origin. I decided to take advantage of this feature to investigate if Bio-CAP is sensitive enough to discriminate the two co-existing alleles. To this end, I designed PCR primers against three different ICRs, *Zac1*, *Snrpn* and *Nespas*, known to be methylated only on the maternal allele (Zhang et al., 2016). While *Zac1*, and *Nespas*, showed exclusively enrichment in CAP700 and CAP1000 fractions (Figure A.9.), *Snrpn* showed also a slight enrichment in CAP300 fraction. Previously, Bio-CAP qPCR analysis of imprinted *Gnas* promoter of murine V6.5 embryonic stem (ES) cells also showed enrichment in both low salt (300 & 500 nM) and high salt (700 and 1000 nM) fractions (Blackledge et al., 2012). Bisulphite sequencing analysis has confirmed in this case that the methylated allele of Gnas was specifically eluted in the CAP300 fraction, while the unmethylated

allele was eluted with the CAP500, CAP700 and CAP1000 fractions (Blackledge et al., 2012). Therefore, my analysis of ICRs suggests that Bio-CAP was able to either exclusively isolate the unmethylated allele or, at least, to separate the two alleles in different fractions.

Table A.1. Promoter regions with known CpG density and methylation status for Bio-CAP PCR primer design

Methylation status / Promoter Classification	Unmethylated	Methylated
Non CGI Promoter (Low CpG density)	*Fabp7*	*Uts2*
Weak CGI Promoter (Intermediate CpG density)	*Msn*	*Usp44*
Strong CGI Promoter (High CpG density)	*Cog8*	*Smarca5*

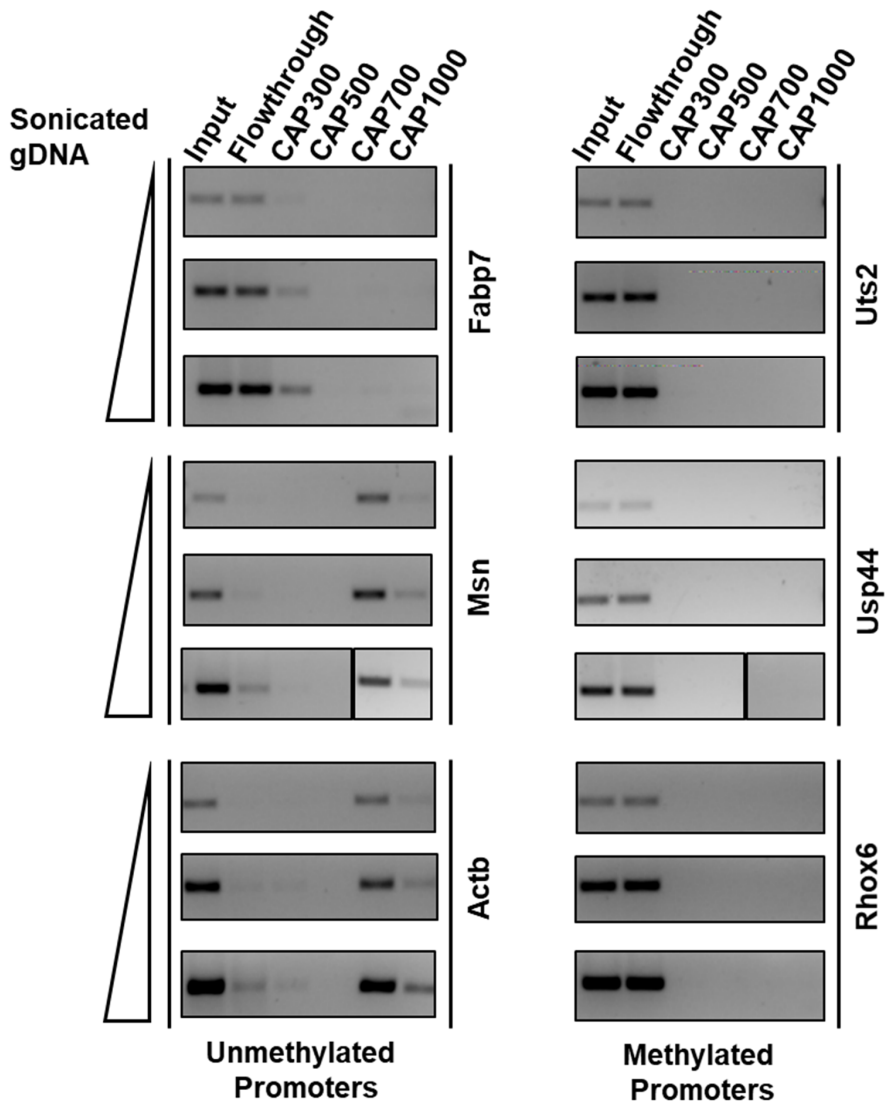

Figure A.8 Bio-CAP captures unmethylated promoters but not methylated promoters

Bio-CAP was carried out using 0.35, 1.75 and 8.75 µg input sonicated gDNA. Bio-CAP isolated DNA was analysed by PCR amplification, carried out with primers designed to the indicated target promoters. The products were analysed by agarose DNA electrophoresis. Parallel analysis of known methylated and un-methylated promoter regions showed that Bio-CAP can specifically enriched un-methylated DNA.

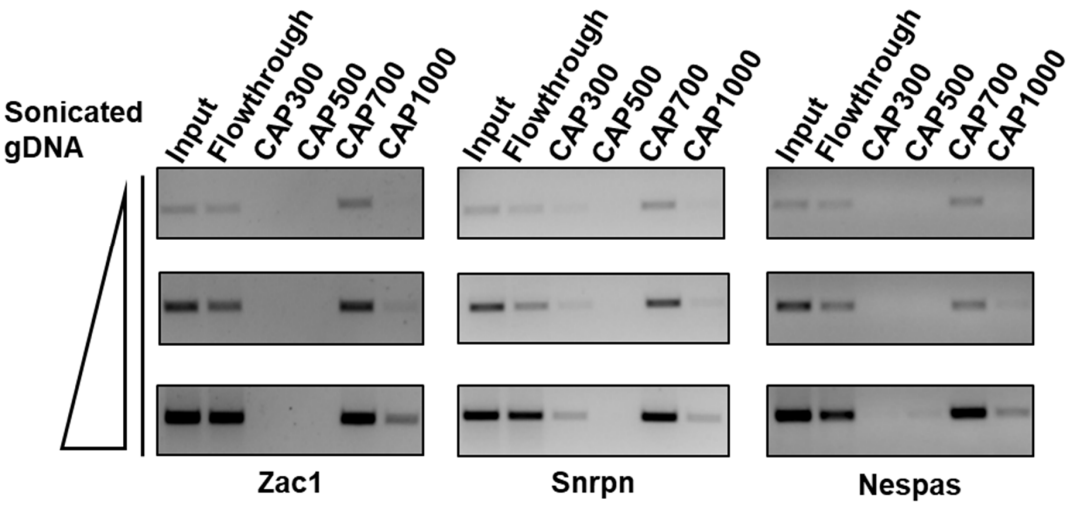

Figure A.9. Bio-CAP can discriminate between the methylated and unmethylated alleles of ICRs.

Bio-CAP was carried out using 0.35, 1.75 and 8.75 µg input sonicated gDNA. ICR PCR products of Bio-CAP fractions were analysed by agarose DNA electrophoresis to assess DNA enrichment of ICRs.

A.4 Discussion

Previously, methylated CpG capture techniques, such as methylated DNA immunoprecipitation (MeDIP) and methylated DNA affinity purification (MAP), have been utilised in combination with either microarrays or high throughput sequencing techniques to generate genome-wide methylation profile as an alternative or supplementary to whole-genome bisulphite sequencing (Reviewed in (Laird, 2010)). However, approximately 98% of CpGs which are sparsely spaced in the genome, are predominantly methylated and around 2% are concentrated in CpG Islands which are mostly unmethylated (Bird, 2002). Furthermore, around 70% of promoter regions contain CpG islands (Saxonov, Berg and Brutlag, 2006). Therefore, due to the smaller proportion of analysed DNA, unmethylated DNA enrichment technique such as CxxC Affinity Purification (CAP) can offer the advantages of low sequencing depth requirement, increased sensitivity of CGI detection and increased cost-effectiveness in comparison to methylated DNA enrichment techniques (Blackledge et al., 2012; Illingworth et al., 2008). Bio-CAP is a modified CxxC Affinity Purification (CAP) technique, previously developed to purify CpG islands, which were predominantly unmethylated (Illingworth et al., 2008). The modification allowed the use of lower amount of input gDNA, lower amount of CxxC protein and made liquid chromatography, used in the original CAP method, dispensable (Blackledge et al., 2012; Illingworth et al., 2008). Motivated by these advantages, I planned to utilise this method for analysing DNA methylation changes on promoters of hTERT-immortalised cells, following prolonged culture with and without telomerase. As previously mentioned, hTERT-immortalised cells exhibit increased DNA methylation at gene promoters (Gordon et al., 2014). Bio-CAP-sequencing, in combination with a system designed to switch telomerase activity on and off, would have allowed me to assess whether telomerase was required for the induction and/or maintenance of DNA methylation on promoters.

In this chapter, I have optimised the production of His6-BirA and His6-CxxC-Avi proteins, which were the two most important component to create Bio-

CxxC protein used in the Bio-CAP technique. My results showed that the Bio-CAP technique is capable of specific enrichment of promoter regions containing non-methylated CpGs with DNA input as low as 350 ng, particularly in the high salt fractions (CAP700 and CAP1000). Furthermore, it is also capable of capturing unmethylated alleles of ICRs. However, non-methylated, CGI-poor promoter such as Fabp7 promoter was enriched in the low salt fractions (CAP300), suggesting that CpG density affects the binding of Bio-CxxC to unmethylated DNA. Therefore, further optimisations are required to identify the salt concentration threshold that specifically discriminates between methylated and unmethylated DNA, particularly at low CpG density.

A.5 Acknowledgements

Primary and Immortalised MEFs used for optimisation of Bio-CAP were acquired from Natalia Torrea. MRC-5 hTERT, DD-hTERT and DD-hTERT ΔPT cell lines were generated by Katrina Gordon. Plasmids for expression of His6-BirA and His6-CxxC-Avi proteins were acquired from Rob Klose. Simon Varzandeh provided the TEV protease used for His6-tag removal from the His6-CxxC-Avi protein.

A.6 References

Bartolomei, M. S. and Ferguson-Smith, A. C. (2011). Mammalian genomic imprinting. Cold Spring Harbor Perspectives in Biology, 3 (7), pp.1–17. [Online]. Available at: doi:10.1101/cshperspect.a002592.

Bird, A. (2002). DNA methylation patterns and epigenetic memory. Genes & development, 16 (1), pp.6–21. [Online]. Available at: doi:10.1101/gad.947102.

Bird, A. P. (1987). CpG islands as gene markers in the vertebrate nucleus. Trends in Genetics, 3, pp.342–347. [Online]. Available at: doi:10.1016/0168-9525(87)90294-0.

Blackledge, N. P. et al. (2012). Bio-CAP: a versatile and highly sensitive technique to purify and characterise regions of non-methylated DNA. Nucleic Acids Research, 40 (4), pp.e32–e32. [Online]. Available at: doi:10.1093/nar/gkr1207.

Blasco, M. A. (2005). Telomeres and human disease: ageing, cancer and beyond. Nature Reviews Genetics, 6 (8), pp.611–622. [Online]. Available at: doi:10.1038/nrg1656.

Bodnar, A. G. et al. (1998). Extension of Life-Span by Introduction of Telomerase into Normal Human Cells. Science, 279 (5349), pp.349–352. [Online]. Available at: doi:10.1126/SCIENCE.279.5349.349.

Counter, C. M. et al. (1998). Telomerase activity is restored in human cells by ectopic expression of hTERT (hEST2), the catalytic subunit of telomerase. Oncogene, 16 (9), pp.1217–1222. [Online]. Available at: doi:10.1038/sj.onc.1201882.

Cruickshanks, H. A. et al. (2013). Senescent Cells Harbour Features of the Cancer Epigenome. Nature Cell Biology, 15 (12), pp.1495–1506. [Online]. Available at: doi:10.1038/ncb2879.

Farcas, A. M. et al. (2012). KDM2B links the Polycomb Repressive Complex 1 (PRC1) to recognition of CpG islands. eLife, 1. [Online]. Available at: doi:10.7554/eLife.00205.

Frommer, M. et al. (1992). A genomic sequencing protocol that yields a positive display of 5- methylcytosine residues in individual DNA strands. Proceedings of the National Academy of Sciences of the United States of America, 89 (5), pp.1827–1831. [Online]. Available at: doi:10.1073/pnas.89.5.1827.

Genereux, D. P. et al. (2008). Errors in the bisulfite conversion of DNA: Modulating inappropriate- and failed-conversion frequencies. Nucleic Acids Research, 36 (22). [Online]. Available at: doi:10.1093/nar/gkn691.

Gordon, K. et al. (2014). Immortality, but not oncogenic transformation, of primary human cells leads to epigenetic reprogramming of DNA methylation and gene expression. Nucleic Acids Research, 42 (6), pp.3529–3541. [Online]. Available at: doi:10.1093/nar/gkt1351.

Hahn, M. A. et al. (2011). Relationship between Gene Body DNA Methylation and Intragenic H3K9me3 and H3K36me3 Chromatin Marks. Feil, R. (Ed). PLoS ONE, 6 (4), p.e18844. [Online]. Available at: doi:10.1371/journal.pone.0018844.

Hanahan, D. and Weinberg, R. A. (2011). Hallmarks of Cancer: The Next Generation. Cell, 144 (5), pp.646–674. [Online]. Available at: doi:10.1016/J.CELL.2011.02.013.

Hayatsu, H., Wataya, Y. and Kazushige, K. (1970). The addition of sodium bisulfite to uracil and to cytosine. Journal of the American Chemical Society, 92 (3), pp.724–726. [Online]. Available at: doi:10.1021/ja00706a062.

Holliday, R. and Pugh, J. E. (1975). DNA modification mechanisms and gene activity during development. Science (New York, N.Y.), 187 (4173), pp.226–232. [Online]. Available at: doi:10.1126/SCIENCE.187.4173.226.

Illingworth, R. et al. (2008). A Novel CpG Island Set Identifies Tissue-Specific Methylation at Developmental Gene Loci. Liu, E. T. (Ed). PLoS Biology, 6 (1), p.e22. [Online]. Available at: doi:10.1371/journal.pbio.0060022.

Illingworth, R. S. et al. (2010). Orphan CpG Islands Identify Numerous Conserved Promoters in the Mammalian Genome. Reik, W. (Ed). PLoS Genetics, 6 (9), p.e1001134. [Online]. Available at: doi:10.1371/journal.pgen.1001134.

Jiang, X. R. et al. (1999). Telomerase expression in human somatic cells does not induce changes associated with a transformed phenotype. Nature Genetics, 21 (1), pp.111–1114. [Online]. Available at: doi:10.1038/5056.

Koyama-Nasu, R., David, G. and Tanese, N. (2007). The F-box protein Fbl10 is a novel transcriptional repressor of c-Jun. Nature Cell Biology, 9 (9), pp.1074–1080. [Online]. Available at: doi:10.1038/ncb1628.

Laird, P. W. (2010). Principles and challenges of genome-wide DNA methylation analysis. Nature Reviews Genetics, 11 (3), pp.191–203. [Online]. Available at: doi:10.1038/nrg2732.

Landan, G. et al. (2012). Epigenetic polymorphism and the stochastic formation of differentially methylated regions in normal and cancerous tissues. Nature Genetics, 44 (11), pp.1207–1214. [Online]. Available at: doi:10.1038/ng.2442.

Larsen, F., Solheim, J. and Prydz, H. (1993). A methylated CpG island 3' in the apolipoprotein-E gene does not repress its transcription. Human Molecular Genetics, 2 (6), pp.775–780. [Online]. Available at: doi:10.1093/hmg/2.6.775.

Laurent, L. et al. (2010). Dynamic changes in the human methylome during differentiation. Genome Research, 20 (3), pp.320–331. [Online]. Available at: doi:10.1101/gr.101907.109.

Li, N. et al. (2010). Whole genome DNA methylation analysis based on high throughput sequencing technology. Methods, 52 (3), pp.203–212. [Online]. Available at: doi:10.1016/j.ymeth.2010.04.009.

Lister, R. et al. (2009). Human DNA methylomes at base resolution show widespread epigenomic differences. Nature, 462 (7271), pp.315–322. [Online]. Available at: doi:10.1038/nature08514.

Milyavsky, M. et al. (2003). Prolonged culture of telomerase-immortalized human fibroblasts leads to a premalignant phenotype. Cancer research, 63 (21), pp.7147–7157. [Online]. Available at: http://www.ncbi.nlm.nih.gov/pubmed/14612508.

Mohn, F. et al. (2008). Lineage-Specific Polycomb Targets and De Novo DNA Methylation Define Restriction and Potential of Neuronal Progenitors.

Molecular Cell, 30 (6), pp.755–766. [Online]. Available at: doi:10.1016/J.MOLCEL.2008.05.007.

Morales, C. P. et al. (1999). Absence of cancer-associated changes in human fibroblasts immortalized with telomerase. Nature Genetics, 21 (1), pp.115–118. [Online]. Available at: doi:10.1038/5063.

Myant, K. et al. (2011). LSH and G9a/GLP complex are required for developmentally programmed DNA methylation. Genome research, 21 (1), pp.83–94. [Online]. Available at: doi:10.1101/gr.108498.110.

Riggs, A. D. (1975). X inactivation, differentiation, and DNA methylation. Cytogenetic and Genome Research, 14 (1), pp.9–25. [Online]. Available at: doi:10.1159/000130315.

Robertson, K. D. and Jones, P. A. (1998). The Human ARF Cell Cycle Regulatory Gene Promoter Is a CpG Island Which Can Be Silenced by DNA Methylation and Down-Regulated by Wild-Type p53. Molecular and Cellular Biology, 18 (11), pp.6457–6473. [Online]. Available at: doi:10.1128/mcb.18.11.6457.

Saxonov, S., Berg, P. and Brutlag, D. L. (2006). A genome-wide analysis of CpG dinucleotides in the human genome distinguishes two distinct classes of promoters. Proceedings of the National Academy of Sciences of the United States of America, 103 (5), pp.1412–1417. [Online]. Available at: doi:10.1073/pnas.0510310103.

Serre, D., Lee, B. H. and Ting, A. H. (2009). MBD-isolated genome sequencing provides a high-throughput and comprehensive survey of DNA methylation in the human genome. Nucleic Acids Research, 38 (2), pp.391–399. [Online]. Available at: doi:10.1093/nar/gkp992.

Shapiro, R., Servis, R. E. and Welcher, M. (1970). Reactions of Uracil and Cytosine Derivatives with Sodium Bisulfite. A Specific Deamination Method.

Journal of the American Chemical Society, 92 (2), pp.422–424. [Online]. Available at: doi:10.1021/ja00705a626.

Trimarchi, M. P. et al. (2012). Enrichment-based DNA methylation analysis using next-generation sequencing: sample exclusion, estimating changes in global methylation, and the contribution of replicate lanes. BMC Genomics 2012 13:8, 13 (8), pp.1–8. [Online]. Available at: doi:10.1186/1471-2164-13-s8-s6.

Vaziri, H. and Benchimol, S. (1998). Reconstitution of telomerase activity in normal human cells leads to elongation of telomeres and extended replicative life span. Current Biology, 8 (5), pp.279–282. [Online]. Available at: doi:10.1016/S0960-9822(98)70109-5.

Weber, M. et al. (2005). Chromosome-wide and promoter-specific analyses identify sites of differential DNA methylation in normal and transformed human cells. Nature Genetics, 37 (8), pp.853–862. [Online]. Available at: doi:10.1038/ng1598.

Xu, J. et al. (2018). MeDEStrand: An improved method to infer genome-wide absolute methylation levels from DNA enrichment data. BMC Bioinformatics, 19 (1). [Online]. Available at: doi:10.1186/s12859-018-2574-7.

Zhang, T. et al. (2016). G9a/GLP Complex Maintains Imprinted DNA Methylation in Embryonic Stem Cells. Cell Reports, 15 (1), pp.77–85. [Online]. Available at: doi:10.1016/j.celrep.2016.03.007.